Studies on the Cellular and Molecular Basis of Salt Resistance in a Halotolerant *Arabidopsis thaliana* Cell Line.

A thesis submitted to the University of Glasgow for the degree of

Doctor of Philosophy

Medhat El-Sheikh

December 2002

Division of Biochemistry and Molecular Biology,
Institute of Biomedical & Life Sciences,
University of Glasgow

ProQuest LLC.
789 East Eisenhower Parkway
P.O. Box 1346
Ann Arbor, MI 48106 – 1346

DECLARATION.

I hereby declare that the work presented in this thesis is the result of my own investigations except where references are mentioned and assistance is acknowledged. Therefore, no part of this thesis has been previously presented for any degree.

Signed.

Medhat El-Sheikh

Date

ACKNOWLEDGMENTS

I would like to express my gratitude to Dr. Peter Dominy for his helpful and critical advice, and patience throughout the period of his work. I also acknowledge the encouragement and financial support of the Egyptian government.

I should like to thank Dr Joel Milner, Dr Chiara Geri (particularly for her advice on the DD-PCR technique), and Dr Edi Cecchini for her helpful suggestions. My thanks are also given to Ms. Janet Laird for her excellent technical assistance.

I would also like to acknowledge the financial help from Professors Richard Cogdell, Alan Taylor, and John Coggins. For their support and patience I am indebted to Drs Alistair Whitelaw and David Miller. Without the help and understanding of the above, this thesis would not have been completed.

Finally, I am extremely grateful to my parents for their encouragement and support during my years at university.

A List of Abbreviations

2,4 D	2,4-Dichlorophenoxyacetic acid
ABC	ATP-binding cassette.
ACC.	accession number.
AD	absorbance density
AHA	gene encoding *Arabidopsis* H^+-ATPase
AHA	*A.thaliana* gene encoding H^+-ATPase.
AKT	gene encoding *Arabidopsis* high-affinity K^+ transporter
Amp	ampicillin
AOS	active oxygen species
At ACA	*Arabidopsis* gene encoding Ca^{2+} ATPase
AtKUPs	*Arabidopsis* gene encoding K^+ Uptake
AtNHX1	*Arabidopsis thaliana* gene encoding N^+/H^+ antiporter.
AtSOS	*Arabidopsis* gene encoding plasma membrane N^+/H^+ antiporter
BCA	*Brassica* gene encoding Ca^{2+} ATPase.
BLAST	basal local alignment sequencing toll
bp	base pair
BSA	bovine serum albumin
CDK	cyclin-dependent protein kinase
cDNA	complementary deoxyribonucleic acid
CFTR	cystic fibrosis transmembrane regulator.
CIAP	calf Intestinal Alkaline Phosphatase.
cpm	counts per minute

CsCL	caesium chloride
DDRT-PCR	differential Display Reverse Transcription PCR.
DEPC	diethylpyrocarbonate
dH_2O	distilled water
Ds	deci-siemens
DNA	deoxyribonucleic acid
ds DNA	double stranded DNA
ds m^{-1}	deci siemens per metre
dsDNA	double stranded cDNA deoxyribonucleic acid
DTT	dithiotheitol.
EBI	the European Bioinformatic institute
EC	electrical conductivity
EDTA.Na2	diaminoethane-tetraacetic acid, disodium salt
ena1	gene encoding a putative *S. cerevisiae* Na^+-ATPase
ena1	*S cerevisiae* genes encodes plasma membrane Na^+-ATPase
ER	endoplasic reticulum.
ESP	exchangeable sodium percentage
FAO	Food and Agricultural Organization of the United Nation.
FDA	fluorescine diacetate
GSTs	glutathion-S-transferase
GS-X	glutathion conjugate.
HHS	habituated high salt.
HKT1	*Triticum sativum* gene encoding a high-affinity K^+transport.

HsNHe	*H sapiens* gene encoding N^+/H^+ antiporter.
KAKs	gene encoding fungal high-affinity K^+ transporters.
KCO1	*Arabidopsis* gene encoding outward rectifing K^+ channel
KST1	*Solanum tuberosum* gene encoding K^+ channel in.
LCA	*Lycopersicon* gene encoding Ca^{2+} ATPase.
LCT1	gene encoding a low-affinity cation transport.
LHA1	*Lycopersicon* gene encoding H^+-ATPasc.
MDR	multi-drug resistance.
MMLV	Moloney Murine Leukemia Virus
MPa	mega Pascal
MRPs	multi-drug resistance associated protein.
MSMO	murashige-Skoog-basal salt medium
NBF	nucleotide binding fold.
NCBI	thc National Center for Biotechnology Information
NIX	nucleotide identification of interest region.
NPABA	*Nicotiana.plumbaginifolia* ATP-binding cassette.
ORF	open reading frame.
OsNHX1	*O sativa* gene encoding N^+/H^+ antiporter.
PAGE	polyacrylamide-gel electrophoresis
PEG	poly ethylene glycol
PEG 8,000	polyethylene glycol 8,000
pH	hydrogen ion concentration unit
PMA	gene encoding *N plumbaginifolia* H^+ ATPase

PMA	gene encoding plasma membrane H^+-ATPase.
PMCA.	plasma membrane calmodulin-stmulated Ca^{2+} ATPase.
PMF	proton motive force
ppi	inorganic pyrophosphate.
Ppm	part of million
psi	pounds per square inch
p-type	plasma membrane-type
Pvp	polyvinyl pyrrolidone
QTL	quantitative trait loci
rpm	revolutions per minute
RT-PCR	reverse transcriptase- Polymerase Chain Reaction
SBF	sodium bile acid symporter family
Sc NHX1	*Sacchromyces cerevisia* gene encoding Na^+/H^+ antiporter.
SDS	sodium dodecyl sulfate
SERCA	sarco-and endoplasmic reticulum Ca^{2+} ATPase.
SKOR	shaker-like K^+ outwardly rectifying channel.
sod2	gene encoding *S. Pombe* Na^+/H^+ antiporter
SOS	salt overly sensitive
SOT	salt overly tolerant
SPFI	sodium sensitive benzofuranyl
ssDNA	single-stranded deoxyribonucleic acid
ssDNA	single strand deoxyribonucleic acid
SV-V	small vacuoles and vesicles

TDS	total dissolved salt
Tm	melting temperature.
TMD	trans-membrane domain.
TMPred	transmembrane proteins structural prediction.
trk1	*S cerevisiae* gene encoding for high-affinity K^+transporters
TSEM	tams section electron microscopy
TUR2	suphonylurea receptor.
Tween 20	polyoxyethylelesorbitan monolaureate
Vac.	vacuole
V-ATPase	vacuolar H^+-ATPase.
VIC	voltage independent channels.
V-PPase	vacuolar pyro-phosphate
V-Ppase	vacuolar H^+-pyrophosphatase.
V-type	vacuolar type
WT	wild type
X-Gal	5-bromo-4chloro-3-indol B-D galactisde
z-sod2	gene encoding Z. *rouxii* Na^+/H^+ antiporter

TABLE OF CONTENTS

Sections			Page No.
Acknowledgments			i
Abbreviations			ii
Table of Contents			vii
Abstract			xiv
CHAPTER ONE: INTRODUCTION			1
General Introduction			1
1.1	Importance of Salinity to Agriculture		1
1.2	Soil Deterioration		3
1.3	Origin of Salts in Soils		5
1.4	Qualifying the Salinity Hazard and Soil Classification		6
1.5	Differences in Plant Growth Response to Salinity		9
1.6	Factors Modifying Crop Salt tolerance		10
1.7	The Major Effects of Salt on Plant Growth		12
1.7.1	Na^+ Toxicity		12
1.8	Mechanisms for Coping with Salt Stress		15
1.8.1	Maintaining High Cytosolic K^+/Na^+ Ratios		15
1.8.1.1		Better Discrimination for K^+ Uptake	16
		(a) High Affinity K^+ Uptake	17
		(b) Low Affinity K^+ Uptake	19
1.8.1.2		Better Discrimination Against Na^+ Uptake	24
1.8.1.3		Na^+ Compartmentation	26
1.8.1.4		Active Na^+ Efflux from Cells	27
1.8.1.4.1		P-type Ion Pumps	28
1.8.1.4.2		Plasma Membrane H^+-ATPase	30
1.8.1.4.2.1		Plasma Membrane Ca^{2+}-ATPase	35
1.8.1.4.2.2		ABC Pumps	39

1.8.1.4.2.3	Vacuolar ATPase	44
1.8.1.4.2.4	Vacuolar Ppase	47
1.9	Secondary Active Transport	48
1.9.1	Sodium Efflux in Plants	48
1.10	Aims of project.	56

CHPTER TWO: MATERIALS AND METHODS 58

2.1 Materials		58
Chemicals		58
2.1.1.1	Oligonucleotide primers	58
2.1.1.2	DNA Modifying Enzymes	58
2.1.1.3	Bacterial Growth Media (Liquid and Solid)	59
2.1.1.4	Antibiotics, IPTG and X-Gal	59
2.1.2	Bacterial strains, Cloning Vectors and Plasmids	60
2.1.3	General Laboratory Procedures	60
2.1.3.1	Filtration.	60
2.1.3.2	pH Measurement	60
2.1.3.3	Autoclaving	60
2.1.3.4	Solutions and Glassware for RNA Work	61
2.1.3.5	Silicon-coating of Sequencing Glass Plates	61
2.1.4	Plant Material	61
2.1.4.1	Growth of Cell Suspension Cultures	62
2.1.4.2	Salt Treatment and Harvesting of Cell Suspension Cultures	62
2.1.4.3	Electron Microscopy	62
2.1.4.4	Toluidine Blue-Stain of Chromosome	62
2.2 Methods		63
2.2.1	Isolation of Plant Genomic DNA	63
2.2.2	Isolation of Total RNA from cell suspension cultures	65
2.2.2.1	Preparation of Phenol	65
2.2.2.2	Isolation of Total RNA	65
2.2.2.3	Isolation of total RNA using Promega kits	67

2.2.3	Amplification and Preparation of Plasmid DNA	68
2.2.3.1	Preparation of Competent Cells	68
2.2.3.2	Transformation	68
2.2.3.2.1	Transformation of Competent Cell	68
2.2.3.3	Tansformation of *E. coli* XL1-Blue MRF' Supercompetent Cells and XL10-Gold Kan Ultracompetent Cells	69
2.2.3.4	Transformation of TOPO 10 *E. coli* Cells	70
2.2.4	Preparation of Plasmid DNA	70
2.2.4.1	Small-Scale Preparation of Plasmid DNA	71
2.2.4.2	Large Scale Preparation of Plasmid DNA	72
2.2.5	Nucleic Acid Precipitation	73
2.2.5.1	Quantification of DNA and RNA	74
2.2.6.	Agarose Gel Electrophoresis	74
2.2.6.1	Electrophoresis of DNA	74
2.2.6.2	Denaturing Electrophoresis of RNA	75
2.2.6.3	Nucleic Acid Markers	75
2.2.6.4	Digestion of DNA with Restriction Endonucleases	76
2.2.7	Extraction and Purification of DNA Fragments from Agarose Gels	76
2.2.8	Blotting of Nucleic Acids	77
2.2.8.1	Northern Blotting	77
2.2.9	Radiolabelling of DNA	78
2.2.9.1	Generation of Radioactive ssDNA probes by Asymmetric PCR	78
2.2.9.2	Measurement of Incorporated Radioactivity	79
2.2.10	Hybridization Analysis	80
2.2.10.1	Hybridization Analysis of RNA	80
2.2.10.2	Washing Membranes	80
2.2.10.3	Auto-radiography	80
2.2.11	Reverse Transcription - Polymerase Chain Reaction (RT-PCR)	81
2.2.11.1	Synthesis of First-Strand cDNA	81
2.2.12	Polymerase Chain Reaction (PCR)	81

2.2.12.1	PCR Amplification of Nucleic Acid	82
2.2.12.2	Purification of PCR Products	82
2.2.12.3	Creating Blunt End DNA (Polishing)	83
2.2.12.4	Cloning the PCR Product	84
2.2.12.4.1	Cloning of Blunt End PCR Fragment	84
2.2.12.4.1.1	Dephosphorylation of Cloned Plasmid	84
2.2.12.4.1.2	Polishing the Purified PCR Products	85
2.2.12.4.1.3	Ligation of Blunt End PCR Fragments into Cloning Vectors	85
2.2.12.4.2	TOPO Cloning Reaction*	86
2.2.12.4.3	PCR Amplification of Plasmid Vector Insert	86
2.2.13	Differential Display Reverses Transcription PCR	87
2.2.13.1	Reverse Transcription of Total RNA	87
2.2.13.2	Amplification of First Stranded cDNA By PCR	88
2.2.13.3	0.6 % Polyacrylamide Sequence Gels	89
2.2.13.4	Re-amplification of cDNA Eluted from Dried Gels	89
2.2.13.5	Synthesis of Double-Stranded cDNA From Total RNA	90
2.2.13.5.1	First Strand cDNA Reaction	90
2.2.13.5.2	Second strand cDNA synthesis	91
2.2.13.5.3	Cleaning the Double Stranded cDNA	91
2.2.13.5.4	Preparation of Radio-labeled cDNA for Reverse Northerns	92
2.2.13.5.5	Measurement of Incorporated Radio-nucleotides into cDNA	92
2.2.14	Slot Blot Analyses	92
2.2.14.1	Slot Blot of Bands	92
2.2.14.2	Slot Blot Hybridization Analysis	94
2.2.15	Database Searches	94
2.2.15.1	Keyword and Homology Searches	94
2.2.15.2	Structural Prediction	94
2.2.15.3	Identification of Interest Regions In	

	Nucleotides Sequences	95
2.2.15.4	Primer Design	95
2.2.15.5	Determination of Endonucleases Sites	96
2.2.15.6	Alignments	96
2.2.16	DNA Sequencing	96

CHAPTER THREE: CHARACTERIZATION OF HHS and WT *ARABIDOPSIS* CELL LINES. 97

3.1	Fluorescence Microscopy	97
3.2	Electron Microscopy	100
3.2.1	Cellular Sequestration/Cellular Trafficking	102
3.2.1.1	Plasma Membrane and Endo-membrane Fusion	102
3.2.1.2	Endomembrane Fusion	104
3.2.1.3	Tonoplast-Endomembrane Fusion	105
3.3	Nuclear and Chromosomal Aberration	106
3.4	Discussion	109

CHAPTER FOUR: CLONING Na^+/H^+ ANTIPORTERS 112

4.1	The Role of Na^+/H^+ Antiporters in Salt Tolerance	112
4.2.	PCR Cloning Approach	113
4.2.1	PCR Cloning Using Degenerate Primers and cDNA Libraries as Template	113
4.3.	RT-PCR Cloning of *At* B04.4 cDNA	115
4.3.1	PCR Cloning of *At* B04.4 Using Specific Primers and Genomic DNA as Template	115
4.3.2	RT-PCR Amplification of *At*B04.4 cDNA	115
4.3.2.1	RT-PCR Cloning of *At* B04.4 Using Oligo dT Primer First Strand Synthesis	116
4.3.2.2	Cloning of *At* Bo4.4 cDNA	116
4.4	RT-PCR Cloning of *At*T9D9.5 cDNA	118
4.5	RT-PCR Cloning of *At* F24D13.3 and *At* F24D13.4cDNAs	119

4.5.1	RT-PCR Amplification of First Strand *At*F24 D13.3 and *At*F24D13.4 cDNA	119
4.6	RT-PCR Cloning of *At*F14H20.5 cDNA	121
4.6.1	RT-PCR Amplification of First Strand *At*F14H20.5 cDNA	121
4.4.1.3	Northern Analysis of *At*F14H20.5	122
4.7	RT-PCR Cloning of *At* T12H17.230 cDNA	123
4.7.1	Cloning and Sequencing of *At* T12H17.230 cDNA	124
4.7.2	Expression of *At*T12H17.230	126
4.7.3	Function Analysis of the *At* T12H17.230 Full-length Gene	126
4.8	RT-PCR Cloning of *At* T20D21.19 cDNA	127
4.8.1	Cloning and Sequence of *At* T20D21.19 A	128
4.9.	Discussion	129

CHAPTER FIVE: TRANSCRIPTOME ANALYSIS OF SALT TOLERANT CELL LINES USING DIFFRENTIAL DISPLAY 133

5.1	Identification of Differentially Abundant Genes Using DD-PCR	134
5.1.1	Re-amplification of cDNA Eluted From Dried Gels	135
5.2.1	Confirmation of Up-and Down-Regulated Gene Expression	136
5.2.2	cDNA Cloning and Sequencing	137
5.3	Discussion	139

CHAPTER SIX DISCUSSION

6.1	**GENERAL DISCUSSION**	141
References		154

Abstract.

Global agricultural output is now severely affected by salinity due in part to the cultivation of primary salinated land, and partly through irrigation with brackish water. Unfortunately, the major crop species are all salt sensitive (glycophytes) and do not perform well in even mildly saline soils. Consequently there is now much attention focussed on developing new crops that are more salt resistant. Progress in this area has been hampered because the model plant, *Arabodopsis thaliana*, is also a glycophyte that will not complete a full life cycle in a one-fifth dilution of sea water. However, at the University of Glasgow a halotolerant cell suspension (HHS) line has been developed from a wild type (WT) *Arabidopsis* culture that grows well in three-quarter strength seawater. The work presented in this thesis was directed towards understanding better how the HHS cope with high salinity.

The morphology of the two cell lines were examined at the fine and untrastructural level. The HHS , and indeed all halotolerant cells lines studied to date, contain an extensive array of small vacuoles and vesicles (SV-V) in their cytoplasm, as well as a large central vacuole; this is not observed in WT cells. It is feasible that the SV-V are involved in the rapid sequestration of toxic ions away from the cytoplasm. There was some evidence for endocytosis and exocytosis but further clarification of the dynamics of SV-V movement is required. There is also some indirect evidence that ABC transporters may be associated with the SV-V.

Attempts were made to clone the first plant Na^+ transporters from plants using genome sequence data to design PCR primers and RT-PCR on message prepared from the HHS cells. Initaially, six putative Na^+ / H^+ antiporters were identified but no PCR products could be generated from three of these. Of the remaining three, two have subsequently

been shown to code for genuine Na^+ / H^+ antiporters (*At*NHX1 and *At*SOS1), and the other may be a new transporter that has not been characterized yet (*At*T12H17.230).

In addition, Differential Display-PCR was used to identify some of the differentially abundant transcripts in WT and HHS cells. Unfortunately, due to a severe fire, this work was not completed. However, the method does work but now *Arabisopsis* DNA chips are routinely available. microarraying appears to be a better approach,

CHAPTER ONE

INTRODUCTION

CHAPTER ONE

INTRODUCTION

1.1. The Importance of Salinity to Agriculture.

In the last 150 years, global agricultural production has increased enormously, necessitated by a rapidly rising population. This rise in output has been achieved by the introduction of modern farming practices (such as the application of fertilizers and extensive irrigation), the development and use of effective crop production agents (pesticides, herbicides and fungicides), and the breeding of superior lines of the major crops. Due to the application of these practices, global cereal yield practically doubled between 1960 and 1990 (Kishore and Shewmaker, 1999). Yields of both rice and wheat crops largely consumed by the rapid growing Asian population, have dramatically increased. Until recently, these technologies have allowed agricultural output to keep pace with increasing population, but there is now evidence that the food production *per capita* is declining (Kishore and Shewmaker, 1999). One solution to this problem is to recruit more marginal land for intensive agricultural use, necessitating heavier inputs ; consequently food self-sufficiency, especially in emerging economies, will be compromised (Kishore and Shewmaker, 1999).

The threat of a Malthusian population crisis highlighted by Ehrlich (1967) appears to have diminished as a slowdown in the rate of population growth has occurred. However, the challenge of feeding a world population growing by up to 160 people every minute (>90 % of them in developing countries) remains daunting. It is forecast that by 2050, world population will increase from the current level of ~ 6 billion to 10 billion people.

Feeding this population will require an astonishing increase in food production. In fact, it has been estimated that the world will need to produce as much food during the next 50 years as was produced since the beginning of agriculture 10,000 years ago (James, 1997)! More than 800 million people are chronically malnourished, and 1,100 million live in absolute poverty (FAO, of the United Nations 1995).

In the foreseeable future, increasing output from conventional agriculture will be our primary response to this problem, with cereal grains playing a pivotal role. The International Food Policy Research Institute has predicted that by the year of 2020, almost 96 % of the world's rice consumption, two-third of the world's wheat consumption, and almost 60 % of the world's maize consumption will be in developing countries (Hoisington, *et al.*, 1999). From forecasts, it has been suggested that wheat should surpass rice in feeding the poor of those nations. Wheat will likely become the most important cereal in the world, with maize close behind; together, these crops will account for ~ 80 % of the cereal import requirements of developing countries (Hoisington, *et al.*, 1999). Many economists stress, however, that increased production in developing countries will be essential for achieving food security. Maize and wheat are each expected to have an annual global demand of ~ 775 million tons and will be of critical consequence in the race between crop production and population growth (Hoisington, *et al.*, 1999).

The challenge over the next 50 years will be not only to feed more people, but to achieve this in a sustainable manner with reduced or none deleterious effects on the natural

environment. Surprisingly the area available for food production has essentially remained constant since 1960 (Evans, 1998). In appears that new land that has been brought into cultivation, and this balanced that lost due to soil erosion, salinity and urbanization (Hoisington, *et al*., 1999).

1.2. Soil Deterioration.

Soil deterioration has many causes, the main factors being inappropriate land-use, erosion, salinization and waterlogging. Over the last 100 years, with the growth in food consumption, the cultivation of soils has increased, both extensively and intensively, but without a parallel increase in soil conservation measures. The side effects of present agricultural practices are loss of fertility and structure of the soil, and deep erosion. Salinity is one of the major causes for loss of existing agricultural land because of its ability to change the fertility of soils and soil properties, and it is also a major constraint preventing the development of new areas. Soil salinization is one of man's oldest environmental problems. The historical records show that human civilizations never remain established in one locality for more than 800 to 2000 years (Ashraf 1994). The major reason for the decline in many of these civilizations seems to have been the destruction of the land resource (Carter and Dale, 1974).

The processes of soil salinization have continued relentlessly throughout history. In fact, the long-term viability of irrigation agriculture has been seriously questioned (Jacobson and Adams, 1958). In California where irrigated agriculture in most areas is less than

100 years old, of the 8.6 million ha. of arable land in production 4.5 million acres are now affected by salinity, and this damage was expected to increase to 5.2 million ha. by the turn of 2000. In the San Joaquin valley, which has 4.5 million ha. of land under irrigation, more than 0.4 million acres were assessed as severely affected by salinity (Lewis, 1984). The global extent of saline soil is believed to range between 400 and 950 x 10^6 ha. and it has been estimated that one third of the 230 x 10^6 ha. currently under irrigation is affected by salinity (Flowers, *et al.*, 1977).

Moreover, the distribution of the 343.5 million ha. of primary saline soils throughout the world was evaluated by Massoud (1974) and Szabolcs (1979), and of this, 53.5 million ha. was located in Africa, 17.4 million ha. in Australia, 1.96 million ha. in North America, 69.4 million ha. in South America, 91.7 million ha. in North and Central Asia, 83.3 million ha. in South Asia, and 20.0 million ha. in South-East Asia. If it were not for the levels of salt already present in these soils, these regions could be turned over for agricultural production.

Salinity is a common problem in irrigated agriculture in India and Pakistan, particularly when wheat and rice, the most important cereals, are grown in the same system. In Pakistan, over 70 % of the ground water pumped is of poor quality and 6 million ha. are salt affected, mainly in the canal-command areas, of which half is cultivable or cultivated to some extent (Farooq, 2001). In India 7 million ha. are salt or sodicity-affected (Farooq, 2001). World-wide, 40,000 ha. are being lost annually from agriculture due to salinity (Al-Katib, *et al.*, 1993).

It is estimated that about a quarter of a million hectares of good agriculture land in South Western Australia have become unproductive due to soil salinity (Malcom, 1982).

1.3. Origins of Salts in Soils.

Salt-affected soils and water are part of the ongoing geochemical processes. Soluble salts originated from the disintegration of minerals and rocks. Normally, salts move from weathering sites into the groundwater system, and then move into streams and finally into oceans. The present-day location of salt is primarily determined by the amount of water which has passed through a system. If rainfall is high, as in humid climates, most salts have been transported into oceans or to deep groundwater reserve systems. In arid environments where rainfall is limited, salts are frequently present in the soil. Society can alter these geological processes and create salinity hazards in many ways, including irrigation, mining, processing plants and other activities (Hoffman, 1999).

Salts may accumulate in landscapes with particular relief and geological conditions. For example, saline conditions are linked to lowlands or depressions where salty water naturally drains, evaporates and salts accumulate. This situation is often associated with restricted internal soil drainage, which leads to high water tables. Another major factor is whether the landscape was previously submerged under saline or fresh water (Hoffman, 1999).

On irrigated lands, irrigation water is the primary source of salts. When new lands are brought under irrigation, or if salinity management is inadequate, soils prone to salt accumulation may be saline, sodic or both. Under these conditions, economical crop production is not feasible without reclamation. The reclamation process, whether it be for saline, sodic or toxic soils, requires large amounts of non-saline water to leach the salts from the intended crop root zone. Frequently, man-made drainage systems must be installed to aid natural drainage in removing the extra water required to leach salt from the soil (Hoffman, 1999).

Generally arable lands are affected by these factors in addition to other minor factors, and become semi-arid, there are already large areas affected by salinity and this is increasing from year to year. As a consequence, the amount of arable land is decreasing, and crop yield is reduced in regions where irrigation is practiced.

1.4. Quantifying the Salinity Hazard and Soil Classification.

Salinity, sodicity and toxicity must be quantified for proper diagnosis and management. Because saline irrigation water or shallow saline groundwater normally causes saline hazards, sampling this water is particularly important. When saline conditions are present or suspected, soil samples from throughout the root zone are critical to determine what management practices are required to minimize or eliminate the saline hazard (Hoffman, 1999). Soils are considered saline if they contain soluble salts in quantities sufficient to interfere with the growth of most crop species. This, however, is not a fixed

amount of salt but depends on the species, the texture and water capacity of the soil, and the composition of the salts. Thus the criterion for distinguishing saline from non-saline soils is arbitrary. According to the definition of the US Salinity Laboratory the saturation extract (the solution extracted from a soil at its saturation water content) of a saline soil has an electrical conductivity (EC) greater than 4 mmho cm^{-1} (or 4 deciSiemens m^{-1} ,(equivalent to ≈ 40 mM NaCl) and an exchangeable sodium percentage (ESP) of less than 15. Although the pH of saline soils can vary over a wide range, it is usually around neutrality, with a tendency toward slight alkalinity. Saline soils with an ESP of greater than 15 are termed saline-alkali soils (or saline-sodic soils), have high pH values, and tend to become rather impermeable to both water and aeration when the soluble salts are removed by leaching. Sodicity, is defined as an excessive proportion of sodium to calcium plus magnesium. The presence of excess sodium deteriorates soil structure and reduces water penetration into and through the soil. Like drought, an excess proportion of sodium to calcium plus magnesium, reduces water availability to the crop. The term, sodicity, has replaced the term 'alkali', when referring to the effects of excess sodium in the soil. These distinction between saline and alkali (sodic) soils are often insufficiently appreciated in nutrient solution studies by adding high concentrations of single salts (mainly NaCl), but maintaining low calcium concentrations. Such large Na^{+} /Ca^{+2} ratios in the substrate are typical for sodic soils but not saline agricultural soils (Mass, 1987).

In evaluations of the suitability of saline soils for crop production, the measurement of EC offers a rapid and simple method for characterizing the salt content. From the EC the solute potential of the saturation extract can also be calculated: solute (osmotic) potential

(MPa) = EC (ds m^{-1})x -0.036. Since the EC is measured in the saturation extract, the salt concentration in the soil solution at field capacity will be about twice that of the saturation extract and even higher when the soil moisture level declines below field capacity. For comparison, the average EC of seawater is in the range of 44- 55 dS m^{-1}, and as a rule irrigation water of good quality must have an EC below 2 dS m^{-1}. For plant growth in saline soils, however, the EC of the saturation extract only is an insufficient indicator of performance, mainly for two reasons:

(a) the actual salt concentration at the root surface can be higher than in the bulk soil: (b), the EC characterizes only the total salt content, not its composition. Although NaCl is usually the dominant salt, others may be abundant in various combinations, depending on the origin of the saline water and the solubility of the salts. Furthermore, in both saline soils and irrigation waters, high boron concentrations might become more critical for plant growth than salt concentrations *per se*.

Furthermore, salinity is quantified using various units of measure. Salt concentration (C) from laboratory analyses is frequently labeled as total dissolved solids (TDS) and reported as milligrams of salt per liter of water (mg/L) or as grams of salt per cubic meter of water (g/m^3). The units of mg/L or g/m^3 are equal to parts of million (ppm). Salinity, the total salt concentration, in units of mg/m^3, is the sum of the concentrations of each salt constituent. An easier and quicker method of quantifying salinity is to measure the electrical conductivity of irrigation water (EC_i) or water extracted from a saturated soil sample (EC_e). The relationship between salt concentration (C) and electrical conductivity (EC) is approximately C = 640 EC. The approximate relationship between the electrical

conductivity of irrigation water (EC_i) and soil salinity is $EC_e = 1.5\ EC_i$, if about 15 % of the applied water is draining from the crop root zone (Hoffman, 1999).

1.5 Differences in Plant Growth Response to Salinity.

Plant species differ greatly in their growth response to salinity. Plant species were classified by Greenway and Munns (1980) into four groups based on two parameters: the threshold EC (the ability of plants to tolerate salinity up a certain levels without a measurable loss in yield), and the rate of yield loss (the linear rate of yield loss with increasing salinity beyond the threshold). Group I are halophytes which grow under relatively high levels of NaCl, a response which can be explained only in part by the role of sodium as a mineral nutrient in these species. Group II which includes halophytic crop species such as sugar beet, are slightly stimulated by low salinity levels. Group III are salt-tolerant crop species (mesophytes) such as barley, and their response to salt tolerance is relatively low. Group IV are salt-sensitive (glycophytes) such as bean, and growth is severely inhibited even at low substrate salinity levels (Greenway and Munns, 1980).

Mass and Hoffman (1977) categorized crop species into four groups on the basis of their salt-tolerance; these categories were tolerant, moderately tolerant, moderately sensitive and sensitive. Barely, cotton and sugar beet are considered tolerant because their threshold salinity level (maximum salinity without yield loss) is above 8.0 dS/m^{-1}. Wheat and soybean are moderately tolerant, their threshold salinity level ranging form 4.9to 6.8 dS/m^{-1}. Moderately sensitive crops include potato, tomato, sugar cane and rice (2.0-4.8

dS/m^{-1}), whereas most fruit trees, carrot and onion are sensitive group where the threshold salinity level is below 2.0 dS/m^{-1}.

For convenience, with respect to their sensitivity to salt, plants are usually rather arbitrarily divided into two or three groups. There is no universally accepted agreement of where the boundaries between these groups lie, but the following definitions will be used through the thesis. Halophytes have adapted to highly saline conditions (500 mM NaCl), although maximum growth often occurs at lower salt conditions (Unger, 1991). Mesophytes can survive between 500 mM and 100 mM NaCl, and include sugar beet and barley; however, optimal growth is achieved at the lower end of this range. Glycophytes grow in < 100 mM NaCl, and include most crop species such as wheat, maize and tomato. The latter group appear to have never colonized saline habitats and hence most of them are adapted to soils with a low Na^+ content, and lack the mechanisms required to tolerate the water deficiency and the ion excesses prevailing in saline soil (Greenway & Munns, 1980). The growth of most glycophytes is severely limited in concentrations as low as 25-50 mM NaCl, to low to produce a significant water stress effect (Lessani and Marschner, 1978).

1.6. Factors Modifying Crop Salt Tolerance.

There are several factors, including those relating to the soil, crop and environmental conditions that interact with salinity to cause a different yield response. Genotypic differences and the stage of growth, are crop factors which may modify the salinity

response (Soltanpour and Follett, 1999). Clearly, from an agricultural perspective, what is important is that resistance is effective at all or critical stages of development and therefore, an understanding of the complex polygenic responses is required. It is likely that some traits are expressed at one stage of growth, and at another stage different sets of genes are expressed whilst others are down regulated. However, it is not easy to demonstrate these complex, polygenic response of salt resistant plants to high salinity. Clearly, as a first approximation, it will be necessary to understand in general terms how cells exposed to the highest level of salinity (*e.g.* root epidermal cells) cope with dehydration and ion toxicity. This information can then be used to determine whether similar mechanisms operate in other tissues at and other stages of development.

Typically, crop-breeding programs have been designed to select for high productivity. Consequently, differences in salt tolerance between genotypes common among field and garden crops (Soltanpour, and Follett, 1999; Hoffman, 1999). While stage of plant growth is another factor in crop salt tolerance, most crops are capable of germinating at higher salinity levels than they can tolerate during later stages of growth. *Zea mays*, for example, will germinate at a salinity level twice as high as the threshold for measurable grain yield loss. Typically, crops are most sensitive at the seedling stage and become more tolerant as plants mature (Soltanpour, and Follett, 1999; Hoffman, 1999), but salt tolerance is usually not a factor at germination.

Rainfall and warm dry weather are the most critical meteorological factors. Rainfall before and during the irrigation season makes it possible to use more saline irrigation

crops) must largely result from the ionic, not the water stress, component of salinity. Upon exposure to high salinity, low plant water potentials are the initial, primary effect (*i.e.* from a 'time' viewpoint). The hydrostatic (turgor) pressure of cells (Ψp), will drop and the solute (osmotic) potential Ψs will also decrease (become more negative) because water will leave cells (Flowers, *et al.*, 1977; Greeway and Munns, 1980):

$$\Psi_{H2O} = \Psi_S + \Psi_P$$

As the cell plasmolyses the tissues becomes more dehydrated. When trugor reaches zero, growth is not possible although the low tissue water potential may itself not have a major inhibitory affect on cellular metabolism. As a consequence of these and other problems sensitive and glycophytic plants undergo irrecoverable wilting, and they are unable to complete their life cycle (Greeway and Munns, 1980; Flowers, *et al.*, 1977; Lessani and Marschner, 1978).

The major response of halophytes and other salt-tolerant plants to high salinity is that after the initial wilting process described above, osmotic adjustment can occur due to ion uptake from the soil solution, and by the synthesis of internal organic solutes. However, to regain turgor, a desiccated plant cell must reverse the water potential gradient so that water flows back into the cell. This is achieved by the accumulation of osmotically active solutes in the vacuole. An energetically cheap way of achieving this is to take up Na^+ and Cl^- ions from the external medium and sequester them in vacuoles. If the solute potential of the vacuole (Ψs^{vac}) can be made more negative than that of the surrounding

soil, water will flow in, and turgor will rise. However, for the cytoplasm to rehydrate, it is necessary for Ψs^{cyt} to decrease in parallel to Ψs^{vac}, and this is achieved by the accumulation of non-toxic compatible solutes (e.g. glycine betaine, proline, and sugars, (Flowers, *et al.*, 1977). By contrast, some glycophytes are unable to adapt osmotically under salt stress because of their inability to accumulate ions from the external medium; however, glycophytes can synthesize compatible solutes.

The second effect is that unless the influx of Na^+ and Cl^- is limited they will rapidly reach toxic concentration within the cell. The toxic effect is thought to arise by unfavorable interactions between these ions and enzymes in the cytoplasm and organelles, causing disruption of cellular metabolism (Greenway and Munns, 1980).

Despite the requirement of chloride as a micronutrient for all higher plants, and of sodium as a mineral nutrient for many halophytes and C_4 species, the concentration of both ions in saline soils by far exceed this demand and results in toxic levels in non-salt-tolerant plants. In many herbaceous crop species, such as grapevine and many fruit trees, growth inhibition and injury of the foliage (marginal chloride necrosis on mature leaves) occurs even at relatively low levels of NaCl (Mass, 1993). Under such conditions water deficit is clearly not a constraint, and at least in *Citrus* species, high chloride sensitivity (and thus chloride toxicity) is the major constraint (Mass, 1993). Many studies have been undertaken to determine whether a high level of sodium or chloride is more toxic to plants. Although such experiments are often difficult to interpret, there is some evidence that sodium rather than chloride toxicity may be more important in wheat (Kingbury and

(Kingbury and Epstein, 1984; Rawson, *et al.*, 1988; Davenport and Tester, 1997). However, some species including soybean, other legumes, and avocado and *Citrus* spp., are particularly sensitive to chloride (Blum, 1988; Gorham, 1992). The third effect is that nutrient ion imbalance may occur by reduced uptake of essential mineral nutrients for plant growth such as potassium, calcium, and phosphate when soil Na^+ and Cl^- levels are high (Grattan and Grieve, 1992; Marshchner, 1986).

The above primary stress factors may generate secondary effects such as oxidative stress, which is largely mediated by active oxygen species (AOS), that can result in lipid peroxidation, protein and DNA damage as well as perturbing the redox balance of the cell (Smirnoff 1993; Zhu , *et al.* 1997).

1.8. Mechanisms for Coping with Salt Stress.

Three key physiological strategies are found in salt-resistant plants that confer some measure of tolerance to salinity. These are:

1- Maintenance of a high cytoplasmic K^+/Na^+ ratio

2- Maintenance of a low cytoplasmic Cl^- concentration.

3- Tolerance and/or avoidance of desiccation (osmoregulation).

1.8.1. Maintenance of High Cytosolic K^+/Na^+ Ratios.

Wild plants that tolerate salt and grow in saline environments have high intracellular salt levels. A major component of the osmotic adjustment in these cells is accomplished by ion uptake. The utilization of inorganic ions for osmotic adjustment suggests that salt-tolerant plants must be able to tolerate high levels of salts within their cells. However, enzymes extracted from these plants show high sensitivity to salt (Flowers, *et al* 1977; Glenn, and Brown, 1999), suggesting that these plants are able to keep Na^+ away from the cytosol. Plants can use four mechanisms for the maintenance of a low Na^+ concentration and/or high K^+/Na^+ ratio (Marshchner, 1995):

A- Better discrimination for K^+ uptake.

B- Better discrimination against Na^+ uptake.

C- Sodium exclusion.

D- Sodium compartmentation.

However, it is not certain which one or combination of these mechanisms salt-resistant plant utilize.

1.8.1.1. Better Discrimination for K^+ Uptake.

Potassium is an essential element, constituting 2% of the total dry weight of a plant, and its concentration in fresh tissues ranges from 10 to 100 mM (Glass, 1988). The cellular roles that K^+ plays have been frequently reviewed *e.g.*, by Kochian and Lucas, (1988) and Maathuis and Sanders, (1996) and can roughly be summarized as:

1- Charge balancing in the cytoplasm, where K^+ is the dominant counter ion for the large excess of negative charge on proteins and nucleic acids.

2- Activation of crucial enzymatic reactions such as those involved with glycolysis.

3- A substantial contribution to the osmotic pressure of the vacuole, and hence to cell turgor which endows non-lignified plant cells with structural rigidity.

High levels of tissue K^+ are accumulated by roots from soil solutions that usually contain only micromolar levels of soluble K^+. As a result, plant roots have evolved uptake mechanism that operate at low external K^+ concentrations ($[K^+]_{out}$) with a high concentrating capacity (Epstein, 1973). When the rate of K^+ uptake is examined over a range of $[K^+]_{out}$, Epstein, and co-workers discovered a biphasic pattern of K^+ uptake by barley roots (Epstein *et al.*, 1963; Epstein, 1966 & 1972). They proposed the presence of two uptake mechanisms working simultaneously at the plasma membrane. Potassium uptake is mediated by both high-affinity and low-affinity mechanisms. High affinity uptake was thought to be mediated by a carrier that functions to sustain K^+ accumulation in plant when external $[K^+]$ is in the micromolar rage (1-200 μM). Whereas, the low-affinity uptake system involves passive transport of K^+ in the high $(K^+)_{out}$ range (> 0.2 mM; Assmann and Haubrick, 1996).

(a) High-affinity K^+ uptake mechanism.

High-affinity K^+ uptake is especially important in the transport of K^+ from the soil into the roots (Epstein, 1966; Schroeder, *et al.*, 1994; Schachtman and Schroeder, 1994). The

first gene for a high-affinity K^+ transporter was isolated by complementation of a K^+ transport deficient *Saccharomyces cerevisiae* with a cDNA library prepared from wheat roots growing in low K^+ (Schachtman and Schroeder; 1994Rubio, *et al.*, 1995). In *situ* hybridization showed the expression of the gene *HKT1* to be localized in cortical cells of roots and mesophyll cells, and along the vascular tissue in leaves. *HKT*1 mRNA was expressed in *Xenopus* oocytes and the resultant electrophysiological currents were initially interpreted as arising from a H^+/K^+ symport (Schachtman and Schroeder, 1994). However, a subsequent study by the same group indicated that this was a misinterpretation, and that *HKT1* probably functions as a Na^+/K^+ co-transporter. They came to this conclusion because K^+ uptake by HKT1 expressed in oocytes or yeast is greatly facilitated by low Na^+_{out} (Rubio, *et al.*, 1995). This result is unexpected, given the known toxicity of Na^+ to plants and the lack of a Na^+ gradiant for driving K^+ uptake into plants. In support of this controversial conclusion is the observation that two point mutations in *HKT1* were identified that increased Na^+ tolerance when expressed in yeast cells relative to complementation with wild-type *HKT1* (Rubio, *et al.*, 1995). Analysis of the ion content of cells showed that the *hkt1* Na^+-resistant mutants have higher K^+: Na^+ ratios than yeast cells expressing wild-type *HKT1* (Rubio, *et al.*, 1995). It will be interest to ascertain whether such mutations can be exploited to improve the salinity tolerance of crop species.

Bacterial K^+ uptake permeases named *KUPs* (Schleyer and Bakker, 1993) and fungal high-affinity K^+ transporters named *HAKs* (Banuelos, *et al.*, 1995) have been identified in plants independently by several laboratories. The plant genes were named *AtKT1* (Quintero and Blatt, 1997), *AtHAK* (Santa-Maria, *et al.*, 1997) or *AtKUP1* (Fu and Luan,

1998; Kim, *et al.*, 1998). Fu and Luan, (1998) isolated and characterized *AtKUP1*, a dual-affinity K^+ transporter from an *Arabidopsis* cDNA library, and this was reported to function in both high and low-affinity uptake. Expression of the cDNA in CY162, a K^+ uptake deficient *S. cerevisiae* mutant, showed dramatically increased K^+ uptake capacity at both low and high external K^+ concentration ranges. In addition, the AtKUP1 protein may function as a K^+ transporter in *Arabidopsis* roots over a broad ranges of $[K^+]$ soils. Perhaps, the most striking feature of AtKUP1-mediated K^+ uptake is its biphasic kinetics which are similar to those of plant roots (Epstein, 1972), but distinct from any of the other known K^+ transporters identified from higher plants.

(b). Low-affinity K^+-uptake mechanism.

The pathway for low-affinity uptake is believed to be provided by inward-rectifying K^+ channels, allowing potassium to enter along an electrochemical gradient when potassium in the soil is relatively abundant (Smart *et al.*, 1996). Rectification is a property of some ion channels whereby they are open at some membrane potentials and are closed at others, resulting in the passing of current in one direction only. The first two plant gene encoding K^+ channels were reported in 1992. The genes *AtAKT1* (Sentenac, *et al.*, 1992) and At*KAT1* (Anderson, *et al.*, 1992), were both cloned from *Arabidopsis thaliana* cDNA libraries by complementing a yeast mutant lacking endogenous potassium transporters (Cy162) and screening for growth on a low K^+ media.

Histochemical analysis of transgenic *Arabidopsis* plant containing the *AtKAT1* promoter fused to the *β-glucuronidase* reporter gene has shown that *KAT1* is primarily expressed in guard cells (Nakamura, *et al.*, 1995). As the influx of K^+ into guard cells is involved in stomatal opening, the expression pattern of *KAT1* suggests that it may represent the inward K^+ channel involved in the stomatal opening (Nakamura, *et al.*, 1995; Assmann and Haubrick, 1996). Construct of the *ATK1* promoter and the *β-glucoronidase* reporter genes show that this channel is localized to non-vascular tissue of mature roots of wheat (Lagarde, *et al.*, 1996).

In addition to *KAT1* and *AKT1*, two other plant K^+ channel genes have been cloned in *Arabidopsis*. The genes *AKT2* and *AKT3* were independently identified by screening *Arabidopsis* cDNA and genomic libraries with *AKT1* fragments and degenerate oligonucleotides from the conserved pore region and renamed *AtAK1*, *AtAK2, AtAK3* (Ketchum and Slyman, 1996).

The protein *St KST1* is a major inward rectifying K^+ channel in *Solanum tuberosum* and was identified by using *KAT1* as a probe to screen a cDNA library made from epidermal cells (Muller-Rober, *et al.*, 1995). The predicted *St KST 1* sequence has an amino acid similarity of 81 % with AtKAT1 and 67% with AtAKT1. St KST1 was found to be expressed in open flower buds, epidermal leaf cells, guard cells and floral organs Muller-Rober, *et al.*, (1995). Additionally, Southern analysis indicated that *KST1* has two copies in the potato genome (Muller-Rober, *et al.*, 1995). Patch clamp measurements have identified inward rectifying K^+ channels capable of mediating K^+ uptake in potato.

Further, *St kst1* is sensitive to low pH showing enhanced conductance, and when coupled with a H^+-ATPase, provide an ideal mechanism for the uptake of K^+ into cells (Muller-Rober, *et al.*, 1995). In line with properties ofa K^+-sensitive channel, StKST1 cation selectivity was determined as $K^+ > Rb$ and NH_4^+; Na^+ and Li^+ are not transported. With such low permeability for Na^+, low affinity K^+ uptake channels such as StKST1 may prove to be a more energy efficient mechanism for maintaining low cytosolic Na^+, than letting sodium in and then pumping it out again, and this may prove to be an important strategy for engineering sodium resistance in plants. The *StKST1* gene is specifically expressed in guard cells as shown by in *situ* hybridization, thereby, providing additional molecular evidence that the encoding channel protein is indeed that K^+_{in} channel involved in stomata opening.

Schachtman, *et al.*, (1997) identified a gene from wheat, *LCT1* that encodes a low-affinity cation transporter. The transporter activity was assayed using radioactive isotopes in yeast cells expressing the cDNA. LCT1 mediated low-affinity uptake of the cation Rb^+ and Na^+, and possibly Ca^{2+}. *LCT1* is expressed in low abundance in wheat roots and leaves (Schachtman, *et al.*, 1997). The precise functional role of this cation transporter is not known, although the inhibition of cation uptake through LCT1 by Ca^{2+} has parallels to the effect of Ca^{2+} on cation uptake (e.g., Na^+) seen in whole plants and may in part explain the role of Ca^{2+} in reducing Na^+ uptake and ameliorating Na^+ toxicity.

Gorham, *et al.*, 1986 demonstrated that under moderately saline conditions hexaploid bread wheat (AABBDD genome) accumulate less sodium and more potassium in

expanding and young leaves than does tetraploid (AABB) macaroni wheat. This K^+: Na^+ discrimination factor has been recognized in the D-genome of *Triticum* and a series of investigations has localized the trait to the 4D chromosome through the use of chromosome substitution lines in which B-genome chromosomes are replaced singly by their D-genome homeologues (Gorham, *et al.*, 1987). Examination of whether differences in the permeability of Na^+ through K^+ uptake channels can account for differences K^+ /Na^+ discrimination has been made. Patch clamp studies in wheat and other glycophytes have found little sodium permeation through voltage-gated potassium channels (Schachtman, *et al.*, 1991; Gassmann and Schroeder, 1994; Tyerman, *et al.*, 1997). Experiments using whole plants have indicated that transport of $^{22}Na^+$ to the shoot tissue is reduced in plants containing this discrimination trait (Gorham, *et al*, 1990). Rates of ions transport into root plasma membrane vesicles were measured in a tetraploid (AABB) and a hexaploid (AABBDD) wheat. Inhibition of Na^+ influx by Ca^{2+} was greater in the hexaploid, but overall it was concluded that neither of the measured transport processes was responsible for the discrimination trait on 4DL (Allen, *et al.*, 1995). The potassium homeostasis of plant cells seems to be controlled by feedback inhibition of the uptake system by intracellular potassium (Glass, 1976 & 1983). This could be caused by the high co-operative binding of K^+ to an intracellular allosteric site of the channel which when occupied, blocks transport (Glass, 1976). It was reported that the roots of a moderatley-tolerant tomato species (*Lycopersicon cheesmanii*) and moderately -tolerant corn (*Zea mexicana*) species, exhibited a higher rate of potassium uptake than the roots of a salt-sensitive domestic tomato (*L. esculentum*) and a salt-

sensitive corn (*Zea.mays*) varieties (Hajibagheri, *et al.*, 1989). Also, salt-adapted tobacco cells have enhanced K^+ uptake capacity (Watad, *et al.*, 1991).

Assman and Haubrick (1996), summarized the data obtained by promoter-reporter gene studies, in *situ* hybridization and RNA blot analysis regarding the expression patterns of plant K^+ in channel genes. Currently, as more data about the expression patterns of ion channels accumulate it becomes more and more evident that, homologous genes of different species are found in the same tissues (Czempinski, *et al.*, 1999).

At KAT1 expression has been shown by promoter-*GUS* (*β-glucuronidase*) fusion experiments to occur in the guard cells of *A. thaliana* (Nakamura, *et al.*, 1995). Transcription of a second member of *At KAT* family (*At KAT2*) has been detected in RNA isolated from *A. thaliana* leaves (Butt, *et al.*, 1997). The *AtAKT1* gene appears to be preferentially expressed in *A.thaliana* roots, as shown by promoter *GUS* studies as well as by RNA blot analysis (Lagarde, *et al.*, 1996). The presence of AtAKT1 homologous protein was demonstrated in plasma membrane-enrich fractions of *Brassica napus* roots (Lagarde, *et al.*, 1996).

A similar transcript from potato, *St SKT1*, has been detected in RNA isolated from roots (Zimmermann, *et al.*, 1998). In addition, a highly homologous cDNA, *St SKT1* was cloned from a tomato root hair cDNA library (Hartje, *et al.* 2000). The *Arabidopsis At AKT2* gene is expressed in leaves but not in roots as demonstrated by RNA bolt analysis (Cao, *et al.*, 1995), whereas expression of the potato *SSKT2* gene has been found throughout the plant (Zimmermann, *et al.*, 1998). The expression of StSKT2 can be ascribed to the vascular tissue, presumably to xylem parenchyma cells as shown by

promoter-*GUS* studies. RT-PCR analyses provide that StSKT3 is weakly expressed in potato leaves, roots and tubers (Zimmermann, *et al.*, 1998).

Transcripts of AtKCO1 have been found by RT-PCR in all *Arabidopsis* tissues investigated, including flowers, leaves, roots, and stem (Czempinski, *et al.*, 1997a). The expression pattern and localization of a putative regulatory β−subunit (*KAB1*) of *Arabidopsis thaliana* K^+ channels was investigated by Tang, *et al.*, (1998). Using immunogold labelling, *KAB1* protein was detected in the plasma membrane as well as in various intracellular membranes in both leaves and roots and indicated that *KAB1* (or a homologous protein) forms complexes with K_{in}^+ channels in different parts of the plant.

The molecular identification and functional analysis of a new *shaker*-like K^+ channel (*SKOR*) in *Arabidopsis* was cloned by Gaymard, *et al.*, (1998). *AtSKOR* which is expressed in root stellar tissues, was shown to be the first member of the *shaker* family in plants having outwardly rectifying properties (Czempinski, *et al.*, 1999).

1.8.1.2. Better Discrimination Against Na^+ Uptake.

Although Na^+ is a major cation present in soil solutions, Na^+ is not considered an essential mineral. In saline soils, high concentrations of Na^+ disrupt K^+ and other mineral nutrition, create hyperosmotic stress, and cause secondary problems such as oxidative stress (Zhu, 2001). Many cytosolic enzymes are activated by K^+ and inhibited by Na^+ (Flowers, *et al.*, 1977; Jones and Pollard, 1983). Little is known about Na^+ uptake but it

is generally believed that Na^+ presumably enters the cell through K^+ uptake channels which are located on root cell plasma membranes (Rubio *et al.*, 1995; Schachtman, *et al.*, 1997). This suggestion is supported by studies on *HKT1* and *LCT* function in yeast or oocytes (see Section 1.8.1.1b). Differences in the permeability of Na^+ through K^+ uptake channels can account for differences in K^+/Na^+ discrimination. However, patch clamp studies in wheat and other glycophytes have found little sodium permeation through voltage-gated potassium channels (Schachtman, *et al.*, 1991; Gassmann and Schroeder, 1994; Tyerman, *et al.*, 1997).

Outward-rectifying ion channels could play a role in mediating the influx of Na^+ into the cells. These channels, which open during the depolarization of the plasma membrane (*i.e.*, shift of the electrical potential difference to more positive values), could mediate the efflux of K^+ and/or the influx of Na^+. One of these channels, known as *NORC* (non-selective outward-rectifying conductance) does not discriminate between cations and is activated by increased cytosolic Ca^{2+} concentrations (Wenger and DeBoer, 1997).

Voltage independent channels (VIC), have a relatively low K^+ to Na^+ selectivity because they are non-selective against monovalent cations, and in some cases divalent cations (Amtmann and Sanders, 1999). In contrast to the voltage-dependent (inward-rectifying and outward-rectifying) channels, VICs are not gated by voltage. In conditions with high external Na^+/K^+ ratios such as a typical saline environment, VICs, if open, would allow massive influx of Na^+ into the cell over a wide range of voltages (Amtmann and Sanders, 1999). The stealth of sodium entry is due to the similarity between the hydrated ionic

radii of sodium and potassium, which makes the discrimination between the two ions by transport proteins difficult. This discrimination problem is the basis for Na^+ toxicity and perturbations in the cellular K^+/Na^+ ratio (Blumwald, *et al.*, 2000). By using site-directed mutagenesis, Uozumi, *et al.*, (1995); Becker, *et al.*, (1996) and Dryer, *et al.*, (1998) reported that most different classes of K^+ channels have specific regions strongly involved in determining cation selectivity which could lead to improved selectivity against Na^+ uptake, and may ameliorate Na^+ toxicity.

Recently, studies in yeast have demonstrated that the magnitude of the cell membrane potential affects net Na^+ influx into cells. Mutations in the yeast PMP3 protein (a H^+ pump) lead to membrane hyperpolarization, increased Na^+ influx, and salt sensitivity, (Navarre and Goffeau 2000).

1.8.1.3. Sodium Compartmentation.

In plants, sodium compartmentation in vacuoles is a key processes for Na^+ detoxification and cellular osmotic adjustment, it has been proposed that this is achieved by the function of Na^+/H^+ antiporters or Na^+-ATPases (Niu, *et al.*, 1995; Serrano and Gaxiola, 1994; Serrano and Rodriguez-Navarro, 2001). The existence of plant Na^+/H^+ antiporters was first inferred from biochemical studies of antiporter activity in vacuoles or tonoplast vesicles in many plant species (Blumwald and Pool, 1985, Hassidim *et al.*, 1990). Transport mechanisms can actively move ions across the tonoplast into the vacuole, removing the potentially harmful accumulation of excessive levels of ions in the cytosol.

These ions, in turn, act as an osmoticum within the vacuole, which then induces water flow into the cell (Glenn *et al.*, 1999). The presence of large, acidic-inside, tonoplast-bound vacuoles in plant cells allows the efficient compartmentation of sodium from the cytoplasm. Recently it has been demonstrated that plants achieve this by activating tonoplast H^+ pumps (V-type ATPases and pyrophosphatases, and using the electrochemical gradient established to drive a Na^+/H^+ antiporters into the vacuole, through the operation of vacuolar Na^+/H^+ antiporters (Gaxiola, *et al.*, 1999; Apse *et al.*, 1999; Zhang and Blumwald 2001).

1.8.1.4. Active Na^+ Efflux from Cells (sodium exclusion).

There is a view that in halophytes Na^+ sequestration in the vacuole is the only mechanism for removing Na^+ from the cytoplasm, and that extrusion from the cell across the plasma membrane is not important (Blumwald et al., 2000; Yeo, 1998). However, Na^+ efflux from cells is considered to be important in mesophytes and glycophytes (Greenway and Munns, 1980). For a number of reasons, arguments against plasma membrane Na^+ efflux do not make sense. First, Na^+ sequestration in the vacuole is required only to regain cell turgor for growth and structural support; once this has been achieved, further increases in the solute potential of the vacuole would result in the establishments of high, potentially decrease turgor pressures and electrolyte levels within the cells. Second, there is no experimental evidence that halophytes develop excessively high turgor pressure when compared with halophytes growing in low salinity (Dr P. Dominy, University of Glasgow, unpublished). Finally, it has been shown that after turgor has been regained, a

range of halophytes (*e.g., sugar beet* and *Casswarina eguisitifola*) do indeed exclude Na^+ at the root soil boundary (P. Dominy, unpublished). Therefore, active extrusion of sodium could occur either by a primary active Na^+-pumping ATPase or by a secondary active Na^+/H^+ antiport mechanism coupled to an electrochemical (H^+) gradient (Serrano and Gaxiola, 1994; Serrano and Rodriguez-Navarro, 2001). Transport studies have provided evidence for Na^+/H^+ antiporters in the plasma membrane of several plants including barley, tobacco, red beet, tomato, and wheat (Blumwald *et al.*, 2000). However, plant plasma membrane Na^+/H^+ antiporter have not been identified at the molecular level. In plants, Na^+/H^+ exchanger activity is believed to be driven by the H^+ electrochemical gradient generated by the H^+ pumps such as the plasma membrane H^+-ATPase (Blumwald *et al.*, 2000). Loss of function of a putative plasma membrane Na^+/H^+ antiporter gene (*SOS1*) decreases salt tolerance in *Arabidopsis* (Shi *et al.*, 2000) and the localization of SOS1 at the plasma membrane has been demonstrated recently (Shi *et al.*, 2002). An alternative mechanisms for sodium extrusion is through a Na^+-ATPase, and although such a mechanism works, very effectively in *S cerevisiae* it has not been detected in higher plants. Therefore, in higher plants, the main mechanism for Na^+ extrusion is believed to be via a Na^+/H^+ antiporter powered by the operation of the plasma membrane H^+-ATPase (Blumwald *et al.*, 2000).

1.8.1.4.1. P-type Ion Pumps In Plants.

The plasma membrane of the plant cell is a selectively permeable barrier that ensures the entry of essential ions and metabolites into the cell. The plasma membrane has proteins

required to transport protons, inorganic ions, and organic solutes across the plasma membrane and tonoplast at rates sufficient to meet the need of the cell. The membrane contains different types of transport proteins: (1), ATP-powered pumps: (2), channel proteins: and (3), co-transporters (Sze, *al et.*,1999; Chrispeels, *et al.*,1999).

The P-type super family of ion pumps includes primary transporters energized by hydrolysis of ATP with a wide range of specificity for small cations and perhaps also phospholipids (Palmgren and Harper, 1999). P-type ATPases are characterized by forming a phosphorylated intermediate in the reaction cycle (hence the name P-type), by being inhibited by vanadate, and by having a number of sequence motifs in common (Serrano, 1989; Axelsen and Palmgren, 1998). Plant P-type ATPases are characterized structurally by having a single subunit, 8 to 12 transmembrane (TM) segments, N and C termini exposed to the cytoplasm, and a large central cytoplasmic domain which includes the phosphorylation and ATP binding sites.

In *Arabidopsis*, the P-type ATPase family can be divided into several major evolutionarily related subfamilies. P_{1B}, P_{2A}, P_{2B}, P_{3A}, P_4, P_5, according to the ions they transport. The P_{1B} ATPase family pump heavy metals. The P_{2A} and P_{2B} ATPases family are Ca^{2+} pumps (14 members in *Arabidopsis*). The, P_{3A} ATPases are the plasma membrane H^+ pump (12 members in *Arabidopsis*). The P_4 ATPases family is involved in the transport of relatively large amphipathic compounds (e.g., bile acids). Finally, the P_5 group, which has only a single member in *Arabidopsis*, has not been characterized at the biochemical level, and is only found in eukaryotes (Axelsen and Palmgren, 1998).

The P-type ATPaes are involved in a wide range of fundamental cellular processes including the following: making and maintaining the electrochemical gradient used as the driving force for secondary transports (H^+ ATPases in plant and fungi and Na^+/K^+-ATPases in animals): cellular signaling (Ca^{2+}-ATPase): and transport of essential micronutrients (Zn^{2+}-ATPase and Cu^{2+}-ATPases): extrusion of toxic ions if they accumulate in amounts that are too high (Gomes *et al.*, 2000).

1.8.1.4.2 Plasma Membrane H^+-ATPases.

Proton ATPases are mainly found in plants and fungi and provide the major electrochemical driving force for solute transport. They are abundant proteins relative to other transporters as their turnover number is low (10^1-10^3 s^{-1}) compared with other secondary transporters (10^3-10^8 s^{-1}). In fact proton pumps can represent as much as 1 to 5% of the membrane protein. The basic function of these H^+ pumps is to energize the membrane to regulate intracellular and extracellular pH, drive active nutrient uptake (chemical balance), and modulate cell turgor (Serrano, 1989, DeWitt, 1994).

The p-type H^+-ATPases depend on metabolic energy obtained directly from the hydrolysis of ATP to translocate H^+ to the cell exterior, generating an electrochemical H^+ gradient. This protonmotive force generated by the H^+-ATPase allows the operation of other secondary transport systems associated with the plasma membrane, which can act as H^+/solute symports, H^+/solute antiports or charge-driven uniports (Leonard, 1984; Sze, 1985; Fommer and Ninnemann, 1995). Thus, Na^+/H^+ antiporters couple the

energetically downhill movement of H^+ into the cell along its electrochemical gradient ($\Delta\mu_H$), to the energetically 'uphill' movement of Na^- ions out of the cytoplasm against their electrochemical gradient.

The *in vivo* activity of the P-type H^+-ATPase, as assessed by proton efflux measurement, seems to increase during osmotic adaptation in carrot (Reuveni, *et al.*, 1987) and tobacco cell cultures (Watad, *et al.*, 1986). It has been demonstrated that in the halophytic plant *Atriplex nummularia*, when exposed to high salinity during growth the *in vivo* activity of the plasma membrane P-type H^+-ATPase increases. Apparently, this phenomenon does not occur in non-halophytic plants (Braun, *et al.*, 1986).

Several plant genes have now been cloned that code for proteins with structural characteristic of p-type cation-translocating ATPase. It has been recognized that there was not just one gene and corresponding polypeptide, but rather a multigene family (Assmann and Haubrick, 1996).

Using information from protein sequences, as well as knowledge of a highly conserved acid sequence found in all P-type H^+-ATPase, an oligonucleotide was synthesized and used to isolate clones encoding H^+-ATPase from an oat cDNA library (Harper, *et al.*, 1989). The oat clone was then used to screen *A thaliana* cDNA and genomic libraries from which different gene clones were isolated, *AHA1*, *AHA2*, and *AHA*3 for *Arabidopsis* H^+-ATPase (Harper, *et al.*, 1989). It is presumed that different family members will have different promoter sequences, allowing expression in a cell-specific, tissue-specific or

developmental stage-specific manner (Sussman, 1991). The location of the *aha3* gene product was studied in *Arabidopsis* by expression of a construct of the *aha3* promoter sequence 5' of the *β-glucuronidase* (*GUS*) reporter gene. In this case expression of *GUS* was found to be located on the plasma membrane of companion cells of vegetative tissue (DeWitt, *et al.*, 1991; DeWitt and Sussman, 1995). Histochemical localization of *GUS* activity under the light microscope demonstrated that *AHA2* is expressed in root hairs and surface tissues of the root (Sussman, 1994). Furthermore, AHA9 appears to be restricted to stamens (Michelet, *et al.*, 1994), and AHA10 to integument layers of developing seed (Harper, *et al.*, 1994). In conclusion, it is believed that several H^+-ATPases generate the proton-motive force used by sucrose carriers in the phloem. However, AHA2 encodes the one that drives mineral absorption from the soil into roots, and *AHA10* is involved in the flow of nutrients that nourish the embryo (Sussman, 1994).

Ewing, *et al.*, (1990) identified and characterized the first two cDNA clones (*LHA1* and *LHA2*) from tomato (*Lycopersion esculentum*) which probably encodes isoforms of plasma membrane H^+-ATPase. In 1994 Ewing and Bennett identified the seven genomic sequences (designated *LHA1-LHA7*) that encoding isoforms of tomato (*Lycopersion esculentum*) plasma membrane H^+-ATPase by screening a genomic library with the highly conserved ATP-binding domain of the cDNA *LHA1*. Three of these genes are expressed differentially in tomato. However, *LHA1* is expressed at a similar level in all tissues examined, *LHA2* is most highly expressed in mature leaves and *Lha4* is most highly expressed in roots and hypocotyls of tomato. In addition, the isoforms *LHA3,*

LHA5, LHA6, LHA7 are expressed at very low or undetected levels in all organs examined (Ewing and Bennett 1994).

Boutry, *et al.*, (1989) reported the isolation and preliminary characterization of three different clones from a root cDNA library of *Nicotiana plumbaginifolia* encoding genes with similarity to the *S. cerevisiae* H^+-ATPase genes (*PMA*). The largest one (PMA2) exhibits a homology of 73% at the amino acid level with a limited protein sequence obtained from purified oat plasma membrane H^+-ATPase (Schaller and Sussman, 1988), and an 82% similarity with the *Arabidopsis thaliana AHA* genes (Harper *et al.*, 1989). It is therefore, concluded that the *N. plumbaginifolia PMA2* gene encodes a plasma membrane H^+-ATPase (Boutry *et al.*, 1989). Three members of *PMA* gene family of p-type H^+-ATPase have now been isolated from genomic and cDNA libraries of *N. plumbaginifolia* (Perez *et al.*, 1992). The three genes are between 65% and 96% identical at the deduced amino acid sequences level. Due to their high similarity, it is most likely that these genes encode H^+-translocating ATPase with similar function. The three genes are expressed in leaf, stem, flower and root tissues, albeit at different levels, according to the organ and gene (Perez *et al.*, 1992). A fourth gene *PMA4* has now been identified with an even higher amino acid sequence identity (95%-97%) to the *Arabidopsis PMA1-3* genes (Moriau *et al.*, 1993), and it was suggested that there may be *PMA* sub-families. Measured *PMA4* transcript levels indicated that this gene is expressed at similar levels in root, stem, leaf, and flower tissues (Moriau, *et al.*, 1993), contrary to the *PMA1-3* subfamily which displays an organ-specific expression pattern (Perez *et al.*, 1992).

In *Arabidopsis thaliana*, at least 12 genes are predicted to encode plasma membrane H^+-ATPases (P-type ATPase Database at http:// biobase.dk/axe/patbase.html). To date, a unique function has not been ascribed to any of the multiple isoforms in *Arabidopsis*. However, it is clear that many of the isoforms have tissue-specific patterns of expression, and differences in their auto-inhibitory domain, which may result in different regulatory properties (Lou, *et a*l., 1999). In tobacco, the co-suppression of at least one H^+ATPase resulting from the attempted over-expression of isoform *PMA4* resulted in pleiotropic effects on sucrose translocation, stomatal opening, growth, and fertility (Zhao, *et al.*, 2000).

Vitart *et al.*, (2001) reported a mutant (*aha4-1*) resulting from a T-DNA insertion in the *Arabidopsis* proton pump isoform *AHA4-1* which interfered with solute transport through the root endodermis. The *aha4-1* mutation results in plants with greatly increased sensitivity to salt stress, as the mutant plant accumulates higher levels of Na^+ and lower levels of K^+ in leaves, which disrupts Na^+/K^+ homeostasis. In plants, salt resistance is thought to depend on an increase in proton pump activity. For example, the exposure of plants to high external NaCl results in hyper-osmotic stress, ionic imbalance and Na^+/Cl^- toxicity (Serrano, 1996). To alleviate Na^+/Cl^- toxicity and re-establish cellular ion homeostasis, transport processes across the plasma membrane involving proton pumps are necessary (eg., Na^+-antiporters) (Niu *et al.*, 1995; Zhu, 2001; Shi *et al.*, 2002).

1.8.1.4.2.1. . Plasma Membrane Ca^{2+}-ATPase.

For decades, it has been known that Ca^{2+} is required to maintain or enhance the selective absorption of K^+ by plants at high concentrations of NaCl (Epstein, 1966; Epstein, 1973). It is assumed that externally supplied Ca^{2+} alleviates Na^+ toxicity by facilitating higher K^+/Na^+ selectivity although it is not known whether this occurs through the direct effect of Ca^{2+} on transporters, or indirectly through Ca^{2+} signaling (Liu and Zhu, 1997a; Zhu, 2000 and 2001). High salinity also increased cytosolic Ca^{2+} that is transported from the apoplast and intracellular compartments (Knight *et al.*, 1997). The resultant transient Ca^{2+} increase potentiates stress signal transduction and may lead to salt adaptation

The vacuole serves as a primary pool of free calcium ions in plant cells and the vacuole is therefore a major source of Ca^{2+} for intracellular calcium signaling. The Ca^{2+}ATPase and Ca^{2+}/H^+ antiporter perform active Ca^{2+} transport into the vacuole . High Ca^{2+}-ATPase activity has been reported for tonoplast vesicles purified from several plant species (Sze *et al.*, 2000). Plant Ca^{2+}-ATPases have been divided into two groups: type IIA and IIB Ca^{2+}-ATPases They have structures similar to mammalian sarco-and endoplasmic reticulum (SERCA pumps). Type IIB Ca^{2+}-ATPases have a structural similarity to the mammalian calmodulin-stmulated Ca^{2+} ATPases (PMCA) in the plasma membrane (Sze, *et al.*, 1999). Type IIA Ca^{2+}-ATPase from tomato (LCA) and type IIB Ca^{2+}-ATPase from Brassica (BCAI) have been shown to be localized in the tonoplast. In *Arabidopsis thaliana*, cDNAs for four isoforms of the type IIA Ca^{2+}-ATPase (*AtECA*) and six isoforms of type IIBCa^{2+}-ATPase (*AtACA*) have been cloned (Sze *et al.*, 2000),These 10

genes form three clusters in the *Arabidopsis* P-type ATPase family (Axelsen *et al.*, 2001). The overall protein sequence identity is rather high ranging from 45% to 92% between the different members; but even so, the genomic organization of the different genes differs fundamentally. Four of the 10 proteins *Arabidopsis* members (*ACA1*, *ACA2*, *ACA4* and *ACA8*) have been cloned and characterized in some detail (Harper *et al.*, 1998; Bonza *et al.*, 2000; Geisler *et al.*, 2000b). Each protein seems to be present in a specific membrane such as the plasma membrane (ACA8) or the membrane of small vacuoles (ACA4, Geisler *et al.*, 2000). An N-terminal calmodulin-binding domain was first identified in the cauliflower P_{2B} ATPase BCA1 (Malmstron, *et al.*, 1997). There is experimental evidence for the presence of calmodulin binding sequences in the N-terminal domain of *ACA2* (Harper, *et al.*, 1998), ACA4 (Geisler, *et al.*, 2000b), and ACA8 (Bonza *et al.*, 2000). In these pumps, the N-terminus is likely to form an autoinhibitory regulatory domain (Geisler *et al.*, 2000b).

Most living cells grown in high external salinity exclude Na^+, and create a Na^+-concentration gradient across their cell membrane. In animal cells, this gradient is generated by the (Na^+, K^+)-ATPase (Skou, 1988) which plays a role in most active transport mechanisms that are Na^+ coupled. In contrast, in eukaryoyic cells with walls, the membrane potential is generated by a H^+-pumping ATPase (Serrano, 1985). Consequently, sodium-pumping ATPase are not widespread in non-animal cells, where sodium extrusion is probably mediated by Na^+/H^+ antiport mechanism (Serrano, 1985 & 1991; Padan, 1992). In plant cells both Na^+/H^+ antiport mechanism (Colombo, *et al.*, 1979; Hassidim, *et al.*, 1990) and a primary sodium pump coupled to ATP hydrolysis

(Cheeseman, 1982) have been proposed. Evidence for a primary sodium pump coupled to an ATP hydrolysis system, however, is very indirect and no information exists on either the protein or the gene involved in a primary sodium pump coupled to an ATP hydrolysis (Wilson and Shannon, 1995).

In 1954, Conway and co-workers demonstrated that yeast cells actively and specifically exclude Na^+, by a system independent of that mediating K^+ uptake. Since then, many reports on the biochemical characteristics of this transport system failed to establish unambiguously the mechanisms involved (Eddy, 1981). Although, precise details of the mechanisms for K^+ and Na^+ transport in Na^+ resistant plant cells are not available, a model has been established in yeast. Genes encoding the K^+ and Na^+ transport systems have been cloned (Gaber *et al.*, 1988; Haro *et al.*, 1991; Ko and Gaber 1991; Garicadeblas, *et al.*, 1993). Haro, *et al.*, (1991) demonstrated that Na^+ tolerance in yeast showed a large dependence on *ENA1*, a gene encoding a putative Na^+-ATPase, (but originally chracterized as a Ca^{2+}ATPase), and on *TRK1*, a gene required for the expression of high-affinity K^+ uptake (Gaber, *et al.*, 1988). Transformation of the acutely Na^+-sensitive *S.cerevisiae Δtrk1Δ ena1* double mutant with the *trk1* and *ena1* genes, restores both discrimination between K^+ and Na^+, and Na^+ efflux capacity indicating that these two transporters play a crucial role in Na^+ resistance (Haro *et al.*, 1993).

The question now arises, do homologous genes result in a similar response in salt-resistant plants? It seems evident that although many mechanisms (including some not considered here) can protect plants from Na^+ stress, the exclusion of Na^+ from the root,

either by decreasing influx or increasing efflux, would be a very effective mechanism of protection (Gorham, 1992a). The Na^+-tolerance of a *Nicotiana* cell culture line was attributed to an enhanced capacity to take up K^+ (Watad, *et al.*, 1991). Clearly, identification of the gene and their corresponding protein that code for K^+ and Na^+ transport could be useful to protein engineering programmes attempting to reduce the salt sensitivity of some plant species.

The *ENE1* (*PMR2*) gene which plays a central role in Na^+ and Li^+ tolerance in *S. cerevisiae* (Garicadeblas *et al.*, 1993) was cloned by its ability to complement a low Li^+ efflux yeast strain for growth in high Li^+ (Haro *et al.*, 1991). A second Na^+-ATPase gene, *ENE2* has now been isolated from *S.cerevisiae* (Garicadeblas *et al.*, 1993). The putative protein encoding by ENE2 differs only in thirteen amino acids from the protein encoded by ENE1 (Garicadeblas *et al.*, 1993). However, *ENE1* and *ENE2* are the first two genes of a tandem array of four highly homologous genes (*ENE1-ENE4*) which probably have similar function (Garicadeblas, *et al.*, 1993). Consequently, the major pathway for Na^+ efflux in *S.cerevisiae* appears to be mediated by ENA1, and it has been estimated that the combination of *ENA2*, *ENA3* and *ENA4* accounts for about half of the Na^+ efflux activity of WT *S.cerevisiae* (Garicadeblas, *et al.*, 1993). Homologues of *ENE1* may occur in plants as suggested by Cheeseman (1982).

The fission yeast, *Schizosaccharomyces pombe*, is also very tolerant of high levels of Na^+ in the growth medium, but Na^+ exclusion is achieved by a very effective Na^+/H^+ antiporter, *SOD2* (Jia *et al.*, 1992). Banuelos *et al.*, (1995a) demonstrated the functional

expression of *ENE1* of *S.cerevisiae* in *S.pombe* by transforming the *ENE1* gene into a Na^+ sensitive, Δ *sod2* deletion mutant of *S. pombe*. The ENA1 protein was expressed and surviving colonies recovered on high Na^+ media, demonstrating that Na^+-ATPase (*ENA1*) and Na^+/H^+ antiporters (*SOD2*) provide an equally efficient mechanism for Na^+ efflux. In addition, over-expression of *ena1* in *S. cerevisiae* was achieved with a construction of the *ENA1* promoter driving the *ENE1* structural gene (Benito, 1997).

1.8.1.4.2.2. ABC Pumps.

ATP-binding cassette (ABC) transporters are primary pumps, which use the energy of ATP hydrolysis to drive transport, but some may also modulate the activity of ion channels (Higgins, 1995; Theodoulou, 2000). ABC transporters are implicated in the excretion or sequestration of secondary metabolites and xenobiotics (extracellular or intracellular into the vacuoles). Like other tonoplast transport proteins, ABC transporters are found throughout the endomembrane system as well as in the plasma membrane (Sidler *et al.*, 1998). Many ABC transporters are relatively specific, but others are able to handle several chemically dissimilar compounds. Substrates assigned to members of this family of transporters include compounds as varied as lipids, inorganic acids, and heavy metal chelates, polysaccharides, bile acids, glutathion conjugates (Rea *et al.*, 1998).

Osmotic and/or ionic stress induces oxidative stress (Moran *et al.*, 1994; Roxas *et al.*, 1997). Most of the meager transgenic improvements in plant salt tolerance reported to date have been achieved through elevating pathways for detoxificating reactive oxygen

species (ROS). Examples including transgenic plants that overexpress glutathione peroxidase, superoxide dismutase and glutathione reductases (Roxas *et al.*, 1997; Allen *et al.*, 1997). Transport of oxidised glutathione (CSSC- a special form of glutathione conjugate) by GS-X pumps may thus function in defense against oxidative stress (Theodoulou, 2000).

Typically, an ABC transporter contains two copies of two structural units: a highly hydrophobic transmembrane domain (TMD), and a peripherally-located ATP binding domain (or nucleotide binding fold, NBF), which together are often sufficient to mediate transport. They may be expressed as separate polypeptides, or as multi-domain proteins (Cole, *et al.*, 1992). In the majority of characterized eukaryotic ABC transporters, the core domains are contiguous on a single multi-domain polypeptide (full molecule) in a forward MD1-NBF1-TMD2-NBF2 or reverse NBF1-TMD1-NBF2-TMD2 configuration. In a few cases one TMD is fused with an NBF to form a half-molecule (Cole, *et al.*, 1992; Higgins, 1992).

The first ABC transporter isolated from plants was an multi-drug resistance (MDR)-like gene from *Arabidopsis thaliana AtPGP1* (Dudler and Hertig, 1992). Further experiments showed that (*At* PGP1 alias *At*MDR1) is localized in the plasma membrane and involved in hypocotyl elongation in light-grown seedlings (Sidler, *et al.*, 1998). Its mode of action, and those of homologues from other plant sources, remain obscure. The second observation indicating that ABC transporters occurred in plants was that glutathione conjugate (GS-X) transport into vacuoles depended directly on Mg-ATP hydrolysis and was independent of the electrochemical potential created by the vacuolar proton pumps

(Martinoia *et al.*, 1993). Many biotic and abiotic compounds are susceptible to conjugation with glutathione, since the chemical determinants of GST substrates are common (Talalay *et al.*, 1998). Recent results indicate that, as in animals, ion fluxes may be mediated or controlled by ABC transporters. Leonhardt, *et al.*, (1997; 1999) showed that stomata opening in *Comelina* guard cells can be induced by treatment with the sulfonylurea glibenclamide and other drugs affecting ion conductance controlled by the sulfonylurea receptor (SUR) and the cystic fibrosis transmembrane regulator (CFTR)in mammalian systems.

In *S. cerevisiae* ABC-type extrusion is one of the three mechanisms of Na^+ efflux across the plasma membrane (P-type ATPases and Na^+/H^+ antiporters being the others). For example the extrusion of Na^+ and Li^+ in *S. cerevisiae* is mediated by the multi-drug resistance (ABC)-ATPase encoded by the *SNQ2* gene (Miyahara, *et al.*, 1996).

The multi-drug resistance associated proteins (MRPs) family are the second most highly represented subfamily of *Arabidopsis* full-molecule ABC transporters. Like the MDRs, the MRPs are forward orientation, full molecules. Unlike the MDRs, however, the MRPs are frequently larger, consisting of at least 1,500 amino acid residues, and usually contain three additional subfamily-specific structures. These additional structures are a 200 amino acid residue hydrophobic N-terminal extention, a transmembrane domain (TMD0) containing five putative transmembrane spans, a linker (L) domain contiguous with nucleotide binding fold (NBF1), which is rich in charged amino acid residues, and a hydrophilic C-terminal extension. The prototypical MRPs, the human MRP1 and the

canalicular organic anions transporter cMOAT (alias MRP2), are glutathione S-conjugate (GS-X) pumps competent in the transport of a broad range of compounds after their conjugation with the ubiquitous thiol tripeptide glutathione (Rea, 1999).

To date, five unique MRP homologs, *At* MRPs 1-5, have been cloned from *Arabidopsis thaliana* (Rea , 1999). AtMRP1, AtMRP2, and AtMRP3 encode functional GS-X pumps with differing substrate selectivities and transport capacities (Liu *et al.*, 2001). The functional characteristics of AtMRP4 and AtMRP5 have yet to be defined. As exemplified by MRP1 and MRP2, and more recently by human MRPs 3-5 and their orthologs from *Arabidopsis*, the ascription of (GS-X) pump is not entirely accurate because these pumps can transport compounds other than GS conjugates (Liu *et al.*, 2001). As it was shown that at least At MRP2 accepts glucuronides as an additional substrate class.

In animals, the transport of natural substrates by multi-drug resistance-associated proteins (MRPs) such as GS-X, bile acids, or glucuronides has been established. In contrast, only a few plant-borne substrates for MRPs have been identified in plants, such as chlorophyll catabolites or glucuronides (Klein *et al.*, 2000; Liu *et al.*, 2001).

The PDRs represent the third subfamily of full-length ABC transporter in *Arabidopsis* and 13 ORF have been identified. Yeast PDR5, a reverse orientation 1511-amino acid protein (Balzi *et al.*, 1994), is the prototype of this subfamily. Considered to be a functional equivalent of the mammalian MDRs, proteins (albeit one having a reverse

orientation and low overall sequence identity), the yeast PDR5 is a plasma membrane protein able to export all of the anti-cancer drugs tested (Kolaczkowski *et al.*, 1996). Genes encoding *bona fide* PDR homologues have not been identified in the human genome, despite their being the most common ABC protein family in yeast (9 out of 29 ORFs), and the fifth most common subfamily in *Arabidopsis*.

There are two reports of PDR5-like genes from plants, the sulphonylurea receptor (TUR2) from the aquaphyte *Spirodela polyrrhiza* (Smart and Fleming,1996), and NPABC1 from *Nicotiana plumbaginifolia* (Jasinski *et al.*, 2001). Initially cloned on the basis of its transcriptional activation by the stress hormone abscisic acid, which in *Spirodela* fronds induces transcription. Transcription of TUR2 was enhanced by a broad range of stress factors, including cold and salinity. By analogy with its yeast homology, TUR2 is suspected to mediate the mobilization and excretion of toxic metabolites whose production or release is elicited by stress factors. The nearest equivalent to TUR2 in *Arabidopsis* is AtPDR12 (67% identity and 82% similarity), closely followed by *At* PDR6, *At* PDR8, and *At* PDR13 (with identities of 60, 59, and 59%, respectively). The tobacco PDR5 homolog NPABC1 appears to encode a 160-KD plasma membrane polypeptide whose levels are enhanced by the treatment of *N. plumbaginifolia* cell cultures with sclareolide, a close analog of the antifungal diterpene, produced by this plant species (Jasinski *et al.*, 2001).

There are many un-answered questions regard to ABC-transporters like, how many kinds of ABC-transporters are present on the tonoplast, what substrates they transport, and how

their activity is regulated (Bethke and Jones, 2000). Clearly, over the next few years many of these questions will be addressed and our understanding of this new class of important ATPases will increase.

1.8.1.4.2.3. Vacuolar ATPase.

Ion transport across the tonoplast of plant cells plays an important role in control of cell homeostasis, cytoplasmic pH regulation, sequestration of toxic compounds and xenobiotics. It also has a role in regulation of cell turgor, the storage of amino acids, sugars, and finally possibly as calcium store for signaling (Barkla *et al.*, 1995). Plant vacuoles are unique among eukaryotic organelles in having two proton pumps, the vacuolar H^+-ATPase (V-ATPase) and H^+-pyrophosphatase (V-PPase) (O'Neil and Spanswick, 1984). These two mechanisms employ high energy metabolites to pump protons into the vacuole and establish a proton electrochemical potential that provide the driving force for secondary transport of numerous ions and metabolites (Barkla *et al.*, 1995; Barkla and Pantoja, 1996).

The V-type H^+-ATPases are associated with a variety of the endomembrane systems, including the endoplasmic reticulum (ER) and golgi apparatus, lysosomes, storage vesicles, coated vesicles, pro-vacuoles, vacuoles (Sze *et al.*, 1992), and even the plasma membrane (Robinson *et al.*, 1996; Sze *et al.*, 1999). Thus, the term V-type ATPase refers to all H^+-pumps that share common biochemical and molecular features, regardless of their actual membrane localization (Smart and Fleming, 1993). The V-type ATPases are

multimeric enzymes localized in endomembranes of eukaryotic cells. The ubiquitous distribution of V-type ATPases pumps in eukaryotes indicates their importance in energizing ion and metabolite fluxes. In yeast, the trafficking of membrane proteins and soluble vacuolar proteins involves V-type ATPases (Moreno and Klionsky, 1994), and in tobacco cells, concanamycin A causes missorting of soluble vacuolar proteins, thereby reflecting the need for an active Golgi complex V-type ATPase in protein sorting (Matsuoka *et al.*, 1997). V-type ATPases might also be involved in membrane fusion (Ungermann *et al.*, 1998 a and b). Sze *et al.*, (1999), suggest that V-type ATPases might energize solute uptake into intracellular vesicles so as to generate a high solute potential and the high membrane tension needed for intermembrane fusion. The processes of membrane trafficking, fusion, protein sorting, and secretion are integral to the biogenesis of vacuoles, cell plate formation during cell division, and secretion of materials (including cell wall components) at the plasma membrane of plant cells (Battey *et al.*, 1999; Marty 1999; and Sanderfoot and Raikhel, 1999). Thus, acidification of many intracellular compartments by V-ATPases could be directly involved in the dynamic processes of an active endomembrane system.

In plant cells that accumulate NaCl, the driving force for secondary active Na^+ transport into the vacuole is believed to be provided by the PMF (proton motive force) generated across the tonoplast by V-type H^+-ATPase and the V-Ppase. Both H^+ pumps may therefore play a fundamental role in energizing Na^+/H^+ antiport activity in cells accumulating significant quantities of NaCl (Barkla and Pantoja, 1996). Several groups have suggested mechanisms for the regulation of V-type H^+-ATPase and V-PPase.

Matsumoto and Chung (1988), suggested that exposure of barley roots to NaCl (200 mM) induce the synthesis of V-type H^+-ATPase sub-units, thus accounting for the increased transport activity. Barkla *et al.*, (1995) demonstrated that in the halophytic plant *Mesembryanthemum crystallinum* growth in 400 mM NaCl increases the activity of this pump and the level of expression of the V-type H^+-ATPase genes. Plants have been shown to have several isoforms for different subunit of the V-type H^+-ATPase. In carrot, three different genes for the 70-KDa catalytic nucleotide-binding subunit A have been cloned and sequenced (Zimniak *et al.*, 1988; Gogarten *et al.*, 1992). Four genes encoding the 70-KDa subunit in tobacco have been cloned (Nanda *et al.*, 1992). In barley, two different clones for B subunit were identified (Berkelman *et al.*, 1994). Increased V-type ATPase activity was found in salt-adapted leaves of the common ice plant *M. crystallinum* (Barkla *et al.*, 1995), and two cDNAs encoding the c-subunit and two isoforms have also been identified (Low *et al.*, 1996). Several subunit isoforms have been found to be expressed in response to salt-stress (Luttge and Ratajczak., 1997), and three cDNAs were identified in *A. thaliana* (Li *et al.*, 1999). Also, genes for the G-subunits (accession Nos.AJ005901 and AG00502) have been found in several plant species. In addition to these reports, the presence of two isoforms of D and E-subunits has also been demonstrated in mung been and pea at the protein level (Kawamura *et al.*, 2000). Schumacher *et al.*, (1999) reported that the V-ATPase subunit genes C-subunit is essential for photomorphogenesis of *A. thaliana,* because the *DET3* gene encodes the C-subunit of the V-ATPase when grown in light, and the *det3* mutant has an organ-specific reduction in size that results in plants with short hypocotyls but normal leaf blades and roots. This phenotype was attributed to deficiencies in cell expansion in the hypocotyl.

The *det3* mutant has reduced amounts of C-subunit mRNA, and reduced V-ATPase activity compared to wild-type plants. Because the phenotype reflects a tissue-specific reduction in growth, it has been proposed that V-type ATPase activity has been compromised in this mutant leading to a loss of osmotic driving force for hypocotyl growth (Schumacher *et al.*, 1999). Golldack and Dietz (2001), reported that the expression of V-ATPase subunits A, B, E, F, and C increased in salt stressed leaves of *M. crystallinum,* but not in the roots. The authors suggest that the increased levels of protein near the xylem indicate the transport of sodium into the central vacuole through vesicle trafficking or provacuoles, similar to intracellular sodium sequestration in *S. cerevisiae* (Nass and Rao, 1998; Gaxiola *et al.,* 1999).

1.8.1.4.2.4. Vacuolar-PPase.

An alternative vacuolar proton pump is the V-Ppase, for which inorganic pyrophosphate (PPi) is required (Rea and Poole, 1993). The V-Ppase is abundant in the tonoplast and may also be present in the plasma membrane of some tissues (Ratajczak *et al.*, 1999). The V-PPase pump is single polypeptide that acts as a dimer, and its substrate (PPi) is one of the simplest high-energy compounds available (Maeshima *et al.,* 2000). However, unlike the V-type H^+-ATPase, it drives free energy from the hydrolysis of cytoplasmic pyrophosphate (PPi) and appears to be present only in plants and phototrophic bacteria (Barkla and Pantoja, 1996). V-Ppases have been cloned from various organisms including land plants, fresh water alga and marine alga. A single copy gene encoding the V-Ppase has been cloned from *Arabidopsis thaliana* (Sarafian *et al.*, 1992).

1.9. Secondary Active Transport (Na^+ /H^+ antiporters).

Antiporters are secondary transporter membrane proteins; they are ubiquitous membrane transport proteins but their abundance is very low compared with the vacuolar proton pumps and TIPs, making them difficult to identify on SDS-polyacrylamide gels (Maeshima, 2000). They also move solutes against the electrochemical gradient at rates of 10^2 to 10^4 molecules per second by using a pH gradient generated from the proton pumps that cooperatively in the same membrane (Maeshima, 2000). Sodium/H^+ antiporters can export Na^+ from the cytosol both to the extracellular space and to the vacuole driven by proton gradients across the plasma membrane and tonoplast (Blumwald *et al.*, 2000). The Na^+/H^+ group of antiporters has long attracted attention in relation to salt tolerance in plants (Blumwald and Poole,1987; Blumwald *et al.*, 2000).

1.9.1. Sodium Efflux in Plants.

Sodium/proton antiporters are postulated to function at the plasma membrane and the tonoplast of cells where they are envisaged to pump Na^+ out of the cytoplasm and into either apoplast or into the vacuole (Mennen *et al.*, 1990). In contrast, to microorganism and animal cells, the presence of a Na^+/H^+ antiporter is not ubiquitous in plant cells (Mennen *et al.*, 1990).

Sodium transport is better characterized at the vacuolar membrane than at the plasma membrane. Secondary active transport of Na^+ into the vacuole via tonoplast Na^+ /H^+

antiporters is believed to be energized by the PMF generated by the activity of the V-type H^+-ATPase and/or the V-Ppase. In salt resistant plants, it is viewed that an active antiporter functions to sequester Na^+ into the vacuole, thereby avoiding toxic levels of Na^+ from accumulating in the cytoplasm (Barkla and Pantoja, 1996). Sodium / proton antiport activity is reported to increase with increasing salt stress (Blumwald and Poole, 1987; Grabarino and DuPont, 1988 & 1989; Du Pont, 1992).

Several studies have provided evidence consistent with the existence of a Na^+/H^+ antiporter in the plasma membrane of a wide rage of plant cells. Mennen *et al.*, (1990) looked in the plasma Na^+ /H^+ antiport activity in 16 crop species and found four (sugar beet, barley, tomato and wheat) which appeared to operate this mechanism. Cooper *et al.*, (1990) found evidence for activity in the halophyte (*Atriplex nummularia*) and glycophyte plasma membranes. Allen *et al.*,(1995)measured activity consistent with a Na^+/H^+ antiporter in wheat plasma membrane fractions, and similar results were obtained with barley whole roots (Ratner and Jacooby, 1986). Evidence has also been found for Na^+/H^+ antiporter activity in plasma membrane vesicles isolated from barly and sugar beet root (P. Dominy, unpublished).

The transport of Na^+ from the cytosol, via the tonoplast antiporter, and accumulation in the vacuole of halophtes and salt-tolerant glygophytes is an important mechanism for averting the damaging effects of Na^+ on key biochemical processes in the cytosol. In certain plants the operation of the Na^+/H^+ antiporter at the plasma membrane excretes Na^+ from the cells, and thus acts synergistically with the tonoplast antiporter in

maintaining low cytoplasmic Na^+ concentrations (Barkla and Blumwald, 1992; Jocoby, 1993).

Nass and Rajini (1998) observed the emergence of new exchanger homologues from other organisms with similarity to the *Sc* NHX1 and they suggested that these newly discovered isoforms are indicative of their common intracellular, possibly endosomal localization. The *Arabidopsis thaliana* genome sequencing project has allowed for the identification of a plant gene (*At* Nhx1) homologous to the *Saccharomyces cerevicsia* Nhx1 gene product (Gaxiola et al., 1999; Apse *et al.*, 1999). Transcripts for At NHX1 are found in root, shoot, leaf, and flower tissues Apse *et al.*, (1998). Endocytosis, or pre-vacuolar compartmentation, of Na^+ has yet to be assessed in plants (Marty, 1999). The pre-vacuole compartments may be sorted for exocytosis or fusion with the tonoplast (Marty, 1999), and docking and fusion steps are through to be mainly regulated by internal membrane receptors, termed SNAREs (Sanderfoot and Raikhel, 1999).

Gaxiola *et al.*, (1999) cloned the *A. thaliana NHX1* from a phage cDNA library of *A .thaliana* by probing with an EST (*Arabidopsis* Biological Resources Center, DNA stock center) containing a partial clone. The full-length clone (2.1Kb) is longer than the ORF reported by the *Arabidopsis* Genome initiative (ATM021B04.4) and has been deposited in GenBank (accession no. AF106324). By using a yeast strain defective in *NIIX1*, they were able to clone the *A. thaliana NHX1* homologue, *AtNHX1*. The ability of the *Arabidopsis At*Nhx1 gene to complement the yeast *NHX1* mutant, and its induction in plants by salt stress, both suggests that yeast and plants may achieve salt tolerance by a similar mechanism.

An alignment of the amino acid sequences of NHX1 homologues from *Arabidopsis* (*AtNHX1*), human (HsNhe6), and yeast (Sc*NHX1*) reveals segments of amino acid identity and similarity within predicted transmembrane domains (Gaxiola *et al.*, 1999). They show that this compartment contains both the chloride *GEF1* and the Na^+/H^+ exchanger *NHX1* and that their function, together with the establishment of a proton gradient, are required for salt tolerance (Gaxiola *et al.*, 1999).

Apse *et al.*, (1999) demonstrated the feasibility of engineering salt tolerant in *Arabidopsis* by overexpression of a pre-vacuolar Na^+/H^+ antiporter from *A.thaliana* in *Arabidopsis* plants. Unlike WT plants, transgenic lines survived for 16 days in soil watered with up to 200 mM NaCl. This salinity tolerance was correlated with elevated levels of *AtNHX1* protein, and vacuolar Na^+/H^+ antiporter activity, and showed increased vacuolar uptake of Na^+ compared with wild type plants.

Sub-cellular localization of the *At* NHX1 protein which has molecular mass of 47KD was detected mainly in the tonoplast and Golgi-endoplasmic reticulum (ER) enriched fractions, and was more abundant in the transgenic plants. Frommer *et al.*, (1999) have suggested that, *NHX1* over-expression in transgenic plants may affect salt tolerance by disrupting the trafficking of the Na^+/H^+ antiporter such that it is localized not only to pre-vacuoles but also to the tonoplast, thereby increasing the capacity for compartmentation of Na^+ away from the cytoplasm. With this strategy, it should be possible to engineer a

whole spectrum of salt tolerant crop plants, enabling then to be irrigated with seawater or water of marginal quality (Frommer *et al.*, 1999).

Fukuda *et al.*, (1999), isolated the full-length cDNA for a rice homologue of *NHX1* from a library constructed from rice roots. The sequence contains 2330 bp with an open reading frame of 1608 bp, which shows homology to other Na^+/H^+ antiporters. It has 12 predicted transmembrane domains and two amiloride (inhibition of Na^+/H^+ antiporters) binding domains in TM3 (LFFIYLLPPI & LIMEFLPPL). The membrane-spanning segments TM5 and TM6 of OsNHX1 also have high similarity with other exchangers. In eukaryotic Na^+/H^+ exchangers, the membrane-spaning domains are well conserved, thus these regions may be important in the transport of Na^+ and/or H^+ (Orlowski and Grinstein, 1997). The expression of the gene was increased by salt stress, is differently expressed in root and shoots, and it was concluded that that *Os* NHX1 plays an important role in the compartmentation of Na^+ into the vacuoles of both the tissues (Fukuda *et al.*, 1999).

Zhang and Blumwald (2001) reported that transgenic tomato plants over-expressing a vacuolar Na^+/H^+ antiporter were able to grow, flower, and produce fruit in the presence of 200 mM NaCl. Salt accumulated in the leaves and not in the fruits. The modification of a single trait significantly improved the salinity tolerance of this crop plant. Their results demonstrate that with a combination of breeding and transgenic plants it could be possible to produce salt-tolerant crops.

Zhang *et al* (2001) engineered a salt-tolerant Canola (*Brassica napus*) plant by overexpressing the *Arabidopsis* protein *At* NHX1, that sequesters cytoplasmic Na^+ in to

the vacuoles. This has been shown to confer a measure of resistance to NaCl stress. The plants were able to grow, flower, and produce seed in the presence of 200 mM NaCl. Although the transgenic plants grown in high salinity accumulated sodium up to 6% of their dry weight, biomass was only marginally affected by the high salt concentration. Moreover, seed yields and the seed oil qualities were not affected by the salinity of the soil. This result clearly demonstrates the feasibility of generating salt-tolerant crops for agricultural use by the manipulation of single traits. This does not agree with the notion that salt tolerance can be only achieved by a complex, co-ordinate expression of many characteristics in a single genotype (*e.g.*, Yeo *et al.*, 1988; Cuarteo and Fernandez-Munoz, 1999).

Liu and Zhu (1998) reported the positional cloning of the *SOS3* locus, which encodes a Ca^{2+} binding protein with three predicted EF hands and which shares significant homology to animal neuronal calcium sensors (NCS) and the yeast calcineurin B sub-unit. Calcineurin is a central component in the signaling pathway that regulates Na^+ and K^+ homeostasis in *S.cerevisiae* (Mendoza *et al.*, 1994). Functionally, SOS3 is also similar to yeast CNB because, like the yeast *cnb* mutant, growth of *sos3* mutant plants is hyper sensitive to Na^+ and Li^+ (Liu and Zhu, 1997a). These result suggested that SOS3 participates in a calcineurin-like pathway in mediating plant salt tolerance (Liu and Zhu, 1997a).

Liu *et al.*, (2000) identified the *SOS2* locus through positional cloning in *Arabidopsis*, and, the transcribed sequence was predicted to encode a protein of 446 amino acids with

an estimated molecular mass of 51 KD. Data base searches revealed that the deduced amino acid sequence is a serine/threonine type protein kinase with an N-terminal catalytic domain similar to that of yeast SNF (sucrose non-fermenting), and human AOMPK kinases. SOS2 mRNA is up regulated by salt stress in the root. Auto-phosphorylation assays demonstrate that SOS2 is an active protein kinase, furthermore, a mutation that abolishes *sos2* auto-phosphorelation render plants hybersensitive to salt stress. This indicated that in *Arabidopsis*, SOS2 protein kinase is necessary for the limited expression of salt tolerance found in this species.

Halfter *et al.*, (2000) reported that SOS3 physically interacts with and activates SOS2 protein kinase. Genetic analysis of *sos2 sos3* double mutants indicate that SOS2 and SOS3 function in the same pathway because they have similar phenotype, SOS2 interacts with SOS3 in the yeast two-hybrid system and invitro binding assay, the interaction being mediated by the C terminal regulatory domain of SOS2. Therefore, it is believed that SOS3 and SOS2 define a novel regulatory pathway important for the control of intracellular ion homeostasis and salt tolerance in *Arabidopsis* (Halfter *et al.*, 2000).

Shi *et al.*, (2000) accomplished the cloning of the *SOS1* locus (which is believed to be a downstream target of the SOS3-SOS2 signaling pathway), and encodes a plasma membrane Na^+/H^+ antiporter that exports Na^+ from the cell. Through a map-based approach, SOS1 is essential for Na^+ and K^+ homeostasis, and the *sos1* mutation renders *Arabidopsis* plants extremely sensitive to growth inhibition by Na^+ in low K^+ environments, and results in lower Na^+ and K^+ levels in the shoot. The *SOS1* gene has 22

introns and in 23 exons, and is predicted to encode a polypeptide of 1146 amino acid residues. Hydrophobicity plots suggest the protein is highly hydrophobic and may contain 10-12 transmembrane domain, depending on the prediction program used for the analysis. Database searches revealed substantial similarities between the transmembrane region of *sos1* and Na^+/H^+ antiporters from Chinese hamsters and bacteria (*Pseudomonas aeruginosa* and *E. coli*).

Phylogenetic analysis suggests that SOS1 clusters with the Na^+/H^+ antiporters from the plasma membrane of lower eukaryotes (SOD2, NHA1) and bacteria Nha1 and NhP; Shi *et al.*, 2000). SOS1 is more distantly related to a cluster of organellar Na^+/H^+ antiporters such as *At*NHX1, *Os*NHX1, *Sc*NHX1 and *Hs*NHE6, which suggested that SOS1 is probably a plasma membrane Na^+/H^+ antiporter in *Arabidopsis* (Shi *et al.*, 2000).

The steady-state level of SOS1 transcript is up regulated specifically by NaCl stress, unlike any other salt stress -responsive genes, and expressed in cells bordering the xylem elements, but this upregulation is reduced in the *sos3* or *sos2* mutant background (Shi *et al.*, 2000). This expression pattern suggests that SOS1 functions in either loading Na^+ in to the xylem for long-distance transport, or retrieving Na^+ from the xylem. The xylem-loading function for SOS1 would be consistent with *sos1* mutant plants accumulating less Na^+ (Shi *et al.*, 2000). Overexpression of SOS1 lowers shoot Na^+ contents and improves salt tolerance in *Arabidopsis* plants and callus tissues.

The expression of SOS1 in a yeast mutant deficient in endogenous Na^+ transporters, resulted in a decrease in Na^+ accumulation and improved salt tolerance (Shi *et al.*, 2000). Confocal imaging of a SOS1-green fluorescent protein in transgenic *Arabidopsis* plants indicated that SOS1 is localized in the plasma membrane (Shi *et al.*, 2002). Analysis of SOS1 promoter ß-glucuronidase transgenic Arabidopsis plants revealed preferential expression of SOS1 in epidermal cells at the root tip and in parenchyma cells at the xylem/symplast boundary of roots, stems, and leaves (Shi *et al.*, 2002). Under sever salt stress (100 mM NaCl), *sos1* mutant plants accumulated more Na^+ than did the wild type. There was also greater Na^+ content in the xylem sap of *sos1* mutant plants exposed to 100 mM NaCl which suggest that SOS1 is critical for controlling long-distance Na^+ transport from root to shoot (Shi *et al.*, 2002).

1.10. Aims of Project.

From the proceeding review it can be seen that the majority of work was focused on the demonstration of Na^+/H^+ antiporters activities in different organelles, particularly vacuolar and plasma membranes, and some work on the regulation of these transporters by NaCl. Almost nothing was done regarding cloning of these genes or any molecular analysis. Therefore, this research project has focused on isolation and characterizing of the Na^+/H^+ antiporter from *Arabidopsis thaliana* HHS cell line. Part of the project was directed towards comparable characterization of the morphology and cytogenetics of WT and HHS cells to reveal some of the cellular mechanisms that allow HHS cells to tolerate high salinity (up to 380 mM NaCl, *cf.* WT cells which do not survive >80 mM NaCl).. In addition, with the rapidly accruing information in the *Arabidopsis* genome-sequencing

project, attempts were made to use this information to clone Na^+ transporters (Na^+ / H^+ antiporters) that may be involved in maintaining low cytoplasmic Na^+ levels in IIHS cells. Finally, comparisons were made between the pattern of transcript abundance in WT and HHS cells using the technique of Differential Display PCR (DD-PCR) to monitor the changes in global gene expression in those cell lines, as this may identify mechanisms that are involved in salt tolerance.

CHAPER TWO

MATERIAL AND METHODS

CHAPTER TWO.

2. MATERIALS AND METHODS

2.1. MATERIALS.

2.1.1. Chemicals.

The chemicals used in this study were purchased from BDH (Poole Dorest) unless indicated otherwise.

2.1.1.1. Oligonucleotide primers.

Primers for PCR were synthesized by `MWG-Biotech GmbH .The primers were supplied desalted, and resuspended to the appropriate concentration in water before use.

2.1.1.2. DNA Modifying Enzymes.

EcoRI, *SacI*, *BamHI* restriction enzymes, T4 DNA ligase and Calf Intestinal Alkaline Phosphatase (CIAP), DNA polymerase I (Klenow large fragment), were purchased from Promega Corporation, USA and were supplied with their reaction buffers. *BglII*, *XbaI* and *XhoI* restriction enzymes, *Taq* DNA polymerase and Expand high fidelity *Taq* PCR system were obtain with their buffers from Boehringer-Mannheim, GmbH. Native *Pfu* polymerase was purchased from Stratagene, Cambridge UK.

2.1.1.3. Bacterial Growth Media (Liquid and Solid).

One percent (w/v) L-broth (1 % bacto-tryptone, 0.5 % yeast extract (both supplied by Difco laboratories, Michigan, USA), 1 % (w/v) NaCl, pH 7.0) with the appropriate antibiotic was generally used for culturing and preparing competent *E. coli* cells. L-broth plates were prepared by adding 1.5 % (w/v) agar (Difco) to the media prior to sterilization.

2.1.1.4. Antibiotics, IPTG, and X-Gal.

All antibiotics used were purchased from Sigma Chemical Co. (UK). Kanamycin and Ampicillin were dissolved in distilled water (50 mg mL^{-1}) and used at a final concentration of 50 μg mL^{-1}. Chloramphenicol was dissolved in ethanol (30 mg mL^{-1}) and used at a final concentration of 30 μg mL^{-1}. All antibiotics were filter sterilized (0.2 µm pore size) and stored in sterile bottles before adding to autoclaved media cooled to 50°C.

X-Gal (5-bromo-4-chloro-3-indolyl β-D galactoside; Life Technologies) was made as a 25mg mL^{-1} stock in dimethylformamide and used at a final concentration of 50 μg mL^{-1}. Isopropyl thiogalactoside (IPTG, Life Technologies, Gaithersburg, USA) was prepared as a 0.1 mM stock in distilled H_2O and used at final concentration of 50 μg mL^{-1}.

2.1.2. Bacterial strains, Cloning Vectors and Plasmids.

E. coli strains $DH_5\alpha$, C41Des and C43Des (Prof. JG Lindsay, University of Glasgow) were grown to prepare competent cells for transformation. *E. coli* XL-Blue MRF' Kan supercompetent cells and XL10-Gold Kan ultracompetent cells (Stratagene Ltd., Cambridge, UK) were used as the host strain for amplifying cloned PCR fragments.

The PCR-Script Amp SK (+) cloning vector (Stratagene, Cambridge UK), TOPO vector (Invetroge) and PET 28A transcription silent vector (Prof. H Nimmo, Glasgow University) were used to clone and maintain blunt end PCR products.

2.1.3. General Laboratory Procedures.

2.1.3.1. Filtration.

Heat labile solutions were sterilized by passing through a sterifil-D CS filter (pore diameter 0.22 μm, Millipore Co.) into a sterile receptacle.

2.1.3.2. pH Measurement.

The pH of all solutions other than phenol were measured using a corning pH meter 220 and a combination electrode (Jenway, pHM6, UK).

2.1.3.3. Autoclaving.

Solutions and equipments were sterilized at 121°C and 0.1MPa pressure for 20 minutes in Laboratory Thermal Equipment Autoclave 225E.

2.1.3.4. Solutions and Glassware for RNA Work.

Solutions and glassware for RNA work were treated with 0.1 % (v/v) diethyl pyrocarbonate (DEPC, Sigma) overnight as described in Sambrook *et al.*, (1989). After treatment with 0.1 % (v/v) diethyl pyrocarbonate the glassware was sterilized by baking in oven at 180°C overnight.

2.1.3.5. Silicon-coating of Sequencing Glass Plates.

One of the two sequencing plates was siliconised with dimethyl-dichlorosilane solution (BDH, analaR ®grade). A few drops of the solution were sprinkled onto the plate in a fume hood and spread evenly over the surface with a paper towel. The plates were then washed twice thoroughly with sterile H_2O.

2.1.4. Plant Material.

2.1.4.1. Growth of Cell Suspension Cultures.

The original *Arabidopsis thaliana* cell suspension culture was supplied by Prof. C. Leaver, University of Oxford, (May and Leaver, 1993). The suspension culture was grown in MSMO media (1X Murashige and Skoog salts M6899, Sigma), containing 3 % (w/v) sucrose, 0.5 mg L^{-1} α-naphthalene acetic acid and 0.05 mg L^{-1} Kinetin, pH 5.8. The culture was grown in continuous light (PPFD 18 μmol m^{-2} s^{-1}) at 25°C, constantly shaken at 150 rpm, and sub-cultured every seven days in a sterile laminar flow hood by transferring 20 ml into a sterile flask containing 180 ml of fresh sterile medium.

2.1.4.2. Salt Treatment and Harvesting of Cell Suspension Cultures.

The cell suspension cultures were adapted from non-treated cell suspension culture by sub-culturing into progressively higher levels of NaCl, starting with 50 mM NaCl and increasing gradually up to 300 mM NaCl. Wild type *Arabidopsis* cells cannot survive in MSMO media supplemented with over 70 mM NaCl.

Cell suspension cultures were harvested for DNA, RNA extraction (sections 2.21.and 2.2.2.2.), 3 or 4 days after sub-culture by centrifugation for 10 minutes at 700 g. The supernatant was removed and the pellet washed in 50 mL fresh growth media, and immediately frozen in liquid nitrogen. Samples were then stored at -80°C until required.

2.1.4.3. Electron Microscopy.

The wild type (WT) and habituated high salt (HHS) cell lines were harvested after 3 days. Samples were settled under gravity, excess growth media removed, and specimens were fixed in 2.5 % Glutaraldehyde in 0.2 M Cacodylate buffer pH 7.2 for 12 hours at room temperature, then rinsed in the same buffer for (3x10 minutes), minutes and post-fixed in the 2 % Osmium tetroxide and in water. The specimens were dehydrated in series of ethanol (30, 50, 70, and 90, 100) and embedded in spurr resin. Sections were cut on an LKB III ultra-microtome at a thickness of 60 nm and picked up on 300 mesh formvar coated grids. The grids were stained with 2 % methanolic uranyl acetate for 5 minute, and lead citrate. The sections were viewed in an Zeiss 902 electron microscope at 80 KV.

2.1.4.4. Toluidine Blue-Stain of Chromosome.

Toluidine blue-stain was performed to study the chromosome numbers in the wild type (WT) and habituated high salt (HHS) *Arabidopsis* cell lines. Cells were grown in (MS) media to middle log phase and collected by gravity-dependent sedimentation, and thin transferred to 3:1 ethanol glacial acetic acid for 1h. fixation. The cells were stained with 1% Toluidine blue to observe the chromosomes

2.2. METHODS.

2.2.1. Isolation of Plant Genomic DNA.

The isolation of high molecular weight DNA was carried out according to the DNA protocol of Woodhead *et al.,* (1998). Twenty grams of cell suspension culture were quickly frozen in liquid nitrogen and ground to fine powder in a pre-chilled mortar and pestle. The frozen powder was then transferred to pre-heated 250 ml Beckman bottle containing 30 ml of 2 X extraction buffer (50 mM Tris HCl, pH 8.0; 0.7 mM NaCl; 10 mM EDTA; 1 % (w/v) CTAB; and 0.4 ml mercaptoethanol). The content of the bottle were mixed gently by inversion, incubated at 65°C for 20 minutes and allowed to cool to room temperature. Then 30 ml of chloroform: octanol (24:1) was added to the bottle and gently mixed by inversion several times until an emulsion was formed. The bottle was spun at 10,000 rpm in Beckman J2HS centrifuge, using JA-14 rotor for 10 minutes at 20°C. Following the spin, the upper aqueous phase was carefully removed to a clean 250 ml Beckman bottle, and a one-tenth volume of 10 % (w/v) CTAB in 0.7 M NaCl was added and mixed gently. Chloroform: octanol extraction was repeated as described above. The aqueous phase containing DNA was transferred to a clean 250 ml Beckman bottle, and the DNA was precipitated with precipitation buffer (50 mM Tris HCl, pH 8.0;

temperature. The DNA was pelleted by centrifugation at 3000 rpm for 15 minutes at 20°C and the supernatant discarded. The bottle was then inverted on paper towels to allow the pellet to dry. After drying, the DNA pellet was dissolved in 4.8 ml of 1 M CsCl /EtBr solution (1 M CsCl; 50 mM Tris HCl, pH 8.0; 10 mM MEDTA; 0.2 mg mL^{-1} EtBr). The DNA solution was then transferred to a sterile 30 ml Oak Ridge tube containing 7 M CsCl / EtBr solution (7 M CsCl, 0.1 % sarkosyl, 0.2 mg mL^{-1} EtBr), mixed gently, and transferred to an ultracentrifuge tube. The tube was capped and centrifuged at 180,000 g for 40 hours at 20°C in fixed angle rotor (T 865.1) of a Sorvall 55B ultracentrifuge. After centrifugation, the DNA band was collected with a sterile plastic pipette and placed into clean 1.5 mL Eppendorf tubes. Ethidium bromide was removed by adding an equal volume of TE saturated *iso*-amyl alcohol. The phases were mixed gently, allowed to separate and the upper phase was removed. The extraction procedure was repeated several times until all of the ethdium bromide (pink colouration) was removed from the aqueous phase.

The aqueous phase was then dialyzed against a 1000 X volume of TE buffer (10 mM Tris HCl, pH 8.0; 1 mM EDTA) using treated dialysis tubing (Sigma) for 2 hours at 4°C, and then overnight against fresh TE buffer (pH 8.0) at 4°. The dialysis tubing was prepared by boiling for 5 minutes in the presence of 0.1 % (w/v) SDS, and allowed to cool prior to use. The DNA solution was transferred from the dialysis tubing into a 1.5 mL Eppendorf tube, the DNA was then precipitated by the addition of a one-tenth volume of 3 M sodium acetate and two volumes of ice-cold ethanol, and the mixture was then stored at -20°C for 2 hours. The DNA was pelleted in a microfuge by centrifugation at 10,000 g for 3 minutes, washed with 70 % (v/v) ethanol, dried and re-dissolved in TE buffer (pH 8.0).

The concentration of the DNA solution was measured as in Section 2.2.6 and finally stored at 4°C until use.

2.2.2. Isolation of Total RNA from cell suspension cultures.

2.2.2.1. Preparation of Phenol.

Five hundred grams of phenol (detached crystals) was melted at 65°C for 30 minutes and 0.1 % (w/w) of 8-hydroxyquinoline was added before the phenol had been cooled. The warm solution was saturated with 300 mL of 1 M Tris-HCl (pH 8.0) and mixed vigorously for 15 minutes. After allowing the solution to settle, the upper phase was then removed by aspiration and replaced with an equal volume of 100 mM Tris-HCl (pH 8.0). The upper phase was aspirated as described above and the pH of the aqueous extract was measured with litmus paper. The aspiration and washing with 100 mM Tris-HCl (pH 8.0) was repeated until the pH of the aqueous extract was greater than 7.8. The upper phase was replaced with 100 mL of 100 mM Tris-HCl (pH 7.8) and the solution stored in a dark bottle at 4°C.

2.2.2.2. Isolation of Total RNA.

All aqueous solutions were prepared with DEPC-treated water, and all glassware was baked at 180°C overnight before use.

One gram of frozen cell suspension culture was ground to fine powder under liquid nitrogen with a DEPC-treated mortar and pestle. The powder was then transferred to a 15 ml glass Corex tube containing 5 mL of TNT solution (50 mM Tris-HCl, pH 7.8; 10 mM

NaCl; 2 % (w/v) Tri-*iso*-propylnaphthalene-sulphonic acid sodium salt [Greyhound Chromatography and Allied Chemical, UK]) and 5 mL of PCI solution (phenol: chloroform: *iso*-amyl alcohol, v/v/v, 25: 24 : 1). The solution was mixed vigorously by inversion until an emulsion was formed and then kept on ice. The tube was then spun at 1000g for 10 minutes at 4°C in Beckman J2HS centrifuge, using JA-20 rotor. Following the spin, the upper aqueous phase was removed with a baked Pasteur pipette and transferred to a clean 15 mL Corex tube containing an equal volume of PCI. The sample was mixed and centrifuged as described previously. After centrifugation, the upper aqueous phase was removed to a clean 15 mL Corex tube containing an equal volume of chloroform: *iso*-amyl alcohol (v/v 24: 1), mixed and centrifuged as before. The aqueous phase containing RNA was transferred to 15 mL glass Corex tube and the RNA was precipitated with 2.5 volume of ice-cold ethanol and 0.1 volume 3 M sodium acetate (pH 6.0), mixed and incubated at -20°C for 2-12 hours.

After precipitation, the RNA was pelted by centrifugation at 10,000 g for 15 minutes in a Beckman J2HS centrifuge using JA-20 rotor at 4°C. The supernatant was discarded and the pellet washed twice with 80 % (v/v) ice-cold ethanol and re-pelted after each wash by centrifugation as before. The resulting pellet was dried under a vacuum, dissolved in appropriate volume of DEPC-treated analar water and stored at -80°C.

The purity and the concentration of the RNA were estimated by measuring the OD at 260 nm and 280 nm (Section 2.2.6). A high purity RNA preparation was taken as having a 260/ 280 nm ratio of 1.8 -2.0. The integrity of the RNA was examined on a 1.3 % (w/v) formaldehyde agarose gel.

2.2.2.3. Isolation of total RNA using Promega kits.

RNA isolation was carried out accordance with the manufacture's instructions (Kobs, 1998). The plant tissue was frozen in liquid nitrogen and ground using a mortar and pestle. Thirty mg of ground tissue was added to 175 μL of RNA lysis buffer followed by 350 μL of RNA dilution buffer, mixed by inversion, and then centrifuged at maximum speed in a microcentrifuge for 10 minutes. The cleared lysate solution was transferred to fresh microcentrifuge tube by pipeting, 200 μL 95 % ethanol was then added mixed by gentle pipetting. The mixture was transferred to the Spin Column Assembly and micro-centrifuged at 12,000-14,000 rpm for 1 minute. The liquid in the collection tube was discarded and 600 μL of SV RNA wash solution was added to the Spin Column assembly which was subsequently centrifuged again at 12,000-14,000 rpm for one minute. The collection tube was emptied as before, 50 μL of freshly prepared DNase incubation mix (40 μL Yellow Core Buffer, 5 μL 0.09 M MnCl and 5 μL of DNase1 enzyme) was added directly to the membrane inside the Spin Column Basket, and incubated for 15 minutes at 20-25°C. After this incubation, 200 μL of SV DNase Stop Solution was added to the Spin Basket and centrifuged at 12,000-14,000 rpm for one minute. Six hundred of SV Wash Solution was added and centrifuged at 12,000-14,000 rpm for one minute. The Collection tube was emptied and 250 μL SV RNA Wash Solution was added and centrifuged at high speed for two minutes. The Spin Basket was then transferred from the Collection Tube to the Elution Tube, 100 μL Nuclease-Free water was added to the membrane and centrifuged at 12,000-14,000 rpm for one minute. The Spin Basket was discarded and the Elution Tube containing the purified RNA was capped and stored at -70°C.

2.2.3. Amplification and Preparation of Plasmid DNA.

2.2.3.1. Preparation of Competent Cells.

Competent cells were prepared using the method described by Sambrook *et al.*, (1989). Bacterial cultures were grown overnight in 10 mL of L-broth medium (Section 2.1.1.3) at 37°C, and shaken at 200 rpm. Five mL of the culture was inoculated into 100 mL of fresh L-broth medium as beforeand grown at 37°C until an OD at 550 nm of 0.35 was reached. Fifty mL of the suspension was transferred to two sterile 30 mL Oak Ridge tubes, centrifuged (in a Beckman J2HS centrifuge using JA-20 fix angle rotor) at 2,000 g for 5 minutes at 4°C and then the supernatant decanted. The bacterial pellet was re-suspended in 10 mL of TFB1 (100 mM RbCl; 50 mM $MnCl_2$; 30 mM potassium acetate; 10 mM $CaCl_2$; 15 % (v/v) glycerol, pH 5.8) and kept on ice for 90 minutes. After incubation, the cell suspension was centrifuged as above and resuspended in 2.8 mL ice-cold TFB2 (10 mM MOPS; 10 mM RbCl; 75 mM $CaCl_2$; 15 % (v/v) glycerol, pH 7.0). The cells were then devided into 0.2 mL aliquots in 1.5 mL Eppendorf tubes, frozen in liquid nitrogen and stored at - 80°C until required.

2.2.3.2. Transformation.

Three methods were used for transformation of competent cells.

2.2.3.2.1 Transformation of Competent Cells.

Frozen competent cells (prepared as described in Section 2.2.3.1) were thawed on ice. Approximately 30 ng of plasmid DNA in a volume of 5-10 μL was added to the Eppendorf tube containing 0.2 mL of the competent cells, and gently shaken before being incubated on ice for 20 minutes. After this period, the cells were heat-shocked at 37°C for 1 minute and incubated on ice for further 2 minutes. L-broth medium (0.8 mL) (containing the appropriate antibiotic) was added to allow expression of the antibiotic resistance encoded on the plasmid. Cells were pelleted by microcentrifuge at 10,000 g for 30 seconds, the supernatant discarded, and the pellet resuspended in 0.1 mL L-broth medium. One hundred μL of serial 1/10 dilutions of the cell suspension were plated on solid medium containing the appropriate antibiotic (Section 2.1.1.3). The plates were allowed to dry and incubated at 37°C overnight. As a control, competent cells were treated as above in absence of plasmid DNA plated on solid medium without antibiotic. As second control, empty plasmid vector was used to transform cells, and these were plated on solid medium containing the appropriate antibiotic.

2.2.3.3. Transformation of *E. coli* XL1-Blue MRF` Supercompetent Cells and XL10-Gold Kan Utracompetent Cells.

Transformation of *E. coli* XL1-Blue MRF` supercompetent cells and XL10-Gold Kan ultracompetent cells was performed in accordance with the manufacture's instructions (PCR-Script Amp Cloning Kit, Stratagene). Frozen competent cells were thawed on ice. Forty μL aliquots of competent cells were transferred into pre-chilled 15 mL Falcon (polypropylene) tubes. Then 0.7μL of 25 mM of β-mercaptoethanol was added to the tube and gently swirled before being incubated on ice for 10 minutes. Two μL of the

cloning reaction prepared as described in Section 2.2.11.4 were added, gently swirled and incubated on ice for 30 minutes. After the incubation, the transformation reaction was heat-shocked at 42°C for 45 seconds and returned to ice for 2 minutes. Then, 0.45 mL of SOC medium (2 % (w/v) tryptone; 0.5 % (w/v) yeast extract; 0.05 % (w/v) NaCl; 1 mM $MgSO_4$; 1 mM $MgCl_2$; 0.4 % (w/v) glucose) was added to the transformation reaction and then the tube was shaken at 37°C for 1 hour. One-hundred, 125, 150 μL of the transformation reaction were then plated on L-broth agar plates containing ampicillin (50 μg mL^{-1}), X-gal (50 μM mL^{-1}), and IPTG (50 μM mL^{-1}). One hundred μL of control transformation reaction (transformed cells with plasmid containing test insert) were plated onto L-broth-chloramphenicol (30 μg mL^{-1}) agar plates. The plates were allowed to dry, and placed at 37°C overnight.

2.2.3.4. Transformation of TOPO 10 *E. coli* Cells.

Transformation of *E. coli* TOP10 cells was performed in accordance with the manufacture's instructions of TOPO TA cloning Kit (Invitrogen, Leek, The Netherlands). Two μL of the TOPO cloning reaction (section 2.2.14.4.2) were added into a tube containing *E. coli* TOP10, mixed and incubated on ice for 5 minutes. The cells were heat-shocked for 30 seconds at 42°C without shaking. The tube was immediately transferred to ice, and 250 μL of SOC medium was added at room temperature. The tube was capped tightly and shaken horizontally (200 rpm) at 37°C for 1 hour. Ten-to-50 μL from the transformation mix were spread on a pre-warmed selective media plates, and incubated overnight at 37°C.

2.2.3. Preparation of Plasmid DNA.

2.2.4.1. Small-Scale Preparation of Plasmid DNA.

Wizard Miniprep DNA purification system (Promega) was used in accordance with the manufacture's instructions.

A single bacterial colony was used to inoculate 5 mL of L-broth medium, supplemented with the appropriate antibiotic, in a sterile 20 mL Bijou tube. The culture was grown overnight at 37°C with constant shaking at 200 rpm. The overnight culture was transferred to 30 mL Oak Ridge tubes, centrifuged (in a Beckman J2HS centrifuge using JA-20 fix angle rotor) at 2,000 g for 5 minutes at 4°C, and the supernatant was then decanted. The bacterial pellet was re-suspended in 300 μL of cell re-suspension solution (50 mM Tris-HCl, pH 7.5; 10 mM EDTA; 100-μg mL^{-1} RNase A). Once fully re-suspended, the mixture was transferred to 1.5 mL Eppendorf tube, 300 μL of cell lysis solution (200 mM NaOH; 1 % (w/v) SDS) was added to the tube and mixed by gentle inversion. Next, 300μL neutralization solution (1.32 M potassium acetate, pH 4.8) was added and the solution and mixed as before. The tube was centrifuge at 10,000 g for 5 minutes in a microcentrifuge and the supernatant removed to a clean 1.5-mL Eppendorf tube. One mL of Wizard Minipreps NAD purification resin was added to the solution and gently mixed. Meanwhile, a 3 mL disposable syringe was attached to a minicolumn and placed onto a vacuum manifold (Promega). The resin/DNA mixture was then transferred to the syringe and a vacuum applied to pull the slurry into the minicolumn. The vacuum was broken, 2 mL of wash solution (200 mM NaCl; 20 mM Tris-HCl, pH 7.5; 5 mM EDTA; 95 % (v/v) ethanol) was added, and the vacuum re-applied. Once the wash solution had passed through, the column was left to dry for 30 seconds. The vacuum was

broken and the minicolumn removed from the syringe and transferred to a 1.5 mL Eppendorf tube. This was centrifuged at 10,000 g for 2 minutes to further dry the resin. The minicolumn was then transferred to a clean 1.5 mL Eppendorf tube 50 μL of TE buffer (pH 7.6) added and then left at room temperature for 1 minutes. Plasmid DNA was eluted by centrifugation at 10,000 g for 20 seconds.

2.2.4.1. Large Scale Preparation of Plasmid DNA.

For this method the Qiagen Midi- Pasmid Purification system (Qiagen Ltd., Sussex, UK) was used in accordance with the manufacture's instructions.

A single colony of bacteria was selected and used to inoculate 25 mL of L-broth containing the appropriate antibiotic and grown at 37°C with constant shaking (200 rpm) overnight.

The cells were harvested by centrifugation in a Beckman J2HS centrifuge using JA-20 fix angle rotor) at 2,000 g for 5 minutes at 4°C. The supernatant was discarded and the bacterial pellet was re-suspended in 4 mL of buffer P1 (100 μg mL^{-1} RNase A; 50 mM Tris-HCl, pH 8.0; 10 mM Na_2EDTA). Then the cells were lysed by adding 4 mL of buffer P2 (200 mM NaOH; 1 % (w/v) SDS), and the solution was then gently mixed by inverting the tube several times before incubation at room temperature for 5 minutes. Four mL of chilled P3 buffer (3 M potassium acetate, pH 5.5) was added to the lysate solution, mixed immediately by gently inverting 4-6 times, incubated on ice for 15 minutes, and then centrifuged at 20,000 g for 30 minutes at 4°C. The supernatant containing plasmid DNA was removed and re-centrifuged at 20,000 g for 15 minutes at

4°C to obtain a particle-free, clear lysate. Meanwhile, a Qiagen column (tip 100) was equilibrated by applying 4 mL of QBT buffer (750 mM NaCl; 50 mM MOPS; 15 % (v/v) ethanol; 0.15 %(v/v) Triton X-100, pH 7.0). The column was allowed to empty by gravity flow. The supernatant obtained after centrifugation was then applied to the Qiagen column and allowed to enter the resin by gravity. The column was then washed twice with 10 mL of QC buffer (100 mM NaCl; 50 mM MOPS; 15 % (v/v) ethanol, pH 7.0). Plasmid DNA was eluted into a sterile 30 mL centrifuge tube by the addition of 5 mL of QF buffer (1.25 M NaCl; 50 mM Tris-HCl, pH 8.5; 15 % (v/v) ethanol). The DNA was precipitated by adding 0.7 volumes of *iso*-propanol, mixed and immediately spun at 20,000 g for 30 minutes at 4°C. The supernatant was discarded and the DNA pellet washed twice in 70 % (v/v) ice-cold ethanol and centrifuged as before. The supernatant was removed and the pellet air-dried before re-dissolving in a suitable volume of TE buffer (10 mM Tris-HCl, pH 8.0; 1 mM EDTA). The concentration of DNA solution was determined as in Section 2.2.6 and stored at -20°C.

2.2.5. Nucleic Acid Precipitation

Nucleic acid were precipitated by either ethanol or *iso*-propanol method. Nucleic acid were precipitated by the addition of a 1/10 volume 3 M Na acetate (pH 5.2) followed either by the addition of two volumes of ice-cold 100 % ethanol or 0.7 volume of ice-cold *iso*-propanol. DNA precipitation was enhanced by chilling the samples at -20°C for at least 20 minutes before centrifugation at 10,000 g for 3 minutes. Nucleic acid pellets were washed in 70 % (v/v) ethanol, briefly centrifuged, air dried, and finally resuspended in an appropriate volume of distilled water or TE buffer (pH 8.0).

2.2.5.1. Quantification of DNA and RNA.

An aliquot of nucleic acid solution to be quantified (usually 5-10 μL) was diluted to 70 μL with distilled or DEPC-treated water. The absorbance of the nucleic acid containing solution was measured by scanning between 220 nm and 350 nm using distilled water as a blank in a Shimadzu UV-2101 PC scanning spectrophotometer. An absorbance at 260 nm (A_{260}) of 1 was taken to indicate the following concentrations:

Form of nucleic acid	Concentration (μg mL^{-1})
Double stranded DNA	50
Single stranded and RNA	38

2.2.6. Agarose Gel Electrophoresis

GIBCO-BRL Life Technologies Ltd, Paisley UK, supplied all agarose (utra PUPE).

2.2.5.2. Electrophoresis of DNA.

The appropriate concentration of agarose (0.5-2.0 % (w/v)) was added to an appropriate volume of 1 X TBE buffer (90 mM Tris-borate, pH 8.0; 2 mM EDTA) required for the gel being cast. The agarose suspension was heated in a microwave oven until all the agarose had completely dissolved. The molten agarose solution was allowed to cool to around 60°C at which point 10 mg mL^{-1} ethidium bromide was added to a final concentration of 0.5 μg mL^{-1}. The molten agarose solution was then poured into the

electrophoresis apparatus and allowed to set for 30 minutes at room temperature. Enough 1 X TBE running buffer was added to just submerge the gel to a depth of approximately 1-2 mm. The DNA samples to be loaded, were mixed with a one-tenth volume of loading dye buffer (50 % (v/v) glycerol; 1 mM EDTA, pH 8.0; 0.25 % (w/v) xylene cyanol FF) heated to 95°C for 30s, and loaded into the wells of the submerged gel. The electrophoresis was carried out at 20-100 volts (constant voltage) at room temperature until the bromophenol blue lower band had migrated two-third of the way down the gel. The gel was visualized under UV light (Spectroline transilluminator, Model TC-312A). The gel was photographed using Polaroid film (Type 665, professional) or with a Bio Gene Image analysis system (Bio Gen Ltd).

2.2.5.3. Denaturing Electrophoresis of RNA.

The appropriate concentration of agarose (1.3 % (w/v) was added to 80 mL of DEPC-treated water. The agarose suspension was then heated in a microwave oven until the agarose had dissolved. Once the agarose solution had cooled to 60°C, 10 mL of 10 X MOPS buffer (200 mM MOPS pH 7.0; 50 mM sodium acetate; 10 mM EDTA) and 10 mL of formaldehyde (37 % (v/v)) were added and the gel was mixed by swirling in a fume hood prior to pouring into the electrophoresis apparatus. The molten gel was then left in the fume hood for 30 minutes to allow the gel to set and then placed into the electrophoresis tank and submerge to a depth of 1-2 mm in 1 X MOPS running buffer. RNA samples (5-20 μg) were prepared in a solution of 50 % (v/v) formamide (Fluka Biochemical, Gillingham, U.K.), 1 X MOPS, 5.92 % (v/v) formaldehyde and 2 μL of 10 mg mL^{-1} ethidium bromide in a volume not greater than 50 μL. This solution was heated

at 56°C for 5 minutes and chilled on ice. A one-fourth volume of loading dye buffer (50 % (v/v) glycerol; 1 mM EDTA, pH 8.0; 0.25 % (w/v) bromophenol blue; 0.25 % (w/v) xylene cyanol FF) was added and the RNA samples loaded onto the gel. The gel was run at a constant voltage of 80 V at room temperature until the bromophenol blue band (front) had migrated two thirds of the distant down the gel. The gel was visualized under UV light.

2.2.5.4. Nucleic Acid Markers.

Nucleic Acid Markers were run with all samples to size the DNA and RNA that was being analyzed. For double stranded (ds) DNA fragments, the following marker were used: 0.075-12 kb, 1 kb ladder (GIBCO-BRL): 0.568-23 kb *Hind III* digested λ phage (GIBCO-BRL): 0.075-12.216 kb DNA Längenstandards (BIO RAD), 1-10 kb (BIO RAD), EZ Load 100bp Molecular Ruler (BIO RAD). For RNA analysis of single stranded RNA, the RNA ladder (GIBCO-BRL) containing marker bands ranging in size between 0.24-9.5 kb was used.

2.2.6. Digestion of DNA with Restriction Endonucleases.

The DNA to be cut with restriction endonucleases was prepared in the appropriate buffer with 1-20 units of restriction enzyme(s). The reactions were incubated at 37°C for 3 - 16 hr as required. All reactions were monitored by running an aliquot of the completed reaction mixture on an agarose gel with uncut DNA and appropriate DNA markers.

2.2.7. Extraction and Purification of DNA Fragments from Agarose Gels.

For this method the QIAquick Gel Extraction Kit (Qiagen Ltd., Sussex, U.K) was used in accordance with the manufacture's instructions. The DNA fragment of interest was initially separated from residual DNA fragments by agarose gel electrophoresis as described in Section 2.2.7.1. The fragment was then excised from the gel with a clean, sharp scalpel and weighed in a 1.5 mL Eppendorf tube. Three volume of buffer QG were added to 1 volume of gel (100 mg taken as equivalent to 100μL), incubated at 50°C for 10 minutes and mixed by vortexing every 2-3 minutes during the incubation. After the gel slice had dissolved completely, 1 gel volume of *iso*-propanol was added to the sample and mixed. A QIAquick spin column was placed in a 2 mL collection tube, the sample applied and then centrifuged in a micro-centrifuge for 1 minute, at 10,000 g. The elute was discarded and the QIAquick spin column placed back in the collection tube. The column was then washed with 0.75 mL of buffer PE, incubated for 2-5 minutes and re-centrifuged for 1 minute as before. The eluent was again discarded and the QIAquick spin column centrifuged once again for 1 minute to remove the residual of PE buffer. The QIAquick spin column was placed into a clean 1.5 mL microfuge tube and 50 μL of buffer EB buffer was added to the center of the QIAquick spin column to elute the bound DNA. The QIAquick spin column was incubated for 1 minute, centrifuged for 1 minute as before, and the eluted DNA stored at -20°C.

2.2.8. Blotting of Nucleic Acids.

2.2.8.1. Northern Blotting.

RNA was separated on a denaturing agarose gel as described in 2.2.7.2. The gel was then blotted as described in Sambrook *et al.*, (1989) with the following alteration. A wick of

Whatman 3MM paper was placed onto a horizontal support, soaked in 20X SSC as blotting buffer (3M NaCl; 300mM *tri*-sodium citrate, pH 7.0) and each end dipped into a reservoir of 300 ml 20X SSC blotting buffer. The gel was placed on the top of the wick with the well side of the gel (top surface) touching it , ensuring that there were no air bubbles between the wick and the gel, and nylon membrane (Hybond-N, Amersham) was cut to a size 1mm larger than the gel in both dimensions and placed on top of the gel. Any air bubbles between the nylon membrane and the gel was removed by a clean plastic pipette. Two pieces of Whatman 3MM paper were cut to the size of the gel, soaked in 20 X SSC blotting buffer and placed on the top of the nylon membrane, again ensuring no air bubbles were entrapped. A frame of cling film was placed around the gel sandwiched between the lower wick and the upper 3 MM paper to ensured that all rising solution passed from the wick through the gel and up into the upper 3 MM paper. A stack of absorbent paper towels was then placed on top of the3 MM paper, (approximately 5 cm in height when compressed). A glass plate was placed on the top of the stack of the towels with a 500g weight on top. The blot was left overnight to allow the nucleic acids to transfer to the membrane, after that the membrane was marked with a pen to identify the position of the wells. The gel and the membrane were examined under UV light to assess the transfer of RNA from the gel to the membrane as the RNA on the membrane was still stained with ethidium bromide, then the RNA was fixed onto the membrane by UV light, and finally washed carefully in 6X SSC (3 M NaCl; 300mM Na-citrate) for 2 minutes to remove any adhering agarose, and left to dry at room temperature.

2.2.9. Radiolabelling of DNA.

2.2.9.1. Generation of Radioactive ssDNA probes by Asymmetric PCR.

Asymmetric PCR was performed on DNA fragments, which had been cloned into plasmid vector. The reactions were performed in a 50 μL volume containing the appropriate template concentration (50 -100 ng of DNA per reaction) and 200 μM dATP, 200 μM dGTP, 200 μM dTTP, 12 μM dCTP, 50- 100 μCi [α-^{32}P] dCTP, 0.5μM T3 primer, 0.1 μM T7 primer, 1X *Taq* buffer (20mM Tris-HCl, pH 8.0; 1mM dithiothreitol; 0.1mM EDTA; 0.1 M KCl; 0.5% Nonidet P40 (v/v); 0.5% Tween 20 (v/v); 50% glycerol (v/v); and 2.5 units of *Taq* DNA polymerase). The amplification was carried out in the thermocycler under the following condition: 1 min at 94°C; 35 cycles (15 s at 94°C, 15 - 20 s at 45°C, 120 s at 72°C, followed by 3 min at the same temperature.

2.2.9.2.. Measurement of Incorporated Radioactivity.

The incorporated radioactivity into nucleic acid probes was estimated in 1μ samples removed from the labeled probe solution before and after purification throughout the Nick column (Section 2.2.15.5.3). The 1μ samples were placed into screw-capped Eppenddorf tubes containing 0.5mL distilled water and inserted into separate scintillation vials and the radioactivity was counted by Cerenkov emission in a LKB 1209 Rackbeta scintillation counter. The percentage of incorporation was determined by comparing the counts of the two radiolabelled sample aliquots before and after passing throughout the Nick column (counts for labeled sample eluted form the column multiply by 100/counts before sample eluted form the column). The specific activity of the labeled probe (cmp incorporated per μg DNA) could then be calculated.

2.2.10.2. Hybridization Analysis.

2.2.10.1. Hybridization Analysis of RNA.

Northern blots were analyzed using the method of Sambrook *et al.*, (1989). Nylon membranes (prepared as described in Section 2.2.10.1.) were pre-hybridized at 42°C in a shaking water bath using a plastic box . Enough pre-hybridization solution (5X SSC; 50 % formaldehyde (v/v); 5X Dedhardt's solution; 0.1 % (w/v) SDS; 100μm L^{-1} denatured, salmon sperm DNA) was used to just cover the filter(s). The radiolabeled probe was denatured, as described above, and added to the pre-hybridization solution. The hybridization was carried out at 37°C overnight.

2.2.10.2. Washing Membranes.

After hybridization, the hybridization solution was discarded. The membrane(s) were briefly washed twice in 2X SSC, 0.1 % (w/v) SDS at room temperature (to remove most of remaining probe from the membrane). The membranes were then washed twice for 15 minutes with an excess of the washing solution (1X SSC, 0.1 % (w/v) SDS) in a shaking water bath at 50°C. The membranes were then washed at increasing stringency depending on the amount of radioactivity bound to the membrane. After washing, the membranes were wrapped in cling film and auto-radio-graphed at -80°C.

2.2.10.3. Auto-radiography.

The wrapped membrane(s) were exposed to Fuji X-ray film (Type RX) in a film cassette with an intensifying screen at -80°C for the appropriate time.

2.2.11. Reverse Transcription - Polymerase Chain Reaction (RT-PCR)

2.2.11.1. Synthesis of First-Strand cDNA.

This reaction was carried out using the Stratagene Reverse Transcription System (RT-PCR) Kit. Any enzymes and reagents used were supplied with this Kit unless otherwise stated.

Total RNA (5-10 μg) previously prepared as described in Section 2.2.2.2 was used separately in a final volume of 38 μL (adjusted with DEPC-treated water). Three μL of oligo (dT) (100 ng μL^{-1}) were added to the reaction and mixed gently. The reaction was incubated at 65°C for 5 minutes and cooled slowly to room temperature (approximately 10 minutes) to allow the primer to anneal to the total RNA. Then 5 μL of 10 X first-strand buffer, 1μL of RNase Block Ribonuclease Inhibitor (40 units μL^{-1}), 2 μL of 100 mM dNTPs (dATP, dCTP, dGTP,dTTP) and 1 μL (50 U μL^{-1}) of MMLV-RT (Moloney Murine Leukemia Reverse Transcriptase) were added in this order to the above reaction tube. The reaction was mixed gently and incubated at 37°C for one hour. Finally, the reaction was heated at 90°C for 5 minutes and then stored on ice. First strand cDNA was also prepared using the alternative Random Primer method (100 ng μL^{-1}) instead of oligo (dT), using the same condition as above.

2.2.12. Polymerase Chain Reaction (PCR)

2.2.12.1. PCR Amplification of Nucleic Acid.

The polymerase chain reaction was used to amplify DNA sequences from *Arabidopsis thaliana* cDNA library, genomic DNA and first strand cDNA . Generally 1-2 U of *Taq* DNA polymerase per reaction was used in 1X *Taq* buffer (20mM Tris-HCl, pH 8.0; 1mM dithiothreitol; 0.1mM EDTA; 0.1 M KCl; 0.5% Nonidet P40 (v/v); 0.5% Tween 20 (v/v); 50% glycerol (v/v), with 2-3 mM $MgCl_2$, 200 pmol dNTPs (dATP, dCTP, dTTP, dGTP) and 50-100 pmol of each primer (forward and reverse). The reaction was performed in a volume of 50 μL in 0.5 mL Eppendorf tubes. The same reagents were used for PCR reactions when the Expand™ High Fidelity *Taq* PCR system or *Pfu* polymerase were used instead of *Taq* polymerase. For each reaction 1 X buffer was required, Expand HF 1 X buffer (20 mM Tris-HCl, pH 7.5; 100 mM KCl; 1 mM DTT; 0.1 mM EDTA; 0.5 % Tween® 20 (v/v); 0.5 % Nonidet® P40 (v/v); 50 % glycerol (v/v)), and *Pfu* 1 X buffer (20 mM Tris-HCl, pH8.0; 2 mM $MgCl_2$; 10 mM $(NH)_2SO_4$; 0.1 5 Triton X-100; 100 μg mL^{-1} nuclease-free BSA) respectivly. All reagents were mixed gently, one drop of mineral oil (Sigma) was layered on top to reduce the evaporation, and the tubes were placed in Hybond OMI Gene PCR thermal cycler.

Typically, the thermal cycler was programmed to denature the samples for 1 minute at 94°C and then complete 35 cycles. Denaturation was performed at 94°C for 1 minute and extension at 72°C for 2 minutes. The annealing temperature depended on the primers being used, and was set initially 5°C below the estimated melting temperature of the primer DNA sequence, and subsequently adjusted to achieve optimization. The melting temperature was calculated from the formula T_m = (3 x GC) + (2 x AT)°C where GC and AT are the number of G+C or A+T base pairs in the primer. For *Pfu* polymerase the PCR reaction condition was the same except the annealing time was longer than above (30- 60

seconds). The PCR products were generally analyzed by agarose gel electrophoresis (Section 2.2.7.1).

2.2.12.2. Purification of PCR Products.

Two methods were used to purify the PCR products before cloning from excess PCR fragments, primers and enzyme. The first, by using the Qiaquick Gel Extraction Kit (Qiagen, Section 2.2.9). The second, by using the Qiaquick Nucleotid Removal Kit protocols. Ten volume of buffer PN was added to the reaction sample and mixed. The Qiaquick spin column was placed on a provided 2 mL collection tube. The DNA sample was applied to the Qiaquick spin column and spun for 1 minute at 7000 g. The flow-through was discarded, the Qiaquick spin column was placed back in the emptied collection tube, centrifuged for an additional 1 minute at 10,000 g. The Qiaquick spin column was then placed in a sterilized 1.5 mL microcentrifuge tube. The DNA was eluted by adding 50 μL of EB buffer (10 mM Tris-HCl, pH 8.5) to the center of the Qiaquick membrane and left for 1 minute before centrifugation at 10,000 g.

2.2.12.3.. Creating Blunt End DNA (Polishing).

The end of purified PCR products generated with *Taq* DNA polymerase were polished to create blunt end DNA. Two methods were used. First, by using the *pfu*-based PCR-Script™ cloning protocol (Stratagene, 1997). Polishing reaction were prepared by adding the following components in order to a 0.5 mL microcentrifuge tube. Ten μL of the purified PCR product (0.5-1μg DNA), 1 μL of 10 mM dNTP mix (2.5 mM of each,

dATP, dCTP, dGTP, and dTTP), 1.3 μL of 10 X polishing buffer and 1 μL of cloned *Pfu* DNA polymerase (0.5 U). The polishing reaction was gently mixed, layered with 20 μL mineral oil and incubated for 30 minutes at 72°C. Finally, the polishing reaction was added directly to the ligation reaction or stored at 4°C until use. Second, by filling 5`-protruting ends using DNA polymeraseI large (Klenow) fragment. The reaction was prepared (in the indicated order) as follows in a 0.5 mL microcentrifuge tube. One-to-4 μg of DNA, 50 mM Tris-HCl (pH 7.2), 10 mM $MgSO_4$, 0.2 mM DTT, 40 mM of dNTP, 20-μg mL^{-1} acetylated BSA and 1 unit of Klenow fragment per microgram of DNA. The reaction was incubated at room temperature for 10 minutes, and heating for 10 minutes at 75°C stopped the reaction. Finally the mixture was purified using QIAquick Nucleotide Removal Kit (Section 2.11.2).

2.2.12.4 Cloning the PCR Product.

Two methods were used for the cloning reaction.

2.2.12.4 1. Cloning of Blunt End PCR Fragment.

2.2.12.4 1.1. Dephosphorylation of Cloned Plasmid.

The plasmid with 5` recessed or blunt end (Section 2.2.11.3) ends were dephosphorylated using calf intestinal alkaline phosphatase(CIAP) before cloning. The dephosphorylation reaction was set up in 1.5 mL microcentrifuge tube in a total volume 30 μL as following: 1-2 μg of purified DNA plasmid: 3 μL CIAP: 10 X reaction buffer (10 mM tris-HCl, pH 7.5): 1 mM EDTA, pH 7.5): 200 mM NaCl: 0.5 % SDS: 1-5 units of CIAP enzyme:

distilled water to a final volume of 30 μL. The reaction was incubated at 37°C for 15 minutes and then a 56°C for 15 minutes. Then a second aliquot of CIAP was added and the incubation at both temperatures was repeated.

2.2.12.4.1.2. Polishing the Purified PCR Products.

The purified PCR products generated with *Taq* DNA polymerase were polished as described in PCR Script Amp Cloning Kit protocol (stratagene, 1998)

Polishing reaction was prepared by adding the following components in order to a 0.5-ml microcentrifuge tube. Ten μL of the purified PCR product, 1 μL of 10 mM dNTP mix (2.5 mM of each, dATP, dCTP, dGTP and dTTP), 1.3 μL of 10X polishing buffer and 1 μL of cloned *Pfu* DNA polymerase (0.5 U). The polishing reaction was gently mixed, layered with 20-μL mineral oil and then incubated for 30 minutes at 72°C. Finally, the polishing reaction was added directly to the ligation reaction or stored at 4°C until use.

2.2.12.4.1.3. Ligation of Blunt End PCR Fragments into Cloning Vectors.

PCR products from section 2.2.14.4.1 were ligated into PET 28A and/or PCR-Script™. The ligation was performed according to the manufacture's instructions given in the PCR-Script Amp Cloning Kit manual.

The ligation was carried out in 0.5 mL microcentrifuge tube by adding the following components: 1 μL of the PCR- Script Amp SK (+) cloning vector (10 ng μL^{-1}): 1 μL of PCR Script 10 X reaction buffer: 0.5 μL of 10 mM rATP: 2-4 μL of PCR product (40:1 to 100:1 insert-to-vector ratio) or 4 μL of the control PCR insert: 1 μL of *Srf* restriction

enzyme (5 $U\mu L^{-1}$): 1 μL of T4 ligase and distilled water to a final volume of 10 μL. The ligation reaction was stored at -20°C until required.

2.2.12.4.2. TOPO Cloning Reaction.

The TOPO reaction was carried out by adding the following component into 0.5 Ependroff tube: 2 μL of fresh PCR product: 1 μL salt solution (1.2 M NaCl and 0.06 M $MgCl_2$): 1 μL TOPO vector: addition of sterile water to a total volume of 6 μL. The reaction was mixed gently, incubated for 5 minutes at room temperature (22 -23°C) and placed on ice or stored at -20°C overnight until the transformation was completed.

2.2.12.4.3. PCR Amplification of Plasmid Vector Insert.

The size of DNA inserts in plasmid vectors were amplified and estimated using PCR amplification with specific primers designed from the ends of each set of gene sequences obtained (Section 2.2.17.4), and /or T3 and T7 primers. The plasmid vector insert was amplified directly from individual bacterial colonies. Approximately one-half of individual fresh bacterial colonies were picked with the tip of a sterile Pasteur pipette and resuspended into 0.5-mL microcentrifuge tubes containing 10 μL of sterile water. The tubes were heated at 95°C for 5 minutes to release and denature the DNA, cooled on ice for another 5 minutes and spun briefly in a microcentrifuge (10,000 g for 20 seconds). Forty μL of the PCR reaction solution was added to each tube in the following order: five μL of 1 X thermophilic *Taq* buffer: 2.5 to 3 mM $MgCl_2$: 200 pmol of dNTPs (dATP, dCTP, dGTP and dTTP): 100 pmol of oligonucleotide primers: 1-2 units *Taq* DNA

polymerase. All the reagents were mixed gently, the mixture was overlaid with one drop of mineael oil (Sigma) to reduce evaporation, and the tubes were placed in a Hybond OMI Gene PCR thermal cycler.

The thermal cycler was programmed to denature the samples for 1 minute at 94°C and then to complete 35 cycles of 94°C for 20 seconds (denaturation), 42-54°C (annealing temperature depended on the primers being used (see Section 2.2 11.1), and 72°C for 2 minutes (extension). At the end of the last cycle the samples were heated at 72°C for a further 3 minutes to ensure full extension of the product and then cooled down to 18°C. The PCR product was electrophoresed on 1 % agarose gel (Section 2.2.7.1).

In addition, on occasions the size of the insert was estimated by restriction enzyme digest and agarose gel electrophoresis with appropriate size markers °C (Section 2.2.4.1 and 2.2.8 respectively).

2.2.13. Differential Display Reverses Transcription PCR.

2.2.13.1. Reverse Transcription of Total RNA.

RNA extracted from treated and untreated cell suspension cultures was purified with a Purescript Kit (Flowgen, Shenstone, Staffs, UK). To remove any potential DNA contaminants, RNA was treated with DNase 1 (Message Clean Kit, GenHunter Corp., Nashville,TN).

Differential Display – PCR (DD-PCR) was carried out with an RNAimage kit No. 3 (GenHunter Corp,) according to the manufacture's instructions but with some modification. First-strand cDNA synthesis was carried out in duiplicate with three

different 1 base anchored primers (H-T_{11}M, where M may be G, A, or C). Reactions (20 μL) containing 200 ng of freshly deleted total RNA, 250 μM dNTPs, 2 μM H-T_{11}M primers, 100 U MMTV reverse transcriptase , 5X RT buffer (125 mM Tris-HCl, 188 mM KCl, 7.5 mM $MgCl_2$ and 25 mM DTT). The PCR reactions were incubated in the thermocycler in the following conditions 65°C for 5 min., then at 37°C for 10 min., before addition of MMLV reverse transcriptase, after that the reaction incubated at the same temperature for further 50 min, finally 75°C for 5 min.

(replace the above with the section from Chapter 5)

2.2.13.2. Amplification of First Stranded cDNA By PCR.

First stranded cDNA was amplified by PCR with one of the eight H-AP primers in combination with one of the three-anchored H-T_{11}M primers. Reactions (20 μL) containing 2 μL of 10X PCR buffer (100 mM Tri-Cl, pH 8.4: 500 mM KCl: 15 mM $MgCl_2$: 0.01 % gelatin), 1.6 μL dNTPs (25 μM), 2 μL of each eight H-AP primers (2 μM), 2 μL H-T_{11}M (2μM), 2 μL of RT-mix from step A (it has to contain the same H-T_{11}M used for PCR), 2 μCi [α-^{32}P] dCTP, 1 U *Taq* polymerase (Boehringer Mannheim UK, Lewes, UK). The reactions were assembled in 200 μL thin-walled tubes (Micro-Tubes; Biogene, Cambridge, UK) and all the PCRs were carried out in an Air Thermo-cycler (model 1605; Idaho Technology, Idaho Falls, ID), under the initial hot start 94°C for 30 s one cycle, 40 cycles of amplification were carried out, each cycle consisted of 15 s at 94°C, 120 s at 40°C, 30 s at 72°C, temperature slope setting = 3 (equivalent to a temperature ramping speed of approximately 1°C s^{-1}). This was followed by a final

holding temperature at 72°C for 5 min. DD-PCR products were analyzed on 0.6 % polyacrylamide sequence gels.

2.2.13.3. . 0.6 % Polyacrylamide Sequence Gels.

Sequencing gel plates, which measured 20-cm x 40 cm, were washed with detergent and one of the two plates was, siliconized as described in (Section 2.1.3.5). Forty-cm spacers with 94 mm thickness were placed between the plates, which were then taped together. Fifty mL of de-gassed sequencing solution (6% acrylamined: bisacrylamid, (3: 2 w/v), 7 M urea, 1X TBE) supplemented with 30 μL of 10% ammonium persulphate (w/v) and 50 μL TMED (Sigma) was mixed and poured between the plates. After placing a 24- well comb in place, the gel was allowed to set at room temperature for a minimum of 2 h. The gels were then re-run for minimum of 30 min at 35 W in TBE buffer. Aluminum plates were fixed to the sequencing plates to ensure even heat distribution. When the gel was electrophoresed for the appropriate time period (usually 2-6 h) at constant voltage or 35-40 W. After electrophoresis, the plates were prized apart carefully ensuring that the gel remained stuck to the unsiliconized plate. The gel was transferred onto 3 MM Whatman paper, covered with Saran Wrap and dried on a lab-drier at 80°C for 2 h. After removing the Saran Wrap the gels were autoradiogarphed for 25 hrs at room temperature.

2.2.13.4. Re-amplification of cDNA Eluted from Dried Gels.

The dried gels were exposed to X-ray at room temperature for 4 to 6 hr. Bands were excited from the dried gels with a scalpel. DNA was eluted from the slices according to

the instructions from the RNA image Kit, but with some modifications. Briefly, the gel slice, along with 3 MM paper, was soaked in a 100 μL of dH_2O for 2 to 4 hr, boiled for 15 min., and then centrifuge for 5 min., to pellet paper and gel debris. The DNA in the supernatant was ethanol precipitated with glycogen (10 mg/mL), and re-suspended in 10 μL of dH_2O. Re-amplification was performed in a total volume of 40 μL containing 3.2 μL dNTPs (250 μM), 4 μL H-AP primers (2 μM), 4 μL H-T_{11}M (2 μM), 4 μL (either undiluted or diluted 1: 10) cDNA, 4 μL 10X PCR buffer, and 0.4 μL *Taq* polymerase (.05 U). PCR conditions were as follows: 15 s at 94°C; 40 cycles (12 s at 94°C, 15 s at 40°C, 30 s at 72°C, temperature slope setting = 3); 5 min at 72°C.

Ten μL of the PCR products were run on 1.5 % agarose gels to check whether the size of re-amplified PCR products were consistent with their size estimated on the DNA sequencing gel. The remainder of the PCR products were used for further work.

2.2.13.5. Synthesis of Double-Stranded cDNA From Total RNA.

Synthesis of double-stranded cDNA from total RNA was prepared according to Roche Molecular Biochemicals instructions.

2.2.13.5.1. Frist Strand cDNA Reaction.

Ten-to-twenty μg of tolal RNA was added to a sterile 1.5 mL reaction tube containing 2 μL of oligo [(dT) T7 promoter] primer 100 pmol μL^{-1}, and the total volume was made up to 21 μL with autoclaved DEPC-treated water and incubated at 70 °C for 10 min in a water bath, and then immediately placed on ice. After that, the following components

were added: 8μL RT-buffer, 5X conc. (vial 1): 4μL DTT 0.1M (vial 3): 2μL AMV25U/μL (vial 2): 1μLRNase inhibitor, (Vial 4): 25U μL^{-1}: 4μL dNTP Mix: 10mM Na^{+}dNTP (vial 7): 1μL dCTP. The contents were mixed gently and incubated for 60 min.at 42°C, and then placed on ice to terminate the reaction.

2.2.13.5.2. Second strand cDNA synthesis.

The following components were pipette into the first strand tube after thawing: 30μL 2nd strand buffer 5X conc. (vial 9): 1.5 μL dNTP Mix, 10mM each (vial 7): 6.5μL 2nd strand enzyme blend (vial 10): autoclaved DEPC-treated water to a final volume of 150μL. The contents were mixed gently and incubated for 2 hours at 16°C; 20μL (20U) T4DNA polymerase was added to the reaction and incubated for 5min., at the same temperature. Seventeen μL 0.2 M EDTA, M pH 8.0 was added to stop the reaction. After ds cDNA synthesis, the residual RNA was digested by adding 1.5μL (15U) RNase1 and incubating for 30min at 37°C; subsequently, 5μL (3U) Proteinase K was add to the reaction and the incubation continued for another 30minutes at 37°C.

2.2.13.5.3. Cleaning the Double Stranded cDNA.

Double strand cDNA was purified by a Nick column according to the manufacture's instructions. The top cap of the Nick column was removed, the excess of liquid was poured from the column and the rinsed with equilibration buffer (TE buffer, pH 8.0). The gel bed was equilibrated with 3 ml of TE buffer, then the sample of double stranded cDNA was added to the column. The column was washed with 400 μL of the buffer and

1 μL of the wash was kept for measuring the un-incorporated radioactive material in the sample. The purified sample was eluted from the column with 400 μL buffer solution and 1 μL was kept for measuring the incorporated radioactive material.

2.2.13.5.4. Preparation of Radio-labelled cDNA for Reverse Northerns.

The cDNAs were synthesized as described before but with an T7-oligo (dT) primer to prime first-strand cDNA synthesis.

A symmetric amplification of the cDNA was carried out in 50 μL reaction containing: 40 ng of cDNA, 500 nM T7 primer (5`GTAATACGATCACTATAGGC), 200 μM dATP, 200 μM dTTP, 200 μM dGTP, 12 μM dCTP, 100 μCi [α-^{32}P] dCTP, 5 U *Taq* polymerase and 5 μL reaction buffer. Amplification was carried out in an air thermocycler under the following conditions: 30 s at 94°C, 35 cycles (10s at 94°C, 20 s at 41°C, 80 s at 72°C, temperature slope setting = 3 [equivalent to a ramp speed of 3°C.s^{-1}], 5 min at 72°C.

2.2.13.5.5. Measurement of Incorporated Radio-nucleotides into cDNA.

The measurement of incorporated radio-nucleotide into the cDNAs was carried out as described in section (2.2.11.2).

2.2.14. Slot Blot Analyses.

2.2.14.1. Slot Blot of Bands.

Ten μL of PCR products was diluted in 90 μL of 0.1X SSC, denatured for 5 minutes at 100°C, and then cooled on ice. The slot blots were assembled as followers: the two

pieces of perspex were connected together. Two sheets of 3 MM Whatman paper were cut to fit inside the rubber lining and placed on the apparatus. A piece of Hybond-N nylon membrane (Amersham International, Little Chalfont, UK), was cut to the required size for the amount of samples, one Whatman sheet was soaked with 0.1X SSC and used to wet the Hybond-N nylon membrane to avoid the bubbles, and placed on the top the 3 MM Whatman papers. The perspex top was placed on the top of the membranes and the side clips was used to clamp the apparatus together. The vacuum line was connected to a vacuum pump (Minifold II, Schleicher and Schuell, Dassel, Germany) and low vacuum was used to dry the membranes before loading the samples. The denatured samples were added into the wells under the low vacuum and allowed to pass through on to the membrane. Once transfer was complete, the membrane was removed. The nylon membrane was placed DNA-side down onto sheet of Whatman 3 MM paper soaked in a tray containing Denaturing Solution (0.5 M NaOH; 1.5 M NaCl) for 5 minutes. The membrane was then carefully drained of excess solution and transferred DNA-side down onto a fresh sheet of Whatman 3 MM paper soaked in Neutralization Solution (1 M Tris-HCl, pH 8.0; 1.5 M NaCl) for a further 5 minutes. Finally, the membranes were rinsed briefly in 2X SSC and left (DNA-side up) on Whatman 3 MM paper to dry overnight. The DNA was fixed onto the membrane by UV radiation. Denatured plasmid DNA from pBluescript II SK$^-$ (stratagene, Cambrige, UK) that contains a partial length (300 bp) actin cDNA clone from *Arabidopsis thaliana* were applied in duplicate slots to each filter.

2.2.14.2. Slot Blot Hybridization Analysis.

The hybridization, membrane washing, and autoradiography were carried out as described in section (2.2.12.1& 2.2.12.2 and 2.2.12.3) respectively, except that the membranes were hybridized for two days.

2.2.15. Database Searches.

2.2.15.1. Keyword and Homology Searches.

The program ENTREZ was used at the NCBI site (http://www.ncbi.nlm.nih.gov) to search for key words, and for nucleotide and amino acid sequences. BLAST2 searches for sequence homology were also performed from the NCBI or EBI site (http://www2.ebi.ac.uk/), to identify sequences with global and local homology (conserved motive sequences).

2.2.15.2. Structural Prediction.

TMPred is one of structural prediction programs found at http://dot.imgen.bcm.tmc.edu:9331/seq-search/struc-predict.html. This program analyses submitted amino acids sequences and predicts the structure of the resulting polypeptide. TMPred is based on statistical analysis of the Tmbase database of naturally occurring transmembrane proteins. The program gives a prediction of the number of transmembrane helices in give polypeptide sequence.

The TMPred output displays a hydropathy plot, as described by Kyte and Doolitte (1982). Each amino acid is given a hydropathy score corresponding to its degree of hydrophobicity. Hydrophobic amino acids have a positive hydropathy score, and

hydrophylic amino acid have a negative hydropathy score. A 'moving-segment' approach is used, in which the average hydropathy score for each segment is calculated and plotted. Region of hydrophobic sequence, *i.e.* positive hydropathy values, indicates areas which are likely to be within a membrane. This information can be related to possible functions.

2.2.15.3 Identification of Interest Regions In Nucleotides Sequences.

The **NIX** program (http://www.hgmp.mrc.ac.uk/) is intended as a toll to aid the identification of interesting regions in Genomic or transcribed nucleic acid sequences and presenting the results as one page of information. NIX analyses DNA sequences to identify promoter regions, transcription and translation start and stop sites, intron / exon boundaries, *etc.*,. Many algorithms have been developed to identify these structural motifs, NIX runs most of these programs and produces a consensus view of the DNA fragmant.

2.2.15.4. Primer Design.

Primer design is crucial for the success of PCRs. Suitable primers were found using both of PRIMER3 and web PRIMER DNA programs found at (http://www-genome.wi.mit.edu/cgi-bin/primer/primer3), and (http://genome.www2.stanford.edu/cgi.bin/SGD/web).

2.2.15.5. Determination of Endonucleases Sites.

Sites of endonuclease attack in given DNA sequences were determined using the web-based program WEB CUTTER found at (http://searchlauncher.bcm.tmc.edu/).

2.2.15.6. Alignments.

ClustalW (http://www2.ebi.ac.uk/clustalww/) was used for multiple sequence analysis. This program aligns DNA or protein sequences from a submitted group, and highlights areas of sequence homology. Phylogenic relationships were presented using Tree View (http://taxonomy.zoology.gla.ac.uk/rod/treeview.html).

2.2.16. DNA Sequencing.

DNA sequencing of the plasmid insert was performed by MWG-Biotech GmbH.

CHAPTER THREE

CHRACTERIZATION OF HHS AND WT ARABIDOPSIS CELL LINES

CHAPTER THREE

3. Characterization of HHS and WT *Arabidopsis* Cell Lines.

Unlike animals, plants can not escape from harsh conditions, therefore, plants have been endowed by nature with a remarkable array of responses and mechanisms to allow survival in many inhospitable environments. Cell suspension cultures have several advantages compared with the intact plant for studying the effects of environmental stress on the cell and molecular biology of plant cells. Cultured cell lines with enhanced tolerance to sodium chloride have been isolated from moderately salt tolerant plants of alfalfa and tobacco (Croughan,*et al.*, 1978; Hasegawa, *et al.*, 1980) and from halophytes such as *Atriplex nummularia L* (Casas, *et al.*, 1991).

This chapter will focus on the morphological adaptations expressed in the HHS (Habituated to High Salt) cell lines of *Arabidopsis thaliana* that can survive in 380 mM NaCl, approximately four times the level of salt that is lethal to wild type *Arabidopsis* cell lines. Fluorescence, electron and light microscopy was used to compare the morphology and ultra-structure of the HHS and WT cell cultures.

3.1. Fluorescence Microscopy.

The HHS cell line was developed from a wild type (WT) cell line that was established by May and Leaver (1993) Preliminary experiments at Glasgow had shown that 70 mM NaCl in the growth medium (see Section 2.1.4.1) was lethal, and completely arrested growth (J. Laird and P. Dominy, unpublished). To establish a salt-resistant cell line, WT cultures were grown near their limit of survival (50 mM NaCl), and each week these cultures used to start fresh cultures

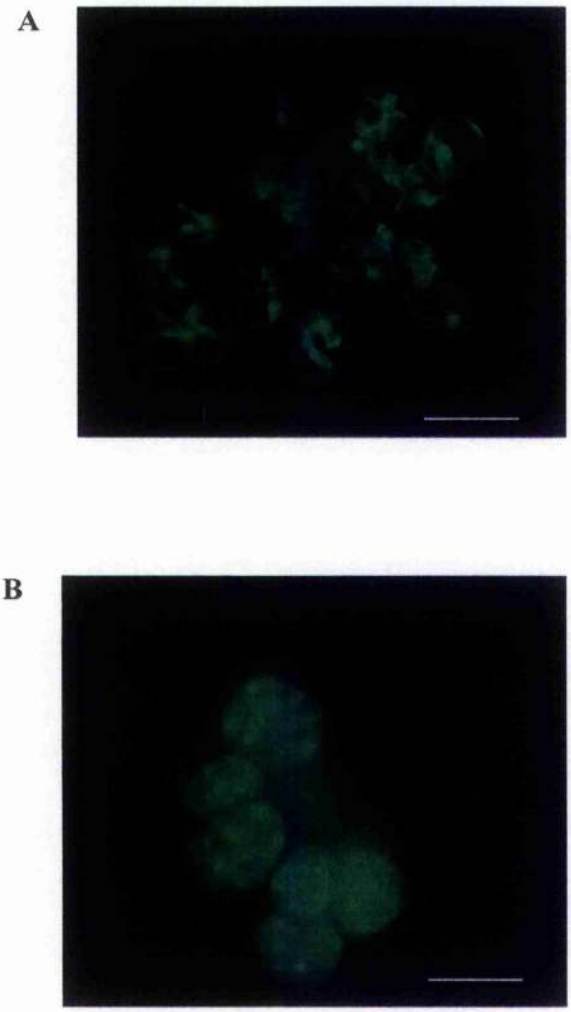

Fig. 3.1. *Arabidopsis thaliana* Cell lines Stained with FDA.

A, *A.thaliana* salt-sensitive cells, note large central vacuoles without fluorescence, and the absence of small intracellular vacuoles and vesicles. B, HHS *Arabidopsis* cell lines stained with the FDA stain. Note the dye appears to accumulate into small vacuoles and intracellular vesicles. Cells (~1ml) from 3 days old cultures were removed and 0.5 µl of FDA (1mg/ml) added. Cells were harvested by gravity after 2 minutes, washed 2 times in growth media (MS, 3% w/v sucrose, or isotonic sorbitol solution, as appropriate), and visualized by fluorescence microscope fitted with fluorescin filters. The scale bar represents 20 µm.

supplemented with either 50 mM or 70 mM NaCl. Each week the cultures exposed to 50 mM NaCl survived, whereas the cultures exposed to 70 mM did not. However, after a year, a level of mutation and/or selection had occurred that allowed cells in 70 mM NaCl to survive. Within one year of this, the salt-adapted cell lines were surviving in 250 mM NaCl, and subsequently, the HHS culture has adapted to 380 mM NaCl.

The conclusion from experiments are that, as long as an adequate supply of energy is provided, *Arabidopsis thaliana* possesses the genetic potential to maintain ionic and osmotic balance, and in effect, to shows halophytic adaptation.

Figure 1 presents typical views of the control (Fig. 3.1A) and HHS (Fig. 3.1B) cells grown in MS medium supplemented with 0 or 300 mM NaCl respectively. In order to show better the arrangements of the endomembrane system, cells were briefly incubated (2 min) with the fluorescent dye fluorescine diacetate (FDA) and washed 2 times in growth medium (MS, 3% w/v sucrose, or isotonic sorbitol solution). Striking differences in the arrangement of the endomembrane system are apparent. Over this incubation period, the control cells took up stain into their cytoplasm, but not into their large central vacuoles which remained clear of florescence (Fig. 3.1A). In contrast, the HHS cells rapidly accumulated FDA into a large numbers of what appears to be small vacuoles (Fig. 3.1B); some staining of the cytoplasm was apparent, and large un-stained vacuoles were also observed (not shown in Fig. 3.1B). FDA is routinely used as a viability stain to confirm whether populations of cells are living or not. The dye is taken up into cells across the plasma membrane as the neutral ion, but then de-protonates to form the mono-anion (pK~5) and at higher pH, the di-anion (pK~6.4). Only the mono-anionic and di-anionic forms are fluoresent with quantum yields of 0.37 and 0.93 nm respectively (Hogland, 2002). The appearance of the small vacuoles in the HHS cell line

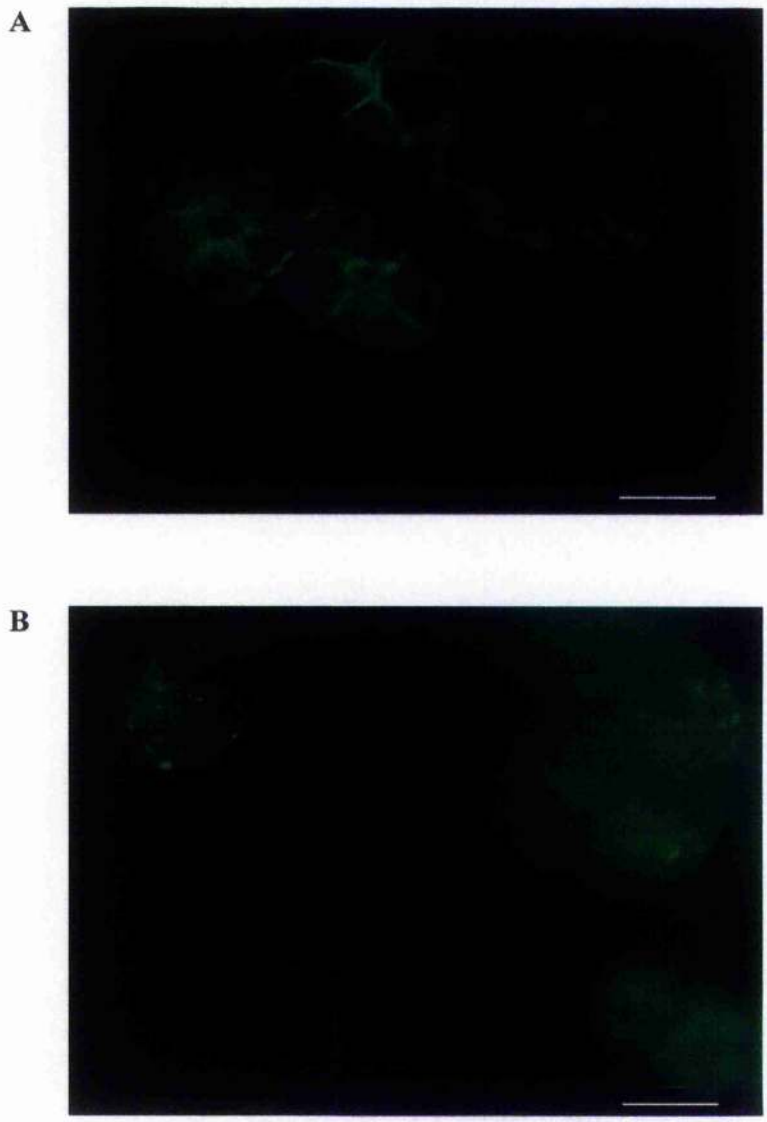

Figure. 3.2 *Arabidopsis thaliana* **Cell Lines stained with BCECF.**

A, *A.thaliana* salt-sensitive cells stained with BCECF, note large central vacuoles without fluorescence and the absence of small intracellular vacuoles and vesicles. B, HHS *Arabidopsis* cell lines stained with the BCECF stain. Note the presence of the bright green fluorescence into small intracellular vesicles, and large unstained vacuoles are also observed. Cells (~1ml) from 3 days old cultures were removed and 0.5 µl of BCECF (1 mg/ml) added. Cells were harvested by gravity after 2 minutes, washed 2 times in growth media (MS, 3% w/v sucrose, or isotonic sorbitol solution, as appropriate), and visualized using a fluorescence microscope fitted with fluorescin filters. The scale bar represents 20 µm.

(Fig. 3.1B) is anomalous. The bright fluorescence from these compartments implies that either the lumen of these vacuoles is positively charged compared with the cytoplasm (promoting the uptake of anionic FDA), and/or their lumen is more basic than the cytoplasm (> pH 8).

In order to check the pH of the lumen of these vacuoles, control and HHS cells were incubated for 2 min in the pH-sensitive fluorescent dye BCECF, washed extensively in growth medium, and then visualized using a fluorescence microscope. Again, control cells took up stain into their cytoplasm, and large unstained central vacuoles were apparent (Fig. 3.2A). In contrast, in BCECF-stained HHS cells, a few, relatively unstained central vacuoles were observed, but many brightly fluorescing small vacuoles/vesicles were present. BCECF can possess 4 or 5 negative charges at high pH (pK~6.9) and the anionic form fluoresces brightly (at 533nm; Hogland, 2002). These findings may be interpreted in a similar way to those from FDA (Fig. 3.1), the bright BCECF fluorescence observed in the small vacuoles may arise from a membrane potential-driven accumulation of this anionic dye in the lumen, and/or from the alkaline interior of these compartments inducing higher fluorescence yield. To establish the mechanisms responsible for the high fluorescence observed from these small vacuoles/ vesicles, control and HHS cell lines cells were incubated with the cationic chloride sensitive dye lucigenin. Lucigenin is a dicationic dye at physiological pH, and emits at 505 nm with a quantum yield of 0.6 (Hogland, 2002). Again, as with FDA and BCECF (Figs. 3.1 and 3.2), after a brief incubation (2 min) WT cells accumulate lucigenin in their cytoplasm; large, unstained central vacuoles are also present. However, in the HHS cells, as before, within 2 minutes small vacuoles in the cytoplasm are observed to fluoresce brightly. Larger, relatively unstained central vacuoles were also observed.

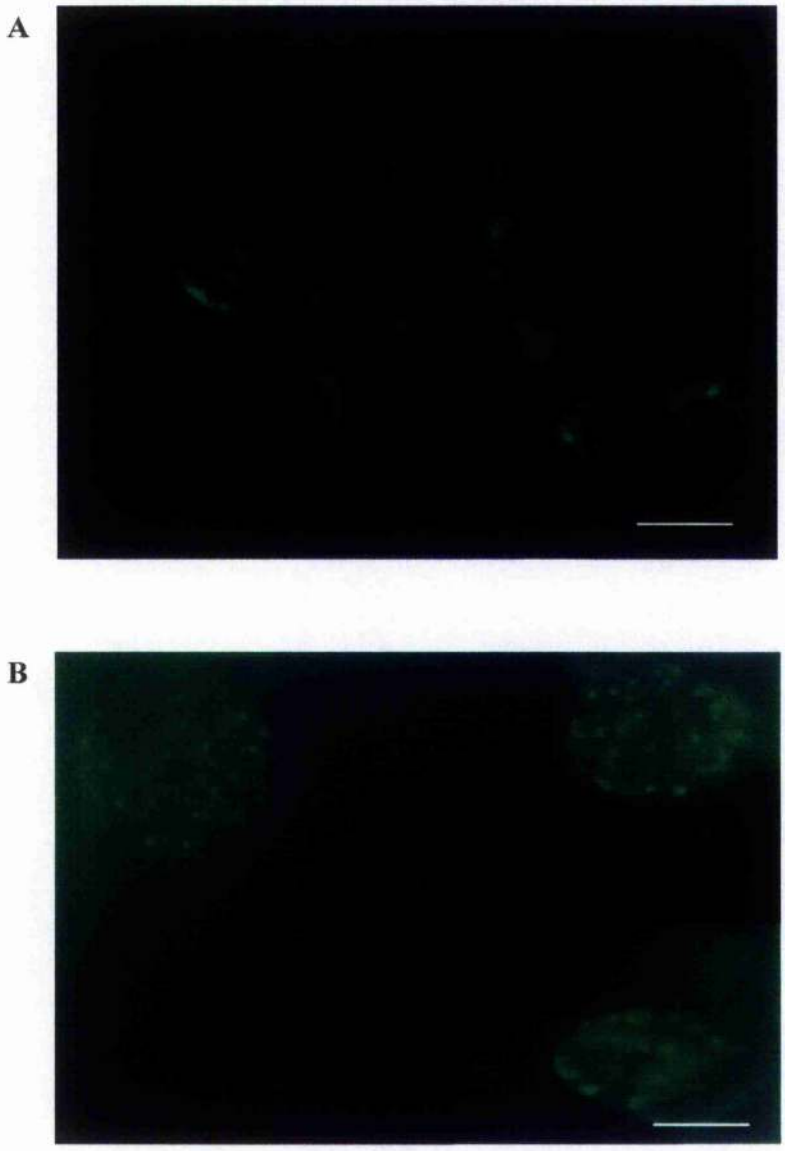

Figure. 3.3. *Arabidopsis thaliana* Cells Stained With the Lucegenin .

A, *A.thaliana* control cells (0 mM NaCl) stained with lucigenin, note large central vacuoles without fluoresce and the absence of small intracellular vacuoles and vesicles. B, HHS *Arabidopsis* cell line (300 mM NaCl). Note intense green staining in the small intracellular vesicles; unstained central vacuoles are also observed. Cells (~1ml) from 3 day old cultures were removed and 0.8 µl of BCECF (1mg/ml) added. Cells were harvested by gravity after 2 minutes, washed 2 times in growth media (MS, 3% w/v sucrose, or isotonic sorbitol solution, as appropriate), and visualized using a fluorescence microscope fitted with fluorescin filters. The scale bar represents 20 µm.

Taken together, the results from the fluorescent stains are difficult to reconcile. It would seem that the rapid appearance of FDA and BCECF (anions), and of lucigenin (cation), in the small vacuoles in the HHS cells can not be explained by membrane potential gradients. However, although FDA and BCECF increase their fluorescence yield with pH, lucegenin is relatively insensitive to pH changes above 8.0, and therefore, the bright fluorescence observed from these vesicles can not be explained on this basis either.

3.2. Electron Microscopy.

The ultra structure of the WT and HHS cell line was further investigated by electron microscopy. Wild type and HHS cells were grown in MS media, 3% w/v sucrose, and 300 mM NaCl (see Section 2.1.4.1 Material and Methods). Fresh cultures were started and cells were harvested after 3 days. Samples were allowed to settle under gravity, excess growth media removed, and samples immediately fixed with 0.1% glutaraldehyde before preparation for thin–section EM (Section 2.1.4.3 Material and Methods). Figure 3.4 presents a TS electron micrograph (TSEM) of a typical HHS cell line preparation. Clearly visible are the cell wall, nuclear membrane, plastids and nucleolus within the nucleus. There is some evidence of nuclear aberrations, as some smaller fragmented nucleoli appear to be present. However, most striking of all is the presence of a large number of small vacuoles (>0.2 μm), and smaller vesicles (<0.2 μm). Presumably, these take up stain and give rise to the bright fluorescence observed with the fluorescence microscope (Figs. 3.1B, 3.2B and 3.3B). Large central vacuoles were also observed in these sections (not shown), although when compared with WT cells grown in low salinity (0 mM NaCl), they were reduced in size (30-40% cell volume *cf.* 80-90% cell volume in WT).

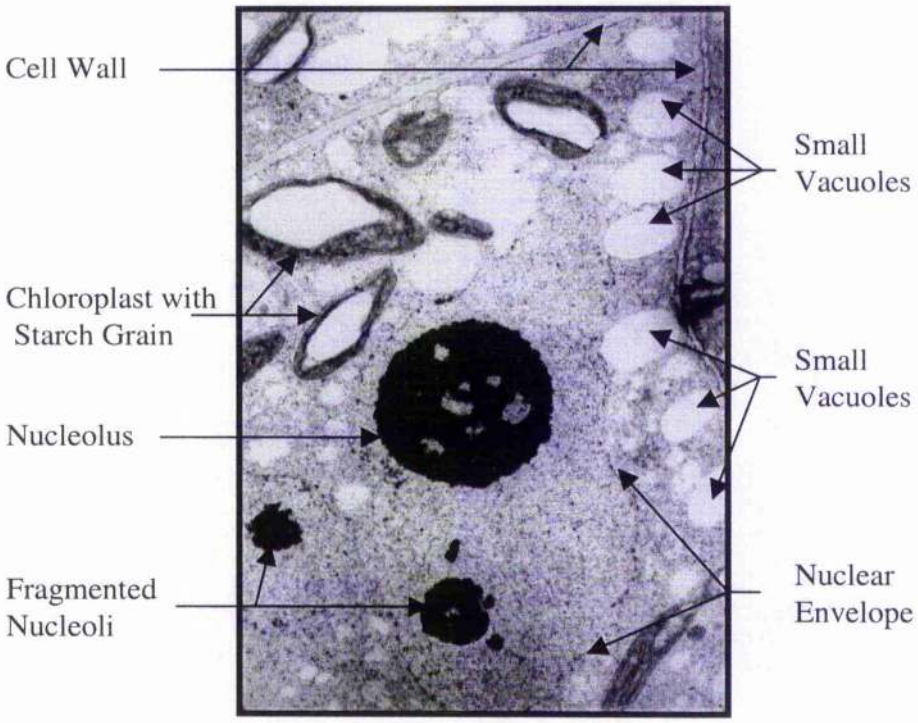

Figure. 3.4 EM Section from the HHS *Arabidopsis* Cell line Grown in High Salt.

The view represents small vacuoles close to the cytoplasm membrane and may represent docking. Also present are a large numbers of endo-membrane compartments of <200 nm dimensions (*i.e.*, vesicles), which may be involved in salt trafficking. Note dark-staining fragmented chromatin. Magnification, 13,000 X.

Figure 3.5 shows a typical TSEM from the WT cell line grown in low salt. Large central vacuoles are present, and a well-defined nucleus with a single nucleolus; plastids and micro-chromatin nucleus are also observed. However, unlike the HHS cells, few small vacuoles/vesicles are seen.

It is conceivable that the brightly fluorescing small bodies observed in Figs 3.1B; 3.2B and 3.3B do not represent the presence of fluorescent dyes in the lumen of the small vacuoles shown in Fig 3.4, but merely reflect the presence of dye bound to the surface of their membranes. To confirm whether or not FDA, BCECF and lucigenin are taken up into these small vacuoles/vesicles, confocal microscopy was used. Samples from WT (0 mM NaCl) and HHS (280 mM NaCl) cell lines were prepared and stained with FDA. The samples were then optically sectioned (Z-plane) with a resolution of 0.8μm using a Zeiss Pascal confocal microscope. Typical images are presented in Fig.3.6. Wild type cells showed a similar cell structure to that described before. Large central vacuoles were observed in all cells and accounted for > 80 % of the cell volume; some fluorescent dye was observed in the cytoplasm of these cells, but not in the central vacuoles (Fig. 3.6A). In contrast, although large central vacuoles were observed in the HHS cells (Fig. 3.6B), their volume was reduced (30-40% cell volume), and many brightly fluorescing small bodies were observed. Careful examination of all of the Z-sectioned images failed to show any rings of fluorescence, which would have been indicative of a section through a vacuole with FDA binding to the membrane. It is therefore concluded that FDA is taken up into the small vacuoles/vesicles shown in Fig 3.4 and gives rise to the brightly fluorescing bodies observed. Presumably, other anionic (BCECF) and cationic (lucigenin) dyes are also taken up into these endo-membrane compartments. Similar results have been obtained (Dr P. Dominy, per.com.) with other

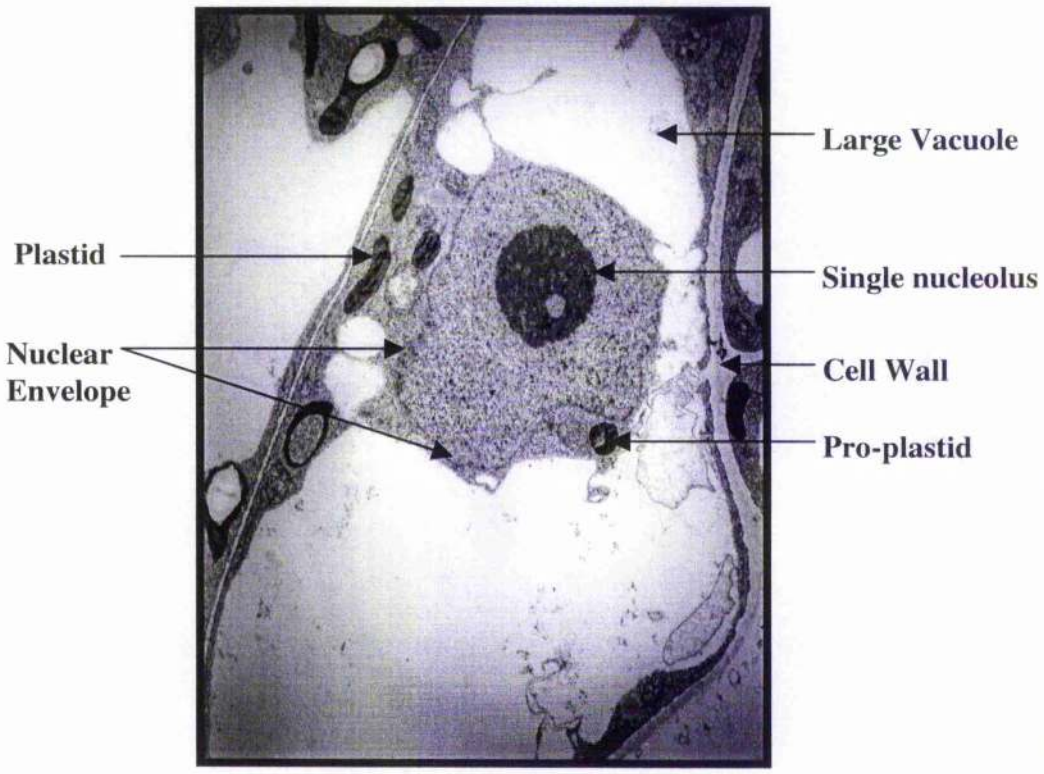

Figure. 3.5. Thin Section EM of Cell from Wild Type *Arabidopsis* Cultures Grown in Low Salt.

Samples were grown as described (Section 2.1.4.1, Material and Methods), harvested after 3 days growth. The samples were spun down (140 to 150 g for 3 to 4 minutes), excess growth media removed. Samples immediately fixed with 0.1% glutaraldehyde before preparation for thin-section EM. Magnification, 13,000X.

fluorescing dyes (anionic SBF1 [Na^+], PBF1 [K^+]: zwitherionic, SPQ [Cl^-]). Further, a rapid rise (<2min) in the fluorescence of these small bodies was observed when the anionic pH-sensitive dye carboxy-SNAFL was used; however, unlike BCECF, carboxy SNAFL quenches with increased pH, and therfore, obsevations that both of these dyes fluoresce brightly in the small vacuoles precludes a role for pH. Taken together, these results suggest that the extensive vacuole/vesicle membrane system in the HHS cell line rapidly accumulate anionic, cationic or zwitherionic solutes. The mechanisms by which this achieved are unclear, but it is unlikely to be driven by membrane potential alone; an active pumping system may be involved (*e.g.*, ABC transporters/GSX-pumps; Theodoulou, 2000).

Regardless of the mechanisms for sequestration of these fluorescent dyes, it is tempting to speculate that the presence of the extensive endomembranous system observed in HHS cells is involved in salinity tolerance/detoxification. For example, these small vacuoles/vesicles may be involved in the rapid sequestration of Na^+ and Cl^- ions from the cytoplasm, or alternatively in trafficking a potentially toxic level of electrolyte between the large central vacuole and the apoplast (exocytosis or endocytosis).

3.2.1 Cellular Sequestration/Cellular Trafficking.

3.2.1.1 Plasma Membrane and Endo-membrane Fusion.

In spite of the limitations of cell suspension cultures, they offer several advantages over the intact root systems to study different environmental stress tolerance mechanisms. One advantage is that all cells must be expressing an appropriate array of responses to allow

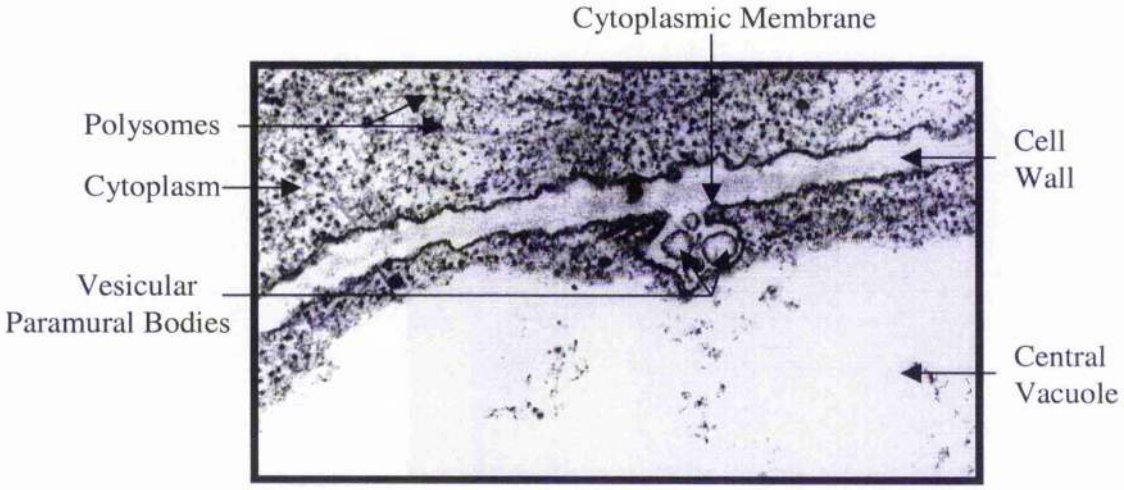

Figure. 3.7. Electronmicrograph of *Arabidopsis* WT Cell Line.

The view illustrate the presence of vesicular Paramural Bodies close to the cell wall, outside the plasma membrane, which may reflect passage of vesicles through the plasma membrane, or extrusions derived from the plasma membrane into the apoplast space. The possible contact point between the tonoplast and the cytoplasmic membranes are also observed. Magnification, 40,000 X.

survival at high salinity; and therefore experimental difficulties that arise from division of labour between tissues is circumvented. One possible mechanism for maintaining ion homeostasis is exocytosis. It is conceivable that salt is sequestered into small vacuoles or vesicles by the operating of pumps and that once loaded, these endomembranes traffick to the cell surface, fuse with plasma membrane, and eject their cargo into the cell wall space.

There is a little ultra-structural evidence to support such a mechanism, but when the HHS *Arabidopsis* cell line is grown in high salt a large number of small vacuoles/vesicles can be observed (Fig. 3.4 and 3.8). Numerous vesicles are aligned close to the plasma membrane, and such an arrangement could be interpreted in terms of the docking of vesicles before fusion (Figs.3.4 & 3.8). Similar observations have been made by Cardale and Field (1971) in their studies of the salt-secreting gland cells of *Tamarix aphylla*, and Shimony *et al.* (1973) in the salt glands of the mangrove species *Aegiceras corniculatum* and *Avicenia marina*. Secretory vesicles dock onto the plasma membrane without fusion, and the two membranes system (endo-membrane and plasmalemma) form junctional complexes where channels on both membranes connect allowing passage of solutes from the vesicles to the exterior (Vassilyev and Stepanova, 1990).

Endomembrane-mediated transport between vacuoles and the plasma membrane is believed to be effected by one of two fundamentally distinct pathways (*i.e.* carrier-mediated or endomembrane-mediated transport). Secretion vesicle membranes fuse and become incorporated with the plasma membrane, as the secreted material is deposited in the extra cytoplasmic space (Thiel and Battey, 1998; Battey, *et al.*, 1999; Blatt *et al.*, 1999; Echeverria, 2000). Exocytosis is an important mechanism in the incorporation of new proteins and lipids into the plasma membrane and cell wall of WT cells *in planta* and in WT cells in culture (Fig

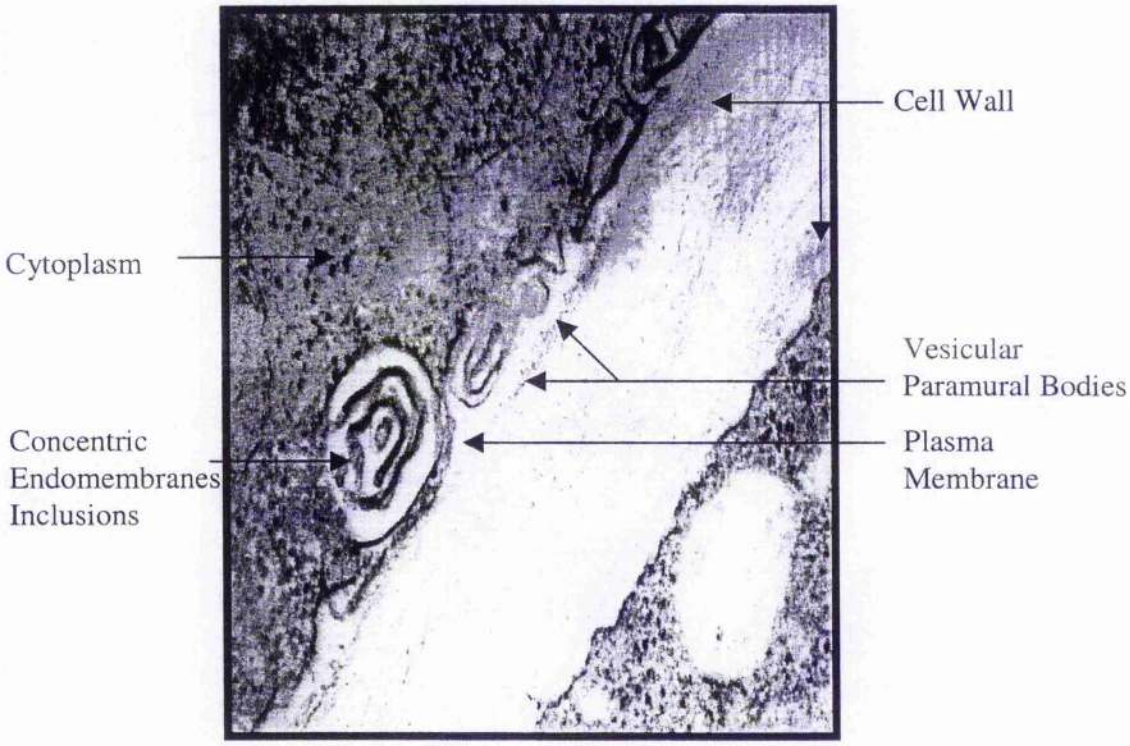

Figure. 3.8. Thin Section EM of the *Arabidopsis* HHS high Salt Grown Cell Line.

Electronmecrograph image of HHS cell line showing plasma membrane/endo-membrane fusion event. Note the contact point between the concentric endo-membranes inclusions (capsulated small vacuoles/vesicles) and the plasma membrane before the release of its content into apoplast space (exocytosis), and the presence of vesicular "Paramural Bodies" between the cell wall and plasmalemma outside the plasma membrane. Magnification, 50,000 X.

3.7); note the extracellular 'paramural bodies' close to the cell wall, which may reflect passage of vesicles through the plasma membrane (as with mucilage secretion in *Plantago* (Hyde,1970).

However, some major differences in the plasma membrane / endomembrane associations were frequently observed in HHS cells (Fig. 3.8). This EM shows structures that may represent plasma membrane / endomembrane fusion event (note the contact point between the concentric (endo?) membranes and the plasma membrane, and the presence of vesicular 'paramural bodies' between the cell wall and plasmalemma.

3.2.1.2. Endomembrane Fusion.

HHS cells grown in high NaCl concentration (280mM) exhibit an abundance of small vacuoles/vesicles and apparent small vacuoles/vesicles fusions (Fig. 3.9). In this EM many single-membraned small vacuoles/vesicles around the periphery of the cell are observed close to the plasma membrane, while others are scattered throughout the cytoplasm. Contact between the small vacuoles / vesicles are also observed (note the small-boxed hooks, Fig. 3.9). These observations suggest that the larger vacuoles result from the dynamic association of smaller vacuoles / vesicles, and it is the latter which are involved in the rapid sequestration of Na^+ and Cl^- ions from the cytosol. Figure 3.10 presents a TSEM of HHS *Arabidopsis* cells grown in high salt (280mM NaCl); the cells contain numerous small vacuoles/vesicles and points of contact (fusion?) can be observed. A higher magnification of a contact point between the endomembranes is boxed (Fig. 3.10). Recent work in plants provides evidence in plants that docking at the plasma membrane is dependent on the formation of SNARE

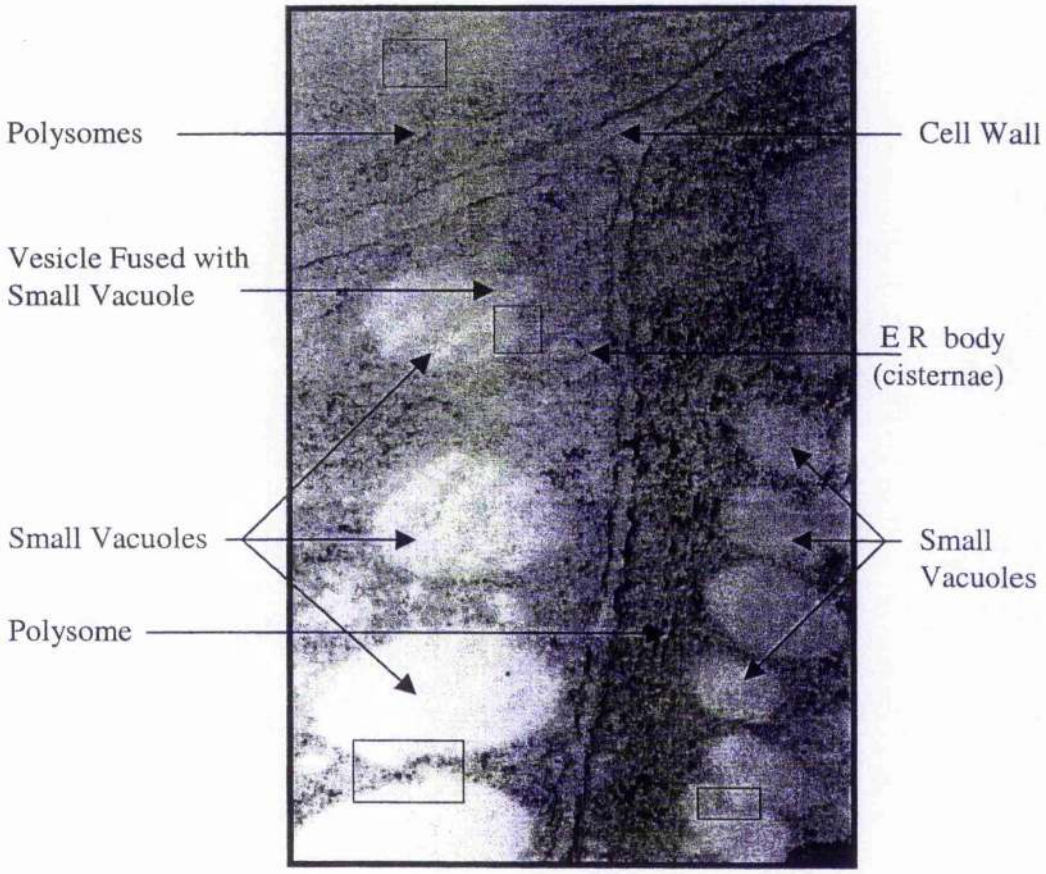

Figure. 3.9. Thin Section EM from the HHS *Arabidopsis* Cell line Grown in High-salt.

The figure represents large numbers of small peripheral vacuoles. Endoendo-membrane fusion (*i.e.*, small vacuoles/vesicles), which requires small vacuoles/ vesicles-to-small vacuoles/vesicles contact are also observed. Note the small boxed hook. This observation suggests that some form of fusion take place between the small vacuoles/vesicles and may allow the solutes to pass between vacuoles/vesicles , and finally eject their cargo into the apoplast space. Magnification, 36,000 X.

vesicle trafficking, fusion and secretion (Ungermann and Wickner 1998, Ungermann *et al.*, 1998).

In comparison, comparable studies on WT *Arabidopsis* cells grown in low salt reveal few small vacuoles/vesicles, but large central vacuoles are observed (Fig 3.5). This suggests that solute trafficking between the central vacuole and the cell wall space appears to occur but at a minimal level and that it is mainly a feature of the salt-tolerant HHS cells.

3.2.1.3. Tonoplast-Endomembrane Fusion.

Under salt stress conditions, cells have to cope with both of ionic and osmotic stress, so they have to deal with an excess of Na^+ in the cytoplasm as well as water deficiency. In order to tolerate high levels of salt, halophytes sequester ions in their vacuoles away from the sites of metabolism (Yeo, 1998). Plant cells are structurally well suited for the sequestration of ions because of the presence of large, membrane-bound vacuoles. It has been proposed that in salt-tolerant plants the compartmentation of Na^+ ions into vacuoles could be achieved through vesicle-mediate transport, or by membrane-bound carriers. The first mechanism requires the movement of solute particles enclosed within numerous small membrane vacuoles / vesicles across the cytosol, and subsequent fusion of pre-vacuoles with the central vacuole (*i.e.* endocytosis; Pincus, 1999).

When TS of salt adapted HHS cells were examined with a transmission electron microscope, numerous small vesicles / vacuoles were observed in the cytoplasm. These may coalesce and eventually fuse with the large central vacuole. Figure 3.11 shows a large number of small vacuoles/vesicles in contact with the tonoplast membrane of large vacuoles. This observation

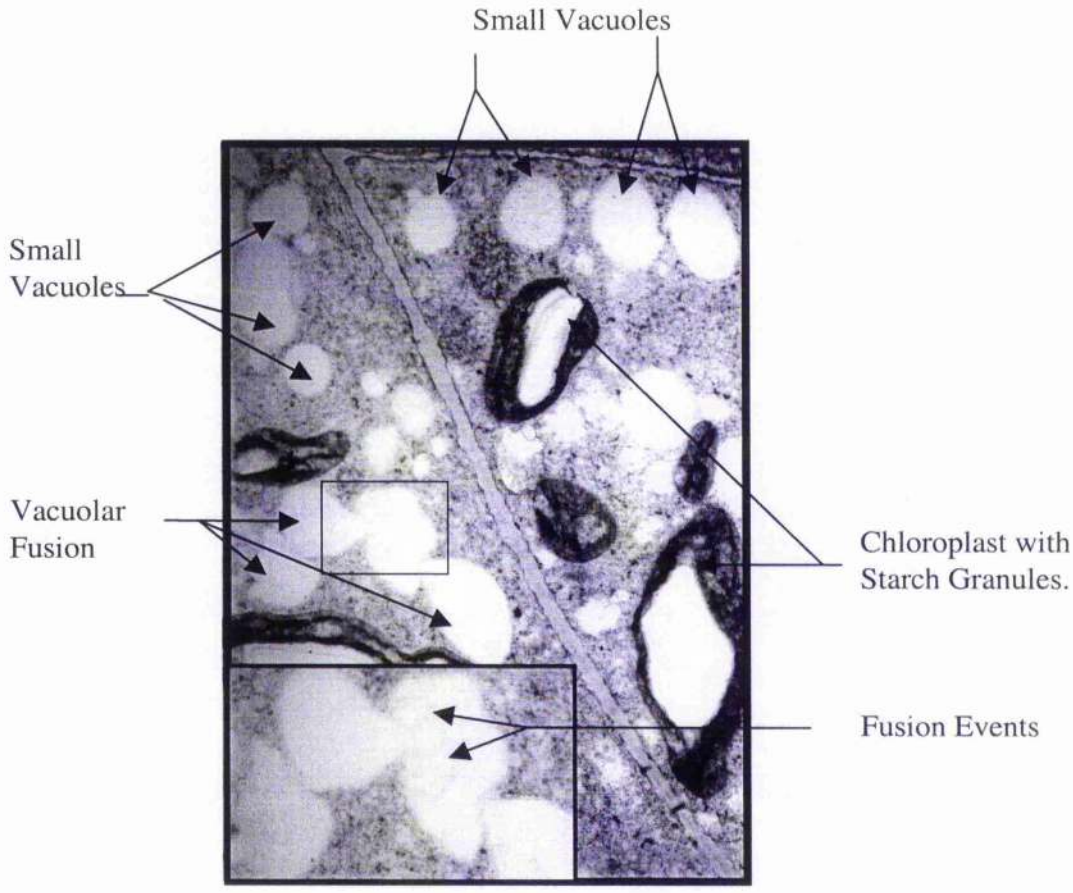

Figure. 3.10. Thin Section EM of HHS Cell Line Showing Possible Endomembrane Fusion Events.

Thin section EM of HHS cells showing possible contact points (fusion) between the endomembrane (*e.g.*, small vacuoles), high numbers of small vacuoles/vesicles appear in the cells. Magnification, 13,000 X. Inset; an enlargement of the boxed area showing possible fusion. Magnification X 26 000.

suggests that the small vacuoles/vesicles may be involved in the rapid sequestration of Na^+ and Cl^- ions from the cytoplasm before they coalesce to form larger pre-vacuoles and subsequently fuse with the central vacuole.

The vacuoles of HHS cells often contained irregular forms of membranous and non-membranous inclusion, as shown in Figs. 3.12 and 3.13. Figure 3.12 shows a TSEM of a large vacuole from an HHS cell that contains an inclusion of membranous material and can be interpreted as arising from a pre-vacuole / vacuole fusion event (autophagey), resulting in compartmentation (Low and Chandra, 1994; Battey, 1999).

Other irregular forms observed in the vacuoles of HHS cells include irregular concentric arrangements of membranous material (Fig. 3.13). It is unclear whether this configuration has arisen by the in-folding of the tonoplast membrane to accommodate osmotically induced changes in the volume of the central vacuole, or from the autophagey partially coated reticulum (Low and Chandra, 1994).

3.3. Nuclear and Chromosomal Aberration.

The HHS cells investigated in this study have clearly undergone some mutations that confer the ability for cells to grow well and survive at high salinity. This contention is supported by comparison of the doubling times of WT cells grown in 0 mM NaCl (~1.9 days) and HHS cells grown in 300 mM NaCl (~3.8 days; P. Dominy, per. comm.). Clearly, HHS cells express proteins involved in salt tolerance that are either not expressed, or expressed at very low levels, in WT cells. It is conceivable that HHS cells have increased their ploidy level, or

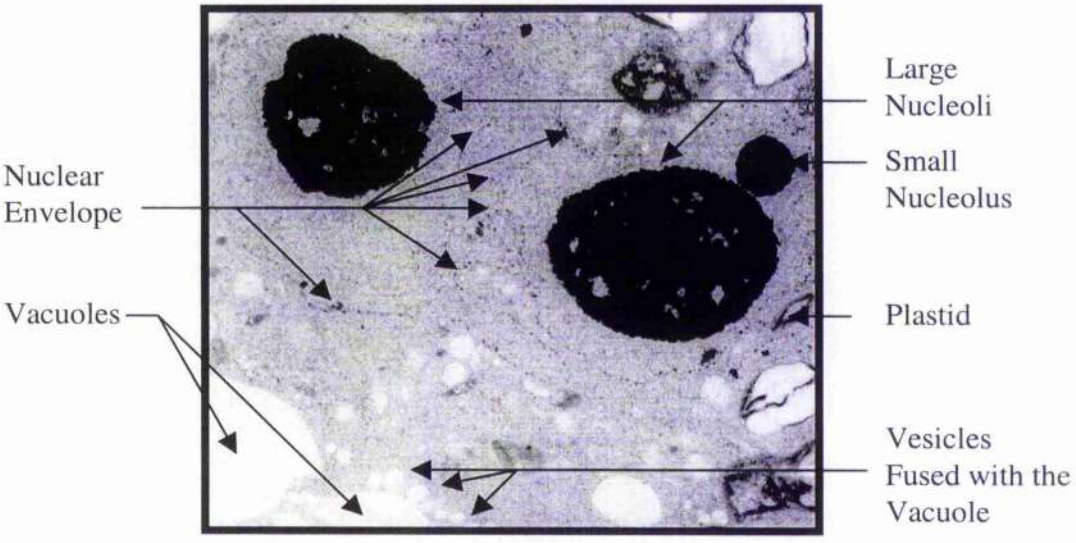

Figure. 3.11. Electron Micrograph of HHS *Arabidopsis* Cell Line Grown in High Salt.

The view showing large number of vesicles scattered in the cytoplasm, and others fused with the vacuole. These vesicles may deposit Na^+ and Cl^- ions into the central vacuole, or to mobilize them in either the apoplast or symplast for long distance transport. The endomytosis (Nucleoli have different size compare with WT, see Fig. 3.5), and the prophase chromosome reduction (the nucleolus smaller than WT) are also presented inside the unclear envelope. Magnification, 13,000 X.

have an altered control of their pattern of gene expression, and this results in the expression of a more effective phenotype for coping with high salinity.

It is conceivable that the HHS cells have increased their ploidy levels by endoreduplication, a process that is known to occur in older leaves of *Arabidopsis thaliana*, particularly when exposed to stress. Endoreduplication arises in somatic cells as a result of several complete rounds of mitotic chromosome duplication without nuclear (and cell) division. In *Arabidopsis* plants, this phenomenon is common with newly emergent leaves being 2n or 4n, but progressing to 8n, 16n, or even 32n as they mature (Doerner, 2000). As a result, large cells with larger-than-normal nuclei tend to develop.

Figure 3.11 presents a TSEM of the nucleus of an HHS cell grown in 280 mM NaCl. Several nuclear aberrations can be observed in this sample. One of the aberrations is the size of the two large nucleoli (~2 – 2.5 μm dia.), which are significantly larger than that observed from WT cells (*ca.* 1 μm dia., *cf.* Fig. 3.5). Large nuclei, with correspondingly large nucleoli, were commonly found in EMs of HHS cells, and therefore appears to give support to an increase in ploidy in this cells line. Comparison of several serial sections through the same nuclei suggest that their size (and that of their corresponding nucleoli) varied and did not always conform to discrete size classes, which would have arisen by simple changes in ploidy (2n, 3n, 4n, *etc.*). This was best demonstrated by measuring the maximum size of nucleoli which in HHS cells ranged from <0.2 μm to >2.5 μm dia. (data not presented). This range in size suggests that other chromosomal aberrations were manifest, in addition to simple ploidy changes.

For example, restitution nuclei may arise where endoreduplication of only part of the full chromosome complement occurred resulting in aneuploid cells. This would be expected to

give rise to cells with different sized nuclei and nucleoli and nucleoli number (*cf.* Figs. 3.4 and 3.11).

In many cases nucleoli that were smaller than the WT (2n) nucleoli were observed in cells from the HHS cell line. Such nuclear aberrations are characteristic of amitosis and prophase chromosome reductions (Miller, 1980). In amitosis, the nucleus does not undergo symmetrical division. Instead, part of the nucleus 'buds off' from the main nucleus in a seemingly uncontrolled fashion, carrying variable amounts of nuclear material with it. Figure 3.4 shows behavior that is consistent with amitosis as fragmented nucleoli appear to be separating off from the main nucleus; such fragments of nucleoli were commonly observed in HHS cells.

Prophase chromosome reduction occurs in cultured cells of many plant species (Nuti Rouchi *et al.*, 1992a). This phenomenon appears to occur in the high salt-grown HHS (but not in WT) *Arabidopsis* cells (Fig. 3.11); note the size of the small nucleolus (*ca.* 500 nm dia.), compared with those of WT cells (*ca.* 1000 nm dia.; Fig. 3.5).

In order to investigate further the chromosome complement of HHS cells, cultures were harvested in mid-log phase of growth (~ 3-4 days after subculture), precipitated under gravity, washed in fresh growth media, and subsequently stained with the chromosome stain, Toluidine Blue (Section 2.1.4.4). Usually high chromosome numbers were observed in cell squashes when visualized by a light microscope (Figs. 3.14 A-D). In Figs. 3.14A-C, there is evidence for ~ 20 chromosomes per HHS cell which is indicative of 2 rounds of DNA synthesis without mitosis. Fig. 3.14D shows an HHS cell squash with ~30 chromosomes, whilst WT cells (Fig. 3.14E) invariably showed 10 chromosomes per cell (*i.e.* 2n, diplod).

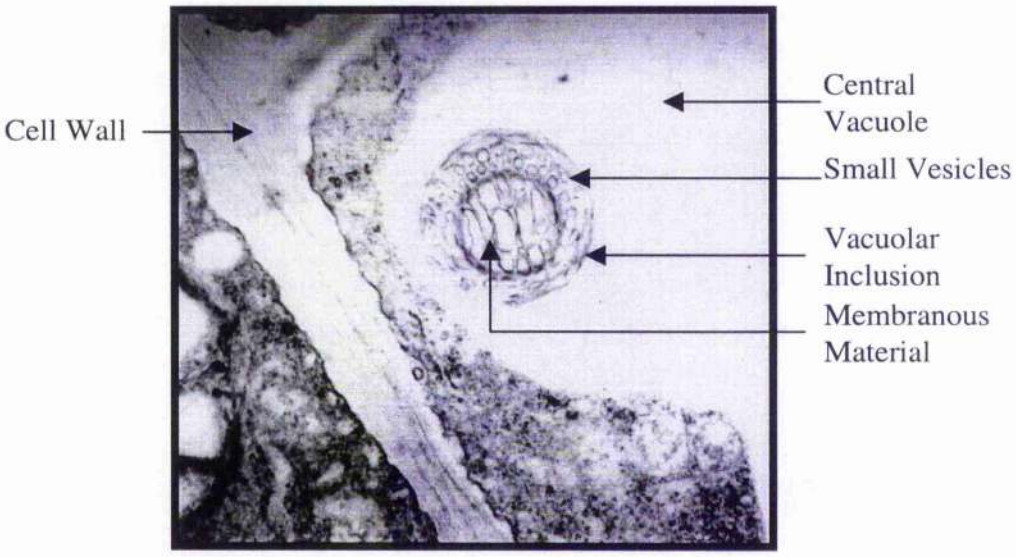

Figure. 3.12. Elecrtonmicrograph View of HHS *Arabidopsis* Cell Line Grown in 280 mM NaCl. .

The view represents one of many irregular membranous structures observed inside the vacuoles. Note, the flocculent vacuolar inclusion, which could be comprise multi-vesicular bodies and /or partially coated reticulum. Magnification, X 36,000.

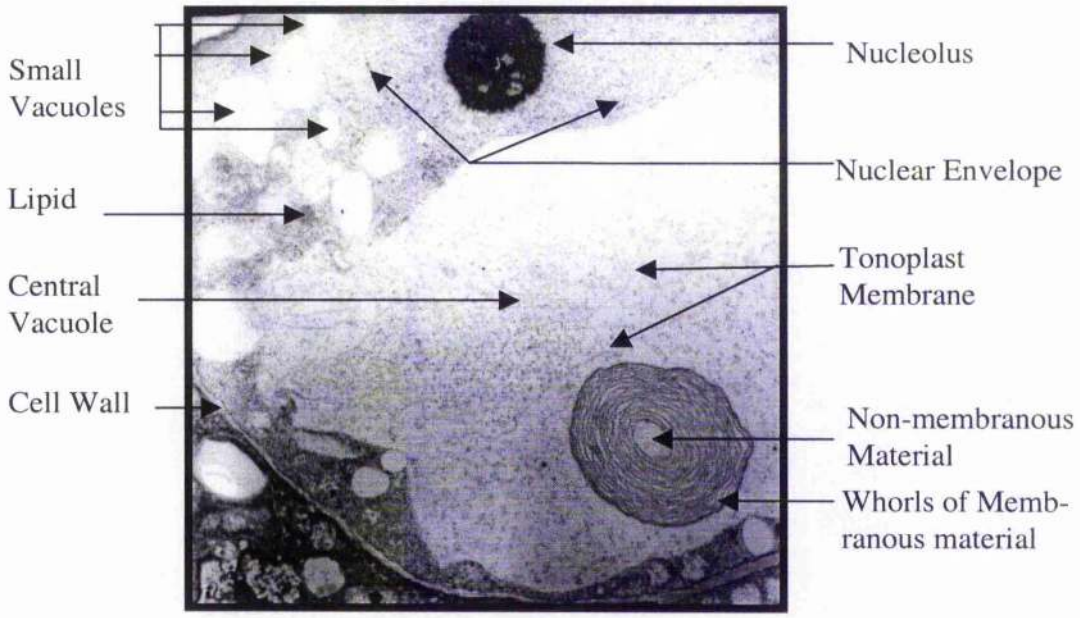

Figure. 3.13. Electronmicrigraph of HHS *Arabidopsis* Cell Line grown in High-Salt.

The figure illustrates small vacuoles fused to each other and the others fused with the tonoplast membrane. Note, vacuolar inclusion and lipid. In addition, an internal invagination of the tonoplast membrane that has a zone of membranous and non-membranous material. Thin zone of non-membranous material is sandwiched between adjacent whorls. Whorls of membranous material could be split from the internal invagenation of the tonoplast membrane. Magnification, 13,000 X.

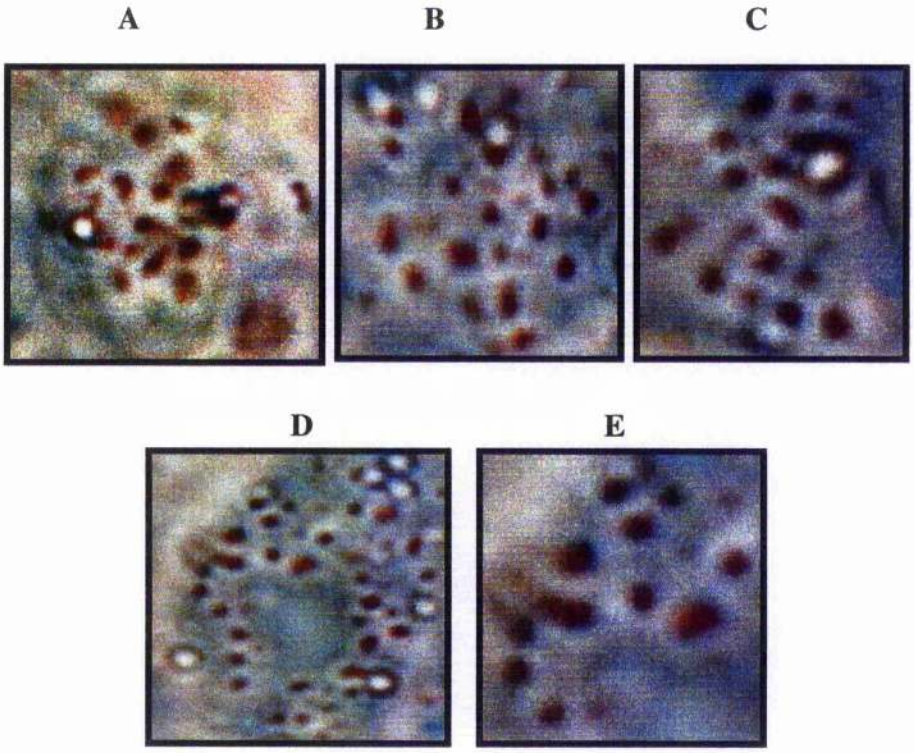

Figure. 3.14. Toluidine Blue-stain of Chromosomes in *Arabidopsis* cells.

Wild type and HHS cells were grown in 0 and 280 mM NaCl, respectively, as described in (Section 2.1.4.1), cells were harvested and stained with Toluidine Blue. Panel A-C, squashes of cells showing~20 chromosomes, indicative of 2 rounds of DNA synthesis without mitosis. Panel D shows a cell squash with ~30 chromosomes, indicative of three successive rounds of DNA synthesis without cell division. Panel E shows WT cell with 2n =10 chromosomes (diploid).

3.4. Discussion.

There is a general belief that despite its many advantages for the study of many fundamental processes in plant biology, *Arabidopsis thaliana* is not a good model for investigating the mechanisms of tolerance to high salinity. *Arabidopsis thaliana* is a glycophyte; it can not undergo a full life cycle in 100 mM NaCl solutions unless aphysiologically high levels of K^+ and Ca^{2+} are present in the growth medium. However, the development of the HHS cell lines that were used in the present study suggests that *A. thaliana* has the genetic potential to tolerate high levels of salinity, and that it is the inability of the intact plants to co-ordinate the expression of the appropriate traits that confines the range of this species to non-saline habitats. Therefore, studies on *A. thaliana* plants may provide us with extensive details on salt sensitivity and very little about salt tolerance. However, these limitations do not apply to studies on the *A. thaliana* HHS cell line, where the many advantages offered by a model plant system can be brought to bear on studying salinity tolerance mechanisms.

In this chapter, preliminary investigations were made on the basic cell biology of HHS cells grown in high salinity (280 – 300 mM NaCl). When compared with WT cells grown in low salinity (0 mM NaCl), several major ultrastructural differences were observed.

Initially, it was hoped to use the HHS cells loaded with ion specific fluorescence probes to measure the flux of Na^+ (using SBFI and Sodium Green), K^+ (using PBFI), Cl^- (using SPQ and lucigenin) and H^+ (using BCECF and carboxy SNAFL) across the plasma membrane. However, it became apparent that these experiments could not be performed as all of these fluorescent dyes were rapidly taken up (less than 2 minutes) by HHS cells and sequestered in an extensive system of small vacuoles that fluoresce brightly (Figs. 3.1, 3.2, 3.3 & 3.6). Electron microscopy showed that HHS cells contain a large numbers of these small vacuoles

(0.2-3 μm), and in addition vesicles (<0.2 μm), and neither of these are as extensively developed in WT cells grown in low salinity (*cf.* Figs. 3.4 & 3.5). Further, cell suspension cultures prepared from the salt tolerant plants of sugar beet and beet root (*Beta vulgaris*), and from the halophytes *Aster tripolium* and *Atriplex hastatda* and show similar small vacuole / vesicle (SV-V) morphology, that also appear to rapidly take up the fluorescent dyes (data not presented). In contrast, suspension cells from glycophytes (*e.g. Solanum tuberosum, Dacus catota*; (Dr P. Dominy, unpublished) do not possess these extensive SV-V arrangements. It is tempting to speculate that this morphology represents a response to high salinity that confers tolerance to salt stress. However, at this stage, the connection between the high level of SV-V and salt tolerance remains merely correlative.

Some evidence has been provided that the SV-V compartments fuse with the plasma membrane (Fig. 3.8) and the tonoplast membrane (Figs. 3.12 & 3.13), and therefore may be involved in trafficking. What is not clear is whether this is exocytosis (of excess ions) or endocytosis (sequestration of ions in the large central vacuole for osmotic adjustment. Comparable observations were made by Shiminy, *et al.*, 1973, for salt glands of the mangrove species *Aegiceras corniculatum* and *Avicenia marina*, and by Vassilyev and Stepannova, (1990) during their ultrastructure work on the salt glands of *Limonium plathyllum*. Further studies using fluorescent dyes and a confocal microscope should establish whether trafficking does occur in HHS cells, and establish the dynamics of the process.

Several nuclear and chromosomal abnormalities appear to have arisen in the HHS cells. These include endoreduplication to produce cells with triploid, tetraploid or higher levels of ploidy, aneuploidy where the copy number of some (but not all) of the chromosomes (or

chromosome fragments) occurs, and prophase chromosome reduction which as the name suggests results in a loss of chromosomal material (Figs. 3.4, 3.11 & 3.14).

CHAPTER FOUR

CLONING Na^+/H^+ ANTIPORTERS

CHAPTER FOUR

4. Cloning Na^+/H^+ Antiporters.

4.1. The Role of Na^+/H^+ Antiporters in Salt Tolerance.

Antiporters are secondary active membrane transporters that require H^+ gradients to drive solute transport. Turn over numbers for such transporters are of the order of 10^2 to 10^4 molecules per second (Maeshima, 2000). Although ubiquitous membrane transport proteins, their abundance is considered to be very low compared with those of proton pumps and MIPs, making them difficult to identify in SDS-polyacrylamide gels (Maeshima, 2000). The group of Na^+/H^+ antiporters has long attracted attention in relation to salt tolerance in plants (Bulmwald and Pool, 1987; Bulmwald *et al.*, 2000). Sodium/proton antiporters catalyze the exchange of Na^+ for H^+ across membranes, exporting Na^+ from the cytosol both to the extracellular space across the plasma membrane, and to the vacuole across the tonoplast (Bulmwald *et al.*, 2000). Several studies have provided evidence consistent with the existence of Na^+/H^+ antiporter activity in both of the plasma membrane and tonoplast vesicles of a wide rage of plant cells (Ratner and Jacooby, 1986; Mennen, *et al.*, 1990; and Jocoby, 1993). The abundance of Na^+/H^+ antiporters are reported to increase with increasing salt stress (Grabarino and DuPont, 1988 & 1989; Du Pont, 1992). Although Na^+/H^+ antiporter activity has been reported in plants since 1985, details on the molecular structure of these proteins has been hampered by the slow progress in cloning the associated genes. Therefore, in the recent past an extensive effort has been directed toward cloning these genes from plants. This chapter reports the results of experiments conducted to clone and characterize these transporters from higher plants.

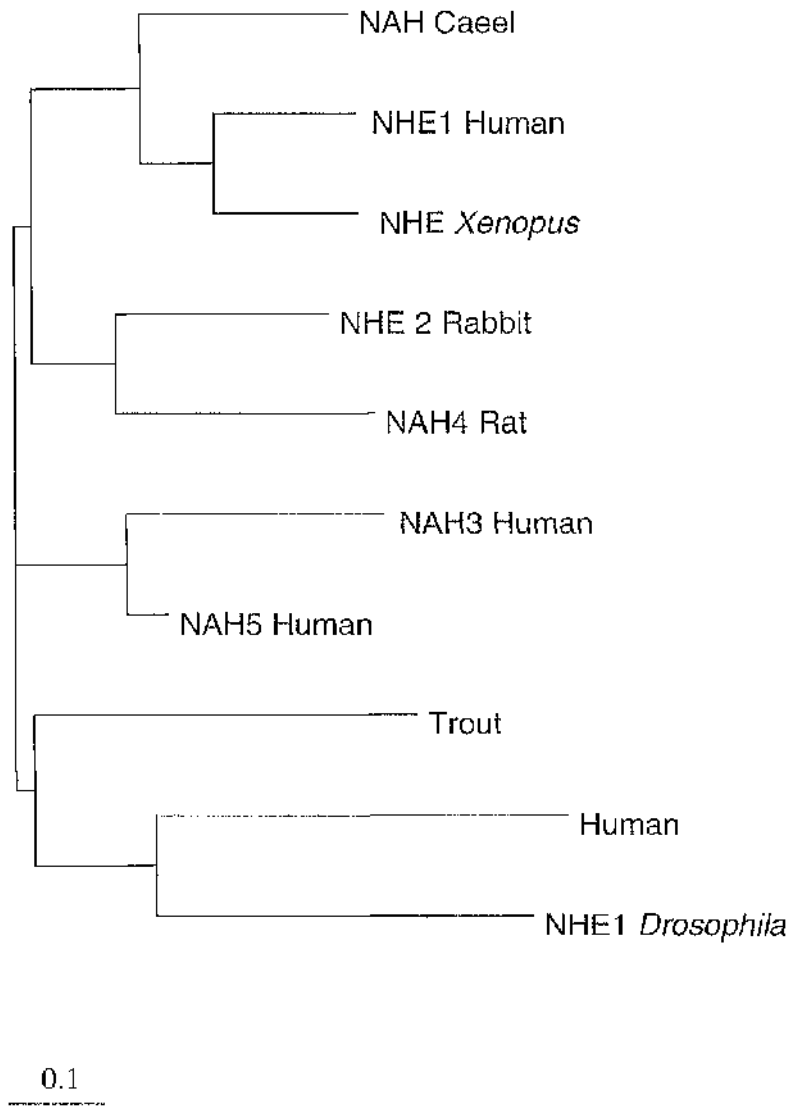

Figure. 4.1 Phylogeney analysis of 10 Na^+/H^+ exchanger proteins (Circa March, 1998).

Multiple sequence alignment and generation of phylogenetic tree were performed with CLUSTALW and Tree View software, respectively. NAH, *C.elegans* (547989): NHE1, Human (544776): NHE, *Xenopus* (1655702): NHE2, Rabit (1709222): NAH4, rat (127814): NAH3, Human (1346659): NAH5, Human (2833257): Trout, (547990): Human, (2944233): NHE1, *Drosophila* (489499). The numbers in brackets are accession numbers and the scale bar represents 0.1 sequence divergence.

4.2. PCR Cloning Approach.

Several attempts to clone plant Na^+/H^+ antiporters by conventional means have failed. These included screening of plant cDNA libraries with heterologous probes, subtractive hybridization and heterologous expression of plant cDNA librarcis in Na^+-sensitive yeast mutants (Dr P. Dominy, per.com.; Prof. A. Rodriguez-Navarro, per.com.; Prof. E. Blumwald, per.com.). However, by 1998, searches of the databases showed ten sequences had been identified from eukaryotes that were reported to represent Na^+/H^+ antiporters. It was decided to attempt to identify regions of conservation at the protein level, and to use the consensus sequence to design PCR primers for cloning plant Na^+/H^+ antiporters.

4.2.1. PCR Cloning Using Degenerate Primers and cDNA Libraries as Template.

Alignments of protein sequences from 10 authentic Na^+/H^+ antiporters from a range of organisms were made and two regions of consensus sequences were identified Fig. A1 (see Appendix 1). Two sets of degenerate primers were designed from the conserved motif domain, and the Arabidopsis codon bias table (Table 4.1) and used in PCR experiments. Phylogenetic analysis was performed by CLUSTAL W and displayed using Tree View software, respectively (Fig.4.1 and Fig. A1 Appendix).

After suitable protocols were found for genomic DNA template, attempts were made to amplify PCR products from two independent cDNA libraries: The "Lacrute" cDNA library of *Arabidopsis* seedling roots (Minet, *et al.*, 1992), and the"Davis" cDNA library of *Arabidopsis* from all organs, also all stages of development (Elledge, *et al.*, 1990).

Table 4.1. A. Degenerated primers designed from Na^+/H^+ exchangers consensus sequences.

Primer Sets	Sequence
Forward	5'-TT(CT) TT(CT) (ACT)T(AGCT) T(AT) (CT) (CT)T(AGCT) (CT) T(AGCT)-3'
Reverse	5'-(CT)TC (AGCT)CC (AG)AA (AGCT)AC (AGCT)A(AG) (AGCT)-3'

Table 4.1. B. Details of the degenerated primer used to amplify genes sequences coding for putative Na^+/H^+ antiporter.

Primer	Length	% GC Content	No. Bases Binding	Annealing Temp. (°C)
Forward	18-mer	24.1	18	43.1
Reverse	16-mer	46.9	16	47.9

Unfortunately, despite extensive attempts the expected product was not found and possibly reflects the low abundance of full-length copies of Na^+/H^+ antiporters in these low salt-grown cDNA libraries.

4.3. RT-PCR Cloning of *At* B04.4 cDNA.

In August 1998, approximately 30% of the *Arabidopsis* genome had been sequenced and a BAC sequence (TM21 B04.4) appeared in the database. BLAST searches suggested this sequence showed some homology at the protein level to some eukaryote Na^+/H^+ antiporters and therefore this sequence may represent the first plant Na^+/H^+. At B04.4 showed a significant similarity to known Na^+/H^+ including ScNHX1 from (*Saccharomyces cerevisiae*), Hs NHE6 (*Homo sapiens*), and DmNHE1 (*Drosophila melanogaster*) as indicated by the alignment and phylogenetic analysis performed by CLUSTALW and Tree View software, respectively (see Fig. 4.2 and Fig. A1.2 Appendix).

It was decided to attempt to clone the full-length cDNA of B04.4 (predicted size 1.4 kbp) using *Arabidopsis* cDNA libraries as template. Three sets of specific primers were designed. Two sets were designed intuitively, and the third set was designed by web-based program PRIMER 3 (http://www-genome.wi.mit.edu/cgi-bin/primer/primer3). The second set of primers contained a linker sequence unlike the other two. Extensive attempts were made to amplify the full-length *At* B04.4 cDNA (predicted size 1.4 kbp) sequence from the Lacrute and the Davis cDNA libraries using (primer set 1 and 2, see Table 4.2), but these failed. This again possibly reflects the low abundance of full-length copies of *At*B04.4 in these low salt-grown cDNA libraries. Consequently, it was decided to use a RT-PCR approach to clone a

Table 4.2. Sets of primers used to amplify gene sequences coding for putative Na^+/H^+ antiporters.

Primer Sets		Sequence
BO4.4 set 1	Forward	5'-ATG TTG GAT TCT CTA GTG TCG-3'
	Reverse	5'-TCA TTT GAT CAT CCA GAG ATT-3'
Bo4.4 set 2	Forward	5'-CTC GAG TCA TTT GAT CAT CCA GAG-3'
	Reverse	5'-GGA TCC ACA ATG GAT TCT CTA GTG-3'
Bo4.4 set 3	Forward	5'-TGT AAC TCA TTT GAT CAT CCA GAG A-3'
	Reverse	5'-GAG GAA CTT TGT TGG ATC TAG-3'
T9D9.5 set1	Forward	5'-ATG GAG CTT TCG ATG TTT GCG-3'
	Reverse	5'-CTA GCG TTT ACC GAG ATC AAT-3'
T9D9.5 set 2	Forward	5'-ATC AAG ATT AAG TCA CTT G-3'
	Reverse	5'-TCC CTC TTT CTA CTC GCT TT-3'
F24D13.3	Forward	5'-TTG AAG TCA TGG AAA TGG GG-3'
	Reverse	5'-ACC ATA GTA TGC TTT CTC CGC-3'
F24D13.4	Forward	5'-TGG CAA TGA CGG AAC TTC AA-3'
	Reverse	5'-TTG GAT ATT CAT AAC ATG G-3'
T12H17.230	Forward	5'-TGT GGA GTG AAA CAA AAT CAA AA-3'
	Reverse	5'-TGA AAA ATC ACA AAG TCC TTT GA-3'
T12H17.230 (Internal)	Forward	5'-TAA TTT CTC GGA GAT GGG TTT G-3'
	Reverse	5'-GAT AGC ATC GGT GTG ACA AGA A-3'
F20D21.19	Forward	5'-TCC ATG CTA CTC CCC ATC TC-3'
	Reverse	5'-TGG GTG GTC CAA TCT CAA AT-3'
F14H20	Forward	5'-TCT TCC TCT GTG TTG TTG CTT C-3'
	Reverse	5'-CAT CTC AAT TCT CAT AGA TCG TTC C-3'

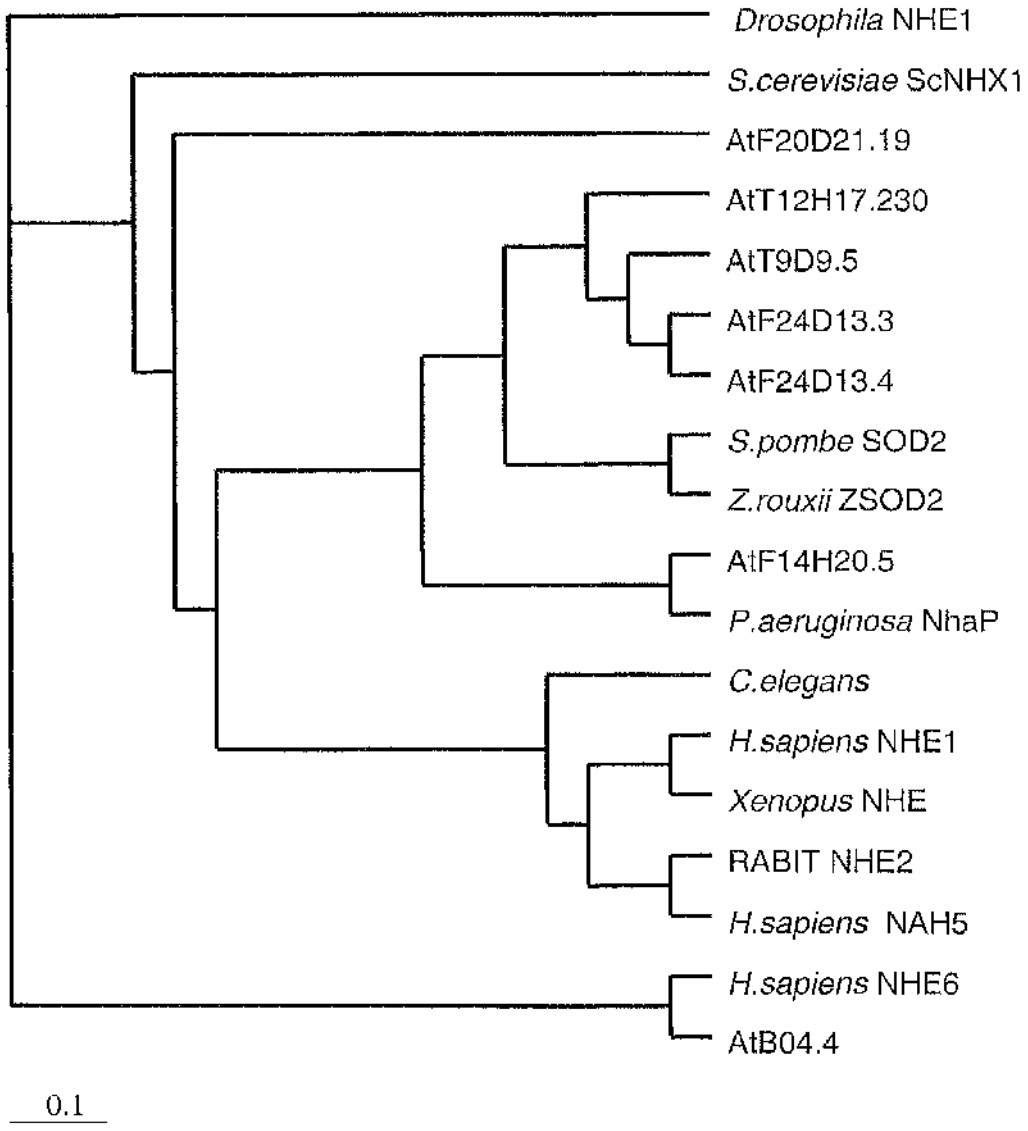

Figure. 4.2 Phylogeny Relationship of Protein sequences for Na^+/H^+ Antiporters from different organisms (Cerca 2000).

Protein sequence for known Na^+/H^+ antiporters from various organisms and seven putative *Arabidopsis* Na^+/H^+ antiporters were aligned using CLUSTAL W and displayed Tree View software, respectively. The scale bar represents 0.1 sequence divergence. The sequence accession numbers are as follows: NHE1 (489499), *Drosophila* ; ScNHX1(NP_010744), S.*cerevisiae*; AtF20D21.19 (AAD25617.1), *Arabidopsis thaliana*; AtT12H17.230 (T04579.1), *Arabidopsis thaliana*; AtT9D9.5 (AAC1692.1), *Arabidopsis thaliana*; AtF24D13.3 (AAC98448.1), *Arabidopsis thaliana*; AtF24D13.4 (AAC98449.1), *Arabidopsis thaliana*; SOD2 (CAA77796.1), *S.pombe*; ZSOD2, *Z.rouxii* ; AtF14H20.5 (AAD20091.1), *Arabidopsis thaliana*; NhaP (BAA31695.1), *P.aeruginosa*; (547990), *C.elegans*; NHE1 (P19634), *H.sapiens* ; NHE (1655702), *Xenopus* ; NHE2 (1709222), RABIT; NHE5 (2833257), *H.sapiens;* NHE6 (NP_006350), *H.sapiens*; and AtB04.4 (AAD16946.1), *Arabidopsis thaliana.*

Table 4.3. A. Details of the various primer sets used to amplify gene sequences coding for putative Na^+/H^+ antiporters.

Primer		Length	% GC Content	No. Bases Binding	Annealing Temp. (°C)
BO4.4 set 1	Forward	21 mer	42.9%	21	55.9
	Reverse	21 mer	33%	21	52
BO4.4 set 2	Forward	21 mer	45.8%	18	61
	Reverse	21 mer	44.4%	18	63.4
BO4.4 set 3	Forward	25 mer	36%	19	58.1
	Reverse	21 mer	42.9%	19	55.9
T9D9.5 set 1	Forward	17 mer	42.9%	21	55.9
	Reverse	17 mer	47.6%	21	57.9
T9D9.5 set 2	Forward	19 mer	39%	19	45
	Reverse	20 mer	41%	20	49
F24D13.3	Forward	20 mer	42.7%	20	49
	Reverse	21 mer	46%	21	52
F24D13.3	Forward	20 mer	41.9%	20	49
	Reverse	19 mer	37%	19	44

Table 4.3. B. Details of the various primer sets used to amplify gene sequences coding for putative Na^+/H^+ antiporters.

Primer		Length	% GC Content	No. Bases Binding	Annealing Temp. (°C)
T12H17.230	Forward	23 mer	43%	23	52
	Reverse	23 mer	51%	23	57
T12H17	Forward	22 mer	40.9%	22	56.5
(Internal)	Reverse	22 mer	45.5%	22	58.4
F14H20	Forward	22 mer	45.5%	22	58.4
	Reverse	22 mer	40%	22	59.7
F20D21	Forward	20 mer	55%	20	59.4
	Reverse	20 mer	45%	20	55.3

cDNA for *At*B04.4 using the *Arabidopsis* HHS cell line grown in high salt (240 mM NaCl see Section 2.1.4.2) after the suitable PCR condition found from genomic DNA as template.

4.3.1. PCR Cloning of *At* B04.4 Using Specific Primers and Genomic DNA as Template.

The primer sets were first tested for suitability using genomic DNA as template. Primer set 1 (Table 4.2) was used with the *Arabidopsis* genomic DNA extracted from untreated cell suspension cultures as a template in the series of experiments designed and carried out to establish the suitable concentration for PCR amplification (i.e., $MgCl_2$, primers and template concentration etc.). After the suitable concentrations of the PCR components were established, a product of the expected size 2.6 kbp (from the annotated *Arabidopsis* database) was resolved by agarose gel electrophoresis Fig. A1.3 (see Appendix). The same conditions with the second set of primers (same sequence as the primer set 1 but with linkers), produced a very faint band of the expected size (data not presented). The third set of primers that were designed by the PRIMER3 program were used with the optimized PCR conditions and these successfully generated the expected band of 2.6 kbp as shown in (Fig.4.3).

4.3.2. RT-PCR Amplification of *At*B04.4 cDNA.

Having established that primer sets 1 and 3 produce products of the expected size from genomic template, attempts were made to amplify a product from cDNA template. An RT-PCR approach was used to clone the full-length of *At*BO4.4 cDNA using an *Arabidopsis* cell

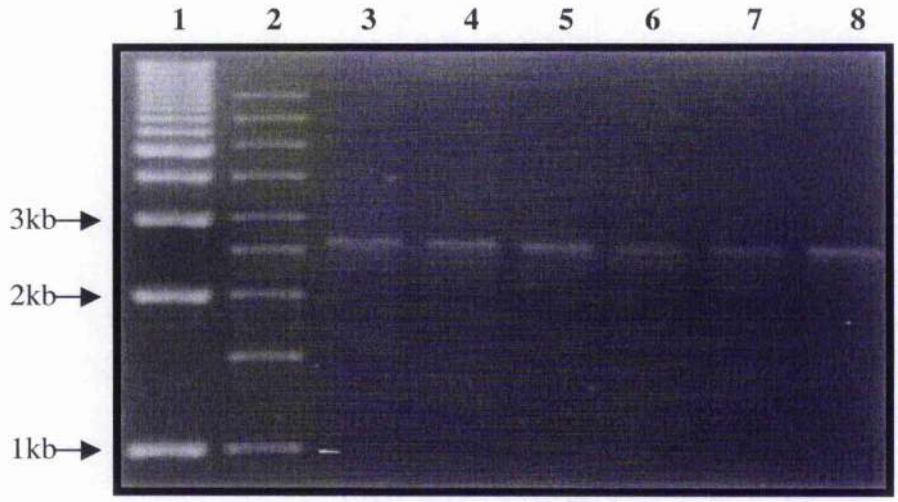

Figure. 4.3 PCR Amplification of *At* B04.4 Fragment From Genomic DNA Template Using Primer Set 3.

The primers were used with *Taq* DNA polymerase in a PCR reaction. The reaction contained 50-100 ng of genomic DNA, 2.5mM MgCl, 50-100 pmol primers, 200μM dNTPs, 1X *Taq* buffer (20mM Tris-HCL, 1mM dithiothreitol, 0.1mM EDTA, 0.1 M KCl, 0.5% Nonidet P40 (v/v),0.5% Tween 20 (v/v),50% glycerol (v/v), pH 8.0 (4°C), and 2.5 units of *Taq* DNA polymerase (final volume of 50 μL). The reaction was started (hot start) by the addition of *Taq* DNA polymerase at 94°C, and followed by 35 cycles of 20 seconds at 47°C (annealing), 120 seconds at 72°C (extension) and 15 seconds at 94°C (denature). The PCR products were analyzed on a 1% agarose gel stained with ethidium bromide (see Chapter2, Section 2.,2.5.2). Lanes 3-8 represent the expected size fragment for PCR product, 2.6kb. Lane 1 represents EZ Load 1kb molecular ruler; lane 2 represents FMC 1-10kb DNA marker.

line grown in high salt (240 mM NaCl) instead of low salt-grown cDNA libraries. Both oligo dT and random primers first strand cDNA synthesis methods were used.

4.3.2.1.. RT-PCR Cloning of *At* B04.4 Using Oligo dT Primer First Strand Synthesis.

RT-PCR was carried out on RNA samples extracted from high-salt grown HHS *Arabidopsis* cells 240 mM NaCl. Total RNA was prepared (Materials and Methods, Section 2.2.2.2) and MMLV (Moloney Murine Leukemia Virus) reverse transcriptase was used to synthesize first strand cDNA by oligo dT, and by random priming (Section 2.2.11.1). Many attempts were made to amplify this sequence, and several bands were generated from the different experiments. However, the primers designed with PRIMER 3 program formed two PCR products and resolved with approximate sizes of 1.4kbp and 1.6kbp (Fig.4.4). The fragment size predicted from the database for *At*BO4.4 cDNA was 1.4 kbp (Section 2.2.15.1 and 2.2.15.3).

4.3.2.2. Cloning of *At* Bo4.4 cDNA.

The resultant 1.4 kbp fragment was excised from the gel, purified (see Section 2.2.7), cloned into PCR -Script Amp SK (+) cloning vector (Section 2.2.12.4.1.3), and transformed into the host *E. coli* strain XL10-Gold Kan ultracompetent cells (Stratagen see Section 2.2.3.3). The initial stages of cloning appeared to work. Colony PCR was conducted on white colonies identified by X-gal selection (see Section 2.2.12.4.1.3) and

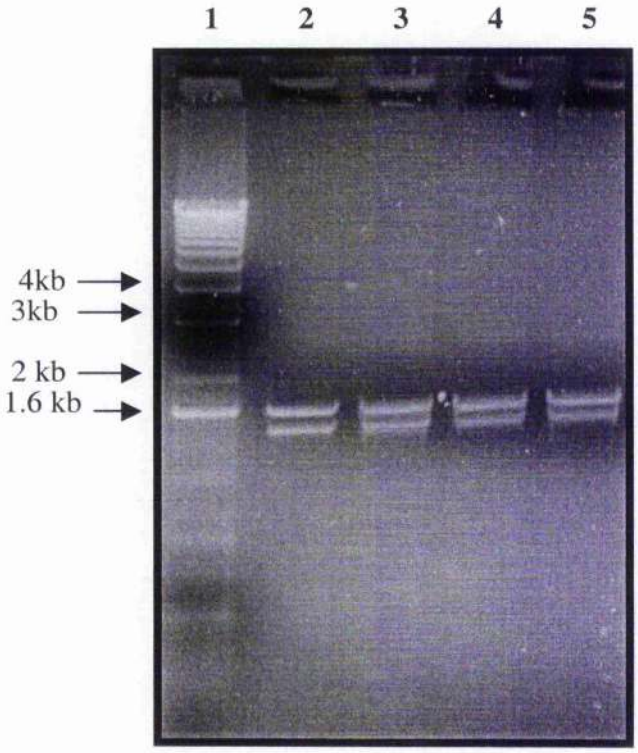

Figure. 4.4 RT-PCR Amplification of a Fragment from *Arabidopsis* cDNA Using *At* B04.4 Primer set 3.

RT-PCR was used to amplify the first strand of *At* B04.4 cDNA prepared from an HHS *Arabidopsis thaliana* cell line grown in high salt (260 mM NaCl). Total RNA was isolated and first strand cDNA prepared using MMLV reverse transcriptase with an oligo (dT) primer. The *At* B04.4 primers were used with high fidelity *Taq* DNA polymerase in a PCR reaction. The reaction contained 2.5 μL first strand cDNA template, 2.6 mM MgCl, 50 pmol primers, 200μM dNTPs, 1X high fidelity *Taq* buffer (20mM Tris-HCl, 100 mM KCl,1mM dithiothreitol (DTT), 0.1mM EDTA, 0.5% Tween 20 (v/v), 0.5% Nonidet P40 (v/v), 50% glycerol (v/v), pH 7.5, and 2.5 units of high fidelity *Taq* DNA polymerase (final volume of 50 μL). The reaction was started (hot start) by the addition of high fidelity *Taq* at 94°C, and followed by 35 cycles of 15 seconds at 47°C (annealing), 120 second at 72°C (extension), and 13 seconds at 94°C (denature). The PCR products were analysed on a 1% agarose gel stained with ethidium bromide. Lanes 2-5 show the expected PCR product, 1.4 kb fragment (lower band). Lane1 contains Marker X.

inserts of the appropriate size (1.4kb) were observed. However, attempts to amplify these clones in *E. coli* failed, as continued growth, particularly in liquid media, was poor.

One possible reason for failure is that sequences coding for membrane proteins can be transcribed and translated in *E.coli* and render the cell membrane 'leaky', resulting in colony death. Amplification of the identified colonies was attempted again but this time no IPTG/X-gal selection was used, thereby reducing transcription of the plasmid-borne sequence to a minimum. However, a similar result was obtained; colonies grow well initially, but died after 3 days.

Another cloning vector was used, PET 28 (Section 2.1.2), which is transcriptionally silent. Clones with the appropriate insert (identified by colony PCR) were selected, but again growth on plates and in liquid culture was poor.

Several *E. coli* hosts strains were used including $DH_5\alpha$, C43Des and C41DEs (Section 2.1.2), which are reported to be good backgrounds for cloning membrane proteins. However, again the initial cloning worked on plates, but continued growth was not, therefore it was not possible to perform a secondary amplification of the positive clones in liquid culture. In April 1999 a publication appeared reporting the isolation of a 1.6 kbp cDNA , longer than that predicted by the database) *At* Nhx1 which was 100% identical to *At*B04.4, and demonstrated function as vacuolar Na^+/H^+ antiporter (Gaxiola *et al.,* (1999). Subsequently, in August 1999, another group published work on the overexpression of *At* Nhx1 (*At*B04.4) in *Arabidopsis* (Apse *et al* ., 1999). Therefore, in view of this strong competition, it was decided to stop work on this sequence and concentrate effort on other putative Na^+/H^+ antiporters in *Arabidopsis*.

4.4. RT-PCR Cloning of *At*T9D9.5 cDNA.

In 1999 another sequenced BAC (T9D9) in the *Arabidopsis* genome database, had been annotated to include a putative Na^+/H^+ antiporter. The sequence contains 12 membrane-spanning α-helices and has some homology to known Na^+/H^+ antiporters. Two sets of primers were designed to amplify the full-length sequence as shown in (Table 4.2). The first set of primers were designed intuitively and included linkers to facilitate cloning, and a second set was designed using the on-line web program PRIMER3 (Section 2.2.15.4). The first set of primers failed to produce any products despite exhaustive attempts to modify the PCR protocols (thermocycle conditions and $MgCl_2$ concentrations). However, the second set successfully amplified a band of the expected size (2.9 kbp, Fig.4.5).

The second set of primers was used with the product of first strand oligo dT primed synthesis *At*T9D9.5 cDNA as a template. After the conditions were optimized, RT-PCR products were electrophoresed on a 1% (w/v) agarose gel (Fig.4.6), and a band of the expected size 2.5 kbp was visualized.

Random primers first strands (as described in Section 2.2.11.1) were also used successfully to generate RT-PCR fragments with the 5' specific primer for *At* T9D9.5. However, as oligo dT first strand synthesis worked, this approach was not persued

The fragment was cut from the gel shown in (Fig.4.6) and purified (Section 2.2.7). The band was subsequently cloned into PCR -Script Amp SK (+) cloning vector (Section 2.2.12.4.1.3), and transformed into the host *E. coli* strain XL10-Gold Kan ultra-competent cells (provided with PCR-Script Amp Cloning Kit- Stratagen see Section 2.2.3.3).

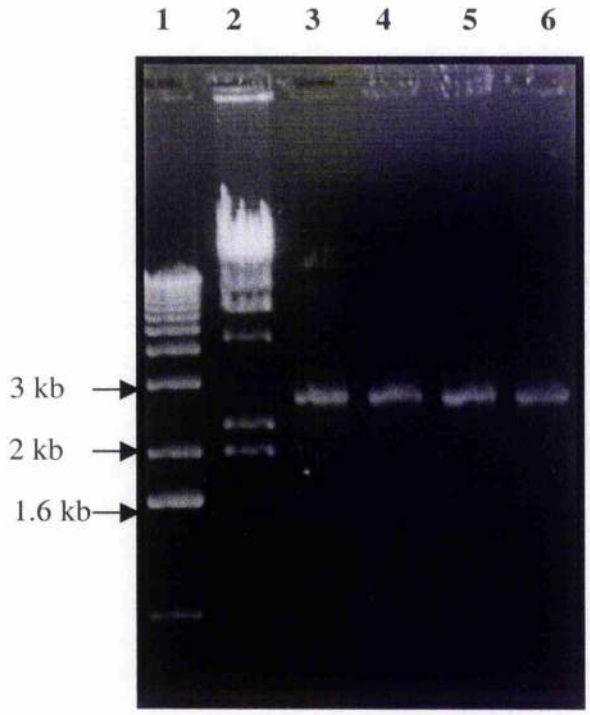

Figure. 4. 5 PCR Amplification of *At T9D9.5* Fragment From Genomic DNA Template Using Primer Set 2.

The primers were designed to bind at a site twenty six bases upstream of the ATG translation start site and twenty five bases down stream of the TGA translation stop sequence. The reaction contained 50-100 ng of genomic DNA, 2.6 mM MgCL, 50-100 pmol primers, 200μM dNTPs, 1X *Taq* buffer (20mM Tris-HCl, 1mM dithiothreitol, 0.1mM EDTA, 0.1 M KCl, 0.5% Nonidet P40 (v/v), 0.5% Tween 20 (v/v), 50% glycerol (v/v), pH 8.0 (4°C), and 2.5 units of *Taq* DNA polymerase (final volume of 50 μL). The reaction was started (hot start) by the addition of *Taq* DNA polymerase at 94°C, and followed by 35 cycles of 20 seconds at 40°C (annealing) ,120 second at 72°C (extension) and 15 seconds at 94°C (denature). The PCR products were analyzed on a 1% agarose gel. Lanes from 3-6 represent the expected PCR product, 2.9kb fragment. Lane 1 represents Marker X; lane 2 represent λ Hind III markers.

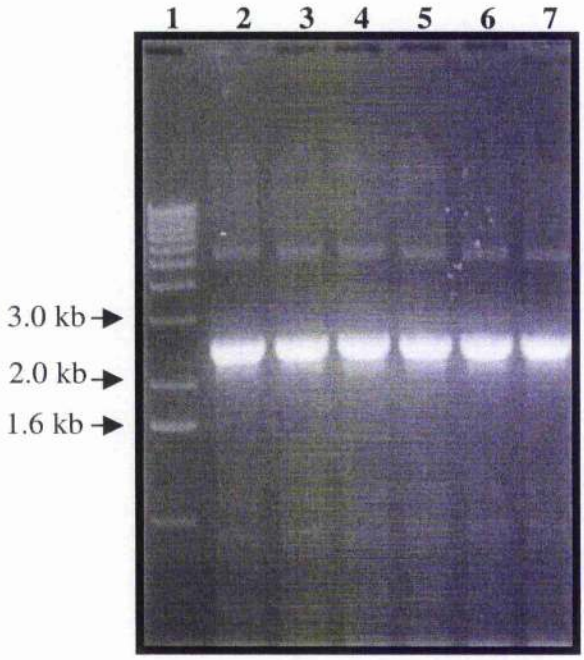

Figure. 4. 6. RT-PCR Amplification of *Arabidopsis* Fragment *At* T9D9.5 cDNA.

RT-PCR was used to amplify the first strand of *At* T9D9.5 cDNA prepared from an HHS *Arabidopsis thaliana* var. Columbia cell line grown in high salt (260 mM NaCl). Total RNA was isolated and first strand cDNA prepared using MMLV reverse transcriptase with an oligo (dT) primer. The *At* T9D9.5 primer set 2 were used with high fidelity *Taq* DNA polymerase in a PCR reaction. The reaction contained 1.5-2.5 μL first strand cDNA template, 2.6 mM MgCl, 50-100 pmol primers, 200 μM dNTPs, 1X high fidelity *Taq* buffer (20 mM Tris-HCl, 100 mM KCl, 1mM dithiothreitol (DTT), 0.1mM EDTA, 0.5% Tween 20 (v/v), 0.5% Nonidet P40 (v/v), 50% glycerol (v/v), pH 7.5, and 2.5 units of high fidelity *Taq* DNA polymerase (final volume of 50 μL). The reaction was started (hot start) by the addition of high fidelity *Taq* at 94°C. A Touch Down PCR programme was used, with annealing temperatures decreasing from 44 °C down to 41 °C in steps of 1 degree. Five cycles were performed at each annealing temperature, and followed by 20 cycles of 15 seconds at 41°C (annealing), 120 second at 72°C (extension), and 20 seconds at 94°C (denature). The PCR products were analyzed on a 1% agarose gel stained with ethidium bromide. Lanes 2-7 show the expected PCR product, a 2.5 kb fragment. Lane 1 represents 1kb ladder marker.

The *At*T9D9.5 cDNA was subsequently amplified and sequenced from both directions at MWG-Biotech (Ebersberg, Germany). The resulting sequence was then used in a BLAST N search (www.ncbi.nlm.nih.gov/). However, the results from BLASTN in T3 primer direction Fig. A1.4 (see Appendix) found 100% identities at the nucleotide level to a patented sequence W00055325, a gene located on chromosome 1of *Arabidopsis* , whereas *At* T9D9.5 is located on chromosome II. Clearly the 5' specific primer designed for *At* T9D9.5 also amplifies another cDNA (W00055325) accession No. AX059463 of the expected size (2.6kb). BLASTN output of the same gene (i.e., *At* T9D9.5) found nearly identical homology 98% identity to *Arabidopsis thaliana* mRNA coding for mitochondrial F1 ATP synthase beta subunit Acc. No. 17939848 in T7 primer direction Fig. A1.5 (see Appendix). No further attempts were made to clone At T9D9.5.

4.5. RT-PCR Cloning of *At* F24D13.3 and *At* F24D13.4cDNAs..

Two other sequences were identified in the *Arabidopsis* database that are putative Na^+/H^+ antiporters *At* F24D13.3 and *At* F24D13.4 these sequences are highly homologous and adjacent on chromosome. Therefore, specific primers were designed to these sequences and tested on genomic DNA template. Many modifications to the PCR protocol were required, but eventually two fragments of approximately the right size (2.9 and 2.7kbp) were amplified (Fig. 4.7 and 4.8).

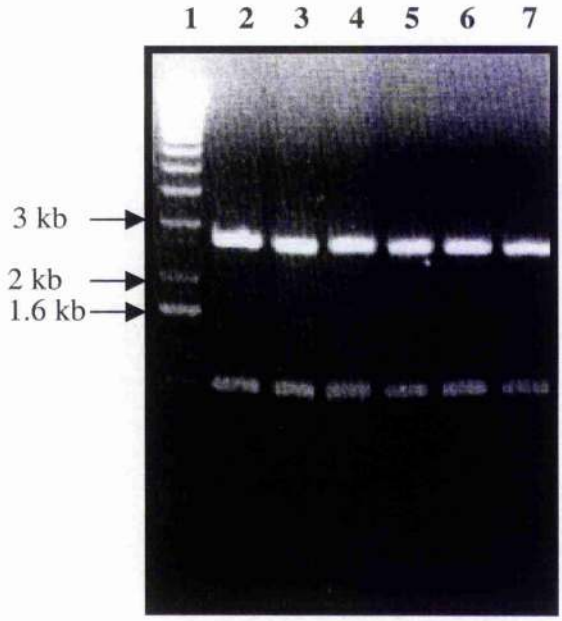

Figure. 4.7 PCR Amplification of *At* F24D13.3 Fragment From Genomic DNA Template.

The primers were used with *Taq* DNA polymerase in a PCR reaction. The reaction contained 50-100 ng of genomic DNA, 2.5mM MgCl, 50-100 pmol primers, 200μM dNTPs, 1X *Taq* buffer (20mM Tris-HCl, 1mM dithiothreitol, 0.1mM EDTA, 0.1 M KCl, 0.5% Nonidet P40 (v/v), 0.5% Tween 20 (v/v), 50% glycerol (v/v), pH 8.0 (4°C), and 2.5 units of *Taq* DNA polymerase (final volume of 50 μL). The reaction was started (hot start) by the addition of *Taq* DNA polymerase at 94°C, and followed by 35 cycles of 20 seconds at 43°C (annealing), 120 second at 72°C (extension) and 15 seconds at 94°C (denature). The PCR products were separated on a 1% agarose gel. Lanes from 2-7 represent the expected PCR product, 2.9 kb fragment. Lane 1 represents a1 kb ladder.

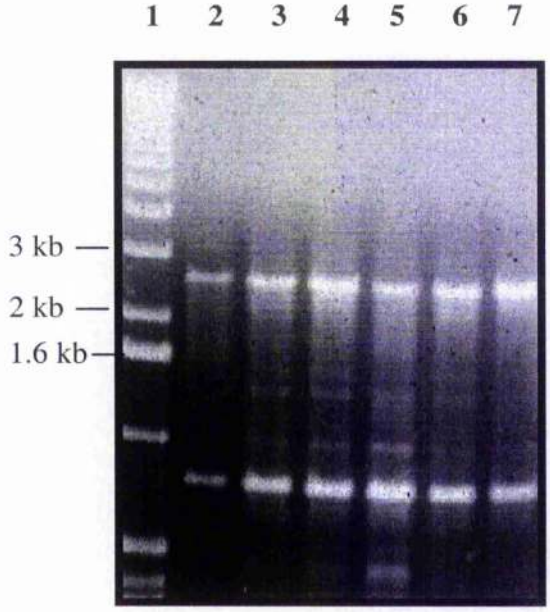

Figure. 4.8. PCR Amplification of *At* F24D13.4 Fragment From Genomic DNA Template.

The primers were used with *Taq* DNA polymerase in a PCR reaction. The reaction contained 50-100 ng of genomic DNA, 2.5mM MgCl, 50-100 pmol primers, 200μM dNTPs, 1X *Taq* buffer (20mM Tris-HCl, 1 mM dithiothreitol, 0.1 mM EDTA, 0.1 M KCl, 0.5% Nonidet P40 (v/v), 0.5% Tween 20 (v/v), 50% glycerol (v/v), pH 8.0 (4°C), and 2.5 units of *Taq* DNA polymerase (final volume of 50 μL). The program was started (hot start) by the addition of *Taq* DNA polymerase at 94°C, and followed by 35 cycles of 20 seconds at 45°C (annealing). The PCR products were analyzed on a 1% agarose gel stained with ethidium bromide. Lanes from 2-7 represent the expected size fragment for PCR product, 2.7kb. Lane 1 represents a1kb ladder.

4.5.1. RT-PCR Amplification of First Strand *At*F24 D13.3 and *At*F24D13.4 cDNA.

These primers successfully amplified a fragment of the expected size to *At*F24 D13.3 using genomic DNA as template. Therefore, the same protocols were subsequently used to amplify a cDNA for *At* F24D13.3 using oligo (dT) primed first strand cDNA. The RT-PCR reaction was carried out with different optimizations, but several bands were generated (Fig. 4.9). Also, the PCR yield was low, suggesting that the copy number of the transcript was very low at the start. The expression level of transporter proteins in plants is generally very low, or this sequence may not be expressed in the cell cultures. However, after many attempts, a cDNA of the expected size to *At* F20D13.3 was amplified as shown in (Fig.4.9). Many experiments were made to improve the PCR products through increasing the number of cycles, but it was unsuccessful. The correct fragment (2.5 kbp) was initially separated from residual DNA fragments by agarose gel electrophoresis, then excised and purified (Section 2.2.7). Many attempts were made to clone this 2.5kbp cDNA using conventional PCR cloning kits (PCR SCRIPT), but these failed, probably due to the low abundance of product. Subsequently, the purified excised gel fragment was cloned into the de-phosphorylated transcriptionally silent vector (PET28). This approach also failed.

Despite the extensive series of experiments made to amplify *At*F24D13.4 cDNA, no PCR products were generated. This may reflect the fact that the *At*F24D13.4, a homologue of *At* F24D13.3 is not expressed, or the primers have the ability to bind at different short sites within the sequence, which may explain the appearance of several bands. Attempts were made to improve the PCR yield for *At*F24D13.4 cDNA but these failed.

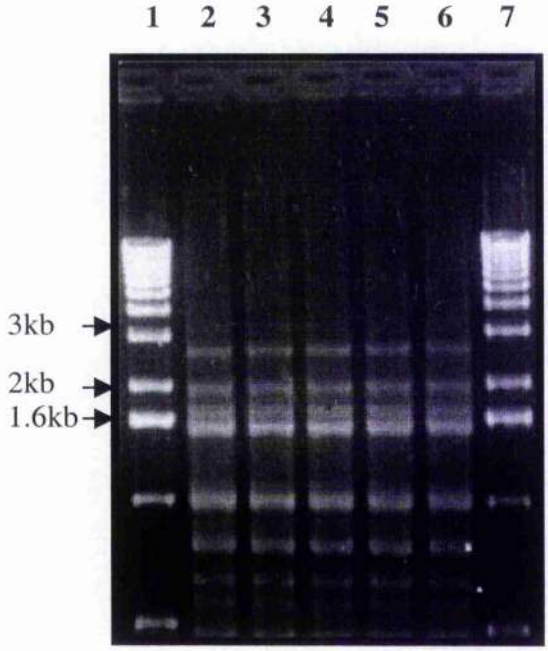

Figure. 4.9. RT-PCR Amplification of *Arabidopsis* Fragment *At* F24D13.3 cDNA.

RT-PCR was used to amplify the first strand of *At* F24D13.3 cDNA prepared from an *Arabidopsis thaliana* var. Columbia cell line grown in high salt (260 mM NaCl). Total RNA was isolated from HHS cells and first strand cDNA prepared using MMLV reverse transcriptase with random primers. The *At* F24D13.3 primer were used with high fidelity *Taq* DNA polymerase in a PCR reaction. The reaction contained 1.5-2.5 μL first strand cDNA template, 2.6 mM MgCl, 50 pmol primers, 200 μM dNTPs, 1X high fidelity *Taq* buffer (20mM Tris-HCl, 100 mM KCl, 1mM dithiothreitol (DTT), 0.1 mM EDTA, 0.5% Tween 20 (v/v), 0.5% Nonidet P40 (v/v), 50% glycerol (v/v), pH 7.5, and 2.5 units of high fidelity *Taq* DNA polymerase (final volume of 50 μL). The reaction was started (hot start) by the addition of high fidelity *Taq* at 94°C. A Touch Down PCR programme was used, with annealing temperatures decreasing from 48°C down to 45 °C in steps of 1 degree. Five cycles were performed at each annealing temperature with 20 cycles of 15 seconds at 44°C (annealing), 120 second at 72°C (extension) and 12 seconds at 94°C (denature). The PCR products were analyzed on a 1% agarose gel stained with ethidium bromide. Lanes 2-6 show the expected PCR product, 2.6 kb fragment. 1 and 7 represent 1 kb markers.

Many attempts were also made to amplify cDNA for *At*F24D13.3 and *At*F24D13.4 using random primers (instead of an oligo dT primer) to generate first strand cDNA template. However, the resulting PCR products were of low yield and produced gel streaking. No further attempts were made to clone cDNAs for either *At*F24D13.3 or *At*F24D13.4.

4.6 RT-PCR Cloning of *At*F14H20.5 cDNA.

Another BAC sequence that has been deposited in the *Arabidopsis* genomic sequence database, BAC clone F14H20, also contains a sequence with homology to known Na^+/H^+ antiporters (F14H20.5). Suitable primers were designed to this sequence (as shown in Table 4.2 and 4.3,), and these used in an attempt to amplify a full-length *At*F14H20.5 genomic sequence. The resulting PCR products were resolved by agarose gel electrophoresis (Fig. 4.10), and a band was observed of the predicted size (6.1 kbp). These results of these experiments suggest that these primers may be suitable for amplifying a full-length cDNA using RT-PCR.

4.6.1. RT-PCR Amplification of First Strand *At*F14H20.5 cDNA.

After suitable conditions were determined Touch Down PCR was carried out with some modifications (see legend to Fig 4.11). RT-PCR products from the reaction were visualized by gel electrophoresis, as shown in (Fig. 4.11), and single bands formed of the expected size (3.5 kbp), as predicted from the NCBI database.

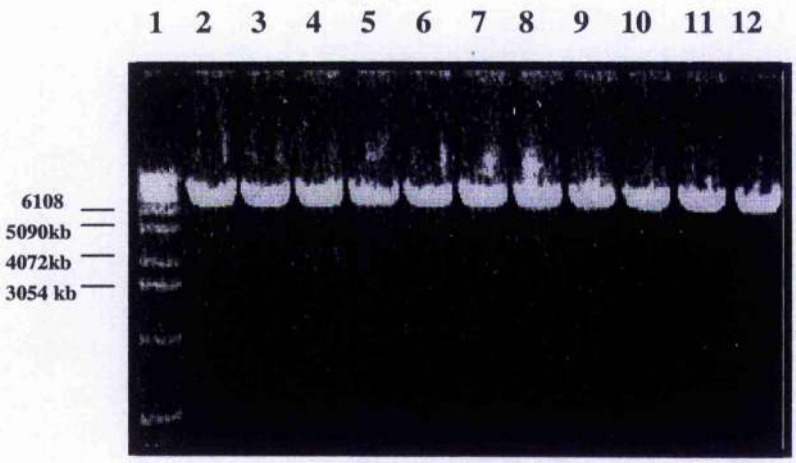

Figure. 4.10. PCR Amplification of *At* F14H20.5 from Genomic DNA Template.

The primers were designed to bind nineteen bases upstream the ATG translation start site and eleven bases down stream the TGA translation stop sequence. The reaction contained 50-100 ng of genomic DNA, 2.6 mM MgCl, 50 pmol primers, 200 μM dNTPs, 1X *Taq* buffer (20 mM Tris-HCl, 1mM dithiothreitol, 0.1 mM EDTA, 0.1 M KCl, 0.5% Nonidet P40 (v/v), 0.5% Tween 20 (v/v), 50% glycerol (v/v), pH 8.0 (4°C), and 2.5 units of *Taq* DNA polymerase (final volume of 50 μL). The reaction was started (hot start) by the addition of *Taq* DNA polymerase at 94°C, and followed by 35 cycles of 30 seconds at 50°C (annealing), 120 second at 72°C (extension) and 30 seconds at 94°C (denature). The PCR products were analyzed on a 1% agarose gel stained with ethidium bromide. Lanes 2-12 represent the expected size fragment for PCR product, 6.1 kbp. Lane 1 contain molecular weight markers x marker, Boehringer Mannheim.

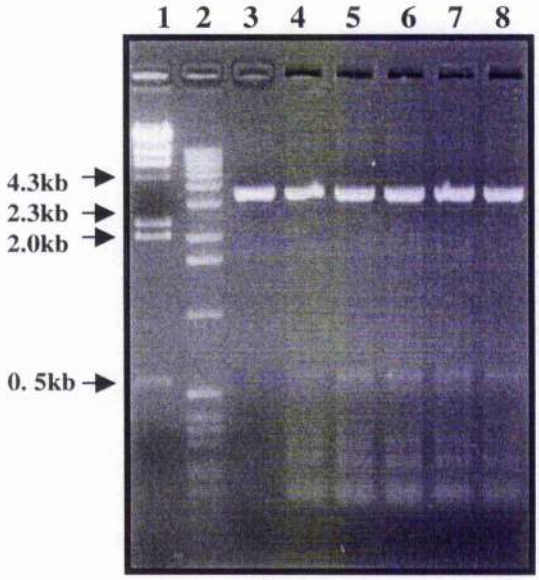

Figure. 4.11. RT-PCR Amplification of *Arabidopsis At*F14H20.5 cDNA.

RT-PCR was used to amplify the first strand of *At*F14H20.5 cDNA prepared from the HHS *Arabidopsis thaliana* (var. Columbia) cell line grown in high salt (260 mM NaCl). Total RNA was isolated and first strand cDNA prepared using MMLV reverse transcriptase with an oligo (dT) primer. The *At*F14H20.5 primers were used with high fidelity *Taq* DNA polymerase in a PCR. The reaction contained 1.5-2.5 μL first strand cDNA template, 2.6 mM MgCl, 50 pmol primers, 200 μM dNTPs, 1X high fidelity *Taq* buffer (20 mM Tris-HCl, 100 mM KCl, 1mM dithiothreitol (DTT), 0.1 mM EDTA, 0.5% Tween 20 (v/v), 0.5% Nonidet P40 (v/v), 50% glycerol (v/v), pH 7.5, and 2.5 units of high fidelity *Taq* DNA polymerase (final volume of 50 μL). The reaction was started (hot start) by the addition of high fidelity *Taq* at 94°C. A Touch Down PCR programme was used, with annealing temperatures decreasing from 51°C down to 48°C steps of 1 degree. Five cycles were performed at each annealing temperature, with 20 cycles at 48°C for 20 seconds (annealing), 120 second at 72°C (extension) and 20 seconds at 94°C (denature). The PCR products were analyzed on a 1% agarose gel stained with ethidium bromide. Lanes 3-8 show the expected PCR 3.5 kb fragment. Lane 1 contains λ Hind III, and lane2 1kb ladder marker.

The product of the RT-PCR using random primer first strand synthesis was estimated to be the same size as that produced from template using oligo dT first strand synthesis Fig. A1.6 (see Appendix). The resulting fragments from the above reaction were excised from the gel and purified as described in (Section 2.2.7), cloned into PCR -Script Amp SK (+) cloning vector (Section 2.2.12.4.1.3), and transformed into the host *E. coli* strain XL10-Gold Kan ultra-competent cells (provided with PCR-Script Amp Cloning Kit- Stratagen; see Section 2.2.3.3). The initial stages of cloning appeared to work. Amplification of the vector insert was carried out by colony PCR on white colonies identified by X-gal selection and inserts of the appropriate size were observed 3.5 kbp Fig. A1.7 (see Appendix). However, subsequent attempts to amplify these colonies in liquid or on solid media resulted in poor growth, and was followed by cell death. Another cloning system was used (PET 28 see Section 2.2.12.4.1.1), but this also failed; the reasons for this are unclear.

4.4.1.3. Northern Analysis of *At*F14H20.5.

Although attempts to perform a secondary amplification of this clone for the sequencing were unsuccessful, it was decided to carry out northern analysis to determine the expression pattern of this gene in the HHS cell line. Northern blot analysis was carried out to investigate *At*F14H20.5 expression in salt stressed (HHS) and unstressed (control) *Arabidopsis* cell lines. Total RNA was isolated from independent untreated (0 mM) and treated (supplemented with 260 mM NaCl) *Arabidopsis* cell suspension cultures 3 days after transfer to the conditioning media. Fourteen micrograms of total RNA were loaded in

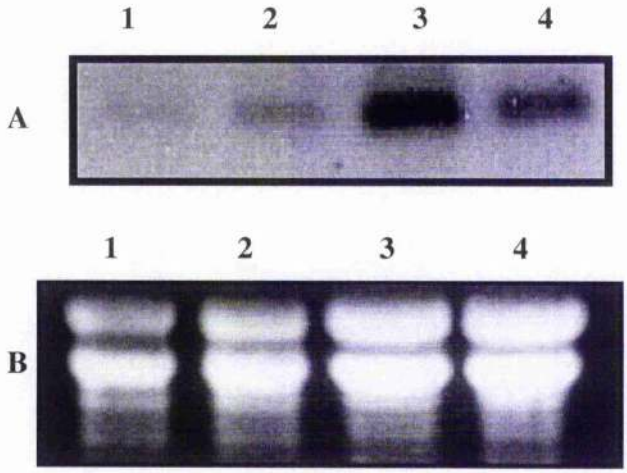

Figure. 4.12. Northern Analysis of *At* F14H20.5 Expression in HHS *Arabidopsis* Cell Line.

Total RNA was extracted from two independent control cell cultures (0mM supplemented NaCl lanes 1 and 2), and two independent HHS cell lines stressed with 260 mM NaCl lanes 3 and 4). Fourteen micrograms of total RNA was loaded in each lane (see Section 2.2.5.3), electrophoresed in a 1.3 % (w/v) agarose gel containing formaldehyde shown in (B), blotted onto a nylon membrane and probed with ^{32}p-labeled *At*T12H17.230 cDNA (RT-PCR amplified fragment of *Arabidopsis* HHS cell lanes stressed with 260 mM NaCl as probe (A). The membrane was ^{32}p-labeled washed at high stringency (0.1 X SSC at 60 °C) and autoradiographed for 3 days at -80.

each lane of a 1.3 % (w/v) formaldehyde agarose gel (Section 2.2.5.3), and then electrophoresed. Northern blot analysis was performed as described in (Section 2.2.8.1) using P^{32}-labeled *At* F14H20.5 cDNA as a probe (synthesized by asymmetric PCR, see Section 2.2.9.1). The membrane was washed at high stringency (0.1 X SSC at 60°C see Section 2.2.10.2), and autoradiographed for 4 days at -80°C (see Section 2.2.10.3).

Expression of *At*F14H20.5 in WT and HHS (0 and 240 mM NaCl respectively) cells is shown in (Fig.4.12 A), the expression of cDNA gene was detected in untreated cells (lane 1 and 2), but strongly expressed in *Arabidopsis* treated cells (lane 3 and 4), suggesting the gene was strongly induced by salt stress, and may have a specific role in Na^+ tolerance. However, it is also possible that the expression levels detected in the HHS cell line, and the slight differences between the treated one (lane 3 and 4), may be because of the independent sources of cell line. However, it is also possible that different abundance of transcript hybridizing to this probe represents differences between the two cell lines, rather than the effect of NaCl stress

4.7. RT-PCR Cloning of *At* T12H17.230 cDNA.

The *Arabidopsis* sequence *At*T12H17.230 has good homology to several prokaryotic and lower eukaryotic genes that code for Na^+ /H^+ antiporters. Figure 4.2 presents the phylogenic relationship between some of these transporters and *At*T12H17.230. The predicted *At*T12H17.230 protein was estimated by the TMPRED program to have 10 or 11 transmembrane α-helices (http://dot.imgen.bcm.tmc.edu.).

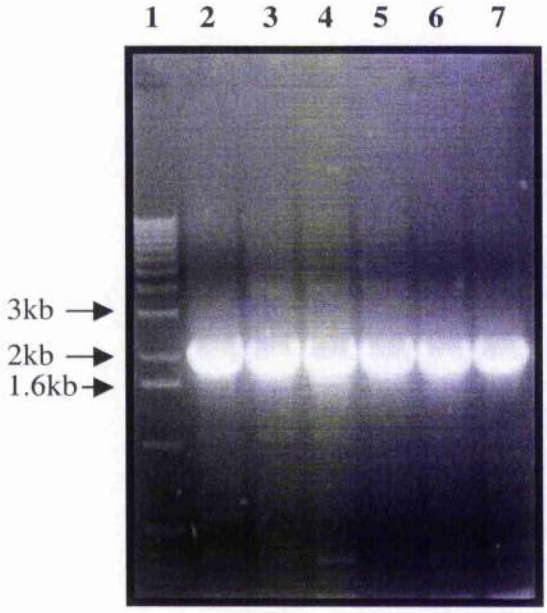

Figure. 4. 13. PCR amplification of *AT* T12H17.230 from Genomic DNA Template.

The primers were designed to bind at a locus twenty nine bases upstream the ATG start site and seventeen bases down stream of the TGA translation stop sequences used in the PCR reaction. The reaction contained 50-100 ng of genomic DNA, 2.5 mM MgCl, 50-100 pmol primers, 200 μM dNTPs, 1X *Taq* buffer (20 mM Tris-HCl, 1 mM dithiothreitol, 0.1 mM EDTA, 0.1 M KCl, 0.5% Nonidet P40 (v/v), 0.5% Tween 20 (v/v), 50% glycerol (v/v), pH 8.0 (4°C), and 2.5 units of *Taq* DNA polymerase (final volume of 50 μL). The program was started (hot start) by the addition of *Taq* DNA polymerase at 94°C, and followed by 35 cycles of 15 seconds at 49°C (annealing), 120 second at 72°C (extension) and 12 seconds at 94°C (denature). The PCR products were analyzed on a 1% agarose gel. Lanes from 2-7 represent the expected size fragment for PCR product, 2.1 kbp. Lane 1 contains a1 kb Ladder marker.

Primers were designed by the web PRIMER3 on-line program that overlapped twenty two bp up stream of the translation start site and twenty five bp down stream of the stop signal in the genomic sequences (Table 4.2 and 4.3). These primers were used with *Arabidopsis* genomic DNA isolated from untreated cell suspension cultures and after optimization, the resulting PCR products were resolved by agarose gel electrophoresis. One band was amplified of the correct size 2.1 kbp, exactly as expected from database information for *At* T12H17.230 genomic sequences (Fig.4.13).

A PCR was set up using amplified *At*T12H17.230 first strand cDNA as template (oligo dT primed), and one fragment was formed of the correct size (1.4 kbp) as predicted by the *Arabidopsis* genome data base (Fig.4.14).

A product of a RT-PCR using random primed first strand synthesis was also produced and estimated to be of the expected size (1.4 kbp).

4.7.1. Cloning and Sequencing of *At* T12H17.230 cDNA.

The amplified 1.4 kbp fragment was run on an agarose gel (Section 2.2.5.2), and the resulting band excised and purified (see Section 2.2.7), cloned into PCR -Script Amp SK (+) cloning vector (Section 2.2.12.4.1.3), and then transformed into TOPO10 host *E. coli* strain and grown without IPTG (Section 2.1.2). Colony PCR amplification of the resulting colony plasmid vector insert was carried out (Section 2.2.12.4.3; Fig. A1.8 see Appendix) to identify clones suitable for sequencing. The *At*T12H17.230 cDNA was sequenced (Section 2.2.16) in both directions (T7 and T3 primers) by MWG-Biotech GmbH (Germany). The two sequences determined from the ends of the clone *At* T12H17.230 did

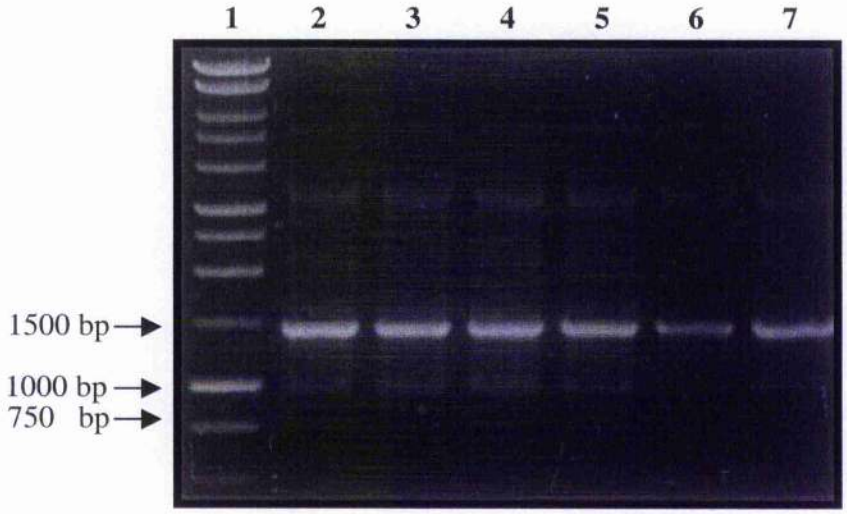

Figure. 4.14. RT-PCR Amplification of *Arabidopsis At*T12H17.230 cDNA.

A RT-PCR was used to amplify the first strand of *At*T12H17.230 cDNA prepared from an *Arabidopsis thaliana* (var. Columbia) HHS cell line grown in high salt (260 mM NaCl). Total RNA was isolated from HHS cells and first strand cDNA prepared using MMLV reverse transcriptase with an oligo (dT) primer. The *At* T12H17.230 primers were used with high fidelity *Taq* DNA polymerase in a PCR reaction. The reaction contained 1.5-2.5 μL first strand cDNA template, 2.5 mM MgCl, 50-100 pmol primers, 200 μM dNTPs, 1X high fidelity *Taq* buffer (20mM Tris-HCl, 100 mM KCL, 1 mM dithiothreitol (DTT), 0.1 mM EDTA, 0.5% Tween 20 (v/v), 0.5% Nonidet P40 (v/v), 50% glycerol (v/v), pH 7.5, and 2.5 units of high fidelity *Taq* DNA polymerase (final volume of 50 μL). The reaction was started (hot start) by the addition of high fidelity *Taq* at 94°C. A Touch Down PCR programme was used, with annealing temperatures decreasing from 52°C down to 49°C in 1 degree steps. Five cycles were performed at each annealing temperature, and followed by 20 cycles of 15 seconds at 49°C (annealing), 120 second at 72°C (extension) and 12 seconds at 94°C (denature). The PCR products were analysed on a 1% agarose gel stained with ethidium bromide. Lanes 2-7 show the expected PCR product, 1.4 kb fragment. Lane1 contains a1 kbp DNA marker ladder.

not overlap, and therefore the full sequence was not determined at this stage. However, BLAST sequences of the *Arabidopsis* genome confirmed that the clone did indeed represent the product of the genomic sequence *At* T12H17.230. Therefore, internal primers were designed from the 5' and 3' sequence (Table 4.2 & 4.3), and these used to generate a PCR fragment that spanned the gap from the cloned cDNA. This fragment was cloned (section 2.2.12.4.1.3). Alignments were made from these 3 sequences and the full-length cDNA sequence deduced (Fig. 4.15). *In silico* translation of the *At*T12H17.230 cDNA produced a protein of 409 amino acids, shorter than the predicted peptide, and estimated by the TMPRED program (http://dot.imgen.bcm.tmc.edu.) to have 10 or 11 transmembrane α-helices. BLAST 2 searches of the database found that the protein shows 87% identity to that predicted for *At*T12H17.230 Fig. A1.9 (Appendix), and the closest homologies were to bacterial Na^+/H^+ antiporters (e-scores of 1e-31, *Pseudomonas aeruginosa*).

Recent database searches have found that the *At*T12H17.230 protein shows 100% identity to *At*4g22840.1 Fig. A1.10 (see Appendix) that appeared on the database on 20 Aug-2002. Further analysis of the databases identified two other identical cDNA confirming the sequence presented in this study and not that presented in the genomic databases is correct. Further, BLAST searches suggest that only one homologue of *At* T12H17.230 exist in *Arabidopsis* (on chromosome 4). CLUSTALW alignments of the predicted *At* T12H17.230 protein with protein sequences from other authentic Na^+/H^+ antiporters are shown in (Fig. 4.2). It appears, that *At*T12H17.230 clusters with the *S. pombe* SOD 2, *P. aeruginosa* NhaP, and *Arabidopsis thaliana At* F14 H20.5 (SOS1) sequences (Fig. 4.16). Further analysis of the AtT12H17.230(At4g22840.1) protein sequence using the MIPS web site

F primer

CGGTGGCGGCCGCTCTAGCCCAAACATCACAAACTCTAAAGAAAAAAA[redacted]AGCGTGATCA

CAACTCCAATAGAGACCCTGCCACCTAAATCAACACTTCGTCTTCTACCACGAGCTGTTTA

TCGCAGTCAACGGATTCAAGTTTTCCCGCCCAACATCTTCTCGAACACTCCTCTGAGTTCT

CCACTTCGCATCGACCCAATCTCTCAAGTTGGCGGATCGAGGAATTTGTGGCGTAGATATG

Internal F

CATCTGATAATTTCTCGGAGATGGGTTTGGATCCTGGAGCTGATCCATTCAAGGTTATTGA

GAAGCCTTCTATAGTGGATAGAATGAAGAAAGCAAACTCAATTCTTCCTCATGTAGTGTTG

GCGAGTACAATATTAGCTCTTATCTATCCTCCTTATTTCACTTGGTTTACTGCGAGGTACT

TTGTGCCCGCTTTAGGTTTTTTGATGTTTGCGGTTGGTATCAATTCAAACGAGAAAGACTT

TCTTGAAGCTTTCAAAAGACCAAAAGCTATCCTCCTCGGTTATGTTGGACAATATCTCGTA

AAGCCTGTCCTAGGTTTCATCTCTGGCCCAGCTGCTGTTTCTCTTTTCCAACTCCCAACTC

CAATTGGTGCTGGAARCATGTTGGTATCATGTGTCAGTGGAGCTCAGTTGTCAAACTATGC

GACATTCCTAACTGATCCAGCACTGGCACCTCTTAGCATCGTCATGACATCTCTATCAACC

Internal R

GCTACTGCGGTTCTTGTCACACCGATGCTATCACTCCTGCTCATTGGGAAGAAACTACCCG

TTGATGTAAAAGGAATGATATCCAGCATTCTTCAGGTTGTAATCGCACCAATCGCTGCAGG

ATTGCTACTAAACAAGTTGTTCCCAAAAGTATCAAATGCAATCCGACCATTTCTCCCGATT

CTATCGGTTCTCGACACAGCTTGCTGCGTTGCAGCACCACTCGCATTGAACATAAACTCGG

TCATGTCTCCATTTGGAGCCACCATATTGTTACTAGTAACAACGTTTCATCTCTCAGCTTT

CCTCGCTGGATACTTCCTTACCGGTTATGTCTTTAGAAACGCTCCAGACGCTAAAGCCATG

CAAAGAACATTGTCCTATGAAACTGGAATGCAGAGTAGCCTTTTGGCTCTAGCGCTTGCTA

CTAAGTTCTTTCAAGATCCTCTCGTGGGGATTCCCCCTGCTACATCTACGGTGGTAATGTC

R primer

ATTGATGGGGTTCACTCTCGTTTT[redacted]CTGGTCTAAGGAAAAGAGTAACGCATTTTAACAT

TTTGATTTTGTTTCACT*

Figure. 4.15. The Nucleotide Sequence of The *At*T12H17.230 cDNA.

The cDNA for a putative Na^+/H^+ antiporter from *Arabidopsis thaliana At* T12H17.230 was synthesized by oligo dT primer and amplified by RT-PCR. The cDNA sequence is 1227 bp with a 5'-ATG translation start site and 5'-GAT translation stop site. The reverse primer (R) binds 6 bases upstream of the ATG translation start site (green) and (F) primer bind 15 bp before 5'-GAT translation stop site. The internal primer sites for amplifying the central part of the cDNA (blue) are also shown.

TAIR programe (www.Arabidopsis.org.com/), confirms 8 to 9 putative membrane spanning α helices, significant alignments for putative conserved domains have been detected to COG0385, predicted Na^+-dependent transporter and SBF, Sodium Bile acid symporter family (Fig.4.16).

4.7.2. Expression of *At*T12H17.230.

The expression levels of *At*T12H17.230 in control (0mM NaCl) and HHS (260 mM NaCl) cells were investigated. Total RNA was extracted from untreated (0mM NaCl) and treated (260-mM NaCl) *Arabidopsis* cell lines grown for three days (mid log phase). Samples were isolated from duplicate cultures of both of control and HHS *Arabidopsis* cells were grown and total RNA extracted from each. Thirteen micrograms of total RNA were loaded in each lane of an agarose gel, and electrophoresed (Section 2.2.6.2; Fig. 4.17 B). Samples were then transferred onto a membrane for northern blot analysis with ^{32}P-labeled *At*T12H17.230 cDNA as probe (Section 2.2.9.1). The membrane was washed with 2 X SSC once at room temperature and twice with high stringency (0.1 X SSC, 0.1 % SDS at 60 ° C for 20 min; see Section 2.2.10.2), and autoradiographed for 3 days at -80°C as described in (Section 2.2.10.3). The *At*T12H17.230 transcript appears to be up regulated in treated cells (lane 3 and 4) compared with untreated cells (lane 1 and 2). Suggesting this sequence may be involved in salt tolerance in HHS cells.

4.7.3. Function Analysis of the *At* T12H17.230 Full-length Gene.

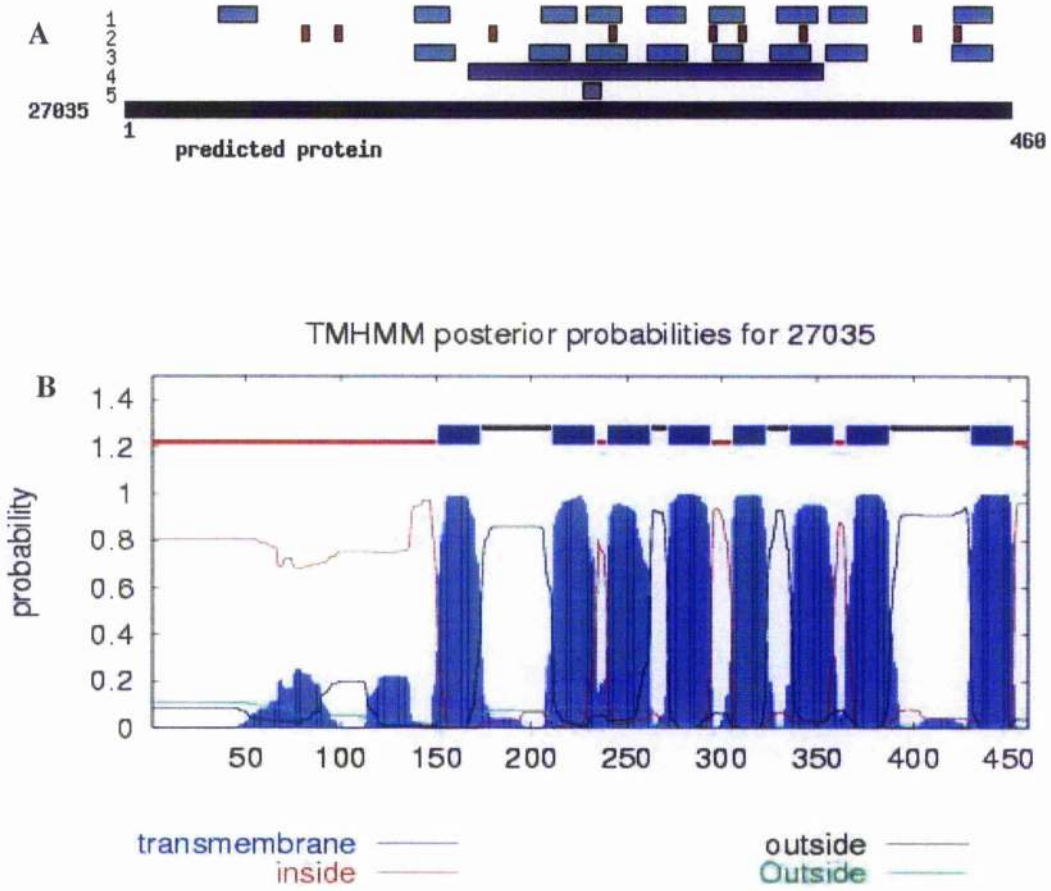

C

MSVITTPIETLHLKSTLRLLPRAVYRSQRIQVFPPNIFSNTSLSSPLRIDPISQGLFILLSSILRRLCLLGTCKIY
TFFSHGFLQPTIYTVGGSRNLWRRYASDNFSEMGLDPGADPFKVCAMGSFLFHSMLCWVIEKPSIVDRMKKANSIL
PHVVLASTILALIYPPSFTWFTSRFFPLEQGFLMFAVGINSNEKDFLEAFKRPKAILLGYVGQYLVKPVLGFIFGL
AAVSLFQLPTPIGAGIMLVSCVSGAQLSNYATFLTDPALAPLSIVMTSLSTATAVLVTPMLSLLLIGKKLPVDVKG
MISSILQVVIAPIAAGLLLNKLFPKVSNAIRPFLPILSVLDTACCVGAPLALNINSVMSPFGATILLLVTMFHLSA
FLAGYFLTGSVFRNAPDAKAMQRTLSYETGMQSSLLALALATKFFQDPLVGIPPAISTVVMSLMGFTLVLIWSKEK
SNTF

Figure. 4.16. Protein Structure of At4g 22840 (old Code AtT12H17.230).

A, TMPred; the translation of the putative full-length open reading frame revealed a protein of 409 amino acids. The protein has 9 (line 1) or 8 (line3) putative membrane spanning α-helices, and 9 N-myristoylation sites (brown, line 2). A region with high similarity to the Na^+-bile acid symporter family (violet, line 4) is also shown. Line 5 (light violet) homology to prokaryote membrane lipoprotein attachment site. B, TMHMM prediction, shows 8 putative membrane spanning α-helices; posterior probabilities (blue) and number of transmembrane helices inside (blue) and outside (brown) are presented, C, protein sequence of AtT12H17.230 (*At*4g 22840).

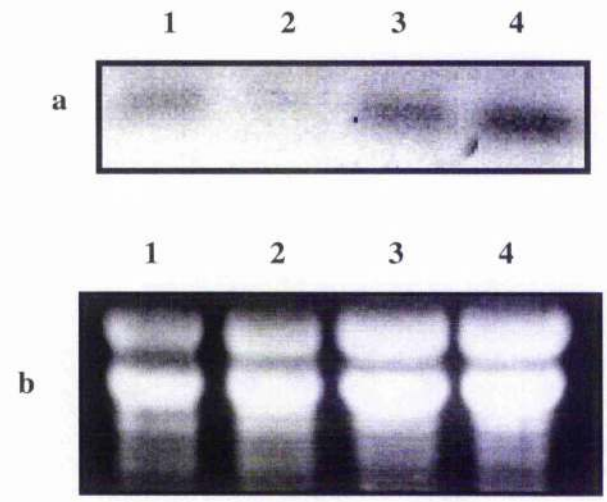

Figure. 4.17. Northern Analysis of *At*T12H17.230 Expression in *Arabidopsis* Cells Exposed to NaCl.

Total RNAs were extracted from two independent control cell cultures (0 mM supplemented NaCl, lanes 1 and 2), and two independent HHS cell lines (treated with 260 mM NaCl lanes 3 and 4). Thirteen micrograms of total RNA were loaded in each lane. Electrophoresed in a 1.3 % (w/v) agarose gel containing formaldehyde. Blotted onto a nylon membrane and probed with ^{32}P-labeled *At*T12H17.230 cDNA (RT-PCR amplified fragment of *Arabidopsis* HHS cell lines treated with 260 mM NaCl as probe). The membrane was washed at high stringency (0.1 X SSC at 60 ^{o} C) and autoradiographed for 3 days at -80. A, northern blot. B, RNA gel.

Several approaches can be used to establish whether *At*T12H17.230.230 has any role in maintaining ionic balance in salt stress-stressed *Arabidopsis* plants. One approach is to over express the *At*T12H17.230 protein in a wild type background, and to study the phenotype of the transgenic line for improved salt-tolerance. Recently, three transgenic T-DNA knockout of lines *At*T12H17.230 have been found. The ID for these knockout lines are as follows: Clone Id; SALK_044369.39.90, Gene Bank Acc. No. 19035143: clone Id; SALK_096300, Gene Bank Acc. No. 22100485: clone Id; SALK_095244, Gene Bank Acc. No. 22099948. Three hundred and sixty-eight bp of sequence was recovered from the left border of the SALK_096300 TDNA line and the sequence lies within an annotated exon of 300 bases of the 5' end of At4g22840. One hundred and eighty-eight bp recovered from the left border of Clone Id: SALK_095244 and the sequence lies within the coding sequence of 300 bases of the 5' end of the gene. Four hundred and fifty-one bp was found the left border of the clone SALK_044369.39.90 and the sequence lies within an annotated exon of 300 bases of the 5' end of the gene.

These knockout lines were being procured for further studies, along with over-expression experiments, when the Bower building fire struck (24/10/2001), and consequently these experiments were not completed.

4.8. RT-PCR Cloning of *At* T20D21.19 cDNA.

First strand cDNA for *At*T20D21.19 was synthesized by reverse transcription of RNA isolated from high salt-grown HHS cells (260mM NaCl), using an oligo dT primer. Specific primers of *At*T20D21.19 (Table 4.2) were used in a PCR to amplify the first

strand. PCR products were electrophoresed on a 1% (w/v) agarose gel (Fig. 4.18), and a number of bands were detected, two of them with sizes of 1.5 to 1.6 kbp, as predicted. The larger one (approximately 1.6 to 1.7 kbp), amplified poorly compared to the other (1.5 kbp).

An RT-PCR reaction was also carried out with the first strand *At* T20 D21.19 cDNA synthesized by random primers as a template. After suitable conditions were found the PCR formed products that were electrophoresed on agarose gels, several bands were formed, and one of them was of the predicted size 1.6 kbp Fig. A1.11 (Appendix). It was decided to use both fragments as estimates of cDNA length are sometimes incorrect. Fragments (1.5 and 1.6 kbp) were excised from each gel and purified (Section 2.2.7), and named *At* T20 D21.19A and *At* T20 D21.19B.

4.8.1. Cloning and Sequence of *At* T20D21.19 A.

The two fragments were cloned into PCR -Script Amp SK (+) cloning vector (Section 2.2.12.4.1.3), and transformed into TOPO10 host *E. coli* strain, and plated on media without IPTG (Section 2.1.2). Colony PCR was used to analyze colonies for inserts of the expected size (see Section 2.2.12.4.3 and Fig. A1.12 Appendix).

*At*T20D21.19 A cDNA was sequenced in both directions (T7 and T3 primers) by MWG-Biotech GmbH (Germany). The resulting sequence was then used in a BLASTN search (www.ncbi.nlm.nih.gov/). However, the results obtained from BLASTN suggested that the nucleotide sequence submitted did not represents the *At*T20D21.19 sequence, but was identical to a gene coding for an ABC transporter Fig. A.1.13 (Appendix).

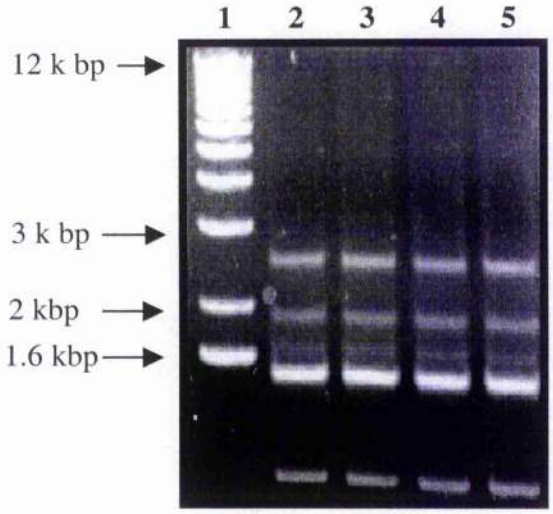

Figure. 4.18. RT-PCR Amplification of *Arabidopsis* Fragment *At*T20D21.19 cDNA.

A RT-PCR was used to amplify the first strand of *At* T20D21.19 cDNA prepared from an *Arabidopsis thaliana* var. Columbia HHS cell line grown in high salt (260 mM NaCl). Total RNA was isolated from HHS cells and first strand cDNA prepared using MMLV reverse transcriptase and oligo dT primers. The *At* T20D21.19 primers were used with high fidelity *Taq* DNA polymerase in a PCR. Five cycles were performed at each annealing temperature, with 20 cycles. The reaction contained 2.5 μL first strand cDNA template, 2.6 mM MgCl, 50 pmol primers, 200μM dNTPs, 1X high fidelity *Taq* buffer (20mM Tris-HCl, 100 mM KCl,1mM dithiothreitol (DTT), 0.1mM EDTA, 0.5% Tween 20 (v/v), 0.5% Nonidet P40 (v/v), 50% glycerol (v/v), pH 7.5, and 2.5 units of high fidelity *Taq* DNA polymerase (final volume of 50 μL). The reaction was started (hot start) by the addition of high fidelity *Taq* at 94°C. A Touch Down PCR programme was used, with annealing temperatures decreasing from 51°C down to 46 °C steps of 1 degree. Five cycles were performed at each annealing temperature, with 10 cycles at 46°C for 15 seconds (annealing),120 second at 72°C (extension) and 12 seconds at 94°C (denature). The PCR products were analyzed on a 1% agarose gel stained with ethidium bromide. Lanes 2-6 show the expected PCR product, 1.6 kb fragment. Lane1 represents a 1kb marker.

The *At*T20D21.19 B cDNA was sequenced in both directions (T7 and T3 primers) at MWG-Biotech GmbH (Ebersberg, Germany). The nucleotide sequences was used to search databases using BLASTN on-line program (Section 2.2.17), to compare it with the nucleotide sequences deposited in *Arabidopsis* sequences database. The results obtained from BLASTN suggested that the nucleotide sequence submitted did not represent the *At*T20D21.19 sequence coding for putative Na^+/H^+ antiporter, but has significant homology to an unknown protein (94%) accession No. 8051670. Part of Blast output is presented in Fig. A.14 (Appendix).

4.9. DISCUSSION:

Two PCR approaches (conventional and RT-PCR) have been used in this study to clone fragments of both genomic DNA and cDNAs coding for putative function Na^+/ H^+ antiporters. Suitable degenerated primers were designed from the consensus regions, and specific primers have been designed from each upstream and downstream target sequence for use with the PCR.

Initially, degenerated primers were used with a conventional PCR approach, but this failed to amplify any fragments from a cDNA library of *Arabidopsis* seedling roots (Minet, 1992), or from all organs, at all stages of developments (Elledge, 1990). This possibly reflects the low abundance of full-length copies of Na^+/H^+ antiporters in these low salt-grown cDNA libraries, or the unsuitability of the degenerated primers. Moreover, attempts made to generate *At* B04.4 a sequence (coding for a putative Na^+/H^+ antiporter from these libraries using two sets of specific primers) failed to generate the expected product. This could be due to the absence of this clone in the libraries.

Specific primers designed from the seven sequences coding for putative Na^+/H^+ antiporters were used with the *Arabidopsis* genomic DNA as a template. After suitable concentrations of each PCR component were established for each sequence, in all cases fragments of expected size were obtained of these seven sequences, six cDNA fragments of the expected size were successfully amplified. Despite an extensive series of experiments, the amplification of *At*F24D13.4 cDNA was not successful. Although the primers worked when genomic template was used no PCR products were formed when first strand cDNA was used as template, which may reflect that the *At*F24D13.4 is not expressed, or the primers bind to different sites, which may explain why several bands were produced (Fig.4.8).

A clone of the expected size for *At* T9D9.5 cDNA was amplified and sequenced. However, BLAST searches suggest it was not a putative Na^+/H^+ antiporter, but an unrelated sequence. These results suggested that, either *At* T9D9.5 is not expressed in cell lines, the primers used were not highly specific for this sequence, or the mature RNA for this sequence is not that predicted in the data base

Two cDNA fragments were amplified but proved difficult to clone (Bo4.4 [*At* Nhx1], and F14H20.5 [SOS1]). The initial stages of cloning appeared to work for both sequences. Colony PCR was conducted on white colonies on X-gal containing plates, and inserts of the appropriate size were observed. However, subsequent attempts to amplify this clone for sequencing failed. It is unclear why the attempts failed to obtain the secondary amplification in liquid medium for plasmid mini-prep or midi-prep. One possibility was that the presence of IPTG for blue / white colony selection during the initial primary screen resulted in the accumulation of toxic protein in *E coli* cells (Dreyer, *et al.*, 1999; Uozumi,

2001). Similarly, the *At* F14H20.5 (SOS1) gene was cloned into PCR-Blunt II-Topo vector (Shi *et al* 2000). This sequence was also difficult to amplify in *E. coli* as are many plant sequences coding for membrane proteins (Covic and Lew, 1996; Theodoulou, 1999). With perseverance it would probably have been possible to pool the low plasmid yield from multi-cultures, and proceed from there. However, as work on *At*B04.4 (*At NHX1*, Gaxiola *et al*., 1999; Apse *et al*., 1999), and *At* F14H20.5 (SOS1), She *et al*., 2000) was published during the course of this work, it was decided to stop further studies on these sequences.

Expression of *At*F14H20.5 (SOS1) in untreated (0 mM NaCl) and treated (260 mMNaCl) cell lines is up-regulated under conditions of salt-stress, and may play a role in Na^+ tolerance. *At*F14H20.5 (SOS1) has been cloned by others using positional cloning (Shi *et al* 2000), and the gene is reported to code for a plasma membrane Na^+/H^+ antiporter, regulated by salt stress and to export Na^+ out from the cells.

The full-length of *At*T12H17.230 cDNA was cloned and the amino acid sequence of the translated gene is 87% identical that predicted in the NCBI database. Translation of the *At*T12H17.230 cDNA sequence results in a protein with 409 amino acid residues, and 8 or possibly 9 membrane spanning α helices (as predicted by TMPred program, and TMHMM Fig.4.16). BLAST2 searches of the full database with the determined cDNA sequence identified the closest homologies to bacterial Na^+/H^+ antiporters (e-scores of 1e-31 *Pseudomonas aeruginosa*). Recent database searches have found that the *At*T12H17.230 protein shows 100% identity to *At*4g22840.1 Fig. A1.10 (Appendix), that appeared on the database on 20 Aug-2002. Further analysis of the databases identified two other identical cDNA confirming the sequence presented in this study is correct. Further, BLAST

searches suggest that only one homologue of *At* T12H17.230 exist in *Arabidopsis* (chromosome 4).

The *At*T12H17.230 was up regulated in high salt-grown HHS cells (260 mM NaCl) compared with the control cells (0 mM NaCl; Fig.4.17), this indicates the gene is induced by salt stress. The function of this gene has not yet been demonstrated. Therefore, it could be located in the plasma membrane like SOS1 (Shi *et al.*, 2000), or may be located in the endo-membrane system in pre-vacuoles like *At* Nhx1 (Gaxiola *et al.*, 1999).

The results obtained from BLASTN searches suggest that *At*T20D21.19 was not cloned. The reasons for this are that the *At*T20D21.19 mRNA population was very low, or the sequence predicted in the database is not correct.. Thus, the true start and stop sites might be upstream or down-stream from that given. Moreover, exon/ intron sizes predicted by programs could be incorrect, resulting in cDNAs with a different size. It therefore appears that miss priming could occur and primers were able to bind at different sites especially with high copy numbers mRNA populations that dominated the PCR reaction.

CHAPTER FIVE

TRANSCRIPTOME ANALYSIS OF SALT TOLERANT CELL LINES USING DIFFERENTIAL DISPLAY

CHAPTER FIVE

5. Transcriptosome Analysis of Salt Tolerant Cell Lines Using Differential Display.

It is generally considered that halophyte cells adapt to high salinity by adjusting their osmotic balance, and by the exclusion and sequestration of excess salt from the cells and tissues. Sodium/proton antiporter activity at the plasma and tonoplast membranes are believed to play a central role in these adaptive strategies, as discussed in chapter 1 (see Section 1.9). These defensive mechanisms function in a co-ordidated fashion to protect the cell from the deleterious effects of toxic ion accumulation.

Plant cellular and molecular responses to high salinity involve complex patterns of gene expression including genes coding for Na^+/H^+ antiporters (Seki *et al.*, 2002). It was decided to monitor changes in global gene expression when the HHS cell lines of *Arabidopsis* are exposed to high salinity (260mM NaCl) as this may identify mechanisms that are involved in salt tolerance. This may be achieved using two methods, DNA microarrays (Seki, *et al.*, 2002) and Differential Display (Muramoto *et al.*, 1999). Differential Display polymerase chain reaction (DD-PCR) was used in preference to *Arabidopsis* DNA microarrays because at that time (Spring, 2001) *Arabidopsis* microarrays were not routinely available. Thus, Differential Display polymerase chain reaction (DD-PCR) was carried out for the identification of transcripts that are differentially expressed in salt-treated HHS cells (260 mM NaCl) and untreated WT cells (0 mM NaCl) of *Arabidopsis.*

5.1. Identification of Differentially Abundant Genes Using DD-PCR.

DD-PCR was carried out with a RNAimage kit No. 3 (GenHunter) according to the manufacture's instructions but with some modification. Total RNA was extracted from WT (0mM NaCl) and HHS (260 mM NaCl) *Arabidopsis* cell lines as described in (Section 2.2.2.3), and three different anchored oligo dT primers (H-T_{11}M) where M either a A, C or G 3' base, were used to synthesize first-strand cDNA fragments by reverse transcription (Section 2.2.13.1). This was followed by a polymerase chain reaction (PCR) to amplify ^{33}P-labelled cDNA fragments using each one of the anchored oligo (dT) and all combinations of the 8 arbitrary primers (*ie.*, 3x8=24 reactions; Section 2.2.13.1). Duplicate samples were run for each of the 24 reactions, for both control and HHS *Arabidopsis* cell lines, (24 reactions x 2 duplicates x 2 cell lines = 96 samples). Labeled cDNAs fragments were fractionated, resolved and compared in polyacrylamide sequencing gels (as described in Section 2.2.13.3 and 2.2.15.4) and autoradiographed. Figure 5.1 presents typical results for seven different arbitrary pairs (1-7). Each pair contained the same anchored oligo (dT) (eg., 5'-AAGCTTTTTTTTTTG-3' H-T11 G) primer and a different arbitrary (H-AP) primer. Examples of differentially abundant cDNA bands are boxed. The abundance of cDNA fragments in samples from the HHS cells was found to be much improved when the anchored oligo (dT) (H-T11 A) primer was used rather than the oligo (dT) H-T11 C and H-T11 G primers. Many bands were equally abundant in both the HHS (salt-treated) and WT (control) samples; however, there were also several examples of fragments that appeared to be differentially abundant (e.g., Fig 5.1, boxed). In total,

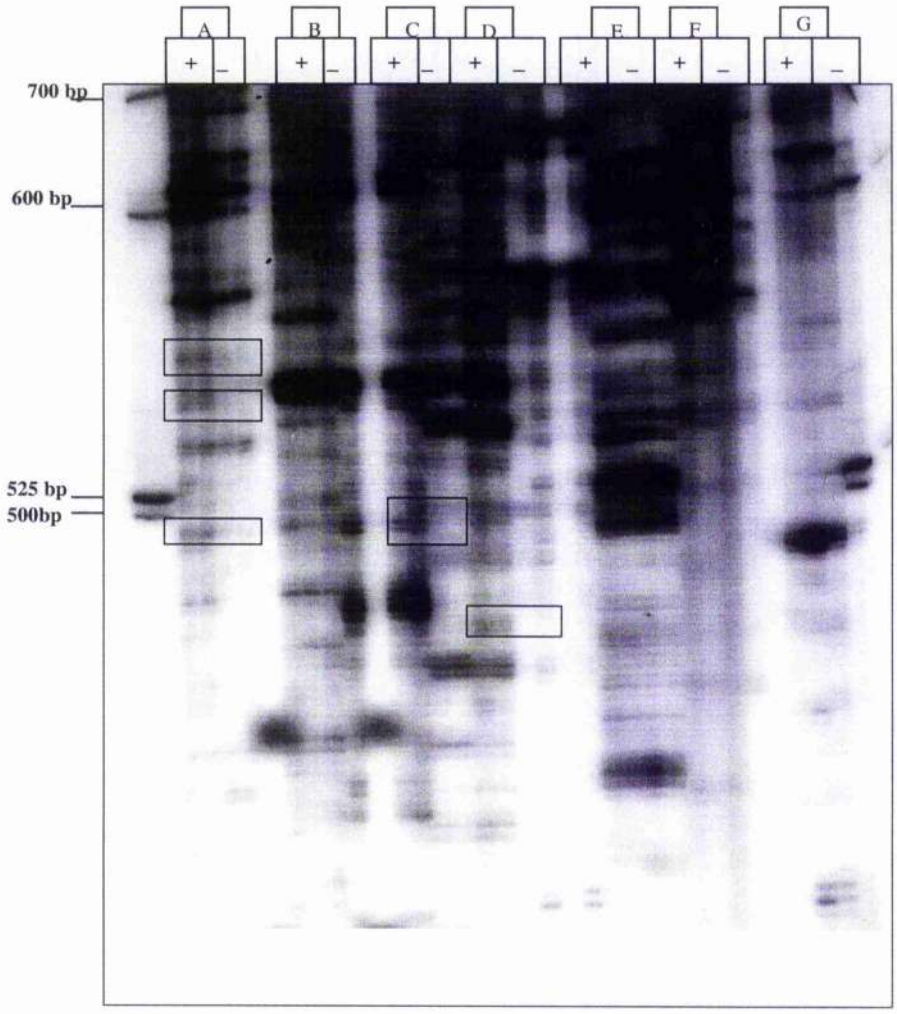

Figure. 5.1. Differential Display Polymerase Chain Reaction Gel of WT and HHS *Arabidopsis* Cells.

DD-PCR products were amplified from RNA isolated from WT and HHS *Arabidopsis* cell lines supplemented with 0 and 260 mM NaCl respectively. In all cases the Results (H-T11G) anchored oligo dT primer was used (5'-AAGCTTTTTTTTTTTG-3') with one of the eight arbitrary primers (H-AP), but only seven of the reactions are shown on this gel(reactions A-G). Duplicate reaction were run for HHS (+) and WT (-) samples, *i.e.*, 4 lanes per primer set. Examples of differentially abundant cDNAs are boxed. Molecular size standards were loaded on the left.

Up to 300cDNA fragments were identified as differentially abundant in these gels, and 172 of the most significant fragments were excised from the gels for further analysis. Of these 172, 100 were initially selected for re-amplification and confirmation of expression pattern; the remainders were stored at -80°C, awaiting further analysis.

5.1.1. Re-amplification of cDNA Eluted From Dried Gels.

The cDNAs bands were excised from gels, eluted and precipitated. The cDNA samples were re-amplified using the same primers (as described in Section 2.2.15.4). The size of the PCR products from this re-amplification was determined by agarose gel electrophoreses (Fig 5.2 A-5.4 C) and compared with that determined from the original labeled cDNAs sequencing gels (*e.g.*, Fig. 5.1). This procedure, successfully amplified cDNA eluted from the sequencing gels. Those samples that failed to amplify may represent bands that are false positives as shown in lanes 9 and 10 (Fig. 5. 2 A), lane 2 (Fig. 5. 2B), lanes 2-7(Fig. 5.3A), lanes 9-10 and 17-24 (see Fig. 5.4 A), lane 2 (Fig. 5.3 C), and lanes 10 and 11 (Fig. 5.4 C). The PCR conditions for the re-amplification of these failed, eluted samples were altered in an attempt to produce the appropriate bands, in addition, and attempts were made to re-amplify the appropriate bands from the original first strand cDNA mixture. After these attempts all 92 of the original 100 selected cDNA fragments appeared to be true positives (*e.g.*, Fig.5.3.B & 5.4B) and 8 bands appeared to be false positives (Malhotra *et al.*, 1998).

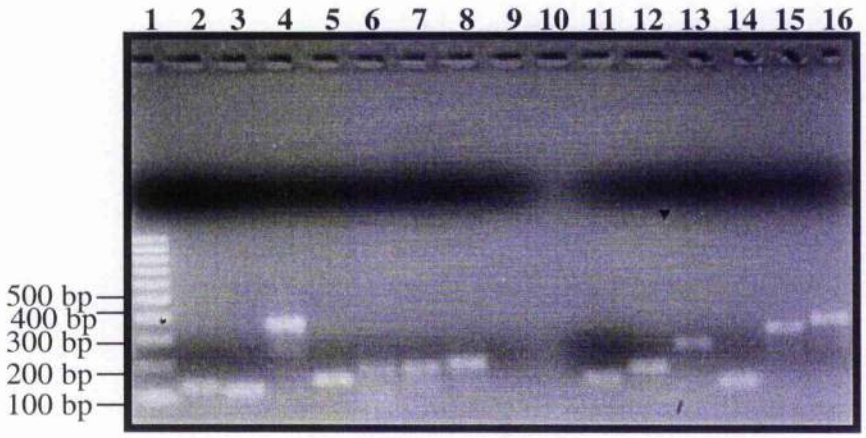

Figure. 5.2 (A). Re-amplification of the cDNA Bands Fractionated on DNA Sequencing Gel: Oligo dT (G) primer.

Re-amplification of cDNA by PCR using the same anchored oligo (dT) 5'-AAGCTTTTTTTTTTTG-3'(H-T11 G) down stream primer in combination with one of eight 13-mer arbitrary (H-AP) upstream primers. The program used was as follows: 15 s at 94°C: 40 cycles (12 s at 94°C, 15 s at 40°C, 30 s at 72°C, temperature slope setting = 3): 5 min at 72°C. The PCR products were analysed on a 1% agarose gel stained with ethidium bromide. Lanes from 2-16 represent the expected size fragment for PCR product that ranged from 150bp to 400bp. No PCR products formed in lanes 9-10 (false positive bands). Lane 1 represents the EZ Load 100 bp molecular ruler.

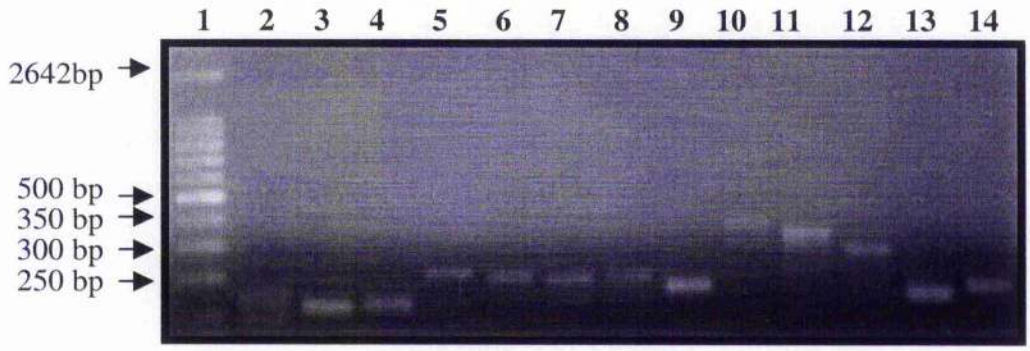

Figure. 5.2 (B). Re-amplification of the cDNA Bands Fractionated on DNA Sequencing Gel: Oligo dT (G) primer.

Re-amplification of cDNA by PCR using the same anchored oligo (dT) 5'-AAGCTTTTTTTTTTTG-3'(H-T11 G) down stream primer and eight different13-mer arbitrary (H-AP) upstream primers. The program used was as follows: 15 s at 94°C: 40 cycles (12 s at 94°C, 15 s at 40°C, 30 s at 72°C, temperature slope setting = 3): 5 min at 72°C. The PCR products were analysed on a 1% agarose gel stained with ethidium bromide. Lanes from 2-14 represent the expected size fragment for PCR product that ranged from 200bp to 400bp. No PCR products formed in lanes 2 (false positive band). Lane 1 contains the DNA-Langenstandards X111molecular weight markers.

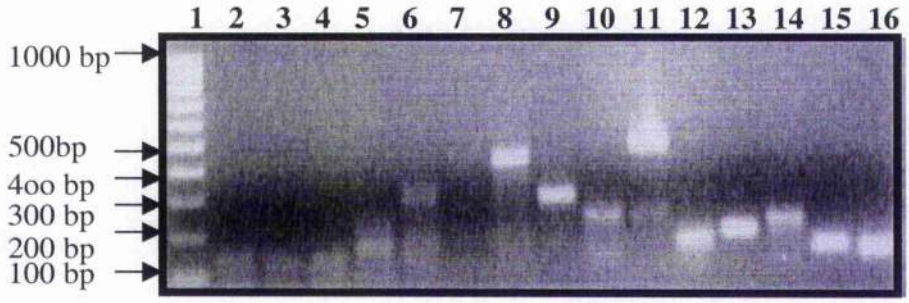

Figure. 5.3 (A). Re-amplification of cDNA Bands Fractionated on DNA Sequencing Gel: Oligo dT (A) primer.

Re-amplification of cDNA bands eluted from dried sequencing gel using the same anchored oligo-dT (H-T11A) down stream primer and different arbitrary (H-AP) upstream primers. PCR conditions were as follows: 15 s at 94°C: 40 cycles (12 s at 94°C, 15 s at 40°C, 30 s at 72°C, temperature slope setting = 3): 5 min at 72°C. The PCR products were analyzed on a 1% agarose gel stained with ethidium bromide. Lanes from 2-7 failed to amplify bands. Lanes from 8-16 represent the expected size fragment for PCR product ranged from 200 bp to 500 bp. Lane 1 contains the EZ Load 100 bp molecular ruler.

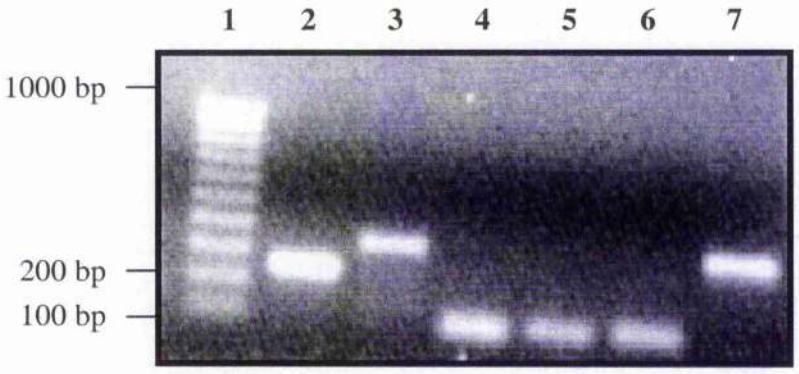

Fig. 5.3 (B). Re-amplification of the cDNA Bands Fractionated on DNA Sequencing Gel: Oligo dT (A) primer.

Re-amplification of cDNA bands, that failed to amplify by PCR (See Fig.5.4 A lanes 2-7), using the same anchored oligo-dT (H-T11A) down stream primer and different arbitrary (H-AP) upstream primers with cDNA eluted bands. The program used was as follows: 12 s at 94°C: 40 cycles (10 s at 94°C, 12 s at 40°C, 30 s at 72°C, temperature slope setting = 5): 5 min at 72°C. The PCR products were analyzed on a 1% agarose gel stained with ethidium bromide. Lanes from 2-7 represent the expected size fragment for PCR product ranged from 100bp to 400bp. Lane 1 contains the EZ Load 100 bp molecular ruler.

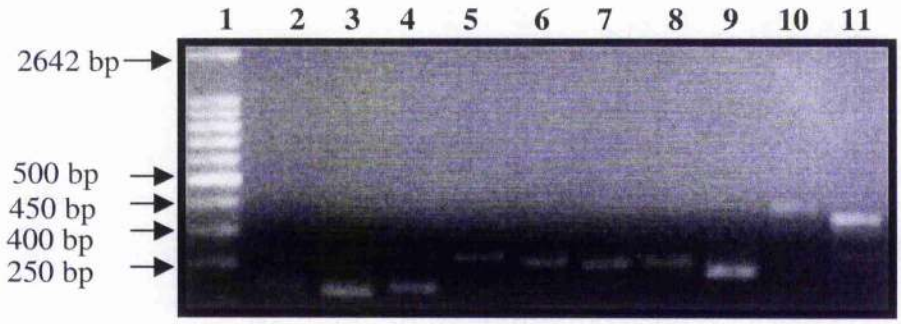

Figure. 5.3(C). Re-amplification of Differential Display cDNA Bands by PCR: Oligo dT (A) Primer.

Re-amplification of eluted cDNA bands by PCR with one of eight 13-mer arbitrary (H-AP) upstream primers in combination with an anchored oligo-dT (H-T11 A) down stream primer. The PCR conditions were as follows: 15 s at 94°C: 40 cycles (12 s at 94°C, 15 s at 40°C, 30 s at 72°C, temperature slope setting = 3): 5 min at 72°C or (See details in the instructions from the RNA image Kit No.3). The PCR products were analyzed on a 1% agarose gel stained with ethidium bromide. Lanes from 2-11 represent the expected size fragment for PCR product that ranged from 250bp to 450 bp. No PCR product formed in lane2 (false positive). Lane 1 contains the DNA-Langenstandards X111 molecular weight markers.

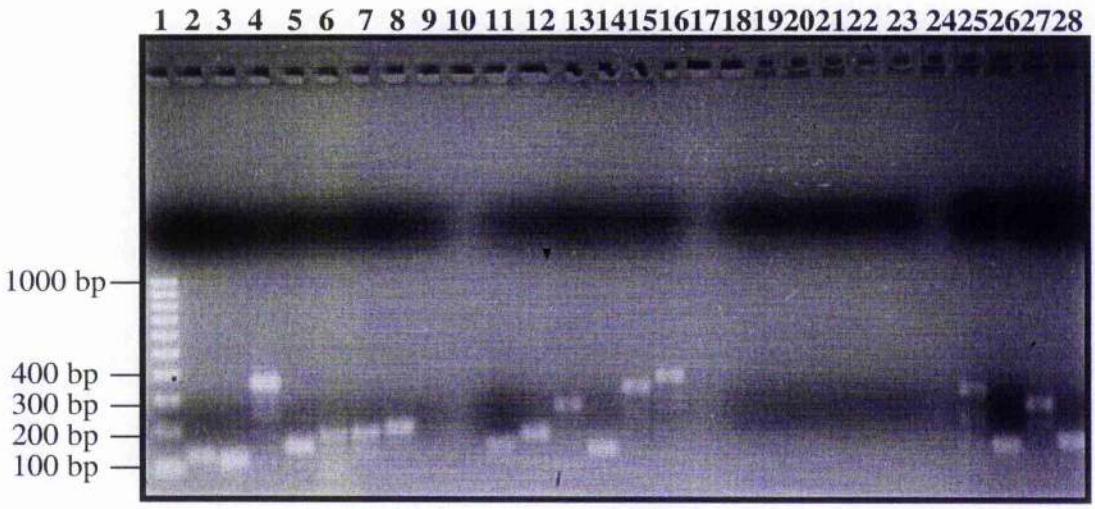

Figure. 5.4(A). Re-amplification of Differential Display cDNA Bands by PCR: Oligo dT(C) Primer.

Re-amplification of eluted cDNA bands by PCR with one of eight 13-mer arbitrary (H-AP) upstream primers in combination with anchored oligo-dT (H-T11 C) down stream primer. The PCR conditions were as follows: 15 s at 94°C: 40 cycles (12 s at 94°C, 15 s at 40°C, 30 s at 72°C, temperature slope setting = 3): 5 min at 72°C or (See details in the instructions from the RNA image Kit No.3). The PCR products were analyzed on a 1% agarose gel stained with ethidium bromide. Lanes from 2-28 represent the expected size fragment for PCR product that ranged from 150 bp to 400 bp. No PCR product formed in lanes 9-10 and lanes 17-24 (false positive). Lane 1 contains the EZ Load 100 bp molecular ruler.

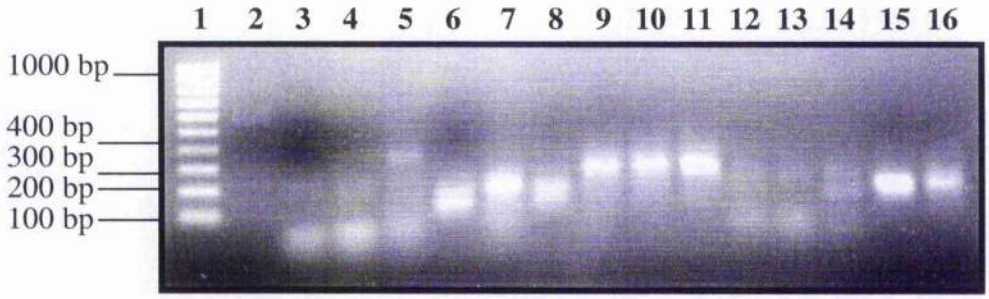

Figure. 5.4 (B). Re-amplification of Differential Display cDNA Bands by PCR: Oligo dT (C) Primer.

Re-amplification of eluted cDNA bands, that failed to amplify (See Fig.5.7A lanes 9-10 and 17-24), using one of eight 13-mer arbitrary (H-AP) upstream primers in combination with the same anchored oligo-dT (H-T11 C) down stream primer with cDNA eluted bands. The PCR conditions were as follows: 12 s at 94°C: 40 cycles (10 s at 94°C, 15 s at 40°C, 30 s at 72°C, temperature slope setting = 6): 5 min at 72°C or (See details in the instructions from the RNA image Kit No.3). The PCR products were analysed on a 1% agarose gel stained with ethidium bromide. Lanes from 2-16 represent the expected size fragment for PCR product that ranged from 200 bp to 400 bp. No PCR product formed in lanes 2-4 and lanes 12-14 (false positive). Lane 1 contains the EZ Load 100 bp molecular ruler.

5.1.2 Confirmation of Up-and Down-Regulated Gene Expression.

To confirm the bands identified by DD-PCR were genuinely differentially expressed, cDNA fragments were analyzed by a modification of the amplified RNA dot blot hybridization procedure (Reverse Northern) of Poirier *et al.,* (1997). Duplicate filters were loaded with re-amplified cDNA PCR products as probe; the majority of these were selected from the cDNAs prepared from the HHS salt-resistant (treated) samples. As a control, a clone of a partial actin cDNA (300bp) from *Arabidopsis thaliana* was applied to each filter. First strand cDNA was then prepared from each of the HHS (260 mM NaCl) and WT (0mM NaCl) pools of total RNA using an oligo (dT) primer with a 3' T7 primer site (Section 2.2.13.5.1). Double strand cDNA was then generated from the first strand cDNA pool (Section 2.2.13.5.2), cleaned (Section 2.2.13.5.3) and multiple single-strand ^{32}P-labelled cDNA generated from ds cDNA template using asymmetric PCR from the T7 primer sequence (Section 2.2.11.5.4). In this way, single strand ^{32}P-labeled sequence was hybridized to unlabelled immobilized probe on the membrane. The two pools of labelled target cDNA were synthesized from salt-sensitive WT (untreated) and HHS (treated) *Arabidopsis* cell lines, denatured, and added to the pre-hybridization solution as described in Section (2.2.14.2). The hybridization, membrane washes and auto-radiography were carried out as described in Sections 2.2.16.1, 2.2.16.2 and 2.2.10.3 respectively, except that the membranes were hybridized for a longer time (two days) compared with hybridization time used with Northern analyses. The

labeled target hybridized strongly to the majority of immobilized probes. Figure 5.5 presents the results from a typical reverse Northern. Comparisons were then made between blots (*i.e.*, duplicate filters applied with labeled target from NaCl treated HHS and untreated WT *Arabidopsis* cell lines). Seventy-two sequences of the original 92 true positives identified by DD-PCR were confirmed by reverse Northern as differentially abundant, and these were selected for further analysis.

5.2. cDNA Cloning and Sequencing.

To gain insight into the genes that altered their expression, the seventy-two partial cDNA sequences identified by DD-PCR and reverse Northern as differentially abundant in response to NaCl stress were cloned for sequencing. The cDNA fragments were cloned directly in (TOPO TA) cloning vector as described in (Section 2.2.12.4.2), and transformed to *E.coli* TOPO 10 (Section 2.1.2). Colony PCR was used to confirm the correct inserts (see Section 2.2.12.4.3). Qiagen Midi-Pasmid preps was then made (Section 2.2.4.2) of these 72 clones, and these were waiting sequencing on 24 October 2001. Unfortunately almost all of the Differential Display clones were destroyed in the Bower Building fire of 24 of Oct 2001. Of those de-frosted samples that were eventually salvaged only 5 proved to be suitable for sequencing.

The cDNA candidates were sequenced at MWG-Biotech GmbH. Identification of the cloned cDNA candidates was achieved by BLAST comparisons with the Gene Bank and the EMBL database to identify possible homologies with known genes.

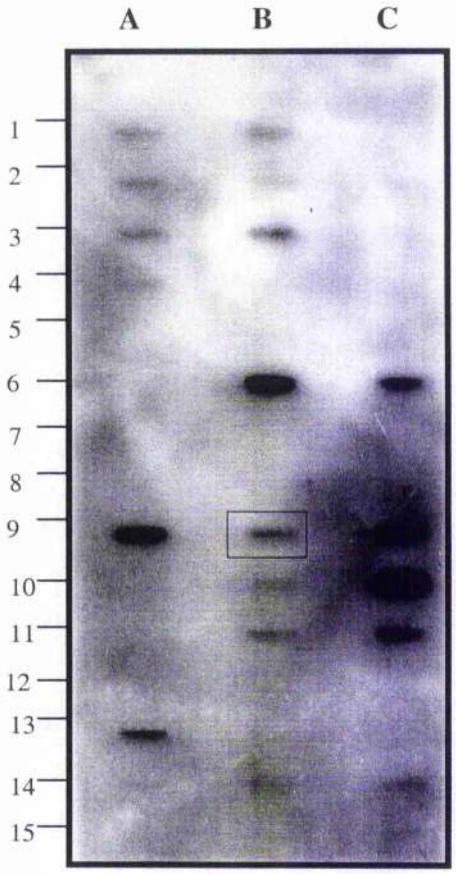

Figure. 5.5. Reverse Northern Analysis of Amplified cDNA Probe Prepared from Salt-treated HHS Cell Line.

Amplified cDNA samples from salt-treated HHS and untreated WT *Arabidopsis* cell lines were applied to the filter in 3 x 15 array, each filter containing 31 PCR products plus pBluescript II SK (which contains a partial length 300 bp actin cDNA clone from *Arabidpsis thalina* as a control (boxed: column B row10, 100 ng). Columns between brackets did not contain samples. The filter was hybridized to the labeled target cDNA, prepared from *Arabidopsis* cell line grown in salt (260mM NaCl) (Section 2.2.15.5.1&2.2.15.5.2). Each PCR product hybridized to the amplified probe as indicated in the figure.

The sequence homology data for these cDNAs are presented in (Table 5.1 and Fig. A2 Appendix).

BLASTN search for the *At* T4A cDNA cloned identified significant homology (99%) to *Arabidopsis thaliana At* 2g41350 an *Arabidopsis* gene coding for unknown protein, id=AAC78538.1, Table 5.1 and Fig. A2.1 (see Appendix).

BLASTN searches revealed the *At*T2C clone to be 100% Identical to an *Arabidopsis thaliana* gene coding for a hypothetical protein (protein_id =AAG51320.1, Table 5.1 and Fig. A2.3 see Appendix).

When BLAST was used to interrogated the EMBL with *At* T4C, sequence homology was found (100%) to both an *Arabidopsis thaliana* mRNA for mitochondrial F1 ATP synthase beta subunit (Acc. No. 17939848 Fig. A2.4 (see Appendix), and an *Arabidopsis thaliana* sequence 208 from patent W00055325 (Acc.No. 12311580, Table 5.1 and Fig. A2.5&A2.6 see Appendix).

BLASTN search for the same sequence (*i.e.*, *At*T4C DD-PCR cDNA clone), also found 94% identity to an *Arabidopsis thaliana* gene coding for stress-resistance and retarded aging in plants (patent: JP 2001512027-A221, Acc. No. 22626544, Table 5.1 or Fig. A2.7 see Appendix).

BLASTN searches for *At*T1A cDNA clone found 99% identity to an human gene sequence, and is clearly a contamination that probably originated in the sample, after salvage.

The other partial-length cDNA sequences (*i.e.*, *At*T2A clone) showed short sequence homology to *Arabidopsis thaliana* clone F23D23. No other matches were found.

Table 5.1. Blast Output of DD-PCR cDNAs Search in the EMBL Database.

Product	Acc. No.	e-Score	Identity	Homologies
T1A	*17551003*	0.0	99%.	*H.s* cDNA clone, a spermatocyte-specific gene.
T2A	*AB062094*	0.005	100%.	*A. thaliana* clone F23D23.
T4A	*AC005662.2*	e-104	99%.	*A. thaliana At* 2g41350 cDNA clone coding for un-known protein..
T2C	*677534.*	1e-20	100%.	*A. thaliana* gene coding for hypothetical protein.
T4C	*17939848*	e-131	100%.	*A..thaliana* mRNA for mitochondrial F1 ATP synthase beta subunit.
T4C	*12311580*	e-115	100%.	*A thaliana* sequence 208 from patent W00055325.

5.3. DISCUSSION:

Reverse transcriptase-polymerase chain reaction (RT-PCR) differential display was used to evaluate transcript abundance in *Arabidopsis* salt-resistant and salt-sensitive cell suspension cultures in order to identify genes, that may be regulated during NaCl treatment.

Total RNA was extracted from *Arabidopsis* salt-resistant and salt-sensitive cell line and first-strand cDNA fragments were synthesized by reverse transcriptase. Three different 1 base anchored oligo dT (H-T_{11}M, where M may be G, A, or C), and eighteen primer sets were used, followed by the Polpolymerase Chain Reaction (RT-PCR) to re-amplify the cDNA fragments that were differentially expressed between *Arabidopsis* salt-sensitive (control) and salt-resistant and cell lines. Labeled cDNAs fragments were fractionated, resolved and compared in polyacrylamide sequencing gels (Fig. 5.1). The cDNAs were eluted from the gel slices and 92 products were re-amplified using the same primers described above. Up-and down-regulated transcripts were confirmed by analyzing partial cDNAs by slot blot hybridization procedure of Poirier *et al.,* (1997). A modified procedure for probe synthesis as (recommended by Dr. Cecchini University of Pisa, per. Com.).

Labeled target from HHS *Arabidopsis* cell line bound strongly to the immobilized probe synthesized and amplified from the HHS samples (*i.e.*, PCR products). However, labeled target from the control cells gave low signals when hybridized to the same HHS immobilized probe. This suggests that the message levels for the sequences selected from the HHS cell line for reverse Northern analysis were indeed more abundant in HHS cells than in control cells, as the hybridization to the

actine probe was the similar. It was hoped that insight would be gained into which genes alter their expression under salt stress by comparing reverse northern filters prepared from WT and HHS samples. Of the seventy-two of the rescued clones, only five proved to be suitable for sequencing. BLASTN searches of the database for sequence homologies to these five clones suggested that one (*At*T1A) was a human sequence that probably contaminated the sample after salvage. However, the other four clones proved to be authentic *Arabidopsis* sequences. Of these, one was a hypothetical protein (*At*T2C, protein_id=AAG51320.1), function (*At*T4A, locus *At*2g 41350). A third clone (*At*T2A, Acc. No. 62094) showed short homology to sequences in BAC f23D23, and has no known function. The fourth authentic clone (*At*T4C) showed strong homology to two *Arabidopsis* sequences, depending on the direction of the transcription. In one orientation, the sequence is reported to code for a β subunit of the F1 ATP synthase, in the other for a patented gene 208(W00055325) that may be involved in salt-resistance and senescence (cf. Patent JP 2001512027-A). These experiments have confirmed that DD-PCR analysis of salt-tolerant *Arabidopsis* cells can identify differences in the pattern of gene expression associated with survival in high salt. In the experiments reported here, 72 clones were identified from one of the Gene Hunter Kits (there are 8 different kits in total), therefore it is reasonable to expect that several hundred, possibly over a thousand, differentially abundant sequences would have been identified if a complete analysis had been undertaken.

CHAPTER SIX

GENERAL DISCUSSION

CHAPTER SIX.

6. GENERAL DISCUSSION.

The major crop species upon which we rely for food are glycophytes, and do not complete a full life cycle in 120 mM NaCl as they do not express the mechanisms required to tolerate the ion excesses that prevail in saline soils (Greenway and Munns, 1980). Therefore, developing crops that grow vigorously in saline solutions is currently one of the prime objectives of plant biologists. Consequently, much interest is currently directed towards understanding how salt tolerant plants respond to high salinity.

To address some of these issues, a salt tolerant cell suspension culture (HHS line) of the model glycophyte *Arabidopsis thaliana* was established at Glasgow University. It was hoped that many of the experimental advantages offered by this plant could be bought to bear on gaining a better understanding of cell salt tolerance mechanisms. The selection of cell cultures that grow vigorously in high salinity should result in an enrichment of the genes (and their proteins) required for maintaining high cytosolic K^+ / Na^+ ratios and low Cl^- concentrations as these are viewed as essential traits for survival in saline conditions.

This study has focused on characterizing some of the cellular mechanisms that allow HHS cells to tolerate high salinity (up to 380 mM NaCl, *cf.* WT cells which do not survive >80 mM NaCl). Part of the project was directed towards characterizing the morphology and cytogenetics of WT and HHS cells. In addition, with the rapidly accruing information in the *Arabidopsis* genome database, attempts were made to use this information to clone Na^+ transporters (Na^+ / H^+ antiporters) that may be involved in maintaining low cytoplasmic Na^+ levels in HHS cells. Finally, comparisons were made between the pattern of transcript

abundance in WT and HHS cells using the technique of Differential Display PCR (DD-PCR).

Preliminary experiments on the HHS cells loaded with ion specific fluorescent dyes demonstrated that it would not be possible to use this approach to characterize ion flux (Na^+, K^+, Cl^- or H^+) across the plasma membrane. Within 2 minutes from adding the dyes to the external medium, small, brightly fluorescing centres were observed in the HHS (but not WT) cells. This response was observed whether anionic, cationic or neutral dyes were used (Figs. 3.1-3.3). Similar observations have been made when the dyes were added to cultures of all of the salt-tolerant cell lines tested to date (sugar beet, red beet, *Aster tripolium*, *Atriplex halimus*, and *Hordeum vulgare*). In contrast, none of the salt-sensitive cell lines tested to date show this behavior (WT *Arabidopsis*, *Solanum tuberosum*, *Daucus carota*). Therefore, there is a good correlation between the appearance of these brightly fluorescing bodies and salt tolerance. Similar observations were made by Shiminy, *et al.*, 1973, in salt glands of the mangrove species *Aegiceras corniculatum* and *Avicenia marina*, and by Vassilyev and Stepannova (1990) in their ultrastructural studies on the salt glands of *Limonium plathyllum*.

Thin section electron microscopy (TSEM) on HHS cells revealed an extensive array of small vacuoles and vesicles (SV-V) in their cytoplasm, in addition to a large central vacuole that typically occupied 40-60% of the cell volume; in contrast, WT cells contained few SV-V and a large central vacuole occupying 80-90% of the cell volume. Consequently, the hypothesis that the SV-V are the repositories for the fluorescent dyes and give rise to the bright bodies observed with a fluorescence microscope was investigated using a fluorescence confocal microscope. These studies showed that the

brightly fluorescing bodies observed in HHS cells (Figs. 3.1 - 3.3) are solid, and confirmed that the dyes, regardless of their charge, are taken up into the lumen of the SV-V.

The questions arises 'is the extensive array of SV-V involved in the sequestration of toxic levels of ions?' Their presence in HHS cells suggests three possible roles.

It is conceivable that the SV-V are static structures that provide a large membrane surface area-to-cytoplasmic volume ratio that facilitates the rapid uptake of toxic levels of ions from the cytoplasm, thereby affording maximum protection to metabolic activity.

Alternatively, the extensive SV-V array may be dynamic and involved in the efflux of excess ions from the cell (exocytosis). Studies of many TSEM of HHS cells suggest the small vacuoles do align near the plasma membrane, and there was also evidence of contact between them (Figs. 3.4 & 3.9). It is conceivable that the extensive SV-V array forms for sequestering Na^+ and Cl^- away from the cytoplasm, and subsequently for effluxing their contents into the apoplast. Exocytosis is known to take place in all plant cells, but this is believed to occur through the secretory pathway and involve golgi-derived vesicles (<200 nm dia.) and the interaction of V-SNARE (vesicle) and T-SNARE (plasma membrane) proteins (Ungermann, *et al.*, 1998). Therefore, although adaptations to the secretory pathway for ion efflux could explain the presence of an extensive array of vesicles, it does not explain the presence of the large number of small vacuoles (>200 nm dia.).

The final explanation for the extensive SV-V arrays is that they are involved in endocytosis. It is well known that halophyte cells that rapidly take up Na^+ and Cl^- and sequester them in their (large central?) vacuoles where they are used as metabolically 'cheap' osmotica to re-establish and maintain cell turgor. It has always been tacitly assumed that Na^+ (and Cl^-) ingresses into the cytoplasm across the plasma membrane and

then diffuse to the tonoplast where active membrane-bound transport systems (*e.g.* Na^+ / H^+ antiporters) use a H^+ gradient to effect their concentration in the central vacuole. However, it is conceivable that Na^+ (and Cl^-) uptake which is required for the maintenance of turgor and growth (expansion), occurs not by direct transport through the cytoplasm, but by endomembrane trafficking. Endocytosis normally occurs through clathrin-coated vesicles that subsequently coalesce to form pre-vacuoles (or endosomes), and these eventually fuse with the tonoplast and empty their cargo into the vacuole. (Hawes *et al.*, 1996). There is also evidence that vesicles that emanate from trans-golgi network can coalesce with pre-vacuoles (Hawes, *et al.*, 1996). In this study, some evidence was found for associations between the tonoplast and small vacuoles (Figs. 3.12 & 3.13), and for the coalescence of small vacuoles (Figs. 3.9 & 3.10).

At this stage, it is not possible to determine which of the three mechanisms outlined above (static endomembrane system, exocytosis or endocytosis) best explains the appearance the extensive array of small vacuoles and vesicles observed in HHS (and all studied salt tolerant) cells. The best way to address this question would be to use real-time confocal microscopy to study the dynamics of the SV-V, and thereby establish if any trafficking is involved. Unfortunately, at the time these studies were undertaken, routine access to a confocal microscope was not possible. In addition, access to a confocal microscope might allow immunofluorescence techniques to be used to distinguish between the three recognized classes of vacuoles in plants (central, lytic and protein storage). It has been shown that the three types of plant vacuoles express a different complement of TIPs (aquaporins) in their membranes, and antibodies are now available for these (Cao, *et al.*, 2000).

Another question concerning the SV-V system that remains unanswered is ' what mechanisms sequester the fluorescent dyes into the lumen of the endomembranes?' A consensus has emerged that Na^+ and Cl^- transport across plant membranes is effected by H^+-coupled co-transporters or ion channels, and driven by pH gradients and/ or membrane potential. Several Na^+ (Gaxiola *et al*,1999; Apse *et al.*, 1999; Shi *et al.*, 2000) and Cl^- (Lupin, *et al.*, 1996) transporters have been identified in plants, and it is conceivable that these (or other similar transporters) are expressed in the SV-V membranes. Preliminary attempts to isolate an SV-V enriched fraction from the HHS cells for biochemical characterization have so far proved futile (J. Price, University of Glasgow, per. comm.), but these experiments are on going. However, the fact that the SV-V appear to accumulate rapidly cations, anions or neutral solutes suggests that either a complex plethora of specific transport mechanisms are expressed in these membranes, or an active non-specific system operates (*e.g.* ABC transporters). Since their discovery in plants just 10 years ago, there has been acute interest in ABC transporters. The first well-characterized system was the GS-X pump which is involved in the sequestration (detoxification) of xenobiotics (*e.g.* herbicides) into the vacuole (Martinoia *et al.*, 1993). It is viewed that the GS-X pump recognizes the conjugates of glutathione ligated to a xenobiotic, regardless of the chemical structure of the xenobiotic. Therefore, as long as glutathione can form a ligand with the xenobiotic (such as a fluorescent dye), a GS-X pump (supplied with ATP) can rapidly sequester the toxic substance in the vacuole (Martinoia *et al.*, 1993). One hundred and thirty ABC transporter sequences have now been identified in *Arabidopsis,* and it is entirely possible that some of the corresponding transporters recognize conjugates of the fluorescent dyes used in this study, regardless of their charge, and are expressed in the

membranes of the SV-V in HHS cells. Some ATP-dependent ABC transporters (*e.g.* HMT1) are known to recognize conjugates of heavy metals (*e.g.* Cd, Pb) and phytochelatins, and to detoxify the cytoplasm by removal to the vacuole (Ortiz *et al.*, 1995). Sodium is also a cation, albeit far more abundant in plant cells than heavy metals, but it is possible that an ATP-dependent ABC transporter loads not only conjugates of fluorescent dyes into the vacuoles, but also conjugates of Na^+. Furthermore, an ABC-type ATPase has been found in the plasma membrane of yeast cells and is one of three mechanisms of for Na^+ extrusion in *S. cerevisiae* (Miyahara, *et al.*, 1996).

It is interesting to speculate on what kinds of genetic adaptations / mutations have occurred in HHS cells that gives rise to salt tolerance. Studies with a light microscope and an electron microscope on the HHS cells have identified many chromosomal and nuclear abnormalities. For example, it was observed that the nuclei of HHS cells were usually larger than those of WT cells. The irregular shape of the HHS cell nuclei in TSEM made the quantification of this observation difficult, but as there is a good correlation between the size of the nucleus, the size of the nucleoli, and the level of ploidy, and so the dimensions of the nucleoli can be used to estimate the chromosome complement of cells. What is clear is endoreduplication was common in HHS cells. The presence of large nucleoli (nuclei) in these cells suggests that several rounds of chromosome duplication occurred without nuclear division (Figs. 3.4, 3.5 & 3.11). Also, in many cases, more than one nucleolus was present in a single HHS cell nucleus, and serial sections through these nuclei showed these nucleoli to range in size. Such observations are indicative of aneuploidy where some, but not all, of the chromosomes undergo division or are lost. In extreme cases, fragmented nucleoli can be observed (Fig. 3.4) which are usually associated

with chromosome fragmentation. Finally, there is also evidence for prophase chromosome reductions, where mitotic divisions result in the loss of whole chromosomes and consequently smaller nucleoli (Fig. 3.11); presumably, such abnormalities arise from malfunctions in spindle assembly and segregation.

Abiotic and biotic stress often produces oxidative stress in plants (Roxas, *et al.*, 1997; Zhu, 2001). In plants, there have been few studies on the effects of abitotic stress on cell cycle progression. However, Logemann *et al.*, (1995) have shown a strong correlation between the down-regulation of cell cycle genes and up-regulation of defense genes following mild oxidative stress in parsley cells. Reichheld *et al.*, (1999), obtained similar results in both BY-2 cell suspensions and whole plants of *Nicotiana tabacum*. They demonstrated that a down-regulation of cell cycle genes (CDKs) occurs under conditions of mild oxidative stress that arise when defense genes are activated (*e.g.* glutathione peroxidase and Cu/Zn superoxide dismutase).

A major part of the effort reported in this thesis was directed towards cloning Na^+ transporters from HHS cells that might be responsible for maintaining a high cytoplasmic K^+ / Na^+ ratio. At the time these experiments began (April 1998), approximately 20% of the *Arabidopsis* genome had been sequenced and annotated, but no plant Na^+ transporters had been identified. Therefore, given the perceived wisdom that Na^+ efflux mechanisms were essential for the survival of plant cells at high salinity, it was decided to attempt to clone the cDNAs for these transporters from HHS cells. Alignments of the protein sequences of 11 putative or authentic Na^+ / H^+ antiporters from animals and yeast identified several regions consensus. Degenerate PCR primers were designed from these consensus motifs with judicious reference to the *Arabidopsis* codon bias. However,

despite many attempts, no convincing PCR products were generated that warranted sequencing.

However, in August 1999, a sequence appeared in the *Arabidopsis* database (BO4.4) that was reported to show some homology to Na^+ / H^+ antiporters from other organisms. Over the next few months several other putative *Arabidopsis* Na^+ / H^+ antiporter sequences were deposited in the data base (T20D21.19, F24D13.4, T9D9.5, F14H20.5, T12H17.230). Therefore, it was decided to design PCR primers to the reported 5' and 3' untranslated regions (5' UTR and 3' UTR) of these genes, and use reverse transcription PCR (RT-PCR) to clone the corresponding cDNAs from HHS cells.

All of the primer sets were first tested for suitability (and for reaction optimization) using genomic DNA as template, and in all cases products of the expected size were generated. Subsequently, each of the primer sets was used with first strand cDNA template (generated by oligo (dT) primed reverse transcription of total RNA isolated from HHS cells).

Of the six putative Na^+ / H^+ antiporter sequences identified, despite exhaustive attempts, cDNAs for two of them (F24D13.4 and T9D9.5) could not be generated from HHS cells. A cDNA of the predicted size for a third (T20D21.19) was cloned and subsequently sequenced, but proved to be an unrelated PCR product. The conclusion is that none of these three sequences are expressed in HHS cells, or alternatively the 5' UTR and 3' UTR of these genes identified in the database which were used for designing primer sets, were not correct. Therefore, although each primer set worked with genomic DNA template (generated products of the predicted size), they did not generate the expected cDNA product from RT-cDNA template.

Two other primer sets (for BO4.4 and F14H20) did produce products of the expected size (~1.4 kbp and 3.5 kbp, respectively) by RT-PCR, and these were subsequently cloned (in pCR SCRIPT, Stratagene) for sequencing. However, although colony PCR indicated that colonies with inserts of the expected size were produced, it proved to be very difficult to grow sufficient amounts of either for plasmid isolation and sequencing. After the initial cloning step, colonies grew on solid selective media, but subsequent growth of selected colonies in liquid cultures repeatedly failed. Extensive attempts to amplify these two clones in *E. coli* failed. These included the following strategies used in most possible combinations: reducing transcription of the inserts in *E. coli* by removal of IPTG from the initial selection plates: use of transcriptionally silent vectors (*e.g.* pET 28): screening of several *E. coli* host strains (including XL1-BLUE, DH5α, TOPO10, XL10-GOLD, C43Des and C41Des). In mid-1999, two publications appeared that reported the cloning and characterization of one of these sequences (BO4.4), and suggesting the protein product of this gene is localized to the tonoplast membrane where it operates as a Na^+ / H^+ antiporter (Gaxiola *et al.*, 1999; Apse *et al.*, 1999). This sequence is now known as *AtNHX1*, and its over expression in *Arabidopsis* (Apse *et al.*, 1999) and *Lycopersicon esculentum* (Zhang & Blumwald, 2001) has been shown to confer improved tolerance to salinity. In mid-2000 a report appeared on the identification and characterization of F14H20.5 (Shi, *et al;* 2000). This sequence was identified from a genetic screen which identified a salt-overly-sensitive mutant (*sos1*) and positional cloning identified is as *AtSOS1*. SOS1 is reported to be a Na^+ / H^+ antiporter localized in the plasma membrane that effluxes Na^+ from the cytoplasm (Shi, *et al.*, 2000); however, no experimental data has been provided to confirm this. In view of the strong competition from other well-

established groups, and the difficulty in maintaining stable clones of *AtNHX1* (BO4.4) and *SOS1* (F14H20.5), further work on these two sequences was stopped in early 2001.

The RT-PCR product of the sixth sequence (T12H17.230) was cloned successfully, sequenced and subsequently confirmed as a cDNA for T12H17.230. The amino acid sequence of the translated gene is 87% identical to that predicted in the NCBI database; no other significant homologies were found. The translated protein consists of 409 amino acid residues, and 8 or possibly 9 membrane spanning α helices (as predicted by the hydropathy calculations from the TMPred and TMHMM programs, Fig.4.16). Northern analyses of *At*T12H17.230 expression indicated that it is strongly up-regulated in HHS cells (grown in 260mM NaCl) when compared with levels in WT cells (grown in 0 mM NaCl), lending support to the idea that the gene product may be involved in salt tolerance. The location and function of the AtT12H17.230 has not yet been determined. Therefore, it may be located in the vacuole like *At*NHX1 (Apse, *et al.*, 1999), or in the plasma membrane like *At*SOS1 (Shi, *et al.*, 2000). The structural relationship between the proteins for known Na^+/H^+ antiporters from different organisms and for AtT12H17.230 was analyzed by CLUSTALW (Fig. 4.2). This analysis revealed that *At*T12H17.230 is more closely related to known plasma membrane transporters such as SOD2 (from *S. pombe*), NhaP (from *P. aeruginosa*) and *At*SOS1 (F14H20.5, from *Arabidopsis*), than other Na^+/H^+ exchangers (*i.e.*, *At*NHX1, *Sc*NHX1 and *Hs*NHE6) that are located elsewhere in the cell. Therefore, it is tentatively suggested that *AtT12H17.230* encodes a plasma membrane Na^+/H^+ antiporter.

Further characterization of the function and localization of *At*T12H17.230 is required. Two approaches can be used to confirm function, over expression in a WT *Arabidopsis*

background to determine if the transgenic plants are overly-salt-tolerant (*OST*), or characterization of the phenotypes of null mutants (knockouts) of *AtT12H17.230* (*i.e. SOS* phenotype). In August 2001 a single knockout line was identified in the Syngenta GARLIC *Arabidopsis* T-DNA knockout collection. A Material Transfer Agreement was prepared to obtain this mutant from Syngenta, but due to the Bower fire, no characterization was undertaken.

A recent search (July, 2002) of the full *Arabidopsis* genome database reveals sequences for over 30 authentic or putative Na^+ / H^+ antiporters have been deposited. Clearly an RT-PCR approach should be successful in cloning most, if not all, of these sequence, especially as the annotation of gene structure is much more reliable now than it was three years ago, and hence primer design should also be more reliable.

Recently, there has been much interest in transcriptosome analyses, that is, the quantification of the abundance of transcripts in cells. It is believed that comparisons of the global pattern of abundance from samples exposed to different treatments (for example low and high salinity), will provide information on the expression of key genes that may be involved in critical responses. Two technologies have been developed for transcriptosome analyses, DNA microarraying and Differential Display-PCR. At the time of writing, DNA microarraying is the method of choice if the microarrays are routinely available; at present, plant biologists are restricted to working with *Arabidopsis* or investing a considerable amount of effort and expense in setting up facilities to generate their own microarrays. In the spring of 2001 when these experiments were begun, *Arabidopsis* microarrays were very expensive and not routinely available in the UK. For this reason, it was decided to investigate the feasibility of comparing the expression patterns in WT and HHS cells using

DD-PCR. Eight commercially available RT-PCR kits are available from GenHunter Corp, and one of these was selected for trial purposes. One hundred differentially abundant (up-regulated) HHS cDNA fragments were identified and selected for further analyses, although many more fragments were observed that either showed more subtle changes or were down-regulated. Of these 100 fragments, 92 were subsequently shown to be true positives, and 72 of these were confirmed by reverse northern analyses (Poirier *et al.* 1997; see Section 2.2.16) to be genuinely differentially abundant. All 72 fragments were re-amplified by PCR and cloned for sequencing. Plasmid preparations from each of these 72 clones were made, and PCR confirmed that each contained the correct sized insert. These 72 preparations were awaiting dispatch for sequencing when the Bower Fire occurred. The defrosted samples and their corresponding clones were salvaged several days after the fire, but of the original 72, only 5 generated any product after PCR re-amplification. Of these 5 sequences, one proved to be a contaminant, but the other 4 were authentic *Arabidopsis* sequences. BLAST2 searches showed one of these (*AtT2C*) was a 'hypothetical protein (locus *At2g41350*), whilst two (*AtT2A* & *AtT4A*) were expressed but had no known function. The fourth authentic clone (*At*T4C) showed strong homology to two *Arabidopsis* sequences, depending on the direction of the transcription. In one orientation, the sequence is reported to code for a β subunit of the F1 ATP synthase, whilst in the other is codes for a patented gene 208(W00055325) that may be involved in salt-resistance and senescence (*cf.* Patent JP 2001512027-A).

These experiments have confirmed that DD-PCR can be used to identify sequences in the *Arabidopsis* HHS cells that may be involved in salt tolerance, but unfortunately due to the Bower Fire, the pilot experiments reported here were not taken to a satisfactory

conclusion. However, in view of the amount of work involved with analyzing fragments generated from just one of the eight commercially available kits, it is recommended that DNA microarraying is the preferred method if the microarrays are available. Affymetrix DNA chips (both the 8,400 gene and 24,000 gene arrays) are now being used at Glasgow University to analyze the global transcript abundance in HHS and WT cells, and this approach will undoubtedly provide insight into the mechanisms that confer salt resistance on these cells.

Appendices

Appendix 1:

Alignments, Gel Electrophoreses, BLAST Output of cDNA Sequences and BLAST Output of the Amino acid Sequences

Figure A1.1 Alignment of 11 sequences coding for Na^+/H^+ antiporters.

Alignment of the deduced amino acid sequences of Na^+/H^+ antiporters from different organisms. The sequences were aligned by program CLUSTALW. The alignment is based on the total amino acid sequences. The amino acid residues conserved in all sequences are colored highlighted. The membrane spanning-segments (M3-M6) of AtB04.4 have high similarity with other exchangers and indicated by blue line. The conserved sequence of Na^+/H^+ exchangers of M3 and M6 (A and B) were used to design degenerated PCR primers for cloning purposes. The sequence accession numbers are as follows: NAH *C.elegans* (accession No. 547989), NHE1 Human (544776), NHE *Xenopus* (1655702), NHE2 Rabit (1709222), NAH4 rat (127814), NAH3 Human (1346659), NAH5 Human (2833257), Trout (547990), Human (2944233), NHE1 *Drosophila* (489499).

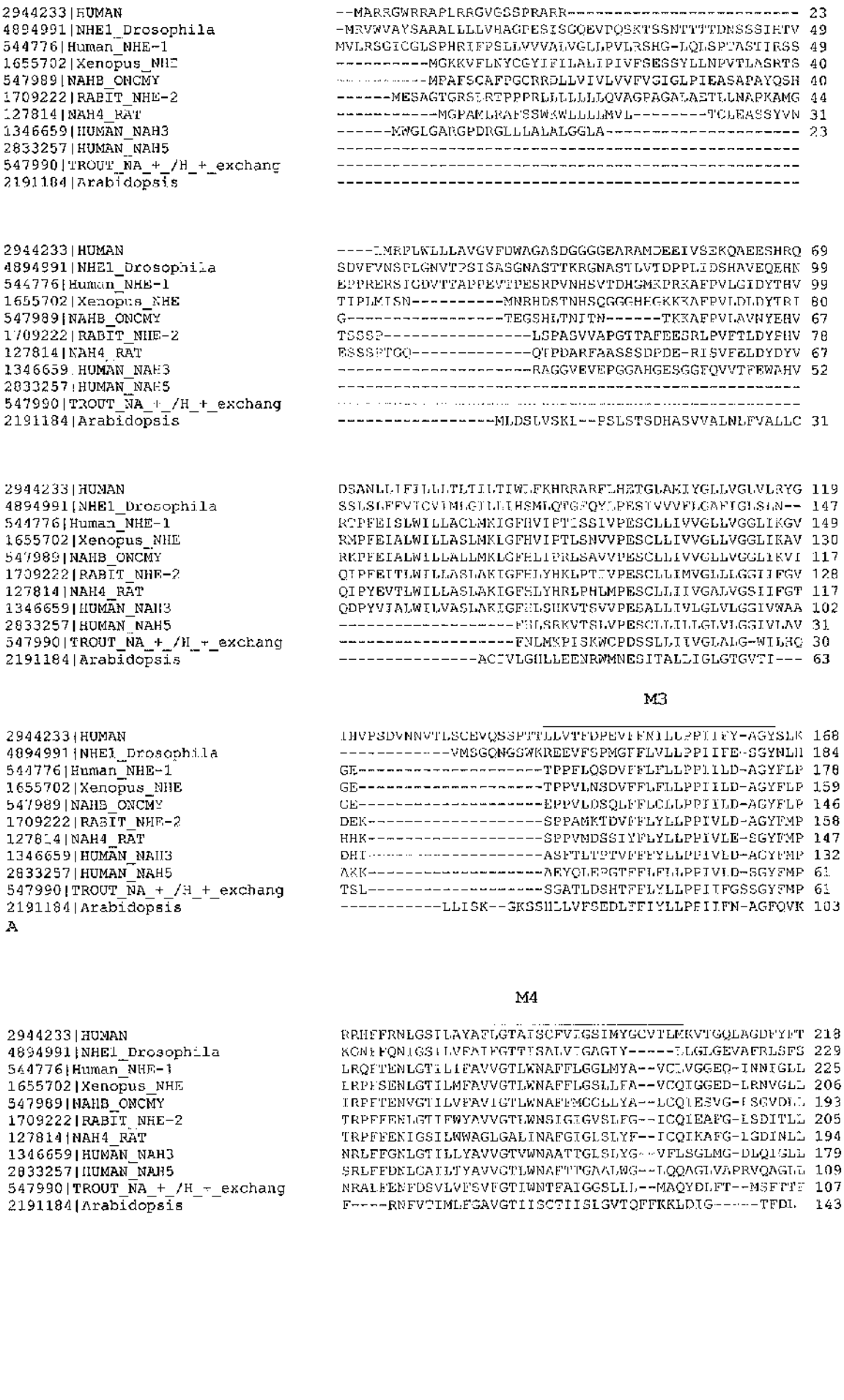
2944233|HUMAN
4894991|NHE1_Drosophila
544776|Human_NHE-1
1655702|Xenopus_NHE
547989|NAHB_ONCMY
1709222|RABIT_NHE-2
127814|NAH4_RAT
1346659|HUMAN_NAH3
2833257|HUMAN_NAH5
547990|TROUT_NA_+_/H_+_exchang
2191184|Arabidopsis
M3
M4
A

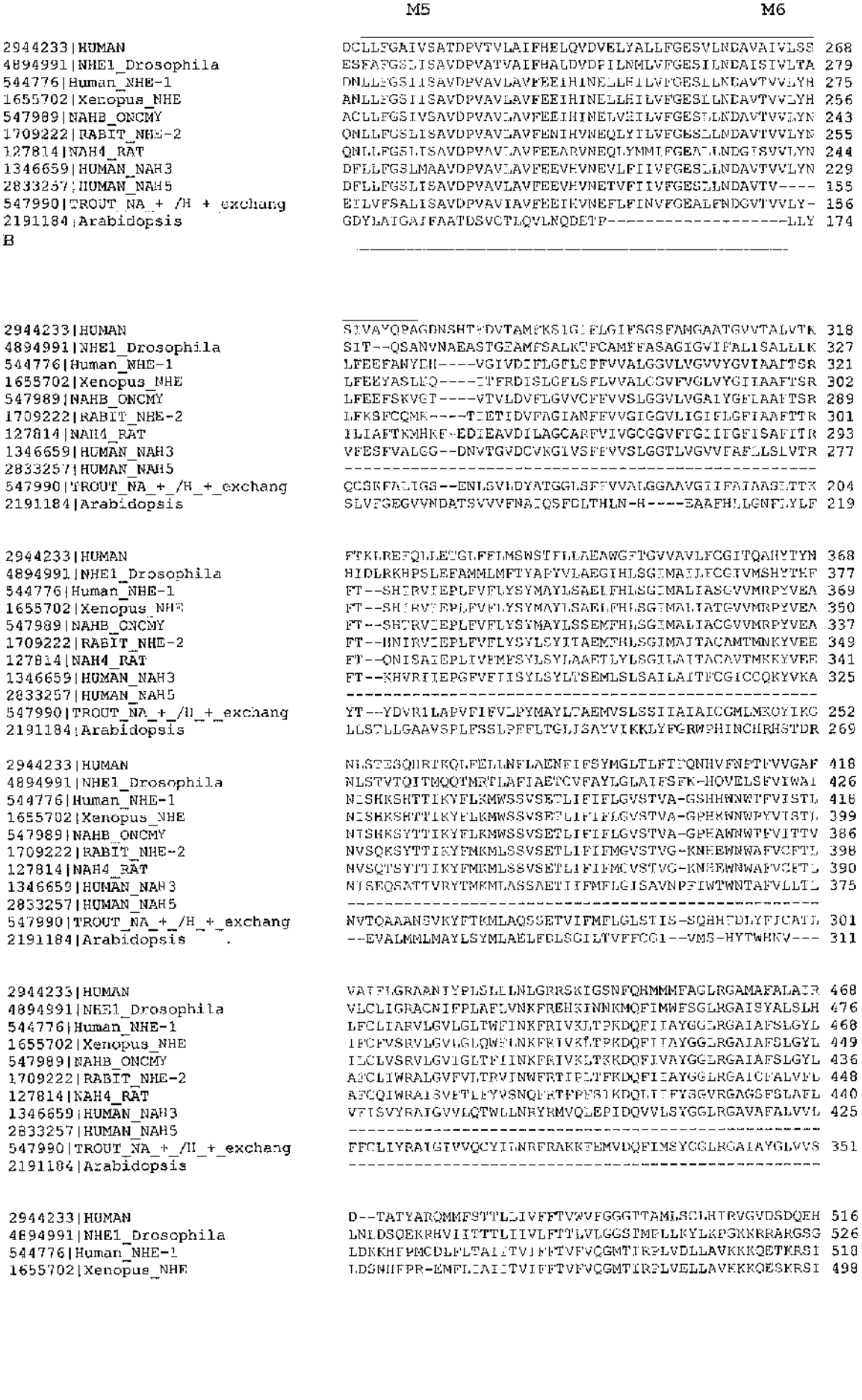
M5
M6
2944233|HUMAN
4894991|NHE1_Drosophila
544776|Human_NHE-1
1655702|Xenopus_NHE
547989|NAHB_ONCMY
1709222|RABIT_NHE-2
127814|NAH4_RAT
1346659|HUMAN_NAH3
2833257|HUMAN_NAH5
547990|TROUT_NA_+_/H_+_exchang
2191184|Arabidopsis
B

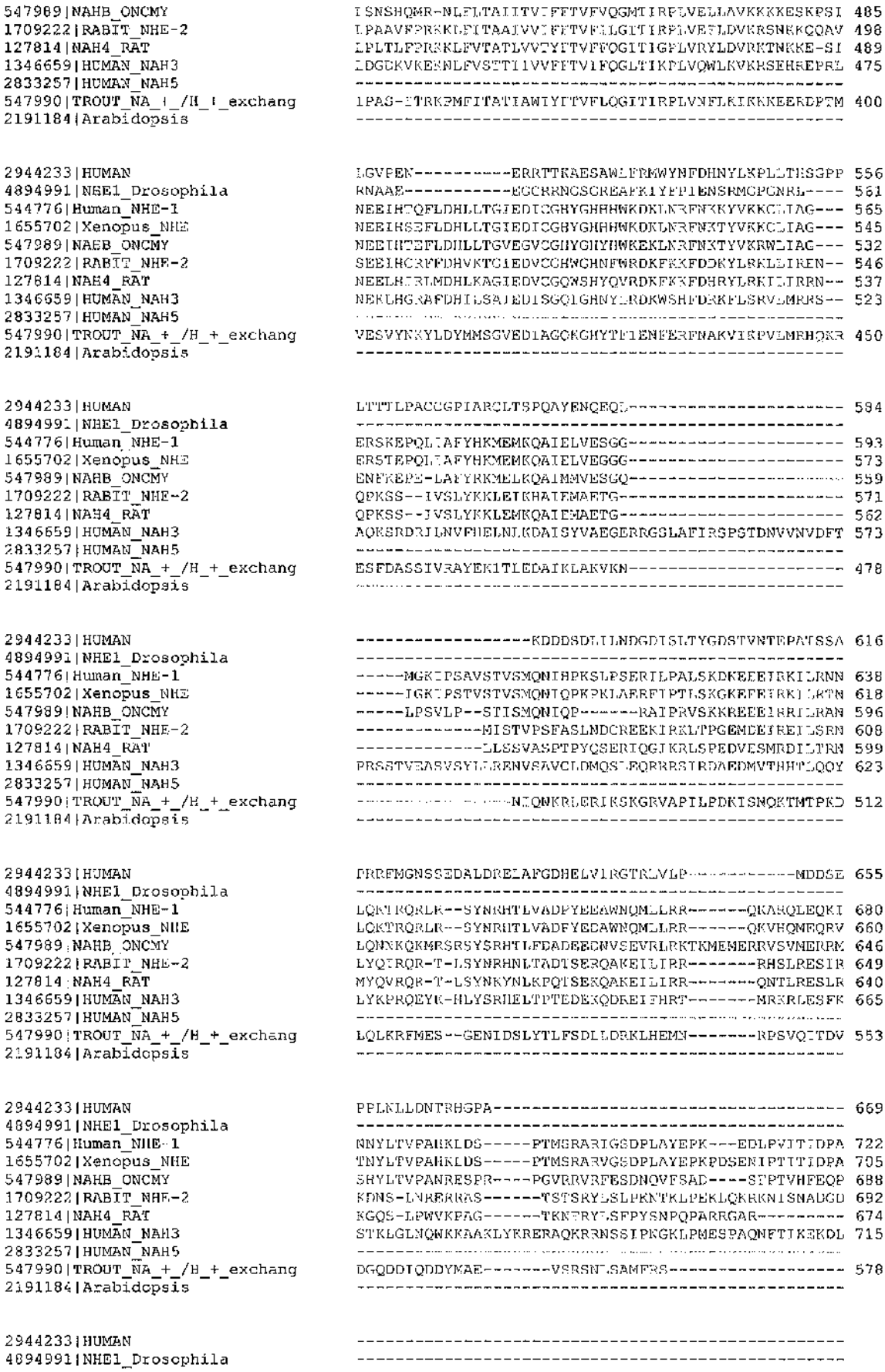

```
544776|Human_NHE-1          SPQSPESVDLVNEELKGKVLGLSRDPAKVAEEDEDD-------------- 758
1655702|Xenopus_NHE         SP----ESVDTVNETQ---------------EEEE---------------- 721
547989|NAHB_ONCMY           SP--PSTPDAVSLEE---------------EEEE---------------- 705
1709222|RABIT_NHE-2         SSDSEADAGTTVLNLQPRARRPLPEPFSKKASQAYKMEWKNEVDAGSGQG 742
127814|NAH4_RAT             AAESTGNPCCWLLIFL---------------------------------- 690
1346659|HUMAN_NAH3          ELSDTEEPPNYDEEMSGGIEFLASVTKDTASDSPAGIDNPVFSPDEALDR 765
2833257|HUMAN_NAH5          ------------------------------------------------- 
547990|TROUT_NA_+_/H_+_exchang ------------------------------------------------- 
2191184|Arabidopsis         ------------------------------------------------- 

2944233|HUMAN               ------------------------------------------------- 
4894991|NHE1_Drosophila     ------------------------------------------------- 
544776|Human_NHE-1          -------------DGGIMMRSKETSSPGTDDVFTPAPSDSPSSQRIQRCL 795
1655702|Xenopus_NHE         ---------------GITMTVREPPSPGADDVFIPQ--ESPNSQRLQRCL 754
547989|NAHB_ONCMY           ---------------VPKRPSLKADIEGPRGNASDNHQGELDYQRLARCL 740
1709222|RABIT_NHE-2         QPSPPAAPRSKEGGTQTPAVLRQPLLSKDQGREDSLTEGGRPKPPPRLVR 792
127814|NAH4_RAT             --------------------LCRAMVEKIWG------PGGQETQPRLLCR 714
1346659|HUMAN_NAH3          SLLARLPPWLSPGETVVPSQRARTQIPYSPGTFRRLMPFRLSSKSVDSFL 815
2833257|HUMAN_NAH5          ------------------------------------------------- 
547990|TROUT_NA_+_/H_+_exchang --------------------TEQLPSETPFHSGRRQSTGDLNATRRADFN 608
2191184|Arabidopsis         ------------------------------------------------- 

2944233|HUMAN               ---------------------------------
4894991|NHE1_Drosophila     ---------------------------
544776|Human_NHE-1          SDPGPHPEPGEGEPFFPKGQ--------- 815
1655702|Xenopus_NHE         SDPGPHPE--EIQPFIPQKKKLIDFVKG 780
547989|NAHB_ONCMY           SDPGPNKDKEDDDPFMSC---------- 758
1709222|RABIT_NHE-2         RASEPGNPKSRLGSDKP----------- 809
127814|NAH4_RAT             NLN---------------------------- 717
1346659|HUMAN_NAH3          QADGPEERPPAALPESTHM---------- 834
2833257|HUMAN_NAH5          ---------------------------
547990|TROUT_NA_+_/H_+_exchang V---------------------------- 609
2191184|Arabidopsis         ---------------------------
```

Figure A1.2 Alignment of 18 Sequences Coding for Na^+/H^+ Antiporters from Different Organisms.

Protein sequence for known Na^+/H^+ antiporters from various organisms and seven putative *Arabidopsis* Na^+/H^+ antiporters were aligned using CLUSTALW. The putative membrane spanning domains of predicted Na^+/H^+ antiporter proteins are highlighted in color and the membrane spanning-segments M3-M6 (blue color line) have high similarity with other exchangers. The sequence accession numbers are as follows: NHE1 (489499), *Drosophila*; ScNHX1 (NP_010744), S.*cerevisiae*; AtF20D21.19 (AAD25617.1), *Arabidopsis thaliana*; AtT12H17.230 (T04579.1), *Arabidopsis thaliana*; AtT9D9.5 (AAC1692.1), *Arabidopsis thaliana*; AtF24D13.3 (AAC98448.1), *Arabidopsis thaliana*; AtF24D13.4 (AAC98449.1), *Arabidopsis thaliana*; SOD2 (CAA77796.1), *S.pombe*; ZSOD2, Z.*rouxii;* AtF14H20.5 (AAD20091.1), *Arabidopsis thaliana*; NhaP (BAA31695.1), *P.aeruginosa*; (547990), *C.elegans*; NHE1 (P19634), *H.sapiens* ; NHE (1655702), *Xenopus* ; NHE2 (1709222), RABIT; NHE5 (2833257), *H.sapiens;* NHE6 (NP_006350), *H.sapiens*; and AtB04.4 (AAD16946.1), *Arabidopsis thaliana.*

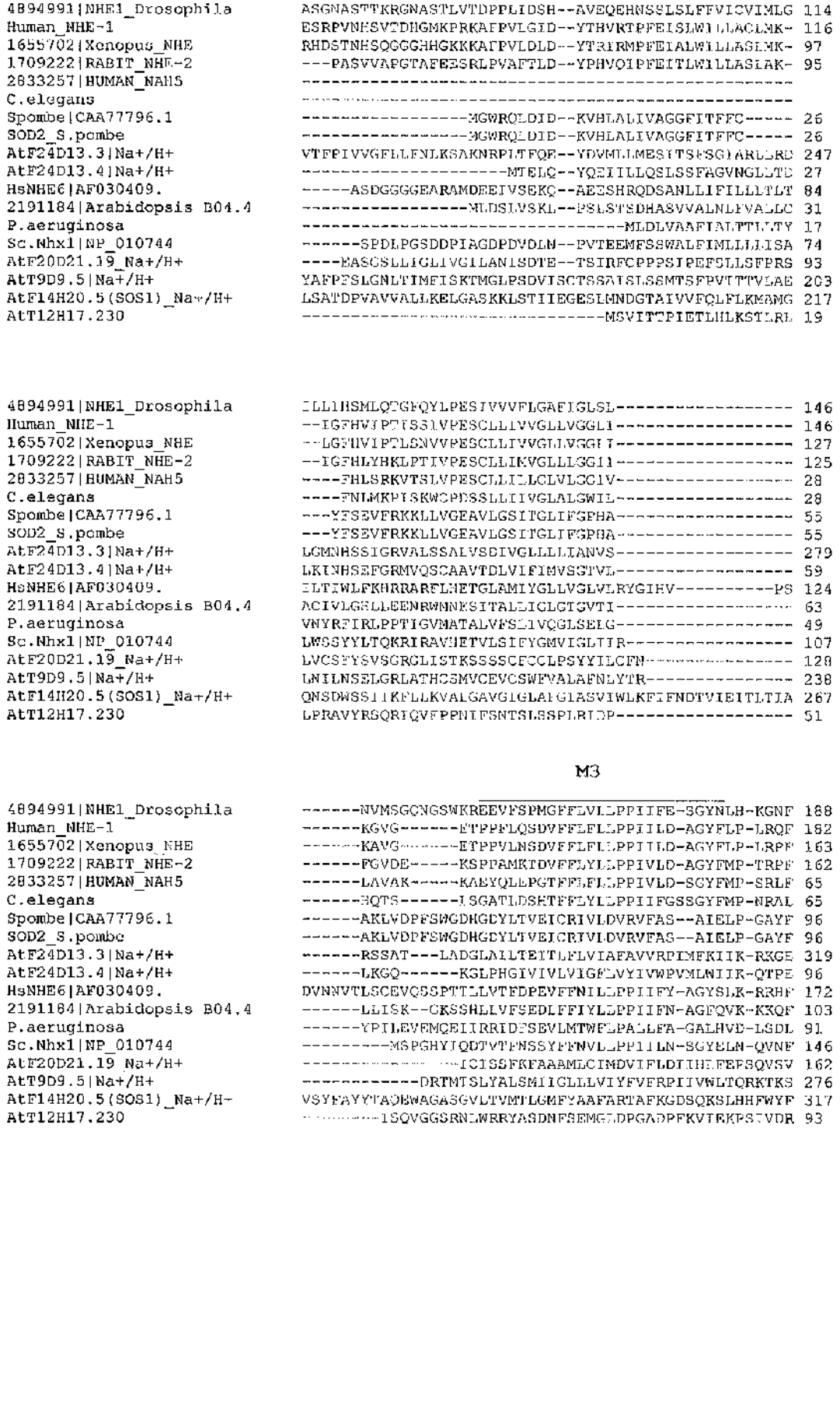
4894991|NHE1_Drosophila
Human_NHE-1
1655702|Xenopus_NHE
1709222|RABIT_NHE-2
2833257|HUMAN_NAH5
C.elegans
Spombe|CAA77796.1
SOD2_S.pombe
AtF24D13.3|Na+/H+
AtF24D13.4|Na+/H+
HsNHE6|AF030409.
2191184|Arabidopsis B04.4
P.aeruginosa
Sc.Nhx1|NP_010744
AtF20D21.19_Na+/H+
AtT9D9.5|Na+/H+
AtF14H20.5(SOS1)_Na+/H+
AtT12H17.230
M3

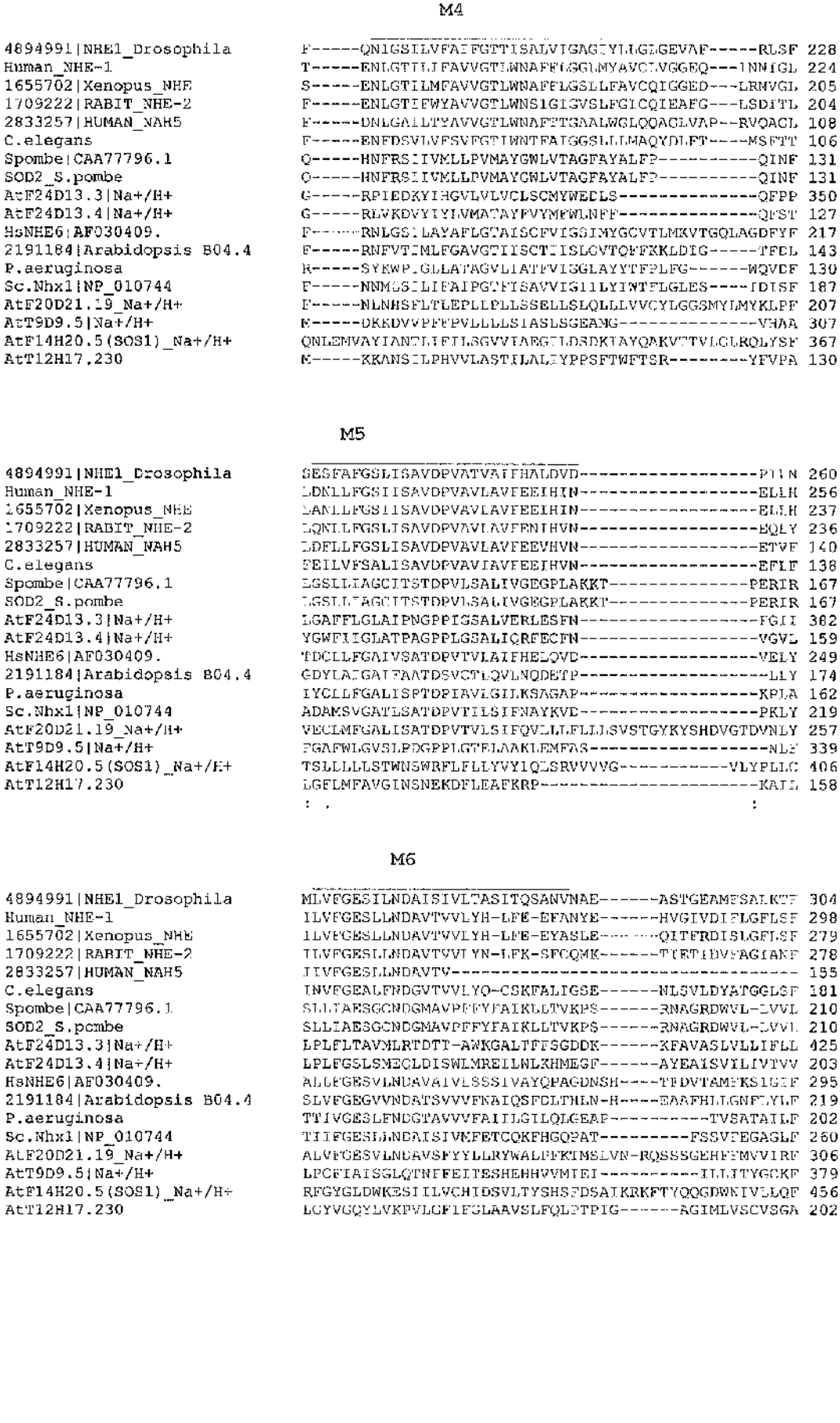
M4
4894991|NHE1_Drosophila F-----QNIGSILVFAIFGTTISALVIGAGIYLLGLGEVAF-----RLSF 228
Human_NHE-1 T-----ENLGTTLIFAVVGTLWNAFFLGGLMYAVCLVGGEQ---INNIGL 224
1655702|Xenopus_NHE S-----ENLGTILMFAVVGTLWNAFFLGSLLFAVCQIGGED---LRNVGL 205
1709222|RABIT_NHE-2 F-----ENLGTIFWYAVVGTLWNSIGIGVSLFGICQIEAFG---LSDITL 204
2833257|HUMAN_NAH5 F-----DNLGAILTYAVVGTLWNAFTGAALWGLQQAGLVAP--RVQACL 108
C.elegans F-----ENFDSVLVFSVFGTIWNTFAIGGSLLLMAQYDLFT----MSFTT 106
Spombe|CAA77796.1 Q-----HNFRSIIVMLLPVMAYGWLVTAGFAYALFP----------QINF 131
SOD2_S.pombe Q-----HNFRSIIVMLLPVMAYGWLVTAGFAYALFP----------QINF 131
AtF24D13.3|Na+/H+ G-----RPIEDKYIHGVLVLVCLSCMYWEDLS----------QFPP 350
AtF24D13.4|Na+/H+ G-----RLVKDVYIYIVMACAYFVYMFWLNFF----------QFST 127
HsNHE6|AF030409. F-----RNLGSILAYAFLGTAISCFVIGSIMYGCVTLMKVTGQLAGDFYF 217
2191184|Arabidopsis B04.4 F-----RNFVTIMLFGAVGTIISCTIISLCVTQFFKKLDIG-----TFDL 143
P.aeruginosa R-----SYKWPLGLLATAGVLIATFVIGGLAYYTFPLFG------WQVDF 130
Sc.Nhx1|NP_010744 F-----NNMLSILIFAIPGTFISAVVIGILLYIWTFLGLES----IDISF 187
AtF20D21.19_Na+/H+ F-----NLNHSFLTLEPLLPLLSSELLSLQLLLVVCYLGGSMYLMYKLPF 207
AtT9D9.5|Na+/H+ K-----DKKDVVPFTPVLLLLSIASLSGEAMG----------VHAA 307
AtF14H20.5(SOS1)_Na+/H+ QNLEMVAYIANTLIFILSGVVIAEGILDSDKIAYQAKVCTVLGLRQLYSF 367
AtT12H17.230 K-----KKANSILPHVVLASTILALIYPPSFTWFTSR---------YFVPA 130
M5
4894991|NHE1_Drosophila GESFAFGSLISAVDPVATVAIFHALDVD----------PIIN 260
Human_NHE-1 LDNLLFGSIISAVDPVAVLAVFEEIHIN----------ELLH 256
1655702|Xenopus_NHE LANLLFGSIISAVDPVAVLAVFEEIHIN----------ELLH 237
1709222|RABIT_NHE-2 LQNLLFGSLISAVDPVAVLAVFENIHVN----------EQLY 236
2833257|HUMAN_NAH5 LDFLLFGSLISAVDPVAVLAVFEEVHVN----------ETVF 140
C.elegans FEILVFSALISAVDPVAVIAVFEEIHVN----------EFLF 138
Spombe|CAA77796.1 LGSLLIAGCITSTDPVLSALIVGEGPLAKKT----------PERIR 167
SOD2_S.pombe LGSLLIAGCITSTDPVLSALIVGEGPLAKKT----------PERIR 167
AtF24D13.3|Na+/H+ LGAFFLGLAIPNGPPIGSALVERLESFN----------FGII 382
AtF24D13.4|Na+/H+ YGWFIIGLATPAGPPLGSALICRFECFN----------VGVL 159
HsNHE6|AF030409. TDCLLFGAIVSATDPVTVLAIFHELQVD----------VELY 249
2191184|Arabidopsis B04.4 GDYLAIGAIFAATDSVCTLQVLNQDETP----------LLY 174
P.aeruginosa IYCLLFGALISPTDPIAVLGILKSAGAP----------KPLA 162
Sc.Nhx1|NP_010744 ADAMSVGATLSATDPVTILSIFNAYKVD----------PKLY 219
AtF20D21.19_Na+/H+ VECLMFGALISATDPVTVLSIFQVLHLFLLLSVSTGYKYSHDVGTDVNLY 257
AtT9D9.5|Na+/H+ FGAFWLGVSLPDGPPLGTFLAAKLEMFAS----------NLF 339
AtF14H20.5(SOS1)_Na+/H+ TSLLLLLSTWNSWRFLFLLYVYIQLSRVVVVG----------VLYPLLC 406
AtT12H17.230 LGFLMFAVGINSNEKDFLEAFKRP----------KAIL 158
M6
4894991|NHE1_Drosophila MLVFGESILNDAISIVLTASITQSANVNAE------ASTGEAMFSALKTF 304
Human_NHE-1 ILVFGESLLNDAVTVVLYH-LFE-EFANYE------HVGIVDIFLGFLSF 298
1655702|Xenopus_NHE ILVFGESLLNDAVTVVLYH-LFE-EYASLE----QITFRDISLGFLSF 279
1709222|RABIT_NHE-2 ILVFGESLLNDAVTVVLYN-LFK-SFCQMK------TIETIDVFAGIAKF 278
2833257|HUMAN_NAH5 ILVFGESLLNDAVTV---------- 155
C.elegans INVFGEALFNDGVTVVLYQ-CSKFALIGSE------NLSVLDYATGGLSF 181
Spombe|CAA77796.1 SLLIAESGCNDGMAVPFFYFAIKLLTVKPS------RNAGRDWVL-LVVL 210
SOD2_S.pombe SLLIAESGCNDGMAVPFFYFAIKLLTVKPS------RNAGRDWVL-LVVL 210
AtF24D13.3|Na+/H+ LPLFLTAVMLRTDTT-AWKGALTFFSGDDK------KFAVASLVLLIFLL 425
AtF24D13.4|Na+/H+ LPLFGSLSMECLDISWLMRELNLKHMEGF------AYEAISVILIVTVV 203
HsNHE6|AF030409. ALLFGESVLNDAVAIVLSSSIVAYQPAGDNSH----TFDVTAMFKSIGIF 295
2191184|Arabidopsis B04.4 SLVFGEGVVNDATSVVVFNAIQSFDLTHLN-H----EAAFHLLGNFLYLF 219
P.aeruginosa TTIVGESLFNDGTAVVVFAILGLQLGEAP----------TVSATAILF 202
Sc.Nhx1|NP_010744 TIIFGESLLNDAISIVMFETCQKFHGQPAT---------FSSVFEGAGLF 260
ALF20D21.19_Na+/H+ ALVFGESVLNDAVSFYYLLRYWALPFKTMSLVN-RQSSSGEHFFMVVIRF 306
AtT9D9.5|Na+/H+ LPCFIAISSLQTNFFEITESHEHHVVMIEI----------ILLITYGCKF 379
AtF14H20.5(SOS1)_Na+/H+ RFGYGLDWKESIILVCHIDSVLTYSHSFDSAIKRKFTYQQGDWNIVLLQF 456
AtT12H17.230 LGYVGQYLVKPVLGFIFGLAAVSLFQLPTPIG------AGIMLVSCVSGA 202

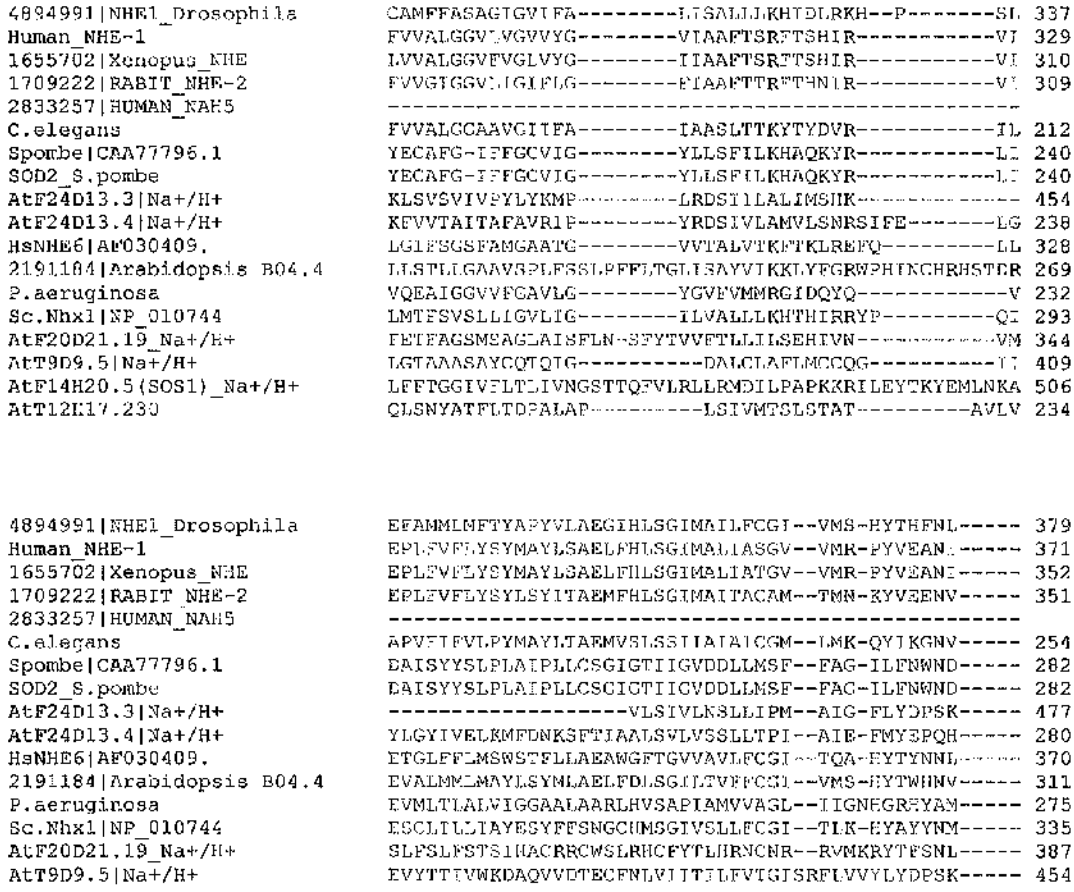
4894991|NHE1_Drosophila
Human_NHE-1
1655702|Xenopus_NHE
1709222|RABIT_NHE-2
2833257|HUMAN_NAH5
C.elegans
Spombe|CAA77796.1
SOD2_S.pombe
AtF24D13.3|Na+/H+
AtF24D13.4|Na+/H+
HsNHE6|AF030409.
2191184|Arabidopsis B04.4
P.aeruginosa
Sc.Nhx1|NP_010744
AtF20D21.19_Na+/H+
AtT9D9.5|Na+/H+
AtF14H20.5(SOS1)_Na+/H+
AtT12K17.230

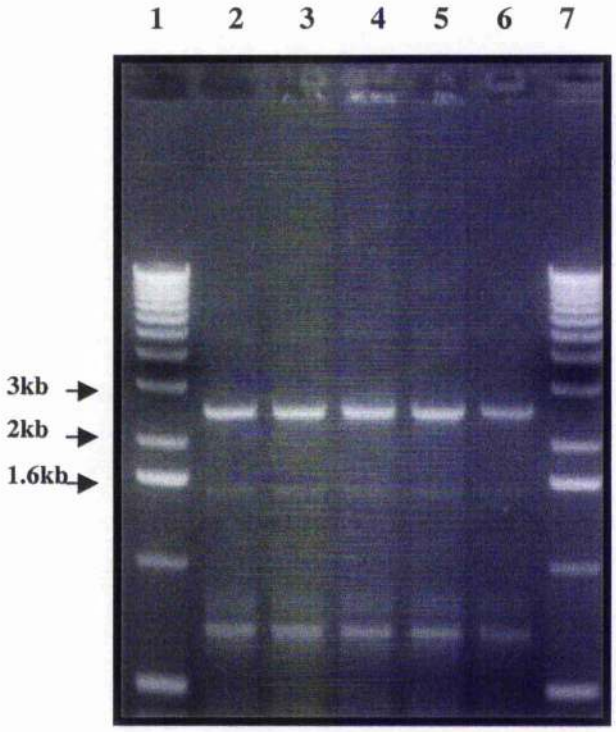

Figure. A1.3. PCR Amplification of *At* B04.4 from Genomic DNA Template Using Primer Set 1.

The primers were designed to bind a site thirty-five bases upstream the ATG Translation start site and thirty base down stream the TGA translation stop sequences. The reaction contained 50-100 ng of genomic DNA, 2.6mM MgCL, 50-100 pmol primers, 200μM dNTPs, 1X *Taq* buffer (20mM Tris-HCL, 1mM dithiothreitol, 0.1mM EDTA, 0.1 M KCL, 0.5% Nonidet P40 (v/v),0.5% Tween 20 (v / v), 50% glycerol (v/v), pH 8.0 (4°C), and 2.5 units of *Taq* DNA polymerase (final volume of 50 μL). The reaction was started (hot start) by the addition of *Taq* DNA polymerase at 94°C, and followed by 35 cycles of 20 seconds at 47°C (annealing),120 second at 72°C (extension) and 15 seconds at 94 °C (denature). The PCR products were analysed on a 1% agarose gel stained with ethidium bromide (see Section2.2.5.2). Lanes from 2-6 represent the expected size fragment for PCR product, 2.6 kb. Lane 1and 7 represent the 1 kb ladder.

Sequence 196 from Patent W00055325
Score=1172bits(591), expect = 0.0
Identities = 589/591(99%)
Strand = Plus/plus

```
Query: 100    aattcgccctatagtgagtcgtattactgttcactggccgtcgttttacaacgtcgtgac 159
              ||||||||||||||||||||||||||||  ||||||||||||||||||||||||||||||
Sbjct: 14655  aattcgccctatagtgagtcgtattacaattcactggccgtcgttttacaacgtcgtgac 14714

Query: 160    tgggaaaaccctggcgttacccaacttaatcgccttgcagcacatccccctttcgccagc 219
              ||||||||||||||||||||||||||||||||||||||||||||||||||||||||||||
Sbjct: 14715  tgggaaaaccctggcgttacccaacttaatcgccttgcagcacatccccctttcgccagc 14774

Query: 220    tggcgtaatagcgaagaggcccgcaccgatcgcccttcccaacagttgcgcagcctgaat 279
              ||||||||||||||||||||||||||||||||||||||||||||||||||||||||||||
Sbjct: 14775  tggcgtaatagcgaagaggcccgcaccgatcgcccttcccaacagttgcgcagcctgaat 14834

Query: 280    ggcgaatggacgcgccctgtagcggcgcattaagcgcggcgggtgtggtggttacgcgca 339
              ||||||||||||||||||||||||||||||||||||||||||||||||||||||||||||
Sbjct: 14835  ggcgaatggacgcgccctgtagcggcgcattaagcgcggcgggtgtggtggttacgcgca 14894

Query: 340    gcgtgaccgctacacttgccagcgccctagcgcccgctcctttcgctttcttcccttcct 399
              ||||||||||||||||||||||||||||||||||||||||||||||||||||||||||||
Sbjct: 14895  gcgtgaccgctacacttgccagcgccctagcgcccgctcctttcgctttcttcccttcct 14954

Query: 400    ttctcgccacgttcgccggctttccccgtcaagctctaaatcgggggctcccctttagggt 459
              ||||||||||||||||||||||||||||||||||||||||||||||||||||||||||||
Sbjct: 14955  ttctcgccacgttcgccggctttccccgtcaagctctaaatcgggggctcccctttagggt 15014

Query: 460    tccgatttagtgctttacggcacctcgaccccaaaaaacttgattagggtgatggttcac 519
              ||||||||||||||||||||||||||||||||||||||||||||||||||||||||||||
Sbjct: 15015  tccgatttagtgctttacggcacctcgaccccaaaaaacttgattagggtgatggttcac 15074

Query: 520    gtagtgggccatcgccctgatagacggtttttcgccctttgacgttggagtccacgttct 579
              ||||||||||||||||||||||||||||||||||||||||||||||||||||||||||||
Sbjct: 15075  gtagtgggccatcgccctgatagacggtttttcgccctttgacgttggagtccacgttct 15134

Query: 580    ttaatagtggactcttgttccaaactggaacaacactcaaccctatctcggtctattctt 639
              ||||||||||||||||||||||||||||||||||||||||||||||||||||||||||||
Sbjct: 15135  ttaatagtggactcttgttccaaactggaacaacactcaaccctatctcggtctattctt 15194

Query: 640    ttgatttataagggattttgccgatttcggcctattggttaaaaaatgagc 690
              ||||||||||||||||||||||||||||||||||||||||||||||||||
Sbjct: 15195  ttgatttataagggattttgccgatttcggcctattggttaaaaaatgagc 15245
```

Figure A1.4 Blast Output of *AtT9D9.5* cDNAT3 Primer Direction Search in the EMBL Database.

Blast output of T3 primer direction from the *AtT9D9.5* cDNA sequences interrogation EMBL database. Nearly identical sequence homology was found at the DNA level (99%) locus (AX059463) Patent W00055325..

Score = 393 bits (198), Expect = e-108
Identities = 217/221 (98%), Gaps = 3/221 (1%)
Strand = Plus / Minus

```
Query: 109 gcttggcgtaatcatggtcatagctgtttcctgtgtgaaattgttatccgctcacaattc 168
           ||||||||||||||||||||||||||||||||||||||||||||||||||||||||||||
Sbjct: 503 gcttggcgtaatcatggtcatagctgtttcctgtgtgaaattgttatccgctcacaattc 444

Query: 169 cacacaacatacgagccggaagcataaagtgtaaagcctggggtgcctaatgagtgagct 228
           ||||||||||||||||||||||||||||||||||||||||||||||||||||||||||||
Sbjct: 443 cacacaacatacgagccggaagcataaagtgtaaagcctggggtgcctaatgagtgagct 384

Query: 229 aattcacattaattgcgttgcgctcactgcccgctttccaagttccgggaaacctgtcgt 288
           ||||||||||||||||||||||||||||||||||||||||||||||||||||||||||||
Sbjct: 383 aatcacattaattgcgttgcgctcactgcccgctttccaagt--cgggaaacctgtcgtt 327

Query: 289 gccagctgcattaatgaatcggccaacgcgcggggagaggc 329
           |||||||||||||||||||||||||||||||||||||||
Sbjct: 326 gccagctgcattaatgaatcggccaacgcgcggggagaggc 286
```

Figure A1.5A Blast Output of *AtT9D9.5* cDNA T7 Primer Direction Search in EMBL Database.

Blast output of T7 primer direction from the *AtT9D9.5* cDNA sequences interrogation the EMBL database. Nearly identical sequence homology was found (98%) to *Arabidopsis thaliana* mRNA coding for mitochondrial F1 ATP synthase beta subunit (p_beta gene). Acc. No. 17939848

Pathogen-induced plant promoters
Score = 581 bits (293), Expected =e-165
Identities = 299/301(99%)
Strand = Plus/Minus

```
Query: 369  gcgcccgctcctttcgctttcttcccttcctttctcgccacgttcgccggctttccccgt 428
            ||||||||||||||||||||||||||||||||||||||||||||||||||||||||||||
Sbjct: 1033 gcgcccgctcctttcgctttcttcccttcctttctcgccacgttcgccggctttccccgt 974


Query: 429  caagctctaaatcgggggctcccttagggttccgatttagtgctttacggcacctcgac 488
            ||||||||||||||||||||||||||||||||||||||||||||||||||||||||||||
Sbjct: 973  caagctctaaatcgggggctcccttagggttccgatttagtgctttacggcacctcgac 914


Query: 489  cccaaaaaacttgattagggtgatggttcacgtagtgggccatcgccctgatagacggtt 548
            ||||||||||||||| ||||||||||||||||||||||||||||||||||||||||||||
Sbjct: 913  cccaaaaaacttgatttgggtgatggttcacgtagtgggccatcgccctgatagacggtt 854


Query: 549  tttcgccctttgacgttggagtccacgttctttaatagtggactcttgttccaaactgga 608
            ||||||||||||||||||||||||||||||||||||||||||||||||||||||||||||
Sbjct: 853  tttcgccctttgacgttggagtccacgttctttaatagtggactcttgttccaaactgga 794


Query: 609  acaacactcaaccctatctcggtctattcttttgatttataagggattttgccgatttcg 668
            ||||||||||||||||||||| ||||||||||||||||||||||||||||||||||||||
Sbjct: 793  acaacactcaaccctatctcgggctattcttttgatttataagggattttgccgatttcg 734


Query: 669  g 669
            |
Sbjct: 733  g 733
```

Figure.A1.5B Blast Output of a *AtT9D9.5* cDNA T3 Primer Direction Search in EMBL Database.

Blast output of T3 primer direction from the *AtT9D9.5* cDNA sequences interrogation the EMBL database. Nearly identical sequence homology was found at the cDNA level (99%) to *Arabidopsis thaliana* gene coding for Pathogen-induced plant promoters Patent: JP2001508661-A / L. Locus BD056961. Accession 22602567.

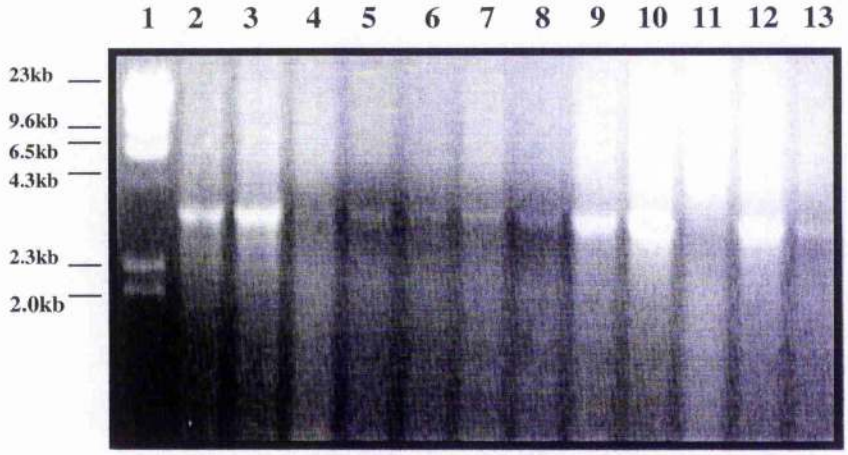

Figure. A1.6. RT-PCR Amplification of *Arabidopsis* Fragment *At*F14H20.5 cDNA.

RT-PCR was used to amplify the first strand of *At*F14H20.5 cDNA prepared from *Arabidopsis thaliana* var. Columbia HHS cell line grown in high salt (260mM NaCl). Total RNA was extracted from HHS cells and the first strand cDNA prepared using MMLV reverse transcriptase and random primers. The *At* F14H20.5 primers were used with high fidelity *Taq* DNA polymerase in PCR reaction. The reaction. reaction contained 2.5 μL first strand cDNA template, 2.6 mM MgCl, 50 pmol primers, 200 μM dNTPs, 1X high fidelity *Taq* buffer (20mM Tris-HCl, 100 mM KCl,1mM dithiothreitol (DTT), 0.1mM EDTA, 0.5% Tween 20 (v/v), 0.5% Nonidet P40 (v/v), 50% glycerol (v/v), pH 7.5, and 2.5 units of high fidelity *Taq* DNA polymerase (final volume of 50 μL). The reaction was started (hot start) by the addition of high fidelity *Taq* at 94°C. A Touch Down PCR programme was used, with annealing temperatures decreasing from 51°C down to 48 °C steps of 1 degree of 20 seconds at 48°C (annealing),120 second at 72°C (extension) and 20 seconds at 94 °C. The PCR products were analyzed on a 1% agarose gel stained with ethidium bromide. Lanes 2-13 show the expected PCR product, 3.5 kb fragment. Lane 1 represents λ Hind III.

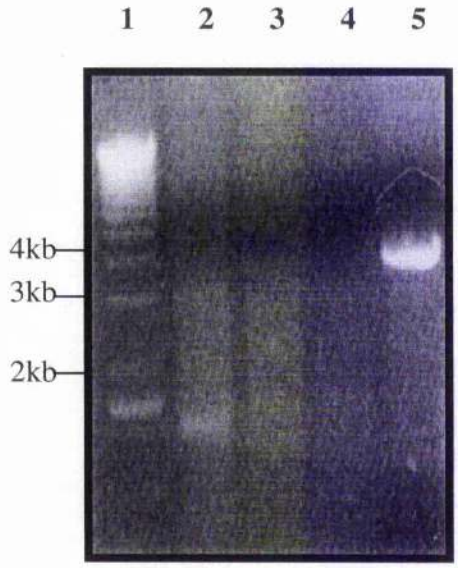

Figure. A1.7 PCR Amplification of Plasmid Vector Insert of *At*F14H20.5 cDNA.

Plasmid vector insert was amplified directly from individual bacterial colonies. The plasmid insert were amplified by colony PCR using T7 and T3 primers, and the products run out on a 1% agarose gel. Lane 2 to lane 4 represent a negative colonies, however lane 5 has a product of the expected size (3.5kbp). Lane 1 represents 1kb ladder marker.

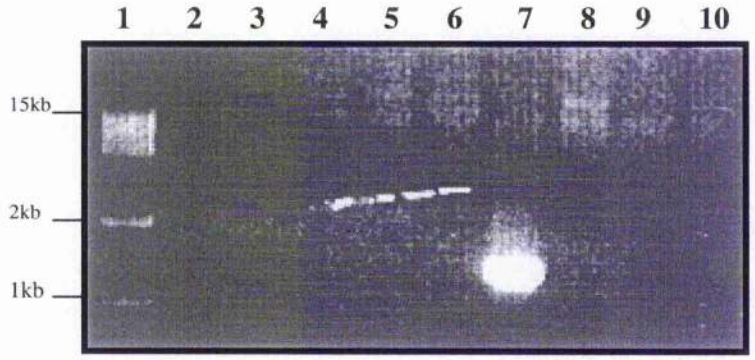

Figure. A1.8. Colony PCR Amplification of Plasmid Vector Insert of *At* T12H 17.230 cDNA.

*At*T12H17.230 cDNA insert was amplified directly from individual bacterial colonies. The size of cDNA inserts in plasmid vectors were amplified by PCR with T3 and T7 primer sites the flank the insert. Positive transforment with the correct size(1.4kb), colony was identified in lane7. Lane 1 represents EZ-Load 1kb molecular ruler.

>gi|7486890|pir||T04579 hypothetical protein T12H17.230 - Arabidopsis thaliana
gi|2827561|emb|CAA16569.1| predicted protein [Arabidopsis thaliana]
gi|3292809|emb|CAA19799.1| putative protein [Arabidopsis thaliana]
gi|7269131|emb|CAB79239.1| predicted protein [Arabidopsis thaliana]
Length = 460

Score = 666 bits (1718), Expect = 0.0
Identities = 404/460 (87%), Positives = 405/460 (88%), Gaps = 51/460 (11%)

```
Query: 1   MSVITTPIETLHLKSTLRLLPRAVYRSQRIQVFPPNIFSNTSLSSPLRIDPISQ------ 54
           MSVITTPIETLHLKSTLRLLPRAVYRSQRIQVFPPNIFSNTSLSSPLRIDPISQ
Sbjct: 1   MSVITTPIETLHLKSTLRLLPRAVYRSQRIQVFPPNIFSNTSLSSPLRIDPISQGLFILL 60

Query: 55  ----------------------------VGGSRNLWRRYASDNFSEMGLDPGADPFK- 83
                                       VGGSRNLWRRYASDNFSEMGLDPGADPFK
Sbjct: 61  SSILRRLCLLGTCKIYTFFSHGFLQPTIYTVGGSRNLWRRYASDNFSEMGLDPGADPFKV 120

Query: 84  --------------VIEKPSIVDRMKKANSILPHVVLASTILALIYPPSFTWFTSRYFVP 129
                         VIEKPSIVDRMKKANSILPHVVLASTILALIYPPSFTWFTSR+F
Sbjct: 121 CAMGSFLFHSMLCWVIEKPSIVDRMKKANSILPHVVLASTILALIYPPSFTWFTSRFFPL 180

Query: 130 ALGFLMFAVGINSNEKDFLEAFKRPKAILLGYVGQYLVKPVLGFIFGLAAVSLFQLPTPI 189
             GFLMFAVGINSNEKDFLEAFKRPKAILLGYVGQYLVKPVLGFIFGLAAVSLFQLPTPI
Sbjct: 181 EQGFLMFAVGINSNEKDFLEAFKRPKAILLGYVGQYLVKPVLGFIFGLAAVSLFQLPTPI 240

Query: 190 GAGIMLVSCVSGAQLSNYATFLTDPALAPLSIVMTSLSTATAVLVTPMLSLLLIGKKLPV 249
           GAGIMLVSCVSGAQLSNYATFLTDPALAPLSIVMTSLSTATAVLVTPMLSLLLIGKKLPV
Sbjct: 241 GAGIMLVSCVSGAQLSNYATFLTDPALAPLSIVMTSLSTATAVLVTPMLSLLLIGKKLPV 300

Query: 250 DVKGMISSILQVVIAPIAAGLLLNKLFPKVSNAIRPFLPILSVLDTACCVGAPLALNINS 309
           DVKGMISSILQVVIAPIAAGLLLNKLFPKVSNAIRPFLPILSVLDTACCVGAPLALNINS
Sbjct: 301 DVKGMISSILQVVIAPIAAGLLLNKLFPKVSNAIRPFLPILSVLDTACCVGAPLALNINS 360

Query: 310 VMSPFGATILLLVTMFHLSAFLAGYFLTGSVFRNAPDAKAMQRTLSYETGMQSSLLALAL 369
           VMSPFGATILLLVTMFHLSAFLAGYFLTGSVFRNAPDAKAMQRTLSYETGMQSSLLALAL
Sbjct: 361 VMSPFGATILLLVTMFHLSAFLAGYFLTGSVFRNAPDAKAMQRTLSYETGMQSSLLALAL 420

Query: 370 ATKFFQDPLVGIPPAISTVVMSLMGFTLVLIWSKEKSNTF 409
           ATKFFQDPLVGIPPAISTVVMSLMGFTLVLIWSKEKSNTF
Sbjct: 421 ATKFFQDPLVGIPPAISTVVMSLMGFTLVLIWSKEKSNTF 460
```

Figure. A1.9. Blast Output of AtT12H17.230 Search in the EMBL Database.

The amino acid sequence deduced from the silico translation of the cDNA revealed that the cDNA encodes a protein of 409 amino acids. BLASTP searches of the EMBL database identified 87% identity to that predicted for At T12H17.230 and has moderate homology to bacterial Na^+/H^+ antiporters (e-values of 1e-31 *Pseudomonas aeruginosa*).

>gi|18416020|ref|NP_567671.1| similar to putative transport protein; protein id: *At*4g22840.1, supported by cDNA: 9746., supported by cDNA: gi_17529349
[Arabidopsis thaliana]
gi|17529350|gb|AAL38902.1| unknown protein [Arabidopsis thaliana]
gi|21436155|gb|AAM51324.1| unknown protein [Arabidopsis thaliana]
gi|21618116|gb|AAM67166.1| unknown [Arabidopsis thaliana]
Length = 409

Score = 697 bits (1798), Expect = 0.0
Identities = 409/409 (100%), Positives = 409/409 (100%)

```
Query: 1   MSVITTPIETLHLKSTLRLLPRAVYRSQRIQVFPPNIFSNTSLSSPLRIDPISQVGGSRN 60
           MSVITTPIETLHLKSTLRLLPRAVYRSQRIQVFPPNIFSNTSLSSPLRIDPISQVGGSRN
Sbjct: 1   MSVITTPIETLHLKSTLRLLPRAVYRSQRIQVFPPNIFSNTSLSSPLRIDPISQVGGSRN 60

Query: 61  LWRRYASDNFSEMGLDPGADPFKVIEKPSIVDRMKKANSILPHVVLASTILALIYPPSFT 120
           LWRRYASDNFSEMGLDPGADPFKVIEKPSIVDRMKKANSILPHVVLASTILALIYPPSFT
Sbjct: 61  LWRRYASDNFSEMGLDPGADPFKVIEKPSIVDRMKKANSILPHVVLASTILALIYPPSFT 120

Query: 121 WFTSRYFVPALGFLMFAVGINSNEKDFLEAFKRPKAILLGYVGQYLVKPVLGFIFGLAAV 180
           WFTSRYFVPALGFLMFAVGINSNEKDFLEAFKRPKAILLGYVGQYLVKPVLGFIFGLAAV
Sbjct: 121 WFTSRYFVPALGFLMFAVGINSNEKDFLEAFKRPKAILLGYVGQYLVKPVLGFIFGLAAV 180

Query: 181 SLFQLPTPIGAGIMLVSCVSGAQLSNYATFLTDPALAPLSIVMTSLSTATAVLVTPMLSL 240
           SLFQLPTPIGAGIMLVSCVSGAQLSNYATFLTDPALAPLSIVMTSLSTATAVLVTPMLSL
Sbjct: 181 SLFQLPTPIGAGIMLVSCVSGAQLSNYATFLTDPALAPLSIVMTSLSTATAVLVTPMLSL 240

Query: 241 LLIGKKLPVDVKGMISSILQVVIAPIAAGLLLNKLFPKVSNAIRPFLPILSVLDTACCVG 300
           LLIGKKLPVDVKGMISSILQVVIAPIAAGLLLNKLFPKVSNAIRPFLPILSVLDTACCVG
Sbjct: 241 LLIGKKLPVDVKGMISSILQVVIAPIAAGLLLNKLFPKVSNAIRPFLPILSVLDTACCVG 300

Query: 301 APLALNINSVMSPFGATILLLVIMFHLSAFLAGYFLTGSVFRNAPDAKAMQRTLSYETGM 360
           APLALNINSVMSPFGATILLLVIMFHLSAFLAGYFLTGSVFRNAPDAKAMQRTLSYETGM
Sbjct: 301 APLALNINSVMSPFGATILLLVIMFHLSAFLAGYFLTGSVFRNAPDAKAMQRTLSYETGM 360

Query: 361 QSSLLALALATKFFQDPLVGIPPAISTVVMSLMGFTLVLIWSKEKSNIF 409
           QSSLLALALATKFFQDPLVGIPPAISTVVMSLMGFTLVLIWSKEKSNIF
Sbjct: 361 QSSLLALALATKFFQDPLVGIPPAISTVVMSLMGFTLVLIWSKEKSNIF 409
```

Figure. A1.10. Blast Output of *At* T12H17.230 Search in the EMBL Database.

The putative At T12H17.230 protein deduced from the silico translation of the cDNA revealed that the cDNA encodes a protein of 409 amino acids. BLASTP searches of the EMBL database identified 100% identity to Atg2284.1similar to putative transporter protein that deposited recently on 20-Aug-2002 in the database. Acc. No. 18416020 and supported by cDNA:9746., supported by cDNA:17529349.

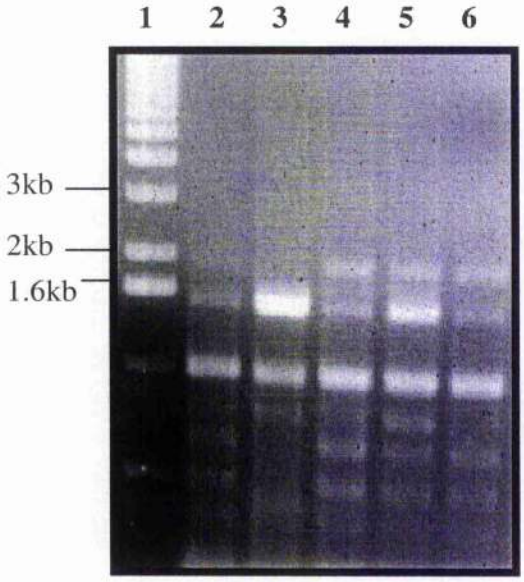

Figure. A1.11 RT-PCR Amplification of *Arabidopsis* Fragment *At*T20D21.19 cDNA.

A RT-PCR was used to amplify the first strand of *At* T20D21.19 cDNA prepared from an *Arabidopsis thaliana* var. Columbia HHS cell line grown in high salt (260 mM NaCl). Total RNA was isolated from HHS cells and first strand cDNA prepared using MMLV reverse transcriptase and random primers. The *At* T20D21.19 primers were used with high fidelity *Taq* DNA polymerase in a PCR. Five cycles were performed at each annealing temperature, with 20 cycles. The reaction contained 1.5-2.5 μL first strand cDNA template, 2.6 mM MgCl, 50 pmol primers, 200μM dNTPs, 1X high fidelity *Taq* buffer (20mM Tris-HCl, 100 mM KCl,1mM dithiothreitol (DTT), 0.1mM EDTA, 0.5% Tween 20 (v/v), 0.5% Nonidet P40 (v/v), 50% glycerol (v/v), pH 7.5, and 2.5 units of high fidelity *Taq* DNA polymerase (final volume of 50 μL). The reaction was started (hot start) by the addition of high fidelity *Taq* at 94°C. A Touch Down PCR programme was used, with annealing temperatures decreasing from 50°C down to 45 °C steps of 1 degree. Five cycles were performed at each annealing temperature, with 10 cycles at 45°C for 15 seconds (annealing),120 second at 72°C (extension) and 12 seconds at 94 °C (denature). The PCR products were analyzed on a 1% agarose gel stained with ethidium bromide. Lanes 2-6 show the expected PCR product, 1.6 kb fragment. Lane1 represents a1kb marker.

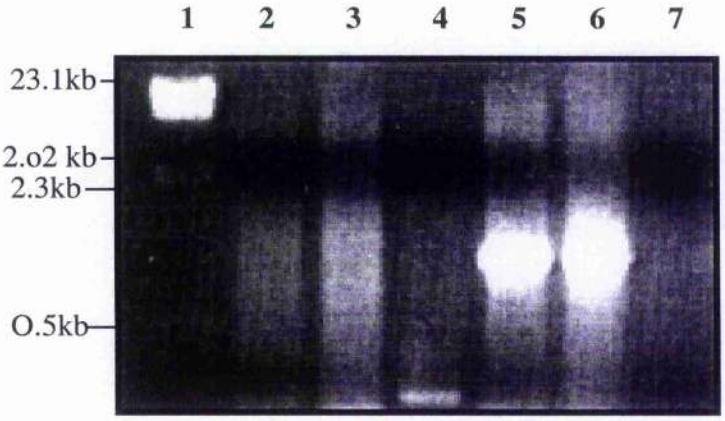

Figure. A1.12 Colony PCR Amplification of Plasmid Vector Insert of *At* F20D21.19 cDNA.

Plasmid vector insert was amplified directly from individual bacterial colonies. The plasmid insert were amplified by colony PCR using T7 and T3 primers, and the products run out on a 1% agarose gel. Lane 5 and 6 represent a positive transforment colonies with inserts of an expected size (1.5kb). However, Lane 2 ;3;4; and lane 7 represent a negative colonies. Line number 1 represents λ Hind III marker.

Score = 1511 bits (757), Expect = 0.0
Identities = 757/757 (100%)
Strand = Plus / Minus

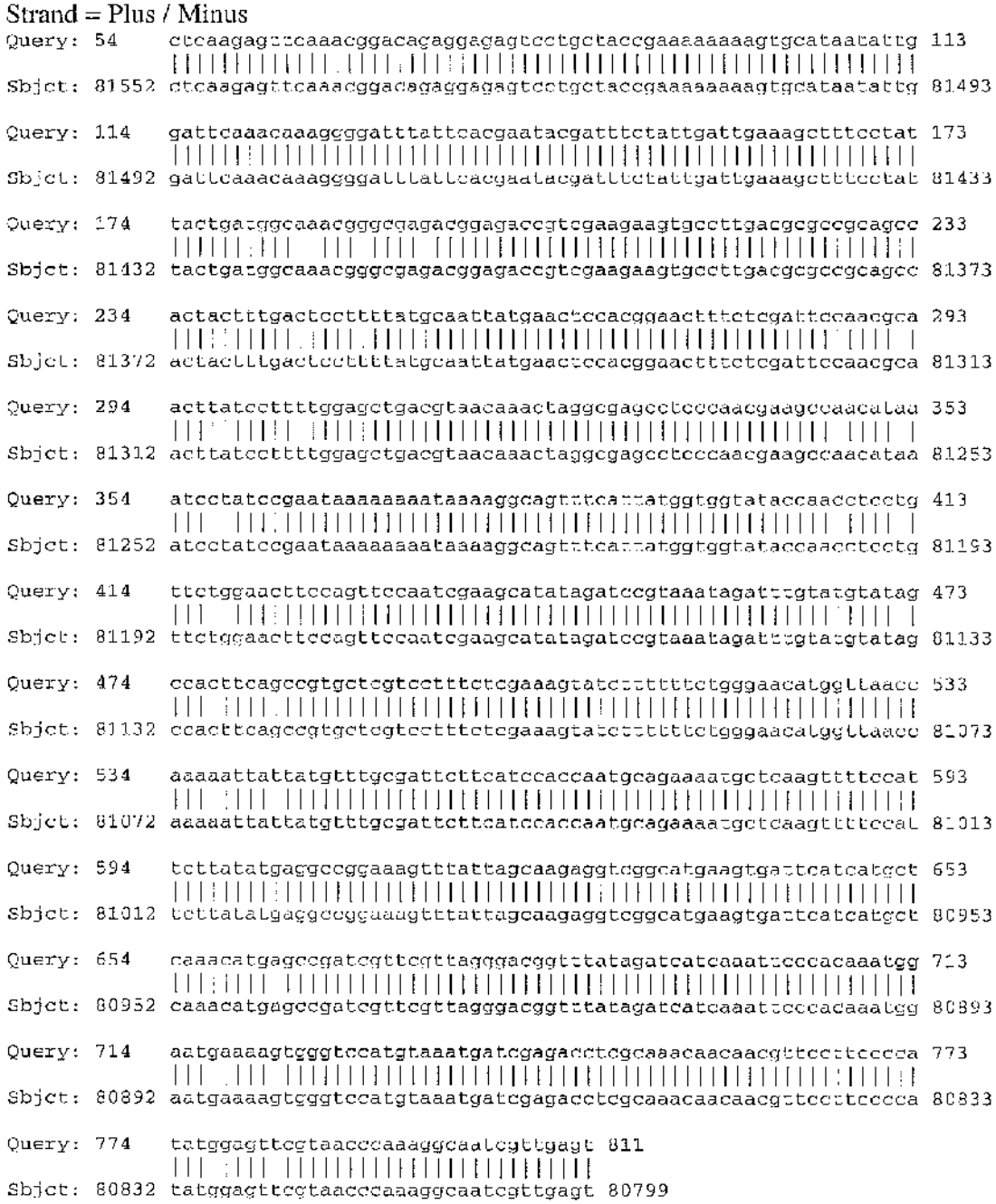

Figure A1.13A. Blast Output of *AtT20D21.19* cDNA Search in the EMBL Database.

Blast output from the *AtT20D21.19* cDNA sequences interrogation the EMBL database. Identical sequence homology was found (100%) to *Arabidopsis* clone T18C6 coding for ATP-binding cassette (ABC). Accession no.20197635.

Arabidopsis thaliana mitochondrial genome, part A.
Score = 1511 bits (757), Expect = 0.0
Strand = Plus / Plus

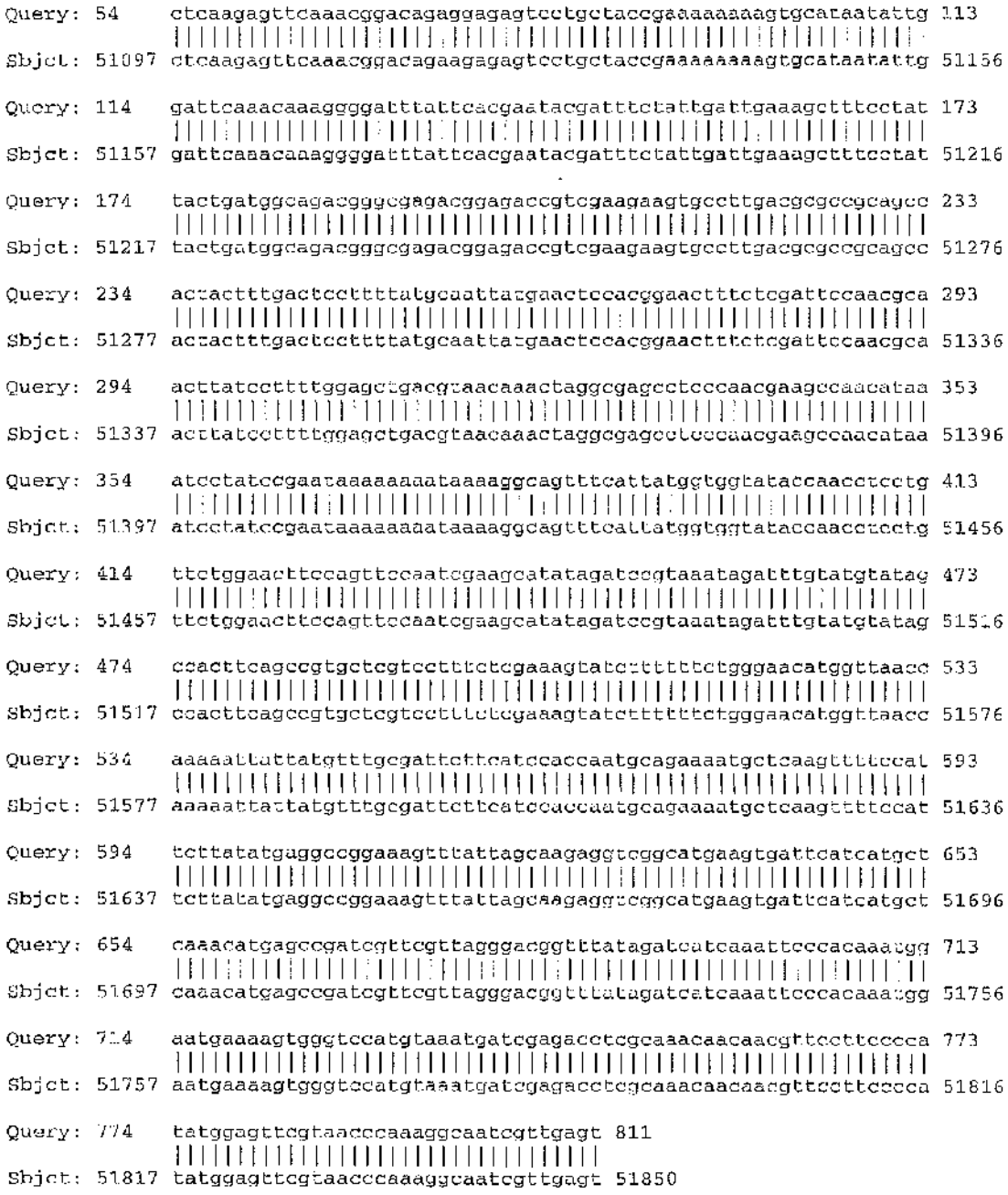

Figure A1.13.B Blast Output of *AtT20D21.19* cDNA Search in the EMBL Database.

Blast output from the *AtT20D21.19* cDNA sequences interrogation the EMBL databas. Identical sequence homology was found to *Arabidopsis thaliana* mitochondrial genome, part A. Identities (100%) to cytochrome C biogenesis. Accession no.1785673.

Sequence 253 from Patent W00055325
Identities =757/757 Expect = 0.0
Strand = Plus / Plus

```
Query:54     ctcaagagttcaaacggacagaggagagtcctgctaccgaaaaaaaagtgcataatattg 113
             ||||||||||||||||||||||||||||||||||||||||||||||||||||||||||||
Sbjct:15239 ctcaagagttcaaacggacagaggagagtcctgctaccgaaaaaaaagtgcataatattg 15298

Query:114    gattcaaacaaaggggatttattcacgaatacgatttctattgattgaaagctttcctat 173
             ||||||||||||||||||||||||||||||||||||||||||||||||||||||||||||
Sbjct:15299 gattcaaacaaaggggatttattcacgaatacgatttctattgattgaaagctttcctat 15358

Query:174    tactgatggcaaacgggcgagacggagaccgtcgaagaagtgccttgacgcgccgcagcc 233
             ||||||||||||||||||||||||||||||||||||||||||||||||||||||||||||
Sbjct:5359   tactgatggcaaacgggcgagacggagaccgtcgaagaagtgccttgacgcgccgcagcc 15418

Query:234    actactttgactccttttatgcaattatgaactccacggaactttctcgattccaacgca 293
             ||||||||||||||||||||||||||||||||||||||||||||||||||||||||||||
Sbjct:15419 actactttgactccttttatgcaattatgaactccacggaactttctcgattccaacgca 15478

Query:294    acttatccttttggagctgacgtaacaaactaggcgagcctcccaacgaagccaacataa 353
             ||||||||||||||||||||||||||||||||||||||||||||||||||||||||||||
Sbjct:15479 acttatccttttggagctgacgtaacaaactaggcgagcctcccaacgaagccaacataa 15538

Query:354    atcctatccgaataaaaaaaataaaaggcagtttcattatggtggtataccaacctcctg 413
             ||||||||||||||||||||||||||||||||||||||||||||||||||||||||||||
Sbjct:15539 atcctatccgaataaaaaaaataaaaggcagtttcattatggtggtataccaacctcctg 15598

Query:414    ttctggaacttccagttccaatcgaagcatatagatccgtaaatagatttgtatgtatag 473
             ||||||||||||||||||||||||||||||||||||||||||||||||||||||||||||
Sbjct:15599 ttctggaacttccagttccaatcgaagcatatagatccgtaaatagatttgtatgtatag 15658

Query:474    ccacttcagccgtgctcgtcctttctcgaaagtatcttttttctgggaacatggttaacc 533
             ||||||||||||||||||||||||||||||||||||||||||||||||||||||||||||
Sbjct:15659 ccacttcagccgtgctcgtcctttctcgaaagtatcttttttctgggaacatggttaacc 15718

Query:534    aaaaattattatgtttgcgattcttcatccaccaatgcagaaaatgctcaagttttccat 593
             ||||||||||||||||||||||||||||||||||||||||||||||||||||||||||||
Sbjct:15719 aaaaattattatgtttgcgattcttcatccaccaatgcagaaaatgctcaagttttccat 15778

Query:594    tcttatatgaggccggaaagtttattagcaagaggtcggcatgaagtgattcatcatgct 653
             ||||||||||||||||||||||||||||||||||||||||||||||||||||||||||||
Sbjct:15779 tcttatatgaggccggaaagtttattagcaagaggtcggcatgaagtgattcatcatgct 15838

Query:654    caaacatgagccgatcgttcgttagggacggtttatagatcatcaaattcccacaaatgg 713
             ||||||||||||||||||||||||||||||||||||||||||||||||||||||||||||
Sbjct:15839 caaacatgagccgatcgttcgttagggacggtttatagatcatcaaattcccacaaatgg 15898

Query:714    aatgaaaagtgggtccatgtaaatgatcgagacctcgcaaacaacaacgttccttcccca 773
             ||||||||||||||||||||||||||||||||||||||||||||||||||||||||||||
Sbjct:15899 aatgaaaagtgggtccatgtaaatgatcgagacctcgcaaacaacaacgttccttcccca 15958

Query:774    tatggagttcgtaacccaaaggcaatcgttgagtt 811
             ||||||||||||||||||||||||||||||||||
Sbjct:15959 tatggagttcgtaacccaaaggcaatcgttgagtt 15992
```

Figure A1.13C. Blast Output of *AtT20D21.19* cDNA Search in the EMBL Database.

Blast output of T3 primer direction from the *AtT20D21.19* cDNA sequence interrogation EMBL database. Identical sequence homology was found to *Arabidopsis thaliana* sequence 253 from Patent W00055325 identities (100%). Accession No. 20198270

```
>gi|23387388|emb|AX506151.1|    Sequence 846 from Patent WO0216655
```

Score = 168 bits (85), Expect = 2e-40
Identities = 143/161 (89%), Gaps = 1/161 (0%)
Strand = Plus / Plus

```
Query: 126 aagatccgcgaaatcttcatgcctgcactcagttccactatgaccgagggtaaaatcgtc 184
           ||||||| |||||||||||||||||||| |||||||| |||||||| || |||||||||
Sbjct: 112 aagatccgagaaatcttcatgcctgcactaagttccacgatgaccgaaggcaaaatcgtc 171


Query: 185 tcgtggatcaaatccgaaggcgacactctctccaaaggtgatagtgttgttgttgttgaa 244
           || ||| | ||||| |||||||| |  |||  |||||: || ||||||||||||||||||
Sbjct: 172 tcttgggttaaatcagaaggcgataaactcaacaaaggagagagtgttgttgttgttgaa 231


Query: 245 tcggataaagctgatatggatgttgagactttctatgatgg 285
           || |||||||||||| |||| |||||||||:|||||||||
Sbjct: 232 tctgataaagctgatatggatgttgagactttctatgatgg 272
```

Figure A1.13D Blast Output of *AtT20D21.19* cDNA T7 Primer Direction Search in the EMBLDatabase.

Blast output of T7 primer direction from *AtT20D21.19* cDNA (A) sequences interrogation the EMBL database. Significant sequence homology was found (89%) identity at the nucleotide level to a *Arabidopsis thaliana* At1g34430 mRNA, sequence coding for dihydrolipoamide S-transferase. Acc.No. 24111344

Score = 93.7 bits (47), Expect = 8e-19
Identities = 153/186 (82%), Gaps = 3/186 (1%)
Strand = Plus / Plus

```
Query: 177 aaatcgtctcgtggatcaaatccgaaggcgacactctctccaaaggtgatagtgttgttg 236
           ||||||| ||  |||||||| | |||||||| |  ||| |||| || || |||||||| |
Sbjct: 212 aaatcgtgtcatggatcaaaacagaaggcgagaaactcgccaagggagagagtgttgtgg 271


Query: 237 ttgttgaatcggataaagctgatatggatgttgagactttctatgatggaattcttgctg 296
           |||||||||| |||||||| |||||||||| || || || || ||||   ||||||||
Sbjct: 272 ttgttgaatctgataaagccgatatggatgtagaaacgttttacgatggttatcttgctg 331


Query: 297 ctattgt-ttc--tgaaggtgaaactgctccggttggtgctccgattggtttgctcgctg 353
           | |||||  ||   |||||||||| |||||||||||||| ||||||| ||| | ||||
Sbjct: 332 cgattgtcgtcggagaaggtgaaacagctccggttggtgctgcgattggattgttagctg 391


Query: 354 agactg 359
           ||||||
Sbjct: 392 agactg 397
```

Figure A1.13E Blast Output of At T20D21.19 cDNA T7 Primer Direction Search in The EMBL Database.

Blast output of T7 primer direction from *AtT20D21.19* cDNA (A) sequences interrogation the EMBL database. Partial homology found (82%) identity at the nucleotide level to *Arabidopsis thaliana* Sequence 846 from Patent WO0216655. Titled (stress-regulated genes of plants). Acc No. 23387388.

Score = 953 bits (480), Expect = 0.0
Identities = 582/616 (94%)
Strand = Plus / Plus

```
Query: 85    cccatctcatgtctccctcaaaataaagaccaaagattggtctatcatgcatagctcctc 144
             ||||||| |||||| ||||||||||||||||||||||||||||||||| ||||||||
Sbjct: 37169 cccatcttttgtctctctcaaaataaagaccaaagattggtctatcatgcaaagctcctc 37228

Query: 145   ttcactaacaaatctggtggccttctttggaaaacgggtgttggcgatgcattggtggag 204
             ||||| ||||||||||||||||||||||||||  |||||||||||||||||||||||||
Sbjct: 37229 ttcaccaacaaatctggtggccttctttggaaagagggtgttggcgatgcattggtggag 37288

Query: 205   gtatctaatcacgggattacggattgaagaactcttgctcttggttggtgagaagggctt 264
             || |||||||||||||||| ||||||||||||||||||||||||||| |||||||||||
Sbjct: 37289 gtgtctaatcacgggattatggattgaagaactcttgctcttggttggcgagaagggctt 37348

Query: 265   cggaccggctattgttttccaaagagatttcagctcttcttgatcatagtctcggcggat 324
             ||||||||||||||| ||||||||||||||||||||||| |||||||||| |||||||
Sbjct: 37349 cggaccggctattgtattccaaagagatttcagctcttcttaatcatagtcttggcggat 37408

Query: 325   tccttctccactaggaaacccgaaaatggaatcaagattgcaaatatcaagagtatactc 384
             |||||||||||| |||||||| |||||||||||||||| || ||||||||||||||||||
Sbjct: 37409 tccttctccacttggaaacccaaaaatggaatcaagatggcgaatatcaagagtatactc 37468

Query: 385   gacatccctaactttgaaagttatgtaaccaagacctcctctctcctctctctccgaatc 444
             |||||||||||||||||||||||||||||||||||||||||| |||||||| ||||||||
Sbjct: 37469 gacatccctaactttgaaagttatgtaaccaagacctcctatctcctctttctccgaatc 37528

Query: 445   atcaacacaaaaatgaaccttgagggttgcaaggagttggcagctctcctatttgtatcc 504
             ||||||||||||||||||||||||||||||||||||||||||||||||||||||||||||
Sbjct: 37529 atcaacacaaaaatgaaccttgagggttgcaaggagttggcagctctcctatttgtatcc 37588

Query: 505   cccacattggcagctcatgaatgttgcaagattggccaattccatcaagtattccatatc 564
             ||||||||||||||||||||||||||||||||||||||||||||||||||||||||||||
Sbjct: 37589 cccacattggcagctcatgaatgttgcaagattggccaattccatcaagtattccatatc 37648

Query: 565   accacaaataccaagctcttgcatcgtttccttatgagggtatctagttccctcaaacttt 624
             ||||||||||||||||||||||||||||||||||||||||||||||||||||||||||||
Sbjct: 37649 accacaaataccaagctcttgcatcgtttccttatgagggtatctagttccctcaaacttt 37708

Query: 625   caactccttcaagtattgatagtactcgctcaggattggctctctcttcctccttggccg 684
             ||||||||||||||||||||||||||||||||||||||||||||||||||||||||||||
Sbjct: 37709 caactccttcaagtattgatagtactcgctcaggattggctctctcttcctccttggccg 37768

Query: 685   gtttcttctcccaac 700
             |||||||||||||||
Sbjct: 37769 gtttcttctcccaac 37784
```

Figure A1.14 Blast Output of *At* T20D21.19 (B) cDNA Search in EMBL Database.

Blast output from the *At* T20D21.19 (B) cDNA sequences interrogation EMBL database. Significant sequence homology was found (94%) to *Arabidopsis* clone T22B15 gene *At* T22B15.12 similar to unknown protein. Accession no.8051670.

Appendix 2:

BLAST Output of DDRT-PCR cDNA Fragments

Score = 381 bits (192), Expect = e-104
Identities = 198/200 (99%)
Strand = Plus / Minus

```
Query:1      tgatctatctcaccagtaaagtttaataaccgagagattgttgcattacaaaacatatgt 60
             ||||||||||||||||||| ||||||||||||||||||||||||||||||||||||||||
Sbjct:60381  tgatctatctcaccagtagagtttaataaccgagagattgttgcattacaaaacatatgt 60322

Query:61     tacatattcccaaaacataatattttctggtttatatcgatcactcatcgtttgtctcaa 120
             ||||||||||||||||||||||||||||||||||||||||||||||||||||||||||||
Sbjct:60321  tacatattcccaaaacataatattttctggtttatatcgatcactcatcgtttgtctcaa 60262

Query:121    gggctgattgtaatacttcttctagtaacttttccgcggctgtaaactgtcttttcttgt 180
             ||||||||||||||||||||||||||||||||||||||||||||||||||||||||||||
Sbjct:60261  gggctgattgtaatacttcttctagtaacttttccgcggctgtaaactgtcttttcttgt 60202

Query:181    cttcgattgctagtgaagct  200
             |||||||||||||| ||||
Sbjct:60201  cttcgattgctagtgcagct  60182
```

Figure A2.1 Blast Output of a *AtT4A* cDNA Search in the EMBL Database.

Blast output from the *AtT4A* partial-length cDNA sequences interrogation the EMBL database. Nearly identical sequence homology was found at the cDNA level (99%) to Arabidopsis gene coding for un-known protein AT2941/F13H10.10.

Score= 101 bits (51) , Expect =1e-20
Identities = 51/51 (100%)
Strand = Plus/Minus

```
Query:1      tgcatgctcgagcggccgccagtgtgatggatatctgcagaattcgcccttt   51
             |||||||||||||||||||||||||||||||||||||||||||||||||||
Sbjct:4474   tgcatgctcgagcggccgccagtgtgatggatatctgcagaattcgcccttt   4524
```

Figure A2.2. Blast Output of a *AtT2C* cDNA Search in the EMBL Database.

Blast output from the *At2C* DD-PCR cDNA sequences interrogation the EMBL database. Identical sequence homology was found (100%) to *Arabidopsis thaliana* gene coding for hypothetical protein; 557-2776" /protein_id =AAG51320.1.

Score = 470 bits (237), Expect = e-131
Identities = 237/237 (100%)
Strand = Plus / Minus

```
Query:304   agcttggcgtaatcatggtcatagctgtttcctgtgtgaaattgttatccgctcacaatt  363
            ||||||||||||||||||||||||||||||||||||||||||||||||||||||||||||
Sbjct:504   agcttggcgtaatcatggtcatagctgtttcctgtgtgaaattgttatccgctcacaatt  445

Query:364   ccacacaacatacgagccggaagcataaagtgtaaagcctggggtgcctaatgagtgagc  423
            ||||||||||||||||||||||||||||||||||||||||||||||||||||||||||||
Sbjct:444   ccacacaacatacgagccggaagcataaagtgtaaagcctggggtgcctaatgagtgagc  385

Query:424   taactcacattaattgcgttgcgctcactgcccgctttccagtcgggaaacctgtcgtgc  483
            ||||||||||||||||||||||||||||||||||||||||||||||||||||||||||||
Sbjct:384   taactcacattaattgcgttgcgctcactgcccgctttccagtcgggaaacctgtcgtgc  325

Query:484   cagctgcattaatgaatcggccaacgcgcggggagaggcggtttgcgtattgggcgc     540
            ||||||||||||||||||||||||||||||||||||||||||||||||||||||||
Sbjct:324   cagctgcattaatgaatcggccaacgcgcggggagaggcggtttgcgtattgggcgc     268
```

FigureA2.3. Blast Output of *AtT4C* DD-PCR cDNA Clone Search in the EMBL Database.

Blast output from the *AtT4C* DD-PCR cDNA clone sequence interrogation the EMBL database. Identical sequence homology was found (100%) to *Arabidopsis thaliana* mRNA for mitochondrial F1 ATP synthase beta. Accession No. 17939848.

Sequence 208 from Patent W00055325
Score = 412 bits (208), Expect = e-115
Identities = 208/208 (100%)
Strand = Plus / Plus

```
Query: 1      agcttggcgtaatcatggtcatagctgtttcctgtgtgaaattgttatccgctcacaatt 60
              ||||||||||||||||||||||||||||||||||||||||||||||||||||||||||||
Sbjct: 43476 agcttggcgtaatcatggtcatagctgtttcctgtgtgaaattgttatccgctcacaatt 43535

Query: 61     ccacacaacatacgagccggaagcataaagtgtaaagcctggggtgcctaatgagtgagc 120
              ||||||||||||||||||||||||||||||||||||||||||||||||||||||||||||
Sbjct: 43536 ccacacaacatacgagccggaagcataaagtgtaaagcctggggtgcctaatgagtgagc 43595

Query: 121    taactcacattaattgcgttgcgctcactgcccgctttccagtcgggaaacctgtcgtgc 180
              ||||||||||||||||||||||||||||||||||||||||||||||||||||||||||||
Sbjct: 43596 taactcacattaattgcgttgcgctcactgcccgctttccagtcgggaaacctgtcgtgc 43655

Query: 181    cagctgcattaatgaatcggccaacgcg 208
              ||||||||||||||||||||||||||||
Sbjct: 43656 cagctgcattaatgaatcggccaacgcg 43683
```

Figure A2.4 Blast Output of *At T4C* DD-PCR cDNA Clone Search in the EMBL Database.

Blast output from the *AtT4C* DD-PCR cDNA clone sequence interrogation the EMBL database. Identical sequence homology was found (100%) to *Arabidopsis thaliana* Sequence 208 from Patent W00055325. Accession No.12311580.

Stress-resistance and retarded aging in plant
Score = 129 bits (65), Expect = 4e-30
Identities = 107/113 (94%), Gaps = 6/113 (5%)
Strand = Plus / Minus

```
Query: 8   cgtaatcatggtcatagctgtttcctgtgt-gaaattgttatccgctcacaattccacac 66
           ||||||||||| ||||||||||||||||||| ||||||||||| |||||||||||||||
Sbjct: 108 cgtaatcatg-tcatagctgtttcctgtgtngaaattgttatc-gctcacaattccacac 51


Query: 67  aacatacgagccggaagcataaagtgtaaagcctggggtgcctaatgagtgag 119
           |||||||||| |||||||||||||||||||| |||||||| ||||||||||||
Sbjct: 50  aacatacgag-cggaagcataaagtgtaaag-ctggggtg-ctaatgagtgag 102
```

Figure A2.5 Blast Output of a *AtT4C* T7 cDNA Search in the EMBL Database.

Blast output from the *AtT4C* T7 DD-PCR cDNA sequences interrogation the EMBL database. Significant sequence homology was found at the DNA level (94%) coding for stress-resistance and retarded aging in plant (Patent: JP 2001512027-A 2 21). Accession No. 22626544.

Sequence 196 from Patent W00055325
Score = 412 bits (208), Expect = e-115
Identities = 208/208 (100%)
Strand = Plus / Minus

```
Query: 1      agcttggcgtaatcatggtcatagctgtttcctgtgtgaaattgttatccgctcacaatt 60
              ||||||||||||||||||||||||||||||||||||||||||||||||||||||||||||
Sbjct: 27214  agcttggcgtaatcatggtcatagctgtttcctgtgtgaaattgttatccgctcacaatt 27155

Query: 61     ccacacaacatacgagccggaagcataaagtgtaaagcctggggtgcctaatgagtgagc 120
              ||||||||||||||||||||||||||||||||||||||||||||||||||||||||||||
Sbjct: 27154  ccacacaacatacgagccggaagcataaagtgtaaagcctggggtgcctaatgagtgagc 27095

Query: 121    taactcacattaattgcgttgcgctcactgcccgctttccagtcgggaaacctgtcgtgc 180
              ||||||||||||||||||||||||||||||||||||||||||||||||||||||||||||
Sbjct: 27094  taactcacattaattgcgttgcgctcactgcccgctttccagtcgggaaacctgtcgtgc 27035

Query: 181    cagctgcattaatgaatcggccaacgcg 208
              ||||||||||||||||||||||||||||
Sbjct: 27034  cagctgcattaatgaatcggccaacgcg 27007
```

Figure A2.6 Blast Output of *AtT4C* DD-PCR cDNA Clone Search in the EMBL Database.

Blast output from the *AtT4A* DD-PCR cDNA clone sequence interrogation the EMBL database. Identical sequence homology was found (100%) to *Arabidopsis thaliana* Sequence 196 Patent W00055325. Accession No.12311568.

Sequence 191 from Patent W00055325
Score = 412 bits (208), Expect = e-115
Identities = 208/208 (100%)
Strand = Plus / Minus

```
Query: 1     agcttggcgtaatcatggtcatagctgtttcctgtgtgaaattgttatccgctcacaatt 60
              ||||||||||||||||||||||||||||||||||||||||||||||||||||||||||||
Sbjct: 38051 agcttggcgtaatcatggtcatagctgtttcctgtgtgaaattgttatccgctcacaatt 37992

Query: 61    ccacacaacatacgagccggaagcataaagtgtaaagcctggggtgcctaatgagtgagc 120
              ||||||||||||||||||||||||||||||||||||||||||||||||||||||||||||
Sbjct: 37991 ccacacaacatacgagccggaagcataaagtgtaaagcctggggtgcctaatgagtgagc 37932

Query: 121   taactcacattaattgcgttgcgctcactgcccgctttccagtcgggaaacctgtcgtgc 180
              ||||||||||||||||||||||||||||||||||||||||||||||||||||||||||||
Sbjct: 37931 taactcacattaattgcgttgcgctcactgcccgctttccagtcgggaaacctgtcgtgc 37872

Query: 181   cagctgcattaatgaatcggccaacgcg 208
              ||||||||||||||||||||||||||||
Sbjct: 37871 cagctgcattaatgaatcggccaacgcg 37844
```

Figure A2.7 Blast Output of *AtT4C* DD-PCR cDNA Clone Search in the EMBL Database.

Blast output from the *AtT4A* DD-PCR cDNA clone sequence interrogation the EMBL database. Identical sequence homology was found (100%) to *Arabidopsis thaliana* Sequence 191 Patent W00055325. Accession No.12311563.

References

Allen, G.J., Wyn Jones, R. G. and Leigh, R.A. (1995). Sodium transport measured in plasma membrane vesicles isolated from wheat genotypes with different K^+/Na^+ discrimination traits. *Plant. Cell Environ.,* **18**: 105-115.

Allen R. D., Webb. R. P., and Schake, S. A. (1997). Use of transgenic plants to study antioxidant defenses. *Free Radic. Biol. Med.,*. **23**: 473-479.

Al-Khatib, M., McNeilly, T., and Collin, J. C. (1993). The potential of selection and breeding for improved salt tolerance in Lucerne *(Mediago sativa L). Euphgtica,* **65**:43.

Amtmann, A., and Sanders, D. (1999). Mechanism of Na^+ uptake by plant cells. *Advances in Potanical Research.* **29**: 76-112.

Amtmann, A., Fischer, M., Marsh, E. L., Stefanovic, A., Sanders, D., and Schachtman, D. P. (2001). The wheat cDNA LCT1 generates hypersensitivity to sodium in a salt-sensitive yeast strain. *Plant physiol.* **126**: 1061-1071.

Anderson, J. A., Huprikar, S. S.,Kochian, L. V., Lucas, W. J. and Gaber, R.F. (1992). Function expression of probable *Arabidopsis thaliana* potassium channel in *Saccharomyces cerevisiae. Proc. Natl. Acad. Sci. USA.,* **89**: 3736-3774.

Apse, M. P., Aharon G. S., Snedden, W. A., Blumwld, E. (1999). Salt tolerance conferred by overexpression of a vacuolar Na^+/H^+ antiport in Arabidopsis. *Science* , **285**: 1256-1258.

Apse, M. P., Aharon, G. S., Snedden, W. A. (1998). Cloning and characterization of plant sodium/ proton antiporters. In: *Abstracts of the 11th International Workshop on Plant Membrane Biology. The society of Experimental Biology, 84.*

Ashraf, M. (1994). Breeding for salinity tolerance in plants. *Crit. Rev. In Plant Sci.* **31:**17-42.

Assmann, S. M., and Haubrick, L. (1996). Transport proteins of the plant plasma membrane. *Curr. Opin.: Cell Biol.,* **8**: 458-467.

Axelsen, K. B., and Palmgren, M. G. (2001). Inventory of the superfamily of P-type ion pumps in *Arabidopsis. Plant Physiol.,* **126**: 696-706

Balzi, E., Wang, M., Letermes, S., VanDyck, L., and Goffeau, A. (1994). PDR5, a novel yeast multidrug resistance conferring transporter controlled by the transcription regulator PDR1. *J. Biol. Chem.,* **269(3)**: 2206-2214.

Banuelos, M. A., Klein, R. D., Alexander-Bowman, S. J., Rodriguez-Navaro. A. (1995b). A potassium transporter of the yeast Schwanniomyces occidentalis homologous to the Kup system of *Escherichia coli* has a high concentrative capacity. *EMBO. J.* **14(13):** 3021-3027.

Banuelos, M. A., Quintero, F. J., and Rodriguez-Navarro, A. (1995a). Function expression of the *ENA1(PMR2)*-ATPase of *Saccharomyces cerevisiae* in *Schizosaccharomyces pombe. Biochim. Biophys. Acta.*, **129**: 233-238.

Barkla, B. J., and Pantoja, O. (1996). Physiology of ion transport across the tonoplast of higher plants. *Annu. Rev. Plant Physiol. Plant Mol. Biol.*, **47**: 159-184.

Barkla, B. J., Zingarelli, L., Blumwald, E., Smith, J. A. C. (1995). Tonoplast Na^+ /H^+ antiporter activity and its energization by the vacuolar H^+-ATPase in the halophytic plant *Mesembryanthemum crystallinum L. Plant Phsiol.*, **109**: 549-556.

Barkla, B. J., and Blumwald, E. (1992). *In research photosynthesis, Vol. IV*, 219-226. *Kluwer, Dordrecht.*

Battey, N. H., James, N. C., Greenland A. J., and Brownlee, C. (1999). Exocytosis and Endocytosis. *The Plant Cell.*, **11**: 643-659

Becker,D. Dreyer, I., Hoth, S., Reid, J., D. Buch, H., Lehnen, M. Palme, K., and Hedrich, R. (1996). Change in voltage activation, Ca^{2+} sensitivity, and ion permeability in H5 mutant of the plant K^+ channel *KAT1. Proc. Natl. Acadi. Sci. UAS.*, **93**:8123 8128.

Benito, B., Quintero, F. J., and Rodriguez-Navarro, A. (1997). Over-expression of sodium ATPase of *Saccharomyces cerevisiae*: Condition for phosphorylation from ATP and Pi. Biochem. Biophys. Acta., **1328**: 124-225.

Berkelman, T., Houtchens, K. A., and DuPont, F. M. (1994). Two cDNA clones encoding isoforms of the B sub-unit of the vacuolar ATPase from barley roots. *Plant Physiol.*, **104**: 287-288.

Bethke, P. C., and Jones, R. L. (2000). Vacuoles and prevacuolar compartments. *Curr. Opin. Plant. Biol.*, **3(6):** 469-75.

Blatt M.R., Leyman B., Geelen D. (1999) Molecular events of vesicle trafficking and control by SNARE proteins in plants. *New Phytol*, **144**: 389-418

Blum, A. (1988). Plant breeding for stress environments. *CRC Press, Boca Raton.*

Blumwald, E., Aharon, G. S., and Apse, P. M. (2000). Sodium transport in plant cells. *Biochimica et Biophysica Acta.*, **1465**: 140-151.

Bulmwald, E., and poole, R. J. (1985). Plant physiology. 78:163-167.

Blumwald, E., and Poole, R. J. (1987). Salt-tolerance in suspension culture of sugar beet. Introduction of Na^+ /H^+ antiporter activity at the tonoplast by growth in salt. *Plant Physiol.*, **83**: 884-887.

Bonza, M.C, Morandini, P, Luohi,L., Geisler, M, Palmgren, M. G., De michelis, M. I. (2000). At-ACA8 encodes a plasma membrane-localized calcium-ATPase of *Arabidopsis* with a calmodulin-binding domain at the N terminus. *Plant Physiol.* **123(4):** 1495-506.

Boutry, M., Michelet, B., and Goffeau, A. (1989). Molecular cloning of family plant genes encoding protein homologous to plasma membrane H^+-translocating ATPase. *Biochem. Biophys. Res. Commun. (by Acad. Press, Inc).*, **162 (2):** 567-574.

Braun, Y., Hassidim, M., Lerner, H., and Renhold, L. (1986). Studies on H^+-translocating ATPase in plant of varying resistance to salinity. I. Salinity during growth modulates the proton pump in the halophyte *Atriplex nummularia. Plant Physiol.*, **81**: 1050-1056.

Butt, A. D., Blatt, M. R., and Ainsworth, C. C. (1997). Expression, evolution and genomic complexity of potassium ion channel genes of *Arabidopsis thaliana. J. Plant physiol.*, **150**:652-660.

Cao, X. Rogers, W. S., Butler, J., Beevers, L., and Rogers, J. C. (2000). Structural Requirements for Ligand Binding by a Probable Plant Vacuolar Sorting receptor. The Plant Cell. **12**, 493-506.

Cao, Y., Ward, J. M., Kelly, W. B., Ichida A. M., Gaber, R. F., Anderson, J.A., Uozumi, N., Schroeder, J. L., & Crawford N. m. (1995). Multiple gene tissue specificity, and expression-dependent modulation contribute to the function discovery of potassium channels in *Arabidopsis thaliana. Plant Physiol.*, **109**:1093-1106.

Carter, V. G., and Dale, T. (1974). Topsoil and civilization. *University of Oklahoma. Press. Norman.*

Cheeseman, J. M. (1982). Pump leak sodium fluxes in low salt corn roots. *J. Membr. Biol.*, **70**: 157- 164.

Chrispeels, M. J., Crawford, N. M., and Schroeder, J. I. (1999). Protein for transport of water and mineral nutrients across the membranes of plant cells. *Plant Cell.*, **11**: 661-676.

Cole, S. P. C., *et al.* (1992). Over-expression of a transporter gene in a multidrug-resistant human lung cancer cell line. *Science*, **258**, 150-1654.

Colombo, R., Bonelli, A. and Lado, P. (1979). Promoting effect of fusicoccin on Na^+ efflux in barley roots: evidence for a Na^+/H^+ antiporter. *Plant Cell Environ.*, 2:281-285.

Conway, E. J., Ryan, H., and Carton, E. (1954). Active transport of sodium ions from the yeast cell. *Biochem. J.*, **58**: 88-127.

Cooper, S., Lerner, H. R., and Reinhold, L. (1990). The mechanism of potassium movement across the liposomal membrnae. Biochem. Biophys. Res. Commun., **173(3):** 1008-1012.

Covic, L., and Lew, R. R. (1996). *Arabidopsis thaliana* cDNA isolated by functional complementation shows homology to serine/threonine protein kinases. *Bichim. Biophys. Acta.* **1305**: 125-129.

Cuarteo, J., and Fernandez-Munoz, R. (1999). Tomato and salinity *Sci. Hortic.* **78**: 83-125.

Czempinski, K. Zimmermann, S., Ehrhardt, T., Müller Röber, B. (1997). New structure and function in plant K^+ channels: KCO1, an inward rectifier with a steep Ca^{2+}-dependency. *EMBO, J.*, **16**:2565-2575.

Czempinski, K., Gaedeke, N., Zimmermann, S., & Müller Röber. (1999). Molecular mechanisms and regulation of plant ion chnnels. *J. Exp. Bot.*, **50**:955-966.

Davenport, R., and Tester, M. (1997). A Na^+ permeable channel from the plasma membrane of wheat root may be major route of toxic Na^+ uptake. *Society for Experimental Biology, Plant Transporter Group workshop. University of Glasgow.*

DeWitt, N. D. (1994). Epitope tagging reporter gene studies identify an *Arabidopsis* plasma membrane proton pump specific for phloem companion cells. *PhD dissertation. (Madison, W: University of Wisconsin).*

DeWitt, N. D. and Sussman, R. M. (1995). Immunocytological location of an epitope-tagged plasma membrane proton pump (H^+-ATPase) in phloem companion cells. *The Plant Cell*, **7**: 2053-2067.

DeWitt, N. D., Harper, J. F., and Sussman, R. M. (1991). Evidence for a plasma membrane proton pump in phloem cells of higher plants. *Plant J.*, **1**: 121-128.

Dreyer, I., Horeau, C., Lemaillet, G., Zimmermann, S., Bush, D. R., Rodriguez-Navarro, A., Schachtman, D. P., Spalding, E. P., Sentenac, H., and Gaber, F. R. (1999). Identification and characterization of plant transporters using heterologous expression systems. *J. Exp. Bot.* **50**: 1073-1087.

Dryer, I. Becker, D., Bregante, M., Ganbale, F., Lehnen, M. Palme, K., and Hedrich, R. (1998). Single mutations strongly alter the K^+ selective pore of the Kin channel *KAT1*. *FEBS. Letters*, **430**:370-376.

Dudler, R., and Hertig, C. (1992). Structure of an mdr-like gene from *Arabidopsis thaliana*. Evolutionary implication. *J. Biol. Chem.*, **267(9):** 5882-5888.

DuPont, F. M. (1992). Salt-induced changes in ion transport; regulation of primary pumps and secondary transports, In: Transport and receptor proteins of plant membranes. (Cook, D. T., and Clarks D. T., eds). 91-100, *New York; Pleum Press.*

Ehrlich, P. R. (1975). The Population Bomb (*Ameron, Mattituck NY*).

Engelman, D. M., Steitz, T. A.,and Goldman, A. (1986). *Annu.Rev.Biophys.Biophy. Chem* .,15,321.

Epstein, E., Rains, D. W., and Elzam, O. E. (1963). Resolution of dual mechanisms of potassium absorption by barley roots. *Proc. Natl. Acad. Sci. USA.*, **49**:684-692.

Epstein, E. (1966). Dual pattern of ion absorption by plant cells and by plants. *Nature*, **212**: 1324-1327.

Epstein, E, (1973). Mechanism of ion transport through plant cell membranes. *Int. Rev. Cytol.*, **34**:123-167.

Epstein, E. (1972). Mineral nutrition of plants: Principles and perspective. (*New York, John Wiley and Sons*).

Evans, L. H. (1998). Feeding the 10 billion. In: Plant and population growth. *Cambridge Univ. press, London.*

Ewing, N. N., Wimmers, L. E., Meyer, D. J., Chetelate, R. T., and Bennett, A. B. (1990). Molecular cloning of tomato plasma membrane H^+-ATPase. *Plant Physiol.*, **94**: 1874-1881.

Ewing, N. N., and Bennett, A. B. (1994). Assessment of the number and expression of p-type H^+-ATPase gene in tomato. *Plant Physiol.*, **106**: 547-557.

Farooq, S. (2001). Salt tolerance in *Aegilops* Species: A success story from research and production to large-scale utilization of salt tolerant wheats. (Biosalin Agriculture in the GCC countries), pp.1-23.

Scott. J., Shirley, R., Liu, L. I., Gloden, A., and Kellely, J. M. (1995). Whole genome random sequencing and assembly of *Haemophilus influenzae Rd. Sci.* **269**: 496-512.

Flowers, A. and Yeo, A. (1995). Breeding for salinity stress resistance: Where next?. *Aust. J. palnt physiol.* **22**: 875-884.

Flowers, T. J., Troke, P. F., and Yeo, A. R. (1977). The mechanism of salt tolerance in halophytes. *Ann. Rev. Plant Physiol.*, **28**:89-121.

Food and Agricultural Organization of the United Nations. (1995). *Dimension of Need: An Atlas of Food and Agriculture* (Food and Agriculture Organization, Rome).

Formmer, W. B., ludewig, U., Rentsch, D. (1999). Taking transgenic plants with a pinch of salt. *Science*, **285**: 1222-1223.

Formmer, W. B., and Ninnemann, O. (1995). Heterologous expression of genes in bacterial, fungi, animal, and plant cells. *Annu. Rev. Plant Physiol. Plant Mol. Biol.*, **46**: 419-444..

Fu, H., Luan, S. (1998). AT KUP1: A dual affinity K^+ transporter from *Arabidopsis*. *Plant Cell*. **10**: 63-67.

Fukuda, A., Nakamura, A., and Tanaka, Y. (1999). Molecular cloning and expression of the Na^+ /H^+ exchanger gene in *Oryzxa Sativa Biochimica. et. Biophysica. Acta.*, **1446**: 149-155.

Gaber, R. F., Styles, C. A. and Fink, G. R. (1988). *trk1* encoded plasma membrane protein required for high-affinity potassium transport in *Saccharomyces cerevisiae. Mol. Cell, Biol.*, **8**: 2848-3859.

Gaedke, N., Klein, M., Kolukisaoglu, U., Forestier, C., Muller, A., Ansorge, M., Becker, D., Mamnum, Y., Kuchler, K., schulz, B., Mueller-roeber, B., and Martinoia, E. (2001). The *Arabidopsis thaliana* ABC transporter At MRP5 controls root development and stomata movement. *EMBO J.* **20**: 1875-1887.

Garicadeblas, B., Rubio, F., Quintero, F. J., Banuelous, M. A., Haro. R., and Rodriguez-Navarro, A. (1993). Differential expression of two gene encoding an isoform of the ATPase involved in sodium efflux in *Saccharomyces cerevisiae. Mol. Gen. Genet.*, **236**: 363-368.

Gassmann, W., and Schroeder, J. I. (1994). Inward rectifying K^+ channels in root hair of wheat. *Plant Physiol.*, **105**:1399-1408.

Gaxiola, R. A., Rao, R., Sherman, A., Grisafi, P., Alper, S. L., Fink, G. R. (1999). The *Arabidopsis thaliana* proton transporters, *AtNhx1* and *Avp1*, can function in

cation detoxification in yeast. *Proc. Natl. Acad. Sci. U. S. A.*, **96 (4):** 1480-1485.

Gaxiola, R. A., Yuan, D. S., Klausner, R. D., and Fink, G. R. (1998). The yeast ClC chloride channel functions in action homeostasis. *Proc. Natl. Acad. Sci. U. S. A.* **95(7)**: 4046-4050.

Gaymard, F., Pilot, G., Lacombe, B., Bouchez, D., Bruneau, D., Boucherez, J., Michaux-Ferriere, N., Thibaud. J-B., and Sentenac, H. (1998). Identification and disruption of plant shaker-like outward channel involved in K^+ release into the xylem sap. *Cell*, **94**:647-655.

Geisler, M., Axelsen, k. B., harper, J.F., Palmgren, M. G. (2000a). Molecular aspects of higher plant P-type Ca2+-ATPases. *Biochim. Biophys. Acta.* **1465**:52-78.

Geisler, M., Axelsen, k. B., harper, J.F., Palmgren, M. G. (2000 b). Molecular aspects of higher plant p-type $Ca2^+$-ATPase. *Biochim. Biophys. Acta* **1465:**52-78.

Glass, A. D. M (1983). Regulation of ion trasport. *Ann. Rev. plant physiol.* **34**: 851-864.

Glass, A. D. M. (1976). Regulation of potassium absorption in barley roots. An allosteric model. *Plant physiol.* **105**:1399-1408.

Glass, A. D. M. (1988). Plant nutrition: An introduction to current concepts. (*Boston, MA: Jones and Bartlett*).

Glenn, E. P., and Brown, J. (1999). Salt tolerance and crop potential of halophytes. *Critical Reviews in Plant Sciences*, **18(2):** 227-255.

Gogarten, J. P., Fichmann, J., Braun, Y., Morgan, L., Styles, P (1992). The use of anti-sense mRNA to inhibit the tonoplast H^+-ATPase in carrot. *Plant Cell*, 4: 851-864.

Golldack, D.and Dietz, K.L. (2001). Salt-induced expression of the vacuolar H^+-ATPase in the common ice plant is developmentally controlled and tissue specific. *Plant, Physiol.* **125(4):**1643-54.

Gomes, E. jakobson, M. K., axelsen, K. B., geisler, M., Palmgren, M. g. (2000) Chilling tolerance in *Arabidopsis* involves ALA1, a member of a new family of putative aminophospholipid translocases. *Plant Cell.*, **12(12):** 2441-2454.

Gorham, J. (1992a). Salt tolerance of plants. *Sci Progress Oxford.* **76**:273-283.

Gorham, J., Forster, B..P., Budrewicz, E., Wyn Jones, R. G., Miller, T. E.,Law, C. N. (1986). Salt tolerance in *Triticeae*: solute accumulation and distribution in

an amphidiploid derived from *Triticeae aestivum cv. Chinese Spring and Thinopyrum bessarabicum. J. Epx. Botany,* **37**: 1435-1449.

Gorham, J., Wyn Jones, R. G. and Bristol, A. (1990). Partial characterization of the trait for enhanced K^+ /Na^+ discrimination in the D genome of wheat. Plant., 180: 590-597.

Gorham,, J. (1992b). Stress tolerance and mechanisms behind tolerance in barley. In: Proceedings of VI International Barley Genetic Symposium (L. Munck, ed), 1035-1049. Munksgaard Copenhagen. ISBN **87** (16): 19601-19605.

Gorham,J., Hardy, C., Wyn Jones, R. G., Joppa, L. R., and Law, C. N. (1987). Chromosomal location od a K^+/ Na^+ discrimination character in the D genome of weat. *Theoretical and Applied Genetics*, **74**: 584-588.

Grabarino, J., and DuPont, F. M. (1988). NaCl induces a Na^+ /H^+ antiporter in tonoplast vesicles from barley roots. *Plant Physiol.*, **86**: 231-236.

Grabarino, J., and DuPont, F. M. (1989). Rapid induction of Na^+ /H^+ exchange activity in barley root tonoplast. *Plant Physiol.*, **89**: 1-4.

Grattan, S. R., and Grieve, C. M. (1992). Mineral element acquisition and growth response of plants grown in saline environments. *Agrc. Ecosystem and Environment.* **38**:275- 300.

Greenway, H., and Munns, R. (1980). Mechanism of salt tolerance in non-halophytes. *Ann. Rev. Plant Physiol.*, **31**:149-190.

Hahlbrock, K. (1995). Gene activation by UV light, fungal elicitor or fungal

Halfter, U., Ishitani, M., and Zhu, J-K. (2000). The *Arabidopsis* SOS2 protein kinase phyically interacts with and is activated by the calcium-binding protein *SOS3. Proc. Natl. Acad. Sci. USA* ,**10**: 1073-1087.

Haro, R., Banuelos, M. A., Quintero, F. J., Rubio, F., and Rodriguez-Navarro, A. (1993). Genetic basis of sodium tolerance in yeast. A model for plants. *Physiol. Plant*, **89**: 868-874.

Haro, R., Garicadeblas, B., and Rodriguez-Navarro, A. (1991). A novel p-type ATPase from yeast involved in sodium transport. *FEBS Lett.*, **291**: 189-191.

Harper, J. F., Manney, L. and Sussman, M. (1994). Evidence for at least ten plasma membrane H^+-ATPase genes in *Arabidopsis* and complete genomic sequence of *AHA10* which is expressed primarily in developing seeds., *Mol. Gent.*, **244**: 572-287.

Harper, J. F., Surowy, T. K., and Sussman, M. R. (1989). Molecular cloning and sequencing of cDNA encoding the plasma membrane proton pump (ATPase) of *Arabidopsis* thaliana. *Proc .Natl. Acad. Sci. USA.*, **86**: 1234-1238.

Hartje, S., Zimmerman, S., Klonus, D., and Mueller-Roeber, B. (2000). Functional characterisation of LKT1, a K^+ uptake channel from tomato root hairs, and comparison with the closely related potato inwardly rectifying K^+ channel SKT1 after expression in *Xenopus* oocytes. Planta, 210(5): 723-731.

Hasegawa, P. M., Bressab, R. A., and Handa, A. K. (1980). Growth characteristics of NaCl selected and nonselected cells of *nicotiana tabacum L. Plant Cell Physiol.*, **21**: 1347-1355.

Hassidim, M., Braun, Y., Lerner, H. R. and Reinhold, L. (1990). Na^+ /H^+ antiport in root membrane vesicles isolated from the *Atriplex* and the glycophyte cotton. *Plant Physiol.*, **94:** 1795-1801.

Hawse, C., Crooks, K., Cloeman,J., Satiat-Jeunemaite, B. (1995). Endocytosis in plants: fact of artifact?. *Plant Cell Environ.*, **18:** 1245-1252..

Higgins, C. F., (1992). ABC transporter: from microorganism to man. *Annu. Rev. Cell Biol.*, **8**: 67-113.

Higgins, C. F., (1995). The ABC of channel regulation. *Cell*, **82**: 693-696.

Hoffman G. J. (1999). Water quality criteria for irrigation. *University of Nebraska, Institute of Agriculture and Natural Resource*,

Hoisington, D., Khairallah, M., Reeves, T., Ribaut, J-M., Skovmsam, B., Taba, S., and Warburton, M. (1999). Plant genetic resources: What can they contribute toward increased crop productivity?. *Proc. Natl. Acadi. Sci. USA.* **96:** 5937-5943.

Holstrom, K., Mäntylä, E., Welin, B., Manadal, A., and Palva E. T. (1996). Drought tolerance in tobacco. *Nature*, **379**:683-684.

Hui-Hua, FU. and Luan, S. (1998). Atkup1: A dual-affinity K^+ transporter from Arabidopsis. *Plant, Cell*, **10**:63-73.

Jacobson, T., and adams, R. M. (1958). Salt and silt in ancient Mesopotamian agriculture. *Sci*, **128**:1251-1258.

James, C. (1997). ISAAA Briefs No. 4 (International Service for the Acquisition of Agro-biotch Applications, Ithaca, NY), 31.

Jasinski, M., Stukkens, Y., Degand, H., Purnelle, B., Machannd-Bryanert, J., and Boudry, M. (2001). A plant plasma membrane ATP binding cassette-type

transporter is involved in antifungal terpenoid secretion. *Plant Cell.*, **13(5):** 1095-1097.

Jia, Z. P., McCullough, N., Martel, R. Hemmingsen, S., and Young, P. G. (1992). Gene amplification at a locus encoding a putative Na^+ /H^+ antiporter confers sodium and lithium tolerance in fission yeast. *EMBO J.*, **11(4)**: 1631-1640.

Jocoby, B. (1993). In handbook of plant crop stress. Vol. 1 (Pessaraki, M., ed), *Marcel Dekker. New York.*

Jones and Pollard, 1983 Effects of salt treatment and osmotic stress on V-ATPase and V-PPase in leaves of the halophyte Suaeda salsa.J Exp Bot. **52(365):**2355-65.

Kawamura, Y., Arakawa, K., Maeshima, M., and Yoshida, S. (2000). Tissue specificity of E subunit isoforms of plant vacuolar H+-ATPase and existence of isotype enzymes. *J. Biol. Chem.* **275**: 6515-6522.

Ketchum, k.A. and Slyman, C. W.. (1996). Isolation of an ion channel gene from *Arabidopsis thaliana* using the H5 signature sequence from voltage-dependent K^+ channels. FEBS Lett. **378(1):**19-26.

Kim, E. J., Kwak, J. M., Uozumi, N., and Schoeder, J. I. (1998). *AtKUP1*: An *Arabidopsis* gene encoding high-affinity potassium transport activity. *Plant Cell*, **10**: 51-62.

Kingbury R. W., and Epstein, E. (1984). *Crop Sci.* 24:310-315.

Kishore, G. M., and Shewmaker, C. (1999). Biotechnology: Enhancing human nutrition in developing and developed worlds. *Proc. Natl. Acad. Sci. UAS*, **96**:5968-5972.

Klein, M., Martinoia, E., Hoffmann-Thoma, G., and Weissenbock. (2000). A membrane-potential dependent, ABC-like transporter mediates the vacuolar uptake of rye flavone glucuronides. *Plant J.*, **21**: 289-304.

Klionsky, D. J., Herman, P. K., and Emr, S. D. (1990). The fungal vacuole: composition, fuction, and biogenesis. *Microbiol. Rev.*, **54**: 266-292.

Knight, H., Trewavas, A. J., and Knight, M. R. (1997). Calcium signalling in *Arabidopsis thaliana* responding to drought and salinity. *The Plant J.* **12 (5):** 1067-1078.

Ko, C. H., and Gaber, R. F. (1991). *trk1* and *trk2* encoded structurally related potassium ion transporters in *Saccharomyces cerevisiae*. *Mol. Cell. Biol.*, 11:4266-4273.

Kochian, L. V., and Lucas, W. J. (1988). Potassium transport in roots. *Adv. Bot. Res.*, **15**:93-178.

Kolaczkowski, A., Soumillion, J. P., Konings, W. N., and Goffeau, A. (1996). Anticancer drugs, ionophoric peptides, and steroids as substrates of the yeast multidrug transporter Pdr5P. *J. Biol. Chem.* **271(49)**: 31543 31548.

Lagarde, D., Basset, M., Lepetti, M., Conejero, G., Gaymard, F., Astruc, S., & Grignon, C. (1996). Tissue-specific expression of *Arabidopsis akt1* gene consistent with a role in K^+ nutrition. *Plant J.*, **9**:195-203.

Leonard, R. T.(1984). Membrane associated ATPase and nutrient absorption by roots. *In*: Advances in plant nutrition. (Tinker, P. B., Lauch, A. eds.), **1**: 209-240. *Praeger Scientific, New York.*

Leonhardt, N., Marin, E., Vavasseur, A and Forestier, C. (1997). Evidence for the existence of a sunfonylurea-receptor-like protein in plants: modulation of stomatal movements and guard cell potassium channels by sunfonylureas and potassium channel openers. *Proc. Natl. Acad. Sci. USA*, **94**: 14156-14161.

Leonhardt, N., Marin, E., Vavasseur, A and Forestier, C. (1999). ATP binding cassette modulators control abscisic acid-regulated slow anion channels in guard cells. *Plant Cell*, **11**: 1141-1152.

Lessani, H., and Marschner, H. (1978). Relation between salt tolerance and distance transport of sodium and chloride in various of crop species. *Aust. J. Plant Physol.*, **5**: 27.

Lewis, L. N. (1984). A vital resource in danger. *Calif. Agri.*, **38**:2.

Li, X, Perera, I. Y, Lin, S., Sze, H. (1999). Cloning and characterization of a genomic clone (AF153677) encoding a 16 Kda subunit c of vacuolar H^+-ATPase (Ava-p4) from *Arabidopsis thaliana* (PGR99-106). *Plant physiol.* 120:1205.

Liu, G., Sanchez-fernandez, R., li, Z-S., and Rea, P. A. (2001). Enhanced multispecifity of *Arabidopsis* vacuolar MRP-type ABC transporter, *AtMRP*. *J. Biol. Chem.*, **276(12)**: 8648-56.

Liu, J., and Zhu, J-K. (1997a). An *Arabidopsis* mutant that requires increased calcium for potassium nutrition and salt totolerance. *Proc. Natl. Sci USA*. **94**: 14960-149.

Liu, J., and Zhu, JK. (1997b). Proline accumulation and salt-stress-induced gene expression in a salt-hypersensitive mutant of *Arabidopsis*. *Plant physiol.*, **114**:591-596.

Liu, J., and Zhu, J-K. (1998). A calcium sensor homology required for plant salt tolerance. *Sci.*, **280**: 1943-1945.

Liu, J., Ishitani, M., Halfter,U., Kim, C. S., and Zhu, J-K. (2000). The *Arabidopsis thaliana SOS2* gene encodes a protein kinase that is required for salt tolerance. *Proc. Natl. Acad. Sci. USA.*, 97: 3730-3734.

Lou, H., Morsomme, P. and Boutry, M. (1999). The two major types of plant plasma membrane H^+-ATPase show different enzymatic properties and confer differential pH sensitivity of yeast growth. *Plant Physiol*, **119**: 627-634.

Low, P. S., and Chandra, S. (1994). Endocytosis in plants. *Annu. Rev. Plant Physiol. Plant Mol. Biol.* **43**:609-931.

Low, R. Rockel, B, Kirsch, M, Ratajczak, R, Luttge, R. (1996). Early salt stress effect on the differential expression of vacuolar H+-ATPase gene in roots ans leaves of *Mesembryanthemum crystallinum. Plant physiol.*, **110**:259-265.

Lukowitz, W., Mayer, U., and Jurgens, G. (1996). Cytokinasis in the *Arabidopsis* embryo involves the syntaxin-related KNOLLE gene product. *Cell*, **84**: 61-71.

Maathuis, F. J. M., and Sanders, D. (1996). Mechanisms of potassium absorption by higher plant roots. *Physiologia Plantarum.*, **96**: 158-168.

Malcom, C. V. (1982). Wheat belt salinity. *A Rev. of Salt Land Problem In South Western Australia. WA-Dep. Agric. Tech. Bul.*, **52**:65.

Maddok, S. E., Lancaster, V. A., Risiot, R., Franklin, J. (1983). J. Exp. Bot., **34**: 915-926.

Maeshima, M. (2000). Vacuolar H^+ -pyrophosphate. *Biochim. Biophys. Acta.*, **1465**: 37-51.

Malhotra, K. Foltz, L., Mahony, W. C.,Schueler, P. A. (1998). Interaction and effect of anneting temperature on primers used in differential display RT-PCR. *Nucleic Acid Research* , **26**: 854-856.

Malmstron, S., Askerlund, P. Palmgren, M. G. (1997). A calmodulin-stimulated Ca2+- ATPase from plant vacuolar membranes with a putative regulatory domain at its N-terminus. *FEBS Lett.*, **400**:324-3228.

Marshchner, H. (1986). Mineral nutrition of higher plants. *London. Academic press.*

Marshchner, H. (1995). Mineral nutrition of higher plants. 2^{nd} *edn London. Academic press.*

Martinoia, E., Grill, E., Tommasini, R., Kreuz, K., and Amerhein, N. (1993). ATP-dependent glutathione S-conjugate 'export' pump in the vacuolar membrane of plants. *Nature*, **364**: 247-249.

Marty, F., (1999). Plant vacuoles. *Plant Cell.*, **11**: 587-599.

Marty, F., and Douce, R. (1996). Ultrastructural and biochemical characterization of autophagy in higher plant cells subjected to carbon deprivation: Control by the supply of mitochondria with respiratory substrates. *J. Cell Biol.* **133**: 1251-1263.

Mass, E. V. (1987). Salt tolerance of plants *In* : *CRC Hand Book of Plant Sciences in agriculture.*, **2**: 57-75. (ed. B. R.Christie). *CRC Press Boca Rton.*

Mass, E. V., and Hoffman, G. J. (1977). Crop salt tolerant-current assessment. *J. Irrig. Drainage Dive. Am. Soc. Civ. Eng.*, 103-115.

Massoud, F. I. (1974). Salinity and alkalinity as soil degradation hazards. FAO/UNDP expert consultation on soil degradation, *FAO, Rome*, 21.

Matsumoto, H., and Chung, G. C. (1988). Increase in proto-transport activity of tonoplast as an adaptive reponse of barley root to NaCl stress. *Plant Cell Physiol.*, **29 (7)**: 1133-1140.

Matsuoka, K., Higuchi, T., Maeshima, M., Nakamura, K. (1997). A vacuolar type H^+ -ATPase in a non-vacuolar organelle is required for the sorting of sorting of soluble vacuolar protein precursors in tobacco cells. *Plant Cell*, **9**: 533-546.

May, M. j., Leaver, J. C. (1993). Oxidative stimulation of glutathione synthesis in Arabidopsis thaliana suspension culture. *Plant Physiol.* **103**:1621-627.

Mendoza I., Rubio, F., Rodriguez-Navarro, A., and Pardo, G, M. (1994). The protein phosphatase calcineurin is essential for NaCl tolerance of *Saccharomyces cerevisiae. J. Biol. Chem.*, 269(12): 8792-6.

Mennen, H. Jacob, B., and Marschner, H. (1990). Is sodium proton antiporter ubiquitous in plant cells?. J. *Plant Physiol.*, **137**: 180-183.

Michelet, B. Lukaszewicz, M., Dupriez, V., and Boutry, M. (1994). A plasma membrane proton-ATPase gene is regulated by development and environment, shows signs of a translational regulation. *Plant Cel*, **6**: 1375-1389.

Miller, R. H. (1980). Amitosis and endocytogenesis in fruit *Malus sylvestris. Ann. Bot.* **46**:567-571.

Miyahara, K., Mizunuma, M., Hirata, D, Tsuchiya E., and Miyakwa, T. (1996). The involvement of the *Saccharomyces cerevisiae* multidrug resistance transporters Pdr5p and Snq2p in cation resistance. *FEBS Letters*, **399**: 317-320.

Moller, J.V., Juul, B, Le Maire, M. (1996). Structural organization , ion transport, and energy transduction of p-type ATPases.*Biochim. Biophys. Acta.* **1286**: 1-51.

Moran, J. F., Becana, M., Iturbe-Ormatxe, I., Frechilla, S., Jluas, R. V., and Aparicio-Tejo, P. (1994). Drought induces oxidative stress in pea plants. *Planta*, **194**: 346-352.

Moreno, S., and Nurse, P. (1994). Regulation of progression through the G1 phase of the cell cycle by the *ruml*$^{+}$ gene. *Nature*, **367**: 236-242.

Moriau, L., Bogerts, B., Jonniaux, JL., Boutry, M. (1993). Identification and characterization of a second plasma membrane H^{+}-ATPase gene subfamily in *Nicotiana plumbaginifolia*. *Plant Mol. Biol.*, **21**: 955-963.

Morris, C. E., and Homann, U. (2001). Cell surface area regulation and membrane tension. *J. Membr. Biol.*, **179 (2):** 79-102.

Müller Röber, B., Ellenberg, J., Provar, N., Willmitzer, I., Busch, H., Becker, D., Dietrich, P., Hotth, S., Herdrich, R. (1995). Cloning and electrophysiological analysis of *kst1*, an inward rectifying K^{+} channel expressed in potato guard cells. *EMBO, J.*, **14**: 2409-2416.

Muramoto, Y., Watanabe, A., Nakamura, T.,and Takabe, T. (1999). Enhanced expression of a nuclease gene in leaves of barley plants under salt stress. *Gene.***8; 234(2):**315-21.

Nakamura, R. L., McKendree, W. L., J. Hirsch, R. E. Sedbrook, J. C., Gaber, R. F., & Sussman, M. R. (1995). Expression of an *Arabidopsis* potassium channel gene in guard cells. *Plant Physiol.*, **109**:371-374.

Nakamura, T., Komano, Y., itaya, E., Tsukamoto, K., Tsuchiya, T., and Unemoto, T. (1994). Cloning and sequencing of Na^{+} /H^{+} antiporter gene from marine bacterium *Vibrio alginolyticus*. *Biochem. Biophys. Acta.*, **1190**: 465-468.

Nanda, A., Gukovskaya, A., Tseng, J., and Grinstein, S. (1992). Activation of vacuolar type proton pumps by protein kinase C: role in neutrophil pH regularion. *J. Biol. Chem.*, **267(32)**: 22740-2746.

Nass, R., and Rao, R. (1998). Novel localization of Na^{+} /H^{+} exchanger in a late endosomal compartment of yeast. *J. Biol. Chem.*, **273(33):** 21054-21060.

Navarre, C. Goffeau, A. (2000). Membrane hyperpolarization induced by detection of PMP3, a highly conserved small protein of yeast plasma membrane (conserved small peptide and the uptake of toxic cations, including Na^{+}). *EMBO. J.*, **19**: 2515-2524.

Nichols, S. J., Pelham, H. R., Ungermann, C., Wickner, W., and Haas, A. (1998). Homotypic vacuolar fusion mediated by t- and v-SNAREs. *Nature*. 387(**6629**): 199-202.

Niu, X., Bressan, R. A., Hasegawa, P. M., and Pardo, J. M. (1995). Ion homeostasis in NaCl stress environments. *Plant Physiol.*, **109**: 735-742.

O'Neil, S. D., and Spanswick, R. M. (1984). H^+-ATPase activity from storage tissue of *Beta vulgaris*. 3. Solubilization and reconstitution of a vanadate-sensitive H^+-ATPase from the plasma membrane of red beet. *J. Membr. Biol.*, **79**: 231-243.

Orlowski, J., and Grinstein, S. (1997). Na^+/H^+ exchangers of mammalian cells. *J.Bio. Chem.*, **272(36)**: 22373-22376.

Ortiz, F., Riscitti, T., McCue, K. F., and Ow, D. (1995). *J. Biol. Chem.* **270:** 4721-4728.

Padan, E. and Schuldiner, S. (1992). Na^+ transport system in prokaryotes. *In*: Alkali Cation transport system in prokaryotes. (Bakker, E. ed), 3-24, *Boca Raton FL: CRC Press*.

Palmgren,M. G., and Harper, J. F. (1999). Pumping with plant P-type ATPases. *J. Exp. Bot.,*. **50**: 883-893.

Perez, C. Michelet, B. Ferrant, V., Bogaerts, P., and Boutry, M. (1992). Differential expression with in a three-gene subfamily encoding a plasma membrane H^+-ATPase in *Nicotiana plumbaginifolia. J. Biol. Chem.*, **267**: 1204-1211.

Pincus, P. (1999). Conformational dynamics of vesicles. *Prc. Natl. Acad. Sci. USA*. **96**:10550.

Poirier,G.M.C., Pyati, J., Wan,J. S., and Erlander, M. G. (1997). Screening differentially expressed cDNAclones obtained by differential display using amplified RNA. Nucleic Acids Res. **25**: 913-914.

Price, J., El-shikh. M., Laird, J., Urwin, N.& Dominy, P. (2001). Engineering sodium exclusion mechanisms in plants, eds. Taha, *et al.*, (Biosalin Agriculture in the GCC countries), pp.1-29.

Quintero,F. J., and Blatt, M. R. (1997). A new family of K^+ transporters from *Arabidopsis* that are conserved across phyla. *FEBS. Lett.* **415(2):** 206-211.

Raschke,, K., Hedrich, R., Beckmann, U., and Schroeder, J. I. (1988). *Bot. Acta.*, **101**: 283-294.

Ratajczak, R, Hinz, G., Robinson, D.G. (1999). Localization of pyrophosphatase in membranes of cauliflower inflorescence cells. *Planta.*, **208(2):**205-211.

Ratner, A. B., and Jacooby. (1986). Effect of K^+ its counter anion and pH on soidium efflux from barley roots. *J. Exp. Bot.*, **27**: 843-852.

Rawson, H. M., Richards, R. A., and Munns, R. (1988). An examination of selection criteria for salt tolerance in wheat, barley and *triticale* genotypes. *Aust. J. of Agri Res.*, **39**:759-772.

Rea, P. A. (1999). MRP subfamily ABC transporters from plants and yeast. *J. Exp. Bot.*, **50**: 895-913.

Rea, P. a., and Poole, R. j. (1993). Vacuolar H^+ translocating pyrophosphatase. *Annu. Rev. Plant Physiol. PlantMol. Biol.*, **44**: 157-180.

Rea, P. A., Britten, C. J., and Sarafian, V. (1992). Common identity of substrate-biding subunit of vacuolar H^+-translocating inorganic pyrophosphatase of higher plant cells. *J. Biol. Chem.*, **262**: 14745-14752.

Rea, P. A., Li, Z. S., Lu, Y. P., Drozdowicz, Y. M., and Matrtioia, E. (1998). From vacuolar GS-X pumps to multispecific ABC transporters. Annu. Rev. Physiol. *Plant Mol. Biol.*, **49**: 727-760.

Reichheld, J-P., Vernoux, F., L. (1999). Specific checkpoints regulate plant cell cycle progression in response to oxidative stress. *The Plant J.*, **17:** 647-656.

Reuveni, M., Colombo, R., Lerner, H. R., Pradent, A., and Proljakoff-Mayber, A. (1987). Osmotically induced proton extruction from carrot cells in suspension culture. *Plant Physiol.*, **85**: 383-388.

Robinson, D. G., Haschke, H. P., Hinz, G., Maeshima, M., and Marty,F. (1996). Immunological deduction of tonoplast polypeptides in the plasma membrane of pea cotyledons. *Planta* **198**: 95-103.

Rodriguez-Navarro, A., Quintero, F. J., and Garciadeblas, B. (1994). Na^+ ATPases and Na^+ /H^+ antiporters in fungi. Bioch. Biophys. *Acta.*, **1187**: 203-205.

Roxas, V. P., Smith R. H., and Allen, E. R. (1997). Over-expression of glutathione s-transferase/glutathione peroxidase enhances the growth of transgenic tobacco seedlings during stress. *Nat. Biotechnol.* **15**: 988-991.

Rubio, F., Gassman, W., Schroeder J. I. (1995). Sodium-driven potassium uptake by the plant potassium trasporter HKT1 and mutation conferring salt tolerance. *Sci.* **270**: 1660-1663.

Sambrook, J. Fritsch, E. F., and Maniatis, T. (1989). Molecular cloning: A laboratory manual. *Cold Spring Harbour Laboratory Press, Cold Spring Harbour, New York.*

Sanderfoot, A. A., and Raikhel, N. V. (1999). The specificity of vesicle trafficking: Coat proteins and SNAREs. *Plant Cell.* **11**: 629-641.

Santa-Maria, G. E., Rubio, F., Dubcovsky, J., and Rodriguez-Navaro. A. (1997). The HAK1 gene of barley is a member of a large gene family and encoodes a high-affinity potasium transporter. *Plant Cell.* **9(12):** 2281-2289.

Sarafian, V., Kim, Y., Poole, R. J., and Rea, P. A. (1992). Molecular cloning and sequence of cDNA encoding the pyrophosphate-energized vacuolar membrane proton pump (H^+-PPase) of *Arabidopsis thaliana. Proc. Natl. Acad. Sci. USA.*, **89**: 1775-1779.

Schachtman, D. P., and Schroeder, J. I. (1994). Structure and transport mechanism of a high-affinity potassium uptake transporter from higher plants. *Nature*, **370**: 655-658.

Schachtman, D. P., Kumar, R., Schroder, J. I., and March, E. L. (1997). Molecular and functional characterization of a novel low-affinity cation transport (LCT1) in higher plants. *Proc. Natl. Acad. Sci. USA.* **94(20):** 11079-11084.

Schachtman, D. P., Tyerman, S. D., and Terry, B. T. (1991). The K^+ /Na^+ selectivily of a cation channel in the plasma membrane of root cells does not differ in salt-tolerant and salt-sensitive wheat species. *Plant physiol.*, **79**:598-605.

Schaller, G. E. and Sassman, M. R. (1988). Phosphorylation of the plasma membrane H^+-ATPase of oat roots by a calcium-stimulated protein kinase. *Planta.*, **173**: 509-518.

Schleyer, M., and Bakker, E. P. (1993). Nucleotide sequence and 3'-end deletion studies indicate that the K (+)-uptake protein kup from *Escherichia coli* is composed of a hydrophobic core linked to a large and partially essential hydropholic C terminus. *J. Bacteriol.* **175(21):** 6925-6931.

Schroeder, J. I., Ward, J. M., and Gassmann, W. (1994). Perspectives on the physiology and structure of inward rectifying K+ channels in higher plants: biophysical implications for K (+)-uptake. *Annu. Rev. Biophys. Biomol. Struct.* **23**: 441-471.

Schuldiner, S. (1993a). In alkali cation transport system in prokaryotes. (Bakker, E. P., ed) 3-24, *CRC Press. Boca Raton, Fl.*

Schumacher, K., Vafeados, D., McCarthy, M Sze, H., Wilkins, TA, et al., (1999). The *Arabidopsis* det3 mutant reveals a central role for the vacuolar H+-ATPase in plant growth and development. *Genes Dev.* **13**:3259-3270.

Seki, M., Ishida, J., Narusaka, M., Fujita, M., Nanjo, T., Umezawa, T., *et al.,* (2000)..Monitoring the expression pattern of around 7,000 *Arabidopsis* genes under ABA treatments using a full-length cDNA microarray *Funct Integr Genomics.* **2(6):**301

Sentenac, H.m Bonneaud, N., Minet, M., Lacroute, F., Salmon, J. M., Gaymaed, F., Grignon, C. (1992). Cloning and expression in yeast of a plant potassium ion system. *Sci.* **256**: 663-665.

Serrano and Rodriguez-Navarro, (2001). Ion homeostasis during salt stress in plants. *Current opinion in cell biology,* **13**: 339-404.

Serrano, R. (1985). Plasma membrane ATPase of plant and fungi. *Boca Rato, FL:CPC Press.*

Serrano, R. (1989). Structure and function of membrane ATPase. *Ann. Rev. Plant, Mol. Boil.*, **40**: 61-94.

Serrano, R. (1991). Transport across yeast vacuolar and plasma membrane. *In*: The molecular and cellular biology of the yeast Saccharomyces; genome dynamics, protein synthesis and energetics. (Broach, J. R., Pringle, J. R. and Jones, E. W. eds). 523-585. *Cold Spring Harbor, NY: Cold Spring Laboratory Press.*

Serrano, R. (1996). Salt tolerance in plants and microorganism: toxicity targets and defense responses. *Intern. Rev. cytol.* **195**: 1-52

Serrano, R., and Gaxiola, R. (1994). Microbial model and salt stress tolerance in plants. *Crit Rev plant Sci.* **13 (2)**:121-138.

Serrano, R., and Gaxiola, R. (1994). Microbial models and salt stress tolerance in plants. *Crit. Rev. in plant Sci.,* **13 (2):** 121-138.

Shi, H. Z., Ishitani, M., Kim, C. S., and Zhu, J-K. (2000). The *Arabidopsis thaliana* salt tolerance gene *SOS1* encodes a putative Na^+/ H^+ antiporter. *Proceeding of the National Academy of Sciences of the USA* **79**: 6896-6901.

Shi, H., Quintero, F. J., Pardo, J. M., and Zhu, J-K. (2002). The putative plasma membrane Na^+/ H^+ antiporter SOS1 controls Long-Distant Na^+ transport in plants. *Plant cell.* **14**: 465-477.

Shimony, C., Fahn, A., and Reinhold, L. (1973). Ultrastructure and ion gradients in the salt glands of *Avicenia marina. New Phytol.* **27**: 27-36.

Sidler, M., Hassa, P., Hasan, S., Ringli, C., and Dudler, R. (1998). Involvement of an ABC transporter in a developmental pathway regulating hypocotyl cell elongation in the light. *Plant cell*, **10**: 1623-1636.

Skou, J. C. (1988). The Na,K-pump. *Methods Enzymol.* **156**:1-25

Smart, C. C and Fleming, A.J (1993). A plant gene with homology to D-myo-inositol-3-phosphate synthase is rapidly and spatially up-regulated during an abscisic-acid-induced morphogenic response in Spirodela polyrrhiza.Plant **4(2)**:279-93.

Smart, C. J, Garvin, D.F., Prince, j. P., lucas, w. J., Kochian, L. V. (1996) The molecular basis of potassium nutrition in plants. *Plant and Soil.* **187:** 81-89.

Smart, C., and Fleming, A. J. (1996). Hormonal and environmental regulation of a plant PDR5-like ABC transporter. *J. Biol. Chem.* **32**: 19351-19357.

Smironoff, N. (1993). The role of active oxygen in the response of plant to water deficit and desiccation. *New Phyto.* **125:** 27-58.

Soltanpour, P. N., and Follett, R. H. (1999). Crop tolerance to soil salinity. *Colorado State, Cooperative Extension.*

Stevens, T. H., and forgac, M. (1997). Structure, function, and regulation of the vacuolar H+-ATPase. *Annu.Rev. Cell Dev. Biol.* **13**:779-808.

Storey, R., and Wyn Jones. R. G. (1975). Betaine and choline level in plants and their relationship to sodium chloride stress. *Plant Sci. Lett.* **4**: 161-168.

Sussman, M. R. (1991). A plethora of plasma membrane proton pumps. In: transport and receptor proteins of plant membranes, molecular structure and function, 5-11, D. T. Cook and D. T. Clarkson (eds). *Plenum. Press. New York.*

Sussman, M. R. (1994). Molecular analysis of protein in plant membrnae of a family of transporters reveal functional subtypes. *Proc. Natl. Acad. USA.*, **29**: 9373-9377.

Szabolcs, I. (1979). Review of research on salt-affected soils. United Nations.

Sze, H. (1985). H^+-translocating ATPase. Advances using membrane vasicles. *Ann. Rev. Plant Physiol.*, **36**: 175-208.

Sze, H., Li, X., and Palmgren, M. G. (1999). Enegrization of plant cell membranes by H^+-pumping ATPases: regulation and biosynthesis. *Plant Cell*, **11**: 677-689.

Sze, H., Ward, J. M., and Lai, S. (1992). Vacuolar H^+-translocating ATPase from plants: structure, function and isoforms. *J. Bioenerg. Biomembr.*, **24 (4)**: 371-381.

Tal, M. (1990). Somaclonal variation for salt resistance. In: *Biotechnology in Agriculture and Forestry. Somaclonal variation in crop improvementI,* ed. YPS Bajaj, 236-257. *Berlin: Springer-Verlag.*

Talalay, P., De Long, M., Prochaska, U. J. (1998). Identification of a common chemical signal regulating the induction of enzymes that protect against chemical carcinogenesis. *Proc. Natl. Acad. Sci. USA*. **85**: 8261-8265.

Tang, X. , Halleck, M. S., Schlegel, R. A., and Williamson, P. (1996). A subfamily of P-type ATPases with aminophospholipid transporting activity. *Science*, **272**: 1495-1497.

Tang, H., Vasconcelos, A. C., Ma, J., & Berkowitz, G. A. (1998). *In vivo* expression pattern of a plant K^+ channel α subunits protein. *Plant Sci.*, **134**:117-128.

Theodoulou, F. L. (2000). Plant ABC trasporters. *Biochem. Biophys. Acta.* **1465**: 79-103.

Thiel, G., and Batey, N. H. (1998). Exocytosis in plants. *Plant Mol. Biol.* **38**: 111-125.

Tse, C. M., brant, M. S., Pouyssegure, J., and Donowitz, M. (1992). Cloning and sequencing of a rabbit cDNA encoding an intestinal and kidney-specific Na^+ /H^+ antiporter isoform (*NHE-3*). *J. Biol. Chem.*, **267**: 9340-9346.

Tyerman, S. D., Skerrett, M. Garrill, A., Findlay, G. P., and Leigh, R. A. (1997). Pathway for permeation of Na^+ and Cl^- into protoplasts derived from cortex of wheat roots. *J. of Ex. Bot.*, **48**:459-480.

Unger, I. A. (1991). Ecophysiology of vascular halophytes. *CRC. Press, Boca Raton.*

Ungermann, C and Wickner, W. (1998). Vam7p, a vacuolar SNAP-25 homolog, is required for SNARE complex integrity and vacuole docking and fusion. *EMBO* 17(**12**): 3269-76.

Ungermann, C., Nichols, S. J., Pelham, H. R., and Wickner, W. (1998). A vacuolar v-t-SNARE complex, the predominant form in vivo and on isolated vacuoles, is disassembled and activated for docking and fusion. *J Cell Biol.* 140(**1**):61-69.

Uozumi, N. (2001). *Escherichia coli* as an expression system for K^+ transport systems from plants. *Am. J. Physiol. Cell Physiol.* **281**: C733-C739.

Uozumi, N., Gassmann, W., Cao, Y., and Schroeder, J. L. (1995). Identification of storage modifications in cation selectivity in an *Arabidopsis* in ward rectifying channel by mutant selection in yeast. *J. Biol. Chem.*, **270**:24276-24281.

Vassilyev, A. E., and Stepannova, A. (1990). The ultrastructure of ion-secreting and non-secreting salt glands of Limonium Platyllum. *J. Exp. Bot.* **41**: 41-46.

Vitart, V., Baxter, I., Doerner, P., and Harper, J. F. (2001). Evidence for a role in growth and salt resistance of a plasma membrane H^+-ATPase in the root endodermis. *The Plant J.* **27 (3)**: 191-201.

Voeberg, G. S., and Shap, R. E. (1991). Growth of maize primary root and low water potential. *Plant, physiol.*, **96**: 1125-1130.

Wang, B, Luttge, u. and Ratajczak, R. (2001) Effects of salt treatment and osmotic stress on V-ATPase and V-PPase in leaves of the halophyte Suaeda salsa.J Exp Bot. **52(365)**:2355-65.

Watad, A-E. A., Pesci, P. A., Reinhold, L., and Lerner, H. R. (1986). Proton fluxes as a response to external salinity in wild type and NaCl-adapted *Nicotiana* cell lines. *Plant physiol.*, **81**: 454-459.

Watad, A-E. A., Reuveni, M., Bressan, R. A., and Hasegawa, P. M. (1991). Enhanced net K^+ uptake capacity of NaCl-adapted cells. *Plant Physiol.*, **95**: 1265-1269.

Wegner, L. H., De Boer, A. H. (1997). Properties of two outward-rectifying channels in root xylem parenchyma cells suggest a role in K^+ homeostasis and long -distance signaling. *Plant Physiology*. **115**:1707-1719.

Wilson, C., and Shannon, M. C. (1995). Salt induce Na^+ /H^+ antiport in root plasma membrane of glycophytic and halophytic species of tomato. *Plant Sci.* **107**: 147-157.

Wyn Jones, R. G. (1981). Salt tolerance *In*: Physiological processes limiting plant productivity. (Johnson. C. B. ed), 271, *Butterworth, London.*

Yeo, A., and Flowers, T. (1986). Ion transport in *Suaeda maritima*: its regulation of growth and implications for the pathway of radial transport of ions across the root. *J. Exp. Bot.* **37**: 143-159.

Yeo, A. R., Yeo, M. E., Flowers, S. A., and Flowers, T. (1988) Screening of rice (*Oryza setiva* L.) genotypes for physiological characters contributing to salinity resistance, and their relationship to overall performance. *Theor. Appl. Genet.* **79**: 377-384.

Yeo, A. R., Lee, K-S, Izard, P.., Boursier, P. J. Flowers, T. J. (1991). Short and long-tern effects of salinity on leaf growth in rice. (*Oryza sativa L.*) *J. Exp. Botany.* **42**: 881-889.

Yeo, A., R. (1998). Molecular biology of salt tolerance in the context of whole-plant physiology. *J. Exp. Bot.* **49**: 915-929.

Zhang and Blumwald (2001). Transgenic salt-tolerant tomato plants accumulate salt in foliage but not in fruit. *Nat Biotechnol.* **19(8):**765-8.

Zhang *et al* (2001 Engineering salt-tolerant *Brassica* plants: characterization of yield and seed oil quality in transgenic plants with increased vacuolar sodium accumulation. *Proc Natl Acad Sci.*. **98(22):**12832-12836.

Zhao, R., Dielen, V., Kinet, J-M., and Boutry, M. (2000). Co-suppression of a plasma membrane H^+-ATPase isoform impairs sucrose translocation, stomatal opening, plant growth, and male fertility. *Plant Cell.* **12**: 535-546.

Zhu , J-K, Hasegawa, P. M, Bressan, R. A. (1997). Molecular aspects of osmotic stress in plants. *CTR Crit Rev Plant Sci.* **16**: 253-277.

Zhu, J-K. (2000). Genetic analysis of plant salt tolerance using *Arabidopsis*. *Plant Physiol.* **124**: 941-948.

Zhu, J-K. (2001). Plant salt tolerance. *Trends in Plant Sic.* **6(2)**: 66-71.

Zimmermann, S. Talke, I. Ehehardt, T., Nast, G., Muller-Rober, B. (1998). Characterization of SKT1 an inwardly rectifying potassium channel from potato, by heterologous expression in insect cells. *Plant physiol.* **116**: 879-890.

Zimmermann, S., Ehrhardt, T., Plesch, G., and Müller-Röber, B. (1999). Ion channels in plant signaling. *Cellular and molecular. Life Sciences*, **55**: 183-203.

Zimmermann, S., Thomine, S., Guern, J., and Barbier-Brygoo, H. (1994). An anion current at the plasma membrane of tobacco protoplast shows ATP-dependent voltage regulation and is modulated by auxin. *Plant J.*, **6**: 707-716.

Zimniak, L. D., Dittrich, P., Gogaretn, J. P., Kibak, H. and Taiz, L. (1988). The cDNA sequence of the 69-Kda subuint of the carrot vacuolar H^+-ATPase: homology to the β−chain of F_1F_0-ATPase. *J. Biol. Chem.*, **263(19)**: 9102-9112.

Appendix 2:

BLAST Output of DDRT-PCR cDNA Fragments